

Aus dem Institut für Transplantationsdiagnostik und Zelltherapeutika
des Universitätsklinikums Düsseldorf
Direktor: Dr. med. Johannes Fischer

Linking Granzyme H to NK-Cell Education –
An Examination of Expression Patterns and Functions.

Dissertation

zur Erlangung des Grades eines Doktors der Medizin
der Medizinischen Fakultät der Heinrich-Heine-Universität Düsseldorf

vorgelegt von
Eva Nora Bongards
2021

Als Inauguraldissertation gedruckt mit Genehmigung
der Medizinischen Fakultät der Heinrich-Heine-Universität Düsseldorf

gez.:

Dekan: Prof. Dr. med. Nikolaj Klöckner

Erstgutachter: Prof. Dr. rer. nat. Markus Uhrberg

Zweitgutachter: Univ.-Prof. Dr. Jörg Timm

To my family.

Zusammenfassung (Deutsch)

Natürliche Killer (NK)-Zellen erwerben bei der Zell-Lizensierung durch das Binden entsprechender Liganden an selbstspezifische inhibitorische Rezeptoren funktionale Kompetenz. NK-Zellen, die keine solchen Rezeptoren exprimieren, werden hyporesponsiv. Die intrazellulären Mechanismen sowie die Unterschiede zwischen lizensierten und nichtlizensierten Zellen sind weitgehend unbekannt. Kürzlich wurde gezeigt, dass die Expression von Granzym (gr) B, eines der wichtigsten NK Zell-Effektormoleküle, auf Proteinebene in lizensierten NK Zellen höher ist als in nichtlizensierten. Das humane grH ist grB in Sequenz und Struktur sehr ähnlich, aber weniger erforscht. Daher wurde eine potenzielle Korrelation zwischen NK Zell-Lizensierung und grH-Expression gesucht und eine Analyse der Expressionsmuster und Funktionen von grH durchgeführt. In vorläufigen Experimenten sahen die Arbeitsgruppen von Prof. Dr. M. Uhrberg, Düsseldorf, und Prof. Dr. L. Walter, Göttingen, dass die Expression von *GZMH* (Genname von grH), aber nicht von anderen Granzymen, insbesondere *GZMB*, auf der mRNA-Ebene in lizensierten NK-Zellen höher war als in nichtlizensierten. Die vorgelegte Studie bestätigt durch Vielfarbdurchflusszytometrie diese Korrelation auf der Proteinebene. Sie ist im Hinblick auf mehrere verschiedene Paare inhibitorischer Rezeptoren (vor allem Killer-Cell Immunoglobulin-Like Receptors (KIRs)) und ihrer Liganden (vor allem humanes Leukozyten-Antigen (HLA)-C) statistisch so hochsignifikant, dass die Verwendung von grH-Expression für die Erstellung eines neuen zeit- und entwicklungsorientierten Modells der NK Zell-Lizensierung, ebenso als Marker dafür, vorgeschlagen wird. Eine Korrelation zwischen NK Zell-Lizensierung und grB-Expression auf der Proteinebene war weniger deutlich und für grA oder grK nicht vorhanden. Sowohl grH- als auch grB-Expression korrelierten außerdem positiv mit der NK Zell-Reife. GrH-Expression korrelierte negativ mit der Expression von KLRG1, eines in NK Zell-Adhäsion involvierten inhibitorischen Rezeptors, und es wird gezeigt, dass der Lizensierungsstatus einer NK Zelle aus grH-Positivität, CD57-Positivität und KLRG1-Negativität vorhergesagt werden kann. Außerdem wurde die Expression (Proteinebene) von grH und grB in Lymphozyten untersucht und verglichen. In Ruhe war sie sehr ähnlich; am höchsten in NK Zellen, dann in absteigender Folge in NK-ähnlichen T Zellen, CD8⁺ T Zellen, CD4⁺ T Zellen und nicht-NK/nicht-T Lymphozyten. Insgesamt war die Expression von grB höher als von grH, auch in den untersuchten NK Zell-Subtypen, bis auf adaptive NK Zellen von Spendern, die eine Cytomegalovirus-assoziierte Expansion des NK Zell-Rezeptors NKG2C aufweisen; hier war die Expression von grH mindestens gleich der von grB. Nach NK Zell-Stimulation war die Expression von grH und grB jedoch unterschiedlich. Stimulation durch Interleukin (IL)-2 und/oder IL-15, oder IL-15 und den anti-CD20 monoklonalen Antikörper (mAb) Rituximab, oder durch K562 Targetzellen, führte zu einer drastischen Reduktion der Expression von grH, aber nicht grB. Außerdem zeigten sich nach Stimulation mit K562 Targetzellen Anstiege in der Expression von CD107a, Interferon- γ und Tumornekrosefaktor- α als erhöht in grH⁻ verglichen mit grH⁺ NK Zellen (lizensiert sowie nichtlizensiert), wohingegen keine Differenz zwischen grB⁻ und grB⁺ Zellen bestand. ‚GrH Erschöpfung‘, in der nach NK Zell-Stimulierung grH ausgeschüttet, jedoch wegen verringerter Transkription nicht nachproduziert wird, könnte ein potenzieller Mechanismus für diese Phänomene sein. Ferner wurde die bislang vorgeschlagene mögliche zytotoxische Rolle von grH hier nicht bestätigt. Es gab keinen Unterschied in der Lyse von Targetzellen zwischen grH-überexprimierenden NK-92 Zellen und Kontrollen. Jedoch korrelierte die Expression von grH positiv mit der des antiapoptotischen BCL-2 in primären NK Zellen, was eine mögliche Funktion von grH im Überleben der es exprimierenden Zellen zeigt. Erstaunlicherweise war der häufig verwendete anti-grB mAb GB11 nicht grB-spezifisch, sondern kreuzreaktiv mit grH in grH-überexprimierenden K562 Zellen. Hinsichtlich der starken Korrelation zwischen Lizensierungsstatus und der Transkription von *GZMH* im Gegensatz zu *GZMB*, sowie der fehlenden Unterscheidung zwischen grB und grH durch den häufig verwendeten anti-grB mAb, muss die Rolle von Granzymen im Lizensierungsprozess neu definiert werden. Zusammenfassend zeigt diese Studie, dass grH-Expression positiv mit NK Zell-Lizensierung korreliert; so stark, dass sie die Basis eines neuartigen zeit- und entwicklungsorientierten Modells dieses Prozesses bilden kann. Die zuvor gezeigte Korrelation zwischen NK Zell-Lizensierung und grB-Expression wird infrage gestellt. Überdies wird statt einer zytotoxischen Rolle von grH, die hier nicht bestätigt werden konnte, eine Rolle des Proteins im Überleben der es exprimierenden Zellen suggeriert. Eine Reduktion in der Expression von grH, jedoch nicht von grB, wurde nach Stimulierung beobachtet und auf grH Erschöpfung zurückgeführt. Somit wird hier eine potenzielle regulatorische und nicht hauptsächlich zytotoxische Rolle des grH vorgeschlagen; die Verringerung in grH-Expression nach NK Zell-Stimulierung könnte dazu beitragen, NK Zell-Autoreaktivität zu vermeiden.

Summary (English)

Natural Killer (NK)-cell education is a process by which functional competence is acquired through engagement of self-specific inhibitory receptors, those cells that lack self-specific inhibitory receptors becoming hyporesponsive. It is well known that this process occurs, but the intracellular mechanisms, as well as phenotypic differences between educated and uneducated NK cells, remain largely elusive. Recently, granzyme (gr) B, one of the crucial effector molecules of NK cells, was shown to be more highly expressed, at the protein level, in licensed than unlicensed cells. Another human granzyme, grH, shares considerable sequence and structural identity with grB but is far less well-studied. Therefore, a link between the crucial NK-cell education and grH expression was sought, and an analysis of grH expression patterns and its function was conducted.

In preliminary experiments Prof. Dr M. Uhrberg's group, Düsseldorf, in cooperation with Prof. Dr L. Walter's group, Göttingen, found that mRNA levels of *GZMH* (gene name of grH), but not of other granzymes, including *GZMB*, were higher in licensed than unlicensed NK cells. The present study now confirms this correlation at the protein level using multicolour flow cytometry. The correlation is highly statistically significant for several different inhibitory receptor (mainly killer-cell immunoglobulin-like receptors (KIRs)) / ligand (mainly human leukocyte antigen (HLA)-C) pairs, and so strong that use of grH expression to formulate a novel temporal and developmental model of NK-cell licensing, and also as a marker of the process, is proposed. A correlation between NK-cell licensing and grB expression at the protein level was less clear, and none was found for grA or grK. Both grH and grB expression also positively correlated with NK-cell maturity. GrH expression negatively correlated with KLRG1, an inhibitory receptor involved in NK-cell adhesion, and an NK cell's licensing status is shown to be predictable from grH-positivity, CD57-positivity and KLRG1-negativity.

GrH and grB protein expression by lymphocytes was also examined and compared. It was found to be very similar at rest, highest in NK cells, then in descending order in NK-like T cells, CD8⁺ T cells, CD4⁺ T cells and non-NK/non-T lymphocytes. Overall, expression of grB was higher than of grH, including in all NK-cell subtypes tested, except for adaptive NK cells from donors with a cytomegalovirus-associated expansion of the NK-cell receptor NKG2C, in which grH levels were at least equal to grB's. Upon NK-cell stimulation, grH and grB expression were different, however. Stimulation with interleukin (IL)-2 and/or IL-15, or IL-15 and the anti-CD20 monoclonal antibody (mAb) rituximab, or with K562 target cells, led to drastic reductions in grH but not grB levels. Furthermore, following stimulation with K562 cells, increases in expression of CD107a, interferon- γ and tumour necrosis factor- α , were higher in grH⁻ than grH⁺ NK cells (both licensed and unlicensed), while no difference was observed between grB⁻ and grB⁺ cells. 'GrH exhaustion', where grH is excreted upon NK-cell stimulation but, due to reduced transcription, is not replenished, could be a possible mechanism for these phenomena.

The previously suggested putative cytotoxic role of grH could not be confirmed here. There was no difference in target-cell lysis between grH-overexpressing NK-92 cells and controls. However, primary NK-cell grH expression positively correlated with that of the anti-apoptotic BCL-2, possibly implicating grH in host-cell survival.

Notably, the commonly used anti-grB mAb GB11 was shown to be non-specific for grB, cross-reacting with grH in grH-overexpressing K562 cells.

Considering that in contrast to *GZMB*, transcription of *GZMH* strongly correlated with licensing status, and considering that the commonly used anti-grB mAb did not distinguish between grB and grH, the role of granzymes in the licensing process has to be redefined.

In sum, this study shows grH expression to be positively correlated with NK-cell licensing, strongly enough so to form the basis of a new temporal and developmental model of the process. In contrast, the previously shown correlation between grB and NK-cell licensing is challenged. Furthermore, instead of a possible cytotoxic role of grH, which could not be confirmed here, a role of grH in host-cell survival is suggested. Moreover, a decrease in grH expression upon stimulation was observed, which stands in contrast to the steady or even increased grB expression and may be due to grH exhaustion. Thus, the author proposes a potential regulatory rather than a mainly cytotoxic role of grH, the decrease in grH expression upon NK-cell stimulation possibly helping to prevent NK-cell autoreactivity.

Abbreviations

Recognised Abbreviations

ADCC	Antibody-dependent cell-mediated cytotoxicity	EGFP	Enhanced green fluorescent protein
AF	Alexa Fluor	FACS	Fluorescence-activated cell sorting
Alpha MEM	Alpha Minimum Essential Medium	FBS	Foetal bovine serum
ANOVA	Analysis of variance	Fig.	Figure
APC	Allophycocyanin	FITC	Fluorescein isocyanate
APC/Cy7	Allophycocyanin-Cyanine 7	FVD	Fixable viability dye
Aqua dest.	Distilled water	GZM	Granzyme (gene)
BCL-2	B-cell lymphoma 2	H₂O	Water
Bid	BH3-interacting domain death agonist	HIV	Human immunodeficiency virus
BLAST®	Basic local alignment search tool	HLA	Human leukocyte antigen
bp	Base pair(s)	HPLC	High-performance liquid chromatography
BSA	Bovine serum albumin	ICAD	Inhibitor of caspase-activated DNase
BV	Brilliant Violet	ie	<i>Id est</i> (that is)
CBMC(s)	Cord-blood mononuclear cell(s)	IFN	Interferon
CCL	CC-chemokine ligand	Ig	Immunoglobulin
CD	Cluster of differentiation	IL	Interleukin
cDNA	Complementary DNA	IMDM	Iscove's Modified Dulbecco's Medium
CMV	Cytomegalovirus	ITAM	Immunoreceptor tyrosine-based activation motif
HCMV	Human cytomegalovirus	ITIM	Immunoreceptor tyrosine-based inhibitory motif
MCMV	Murine cytomegalovirus	ITZ	Institute of Transplantation Diagnostics and Cell Therapeutics
DAP10, and DAP12	DNAX-activating protein 10, and 12	kb	Kilobase(s)
DMEM	Dulbecco's Modified Eagle Medium	KIR	Killer-cell immunoglobulin-like receptor
DMSO	Dimethyl sulfoxide	KLRG1	Killer-cell lectin-like receptor G1
DNA	Deoxyribonucleic acid	LAK cells	Lymphokine-activated killer cells
DNAM-1	DNAX-accessory molecule-1	LB	Lennox broth
dNTP	Deoxynucleoside triphosphate	LFA-1	Lymphocyte function-associated antigen 1
DPBS	Dulbecco's Phosphate-Buffered Saline	M-MLV	Moloney murine leukaemia virus
ds	Double-stranded	mAb	Monoclonal antibody
DSMZ	German Collection of Microorganisms and Cell Cultures GmbH	MFI	Mean fluorescence intensity
<i>E. coli</i>	<i>Escherichia coli</i>	MHC	Major histocompatibility complex
EDTA	Ethylenediamine tetraacetic acid		
eg	<i>Exempli gratia</i> (for example)		

Abbreviations

MIC	MHC class I polypeptide-related sequence
mRNA	Messenger RNA
n	Number of samples/sample size
NCBI	National Center for Biotechnology Information
NCR	Natural cytotoxicity receptor
NK cells	Natural killer cells
ns	Non-significant
ORF	Open reading frame
PBMC(s)	Peripheral-blood mononuclear cell(s)
PC5.5	Phycoerythrin-Cyanine 5.5
PCR	Polymerase chain reaction
PE	Phycoerythrin
PE/Cy5	Phycoerythrin-Cyanine 5
PE/Cy7	Phycoerythrin-Cyanine 7
PEI	Polyethylenimine
PI	Propidium iodide
PS	Phosphatidylserine
RM	Repeated measures
RNA	Ribonucleic acid
RNA-Seq	RNA deep sequencing
RNasin	Ribonuclease inhibitor
RPMI	Roswell Park Memorial Institute
S.O.C.	Super optimal broth with catabolite repression
SEM	Standard error of the mean
SFFV	Spleen focus forming virus
SHP	Src homology region 2 domain-containing phosphatase
Smac/ DIABLO	Second mitochondria-derived activator of caspase/direct inhibitor of apoptosis-binding protein with low pI
ss	Single-stranded
SSP	Sequence-specific primers
SV40	Simian virus 40
TBE Buffer	Tris/Borate/EDTA Buffer
TE Buffer	Tris/EDTA Buffer
Tm	Melting temperature
TNF	Tumour necrosis factor
UKD	University Hospital Düsseldorf
ULBP	UL16-binding protein
vs	<i>Versus</i>
XCL	X-C motif chemokine ligand

Customised Abbreviations

CB	Cord blood
DN	Double-negative (inhibitory KIR and NKG2A-negative)
dp	Double-positive (positive for two inhibitory receptor types)
gr	Granzyme (protein)
h.-i.	Heat-inactivated
Lic	Licensed
MC(s)	Mononuclear cell(s)
PB	Peripheral blood
s.-f.	Sterile-filtered
sp	Single-positive (positive for a single inhibitory receptor type)
tp	Triple-positive (positive for three inhibitory receptor types)
Unlic	Unlicensed

Units and Symbols

&	Ampersand
#	Number
%	Percent
°C	Degrees Celsius
×g	Times gravity (unit of relative centrifugal force)
∞	Infinity
~	Approximately
=	Equals
≅	Corresponds to
<	Less than
>	Greater than
≥	Greater than or equal to
nm	Nanometre(s)
µm	Micrometre(s)
mm	Millimetre(s)
cm	Centimetre(s)
ng	Nanogram(s)
µg	Microgram(s)
mg	Milligram(s)
g	Gram(s)
µl	Microlitre(s)
ml	Millilitre(s)
l	Litre
pmol	Picomole(s)
µM	Micromolar
mM	Millimolar
M	Molar (moles/l)

Abbreviations

mA	Milliampere	IU	International units
min	Minute(s)	TU	Transduction units
h	Hour(s)	V	Volt(s)
rpm	Revolutions per minute	v/v	Volume/volume
RT	Room temperature	w/v	Weight/volume
U	Unit(s)	μF	μFarad(s)

Table of Contents

1	Introduction	1
1.1	Natural Killer Cells – an Overview	1
1.2	NK-Cell Development	2
1.3	NK-Cell Receptors	3
1.3.1	NK-Cell Receptors and Means of NK-Cell Activation – an Overview	3
1.3.2	KIRs	4
1.3.3	The CD94/NKG2 Family of Receptors	8
1.3.4	Natural Cytotoxicity Receptors and Immunoglobulin-Like Transcripts	9
1.4	NK-Cell Education	9
1.4.1	(Classical) NK-Cell Education – an Overview	9
1.4.2	NK-Cell Education by Non-Classical MHC	11
1.4.3	Comparative Analyses of Licensed vs Unlicensed NK Cells	11
1.4.4	NK-Cell Education – Different Models	11
1.4.5	NK-Cell Education – Clinical Relevance	13
1.5	Granzymes	14
1.5.1	Overview and Functions	14
1.5.2	Granzyme Expression by Lymphocytes	15
1.5.3	Genomic Organisation of Granzymes and Comparison between GrB and GrH	15
1.5.4	The Putative Cytotoxic Role of GrH	16
1.6	Aims of this Thesis	17
2	Materials and Methods	18
2.1	Materials	18
2.1.1	Dyes Used for Flow Cytometry	18
2.1.2	Cell Culture	19
2.1.3	Other Reagents	20
2.1.4	Reagents Used for Molecular Biology	20
2.1.5	Cells Used	22
2.1.6	Primers Used in but not Designed within this Study	23
2.1.7	Vectors	24
2.1.8	Commercially Available Kits	25
2.1.9	Plastic- and Glassware	25
2.1.10	Devices and Software	26
2.2	Methods	27
2.2.1	Isolation of Mononuclear Cells	27
2.2.2	Counting Cells Using a Counting Chamber	27
2.2.3	Cryopreservation of Cells	27
2.2.4	Thawing Cells	28
2.2.5	Culture of Cell Lines	28
2.2.6	Flow Cytometry and Fluorescence-Activated Cell Sorting	28
2.2.7	Functional Assays	29
2.2.8	Nucleic Acid Purification and cDNA Generation	32
2.2.9	Agarose Gel Electrophoresis	33
2.2.10	HLA and KIR Typing	33
2.2.11	GrH and grB Overexpression and Preparation for Knockdown of grH and grB	35
2.2.12	Statistics	46
2.2.13	General Statements	46
3	Results	47
3.1	NK-Cell Licensing and <i>GZMH</i> mRNA Levels – Transcriptome Data	47
3.2	Donor Characteristics	48

Table of Contents

3.3	General Gating Strategy	48
3.4	GrH Antibody Selection	49
3.5	GrH and GrB Expression by Lymphocytes	50
3.5.1	GrH and GrB Expression by NK Cells, NK-Like T Cells, T Cells and Non-NK/Non-T Cells	50
3.5.2	GrH and GrB Expression by CD56 ^{dim} and CD56 ^{bright} NK Cells.....	51
3.5.3	GrH Expression by PB and CB-Derived CD56 ^{dim} NK Cells	52
3.6	NK-Cell Education and GrH Expression; GrB for Comparison	52
3.6.1	Staining Strategy and Receptor-Based Definition of NK-Cell Populations.....	52
3.6.2	Correlation between NK-Cell Licensing and GrH Expression.....	53
3.6.3	GrH Expression by NK Cells Expressing more than one Type of Receptor	56
3.6.4	NK-Cell Licensing and GrB Expression	58
3.6.5	NK-Cell Licensing and GrA and GrK Expression	60
3.6.6	GrH Expression by Licensed NK Cells in CB.....	61
3.7	NK-Cell Maturity and GrH Expression	62
3.8	Correlation between Expression of GrH, CD57, KLRG1, CD11c and DNAM-1	65
3.9	Functional Analyses of Primary NK Cells with Regard to GrH Expression	68
3.9.1	Soluble Mediator-Induced NK-Cell Stimulation.....	68
3.9.2	Target Cell-Mediated NK-Cell Stimulation.....	71
3.10	Overexpression of GrH in NK-92 Cells and Primary NK Cells	76
3.10.1	Overexpression in NK-92 Cells	76
3.10.2	Overexpression in Primary NK Cells	81
3.11	Examination of GrH with Regard to Cell Survival and Apoptosis	82
3.11.1	Correlation between Expression of GrH and BCL-2 and Licensing	82
3.11.2	Serum-Starvation Assay	83
3.12	GrH and GrB Overexpression in K562 Cells to Test Antibody Specificity	85
4	Discussion	87
4.1	The Positive Correlation between NK-Cell Education and GrH Expression	87
4.1.1	A Novel Temporal and Developmental Model of NK-Cell Licensing.....	87
4.1.2	The Number of Self-Specific Inhibitory KIRs and GrH Expression.....	89
4.1.3	GrH Expression in Cord Blood-Derived NK Cells, and the Novel Licensing Model.....	89
4.1.4	Effect of Non-Discrimination between 2DL3 and 2DL2	89
4.2	GrB Expression, NK-Cell Licensing and Lack of Antibody Specificity	89
4.2.1	Antibody Non-Specificity and the Putative Link between Licensing and GrB Expression	89
4.2.2	Further Implications of the Lack of GB11-Specificity	90
4.3	The Polyclonal Anti-GrH Antibody	91
4.4	A Single Base Change in the GZMB Insert Sequence	92
4.5	GrH and GrB Expression by Different Types of Lymphocytes	92
4.6	NK-Cell Stimulation and GrH Expression, as well as GrB for Comparison	93
4.6.1	Decreases in Expression of GrH but not GrB upon NK-Cell Stimulation.....	93
4.6.2	CD107a and Cytokine Expression in GrH ⁻ vs GrH ⁺ NK Cells Upon Stimulation with Target.....	94
4.7	Correlation between GrH and CD57-Positivity and KLRG1-Negativity	95
4.8	Lack of GrH Cytotoxic Activity but Potential Involvement in Host-Cell Survival	96
4.8.1	GrH Cytotoxicity in the Literature and Lack thereof in this Study	96
4.8.2	Possible Involvement of GrH in Host-Cell Survival	98
4.9	Direct Antiviral and GrB-Disinhibiting Roles of GrH	99
4.10	Conclusions	100
	Bibliography	101

1 Introduction

This study shows that expression of granzyme (gr) H strongly positively correlates with natural killer (NK)-cell education, the crucial process by which NK-cell functional competence is acquired through engagement of self-specific inhibitory receptors. Given our – as yet – incomplete grasp of the mechanisms of NK-cell education, this finding is highly significant, particularly in light of the importance of granzymes as some of the main effector molecules of NK cells. To gain a better understanding of grH and its relevance, this study also conducts a more detailed examination of grH expression patterns and functions.

This introduction first gives a general overview of NK cells, their responses and development, and then of the main receptor families NK cells express, to provide the appropriate background before an outline of NK-cell education itself is given. An overview of the role of granzymes in NK-cell biology, with a focus on grH, follows. Finally, the aims of this thesis are stated.

1.1 Natural Killer Cells – an Overview

NK cells were originally identified because of their notable lack of T and B-cell markers and their ability to recognise and kill tumour cells without prior sensitisation (1),(2),(3). NK cells constitute ~5-15% of circulating lymphocytes in healthy individuals (4), and are also found in tissues including the bone marrow, spleen, lymph nodes, liver and lung (5). Defined most simply by surface expression of CD56 and lack of CD3, an invariant complex associated with the T-cell receptor (6),(7), NK cells are a crucial cytotoxic mediator and therefore a critical component of the immune defence against virus-infected and tumour cells. For instance, the importance of NK cells in early antiviral defences was demonstrated, amongst others, by Bukowski *et al.*, who showed that mice, a species that represents a good model for the study of human NK-cell function, develop decreased or increased resistance against murine cytomegalovirus (MCMV) following NK-cell depletion and adoptive transfer respectively (8). Mouse studies also provided early evidence for the essential role of NK cells in anti-tumour immunity, showing that tumour cells injected into mice that had been subjected to antibody-mediated NK-cell depletion displayed enhanced growth and metastasis than when injected into non-pre-treated mice (9). Human studies, too, have illustrated the immense importance of NK cells in human health and disease. For example, in an 11-year follow-up study of a Japanese cohort, Imai *et al.* showed that reduced peripheral-blood natural cytotoxicity was associated with higher general cancer risk (10).

NK cells have also been remarkably found to be important for eutherian mammalian placentation (11),(12): uterine NK cells have been shown to be crucial for the remodelling of maternal uterine spiral arteries for adequate placental blood supply (13), and protection from pregnancy disorders like preeclampsia, which are due to failure of normal placentation, has been correlated with particular uterine NK-cell receptor/ligand pairs (14).

Upon activation, NK cells display a variety of responses. These include target-cell cytotoxicity, particularly via the secretion of perforin and granzymes (7),(15), but also via expression of death ligands like Fas ligand (FasL) and TNF-related apoptosis-inducing ligand (TRAIL), and via secreted and membrane-bound cytokines (16),(17). The responses also include immunomodulation through secretion

Introduction

of pro-inflammatory cytokines like tumour necrosis factor (TNF)- α and interferon (IFN)- γ (18),(19),(20),(21), anti-inflammatory cytokines such as interleukin (IL)-10 (22), and chemokines (23).

Although they were once assigned mainly to the innate immune system, evidence implicating NK cells as crucial modulators and even drivers of the adaptive immune response is mounting. For instance, through release of the chemokines CC-chemokine ligand (CCL) 5, X-C motif chemokine ligand (XCL) 1 and XCL2, NK cells have been shown to recruit dendritic cells to solid tumours, which increases the potential for antigen presentation to, and regulation of, T cells and therefore anti-tumour responses (23). Furthermore, depletion and adoptive transfer experiments in mice have shown IFN- γ secreted by NK cells recruited to lymph nodes to be necessary for polarisation of early T-cell responses (21). Importantly, NK cells expressing the stimulatory receptor CD94/NKG2C have been shown to expand following human CMV (HCMV) infection and to develop a mature phenotype with adaptive, memory-like functionality (24),(25),(26),(27),(28).

1.2 NK-Cell Development

In order to be able to appreciate the different subpopulations of NK cells, a brief description of NK-cell development, including NK-cell receptor acquisition, is necessary.

NK cells can be subdivided into two basic populations based on the intensity of CD56 expression: CD56-high-expressing CD56^{bright} NK cells (residing mainly in lymphoid tissue) and CD56-low-expressing CD56^{dim} NK cells (found mainly in peripheral blood) (6),(29). NK cells are thought to arise, in several stages, from CD34⁺ haematopoietic stem cells, the more mature CD56^{dim} NK cells arising from the less mature CD56^{bright} NK cells (**Fig. 1**), as reviewed by, among others, Lorenzo Moretta in 2010 and Yu *et al.* in 2013 (30),(31). Several factors influence this process. For example, the cytokine IL-15, which is used in this study to stimulate NK cells, has been shown to be critical in the differentiation of NK cells from CD34⁺ bipotential T/NK-cell progenitor cells (32), later aiding survival of peripheral NK cells (33), as well as in the induction of their effector functions (34).

The appearance of surface expression of the heterodimer of CD94 and the lectin-like NKG2A receptor coincides with high expression of CD56 (35). Most CD56^{dim} NK cells continue to express CD94/NKG2A, though it is often lost eventually (36). Distinguishing features of CD56^{dim} NK cells include expression of the Fc receptor CD16 (Fc γ RIII), as it is expressed by only a small proportion of CD56^{bright} NK cells (37),(38), the appearance of surface expression of killer-cell immunoglobulin-like receptors (KIRs), as well as maturation of and increased abundance of cytolytic granules (35),(39). Fully mature, terminally differentiated NK cells can be identified by the marker CD57 (36),(40).

NK-cell development in general, and receptor acquisition in particular, follow a tightly regulated path. CD94/NKG2A-single-positivity is thought to be acquired first, followed by the appearance of activating receptors, and co-expression of inhibitory KIRs; KIR-single-positivity eventually occurs by subsequent loss of CD94/NKG2A (30),(36),(41),(42),(43).

Fig. 1 shows a schematic representation of NK-cell development from haematopoietic stem cells.

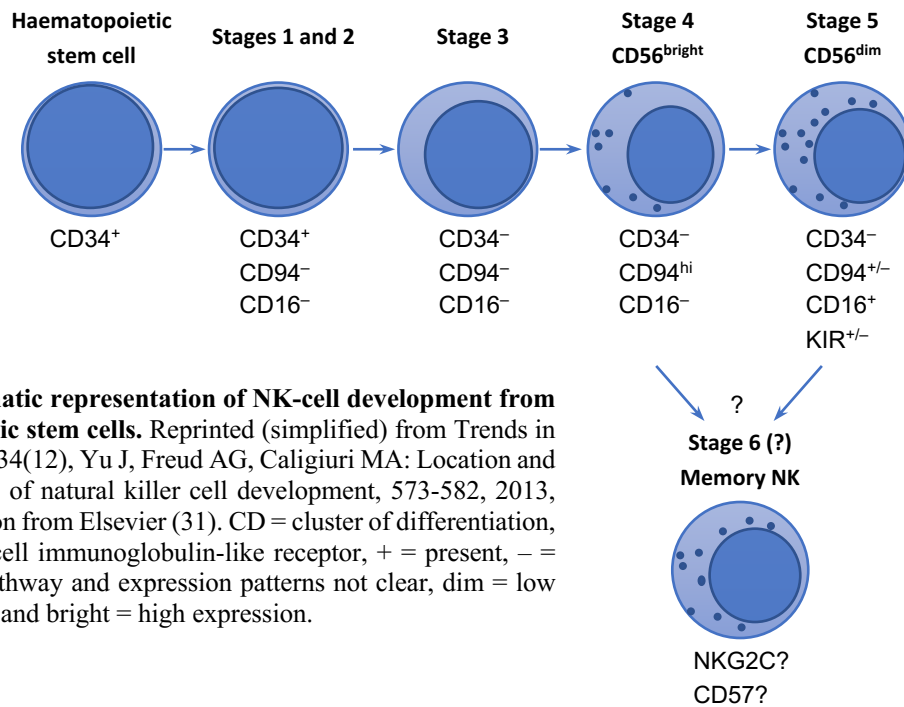


Fig. 1: Schematic representation of NK-cell development from haematopoietic stem cells. Reprinted (simplified) from Trends in Immunology. 34(12), Yu J, Freud AG, Caligiuri MA: Location and cellular stages of natural killer cell development, 573-582, 2013, with permission from Elsevier (31). CD = cluster of differentiation, KIR = killer-cell immunoglobulin-like receptor, + = present, - = absent, ? = pathway and expression patterns not clear, dim = low expression, hi and bright = high expression.

CD56^{dim} and CD56^{bright} NK cells differ in their effector functions and responses to stimulation. While CD56^{bright} NK cells have been ascribed a more prominent role in the response to and production of cytokines, CD56^{dim} NK cells have been found to be more responsive to target-cell than cytokine-induced stimulation, with a larger role in target-cell cytotoxicity (44),(45),(46). Only more recently, CD56^{dim} NK cells have been shown to also be very capable cytokine producers (47),(48).

An important example of a cytokine that acts differentially on CD56^{bright} and CD56^{dim} NK-cell function and development is IL-2. It is also used in this study. Via its heterotrimeric receptor, which shares two subunits with the IL-15 receptor (49), IL-2 has been shown to induce brisk proliferative responses in CD56^{bright} NK cells and enhanced effector functions in CD56^{dim} NK cells (34),(50). Interestingly, activation-induced cell death, a process important in negative selection of NK cells, also relies on IL-2, this time in concert with activating signals through receptors like CD16 and CD44 (51),(52),(53).

1.3 NK-Cell Receptors

Following the brief overview of NK-cell responses and NK-cell development, it is important to discuss the role of NK-cell receptors. Not only do these receptors determine to what challenges an NK cell can respond, but they are also crucial for defining an NK cell's education status, as explained in section 1.4.

1.3.1 NK-Cell Receptors and Means of NK-Cell Activation – an Overview

NK cells express a variety of germline-encoded cell-surface receptors, the downstream signals of which are integrated to fine-tune any given NK cell's response to an immunological challenge (54),(55). Unlike T-cell responses, NK-cell responses are not major histocompatibility complex (MHC)-restricted, an NK cell's activation being mainly independent of the presentation of peptide by self-MHC (56). NK cells express both activating and inhibitory receptors, which are classified into several different families.

Introduction

In the healthy state, recognition particularly of MHC class I by inhibitory NK-cell receptors, especially by inhibitory KIRs (classical MHC class I) and by CD94/NKG2A (non-classical MHC class I) (see below for more detail) leads to NK-cell inhibition. This allows NK cells to monitor and be inhibited by the presence of 'self' (ie MHC class I). When MHC class I is downregulated, like in virus-infected or tumour cells, the inhibitory signal disappears and, in the presence of activating signals, leads to NK-cell activation and often destruction of target cells: the classical missing-self response (57),(58) (**Fig. 2**).

Activating NK-cell receptors, on the other hand, recognise a wider variety of signals (**Fig. 2**). These include 'induced self'-ligands, which are brought about by cellular stress, like the distant MHC class I relatives MHC class I polypeptide-related sequence (MIC) A and MICB, which are bound by the prominent NK-cell activating receptor NKG2D (59). Activating signals also include non-self ligands expressed by infected cells, an example being influenzaviral haemagglutinins, which are recognised by the activating natural cytotoxicity receptors (NCRs) NKp46 and NKp44 (60),(61). Somewhat less prominent is recognition of conserved microbial products like viral RNA and DNA, which provide non-self ligands for Toll-like receptors, which are also expressed by NK cells to some extent (62),(63). Importantly, through expression of the Fc receptor CD16, NK cells are able to recognise antibodies, which can lead to antibody-dependent cell-mediated cytotoxicity (ADCC) against antibody-coated target cells (37).

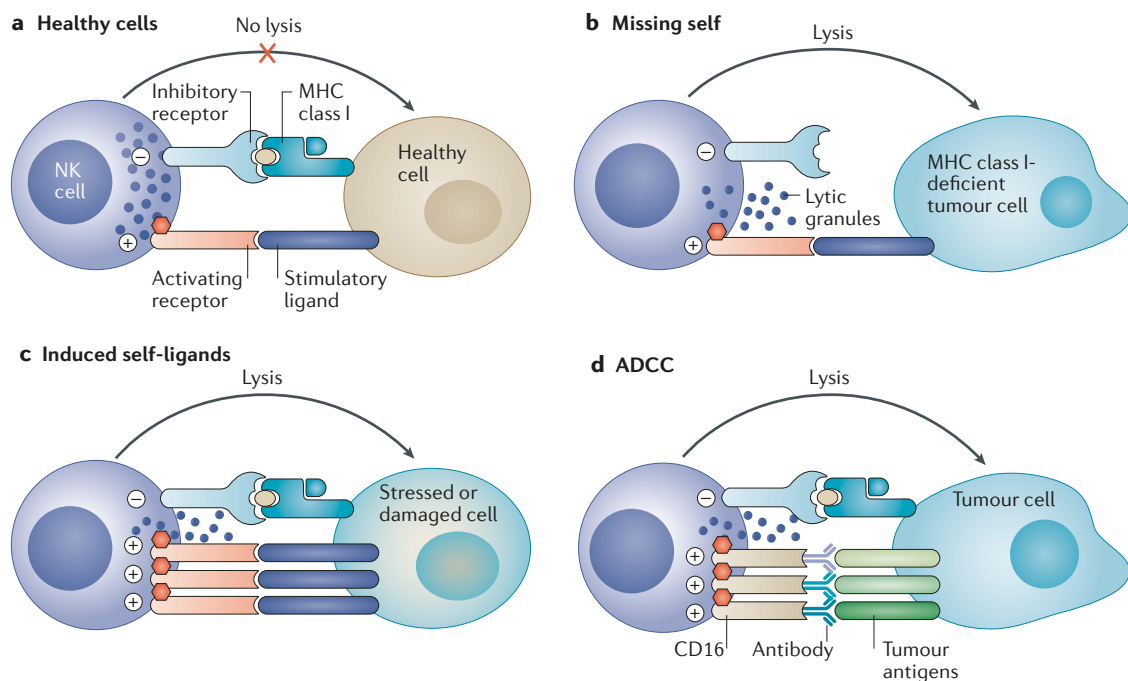


Fig. 2: Overview of the main ways of NK-cell activation. Reprinted with permission from Springer Nature Customer Service Centre GmbH: Springer Nature, Nature Reviews Cancer: NK cells and cancer: you can teach innate cells new tricks, Morvan MG, Lanier LL, 2015 (64) <https://www.nature.com/articles/nrc.2015.5>, accessed 07/09/2019. ADCC = antibody-dependent cell-mediated cytotoxicity, MHC = major histocompatibility complex.

It is important to now describe some of the NK-cell receptor families, particularly KIRs, in more detail.

1.3.2 KIRs

The KIR family of receptors, which, as mentioned above, recognise classical MHC class I antigens (or human leukocyte antigens (HLA)) (65),(66), are some of the most important human NK-cell receptors and are crucial for NK-cell education (46).

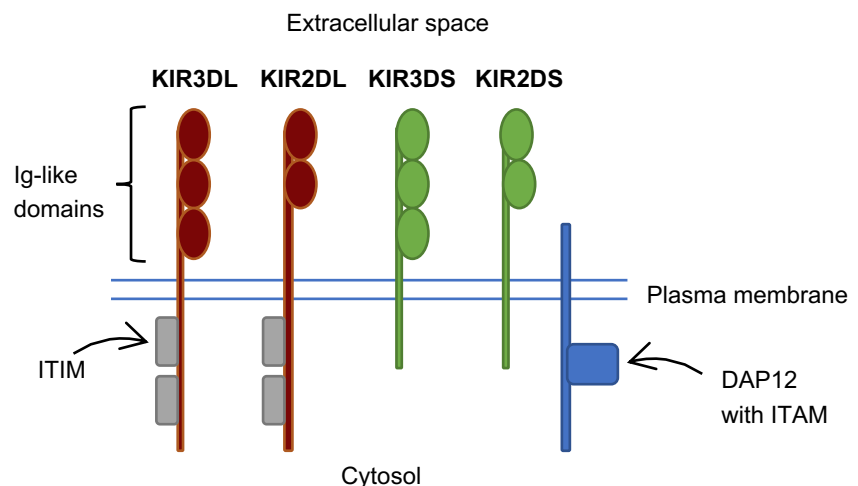
1.3.2.1 Nomenclature and Structure

The KIR family comprises both inhibitory and activating transmembrane receptors that are expressed by NK cells and a subset of T cells (67),(68),(69). Most NK cells have been found to express between zero and two different self-HLA class I-specific KIRs (70). HLA proteins are critical in immune responses due to their presentation of processed peptide antigen to T cells and their function as NK-cell ligands (71). There are two main classes of HLA, HLA class I and HLA class II, with several classical (HLA-A, B and C (class I) and HLA-DR, DP and DQ (class II)) and non-classical subclasses (72),(71). Unlike HLA class II molecules, which are a complex of class II α and β chains, the α chains of classical HLA class I molecules complex with the protein β 2-microglobulin (72).

14 or, if one considers *KIR2DL5A* and *KIR2DL5B* to be distinct, 15 *KIR* genes and two pseudogenes (the latter denoted by the letter 'P'), have been identified in 15 distinct *KIR* loci within the leukocyte receptor complex on chromosome 19q13.4 (73).

KIRs are classified according to the length of their cytosolic tail, a short (S) tail signifying an activating receptor and a long (L) tail signifying an inhibitory one (67),(68). *KIR2DL4* is an exception, the type of response (activating or inhibitory) being context-dependent (74). Furthermore, each KIR possesses either two or three immunoglobulin (Ig)-like domains, conferring the terminology of KIR2D or KIR3D respectively (67),(68). Like most inhibitory NK-cell receptors, the cytoplasmic portions of inhibitory KIRs contain one or two immunoreceptor tyrosine-based inhibitory motifs (ITIMs) (74),(75). These recruit protein tyrosine phosphatases that then transduce the inhibitory response via recruitment of the phosphatases Src homology region 2 domain-containing phosphatase (SHP)-1 and SHP-2 (74),(75). In contrast, the activating response by KIRs depends on their association with the transmembrane adaptor protein DAP12, which contains an immunoreceptor tyrosine-based activation motif (ITAM), and which is necessary for signal transduction (76). **Fig. 3** shows a schematic representation of the structure of KIRs.

Fig. 3:
Schematic representation of the structure of KIRs.
Ig-like = immunoglobulin-like, ITAM = immunoreceptor tyrosine-based activation motif, ITIM = immunoreceptor tyrosine-based inhibitory motif. Author's illustration.



1.3.2.2 KIR Haplotypes

KIR genes are in linkage disequilibrium with one another, leading to their organisation into haplotypes (77). The KIRs display an extraordinary degree of diversity, owing mainly to their polygenicity, variable gene content, extensive polymorphism, and stochastic combinatorial expression (74),(77),(78),(79). Their ligands' genes, the *HLA* genes, are also organised into haplotypes, and are the most polymorphic human genes identified so far (72). Thus, through the extraordinary degree of KIR diversity in

Introduction

conjunction with the vastly polymorphic nature of their HLA class I ligands, as well as the independent segregation of *KIR* and *HLA* genes (which reside on different chromosomes), highly diverse, almost person-unique, receptor-ligand repertoires are achieved (74),(77),(80).

Two groups of *KIR* haplotypes have been identified within the human population based on gene content: group *A* and group *B* haplotypes (77). Group *A* haplotypes have been associated with some protection from viral infections such as hepatitis C virus (81), while group *B* haplotypes have been associated with a lower risk of disorders of pregnancy like preeclampsia (14), indicating that an evolutionary equilibrium exists between the two haplotype groups (82).

Both haplotype groups contain the framework genes *KIR3DL3*, *KIR3DP1*, *KIR2DL4* and *KIR3DL2* (83), with two variable regions in between. Encoding seven genes and two pseudogenes, the more common group *A* haplotypes have a lower and less variable gene content, as well as less copy number variation, than group *B* haplotypes, but display more allele combinations (77),(78),(84). Group *A* haplotypes encode mainly inhibitory KIRs, the most important being *KIR2DL3*, *KIR2DL1* and *KIR3DL1*, and only one activating receptor, *KIR2DS4*, in addition to containing the framework gene *KIR2DL4* (77). *KIR2DS4* is frequently non-functional, owing to a 22-nucleotide deletion (85). Group *B* haplotypes can encompass those genes present in group *A* haplotypes, but contain additional activating receptor genes (77) and group *B* haplotype-unique inhibitory *KIR* genes: *KIR2DL5*, *KIR2DS1*, *KIR2DS2*, *KIR2DS3*, *KIR2DS5*, as well as *KIR2DL2* and *KIR3DS1*, alleles of *KIR3DL3* and *KIR3DL1* respectively (78). **Fig. 4** gives a schematic representation of a group *A* and a representative group *B* *KIR* haplotype. **Table 1** shows some common *KIR* genotypes and the haplotypes to which they correspond.

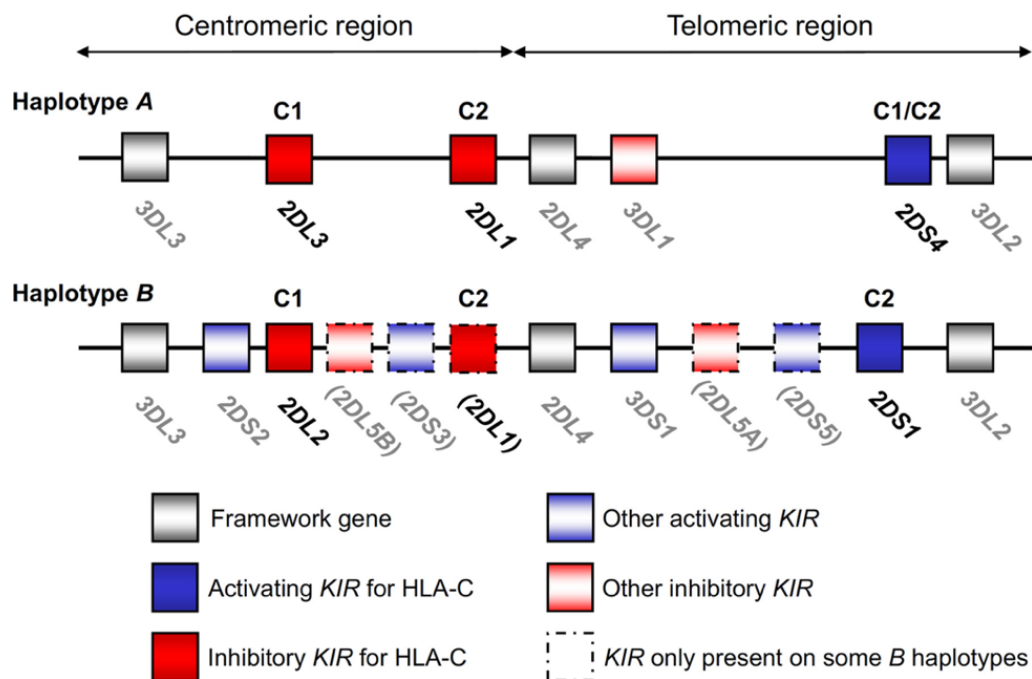


Fig. 4: Schematic representation of a group *A* and a representative group *B* *KIR* haplotype. Pseudogenes are not included. Reprinted from J Leukoc Biol. 90(4), Chazara O, Xiong S, Moffett A: Maternal KIR and fetal HLA-C: a fine balance, 703-16, 2011 (86), with permission.

Table 1: Common *KIR* genotypes and the haplotypes to which they correspond. Table adapted by permission from Springer Nature Customer Service Centre GmbH: Springer Nature, Immunogenetics: Definition of gene content for nine common group B haplotypes of the Caucasoid population: *KIR* haplotypes contain between seven and eleven *KIR* genes, Uhrberg M, Parham P, Wernet P, 2002 (87) (<https://link.springer.com/article/10.1007%2Fs00251-002-0463-7>, accessed 08/08/2019).

Haplotype	Genotype	2DL1	2DL2	2DL3	2DL4	2DL5	3DL1	3DL2	3DL3	2DS1	2DS2	2DS3	2DS4	2DS5	3DS1
AA	1														
Bx	2														
Bx	3														
Bx	4														
Bx	5														
Bx	6														
Bx	7														
Bx	8														
Bx	9														
Bx	10														
Bx	11														
Bx	12														
Bx	13														
Bx	14														
Bx	15														
Bx	16														
Bx	17														
Bx	18														
Bx	19														
Bx	20														
Bx	21														
Bx	22														
Bx	23														
Bx	24														
Bx	25														
Bx	26														
Bx	27														
Bx	28														
Bx	29														
Bx	30														
Bx	31														
Bx	32														
Bx	33														
Bx	34														
Bx	35														
Bx	36														
Bx	37														
Bx	38														
Bx	39														
Bx	40														

A/A = homozygous for group *A* haplotypes. *Bx* = either hetero- or homozygous for group *B* haplotypes. Grey = *KIR* gene present, white = *KIR* gene absent.

1.3.2.3 *KIR* Ligands

Ligands have been identified for many but not all *KIR*s (**Table 2**), the most important being the classical HLA class I antigens mentioned above. Epitopes on all three classical HLA class I molecules HLA-A, B and C can be recognised by *KIR*s (71), however, the dominant HLA class I molecule in shaping NK-cell responses is HLA-C (88),(89). HLA-C alleles are divided into two main groups, the HLA-C1 and HLA-C2 allotypes, originally distinguished based on differential recognition of target cells by NK cells now known to express *KIR*s with different HLA-C specificities (77),(88),(90),(91). The two allotypes result from amino acid dimorphisms at positions 77 and 80 of the $\alpha 1$ domain of HLA-C, HLA-C1 having

Introduction

a serine residue at position 77 and an asparagine at position 80, and HLA-C2 having an asparagine at position 77 and a lysine at position 80 (88),(90),(91).

Table 2: The KIRs and their known ligands.

KIR	Ligand	References
KIR2DL1	HLA-C2	(92),(93),(94),(95)
KIR2DL2	HLA-C1, HLA-C2 (weaker though functionally relevant avidity)	(70),(92),(93),(94),(95), (96)
KIR2DL3	HLA-C1, (HLA-C2 Cw*0501, Cw*0202 and Cw*0401 (weaker interactions; functional relevance not clear))	(70),(92),(93),(94),(95), (96)
KIR2DL4	HLA-G?	(97),(98),(99)
KIR2DL5A		
KIR2DL5B		
KIR2DS1	HLA-C2	(100),(101)
KIR2DS2	HLA-C1 (peptide-dependent), HLA-A11	(102),(103)
KIR2DS3		
KIR2DS4	HLA-C1, HLA-C2, some HLA-A11 epitopes	(104)
KIR2DS5	Some HLA-C2 epitopes	(105)
KIR3DL1	HLA-Bw4 on HLA-A and HLA-B	(106)
KIR3DL2	HLA-A3/-11	(107),(108)
KIR3DL3		
KIR3DS1	Open conformers of HLA-F (non- β 2-microglobulin- or peptide-bound)	(109)

? = ligand not definitively confirmed, blank = no ligand identified to date.

1.3.3 The CD94/NKG2 Family of Receptors

The lectin-like NKG2 transmembrane receptors expressed by NK cells and a subset of T cells represent, arguably, the most important family of both inhibitory and activating NK-cell receptors besides KIRs (110). Hence, a description of this family is warranted, particularly since CD94/NKG2A has also been shown to be involved in NK-cell education (111),(112).

Unlike the genes encoding KIRs, the genes encoding the NKG2 family lie within the natural killer complex on chromosome 12p13.1 (113).

The inhibitory NKG2A and the stimulatory NKG2C, complexed with CD94, bind to the non-classical HLA class I HLA-E expressed by target cells in complex with peptides derived from the signal sequence of other class I MHC molecules, making NKG2 receptors another crucial mechanism for monitoring of HLA class I expression by NK cells (114),(115). After inhibitory KIRs, NKG2A/CD94 actually represents the main inhibitory receptor important for shaping NK-cell receptor repertoires (82),(115). NKG2D, a prominent stimulatory receptor, does not associate with CD94, instead forming a homodimer, and binds the stress-induced ligands MICA and MICB, as well as UL16-binding protein (ULBP)1, 2, 3 and 4 (59),(116),(117),(118).

As alluded to in section 1.1, NK cells expressing CD94/NKG2C have been shown to expand following HCMV infection and to develop a mature, self-specific KIR⁺NKG2A⁻NKG2C⁺CD57⁺ phenotype with adaptive, memory-like functionality (24),(25),(26),(27),(28),(119). These cells are highly effective killers of HCMV-infected cells through ADCC, but are less responsive to cytokines (120),(121). Their memory-like functionality has been demonstrated after their transplantation from HCMV-seropositive

Introduction

donors to HCMV-seropositive recipients, where they exhibited more expansion and cytokine production than after transplantation to HCMV-seronegative recipients (27).

Structurally, the cytoplasmic domain of NKG2A harbours two ITIMs, similar to inhibitory KIRs (110). CD94/NKG2C, on the other hand, like activating KIRs, associates with the ITAM-containing DAP12 (110),(122). NKG2D associates with the adaptor protein DAP10 instead, which, instead of an ITAM, harbours a YINM motif, which recruits different kinases for transduction of an activating response than ITAMs do (116),(123).

The roles of the less well-studied family members, NKG2B, a stemless splice variant of NKG2A, as well as NKG2E, NKG2F and NKG2H are less clear (115),(124),(125),(126),(127),(128).

1.3.4 Natural Cytotoxicity Receptors and Immunoglobulin-Like Transcripts

A further important class of NK-cell receptors are the NCRs. They comprise activating receptors expressed mainly by NK cells that trigger NK cell-mediated cytotoxicity upon ligation, the key ones being NKp46, NKp44 and NKp30 (129). NKp46, one of the main NK-cell activating receptors (130), and NKp44 have been shown to recognise, for example, influenzaviral haemagglutinins (60),(61), as mentioned above, while NKp30 binds, among others, the tumour cell-surface antigen B7-H6 (131).

Another class of NK-cell receptors that recognise HLA are the immunoglobulin-like transcripts (ILTs). An example thereof is the inhibitory receptor ILT2 (LILRB1), which recognises the non-classical HLA class I HLA-G, predominantly expressed by extravillous trophoblast in the placenta, and which may therefore be one of the factors influencing human placentation (132),(133).

1.4 NK-Cell Education

Having given an overview of NK cells, including their responses, development and receptors, NK-cell education can now finally be introduced. An outline of classical education is given first, followed by a brief mention of non-classical NK-cell education, then an outline of what is known regarding phenotypic differences between educated and non-educated NK cells, then a description of the different models of the process that have been proposed, and finally the clinical relevance of NK-cell education.

1.4.1 (Classical) NK-Cell Education – an Overview

NK-cell education is a process by which NK cells acquire enhanced cytotoxic and cytokine-producing competence in a quantitative manner dependent on engagement of self-MHC class I-specific inhibitory receptors, KIRs in humans (Ly49 in mice) and CD94/NKG2A, by self-MHC class I (46),(134),(111),(112) (see **Table 2** for a list of KIRs and their ligands). NK cells that lack self-MHC class I-specific inhibitory receptors, even when fully mature, remain ‘uneducated’ or ‘unlicensed’ and become hyporesponsive (134),(46). In terms of terminology, ‘classical education’ or ‘licensing’ refers to education via a self-specific inhibitory KIR and classical self-MHC class I (135), and is addressed in the most detail here.

Studies from as early as the 1990s have described a lack of cytotoxic activity against HLA class I-null K562 target cells by NK cells from donors with MHC class I deficiency (136),(137), which was later attributed to these NK cells being unlicensed. Licensed NK cells, on the other hand, have enhanced functional potential, particularly in the missing-self response. For instance, Yawata *et al.* demonstrated in 2008 that NK cells expressing a host-MHC-specific inhibitory KIR showed increased degranulation and IFN- γ production in response to MHC class I-deficient 721.221 target cells, when compared to NK cells that expressed only non-host-specific inhibitory KIRs (112).

Educated NK cells have also been shown to display a survival advantage compared with uneducated NK cells. Felices *et al.* demonstrated in 2014 that serum starvation led to preferential death of uneducated rather than educated NK cells and that withdrawal of IL-15 led to upregulation of proapoptotic molecules like Bim and Fas within uneducated but not educated NK cells (53).

In addition to enhancing functional responsiveness of licensed NK cells, education ensures NK-cell self-tolerance. NK cells that do not express any self-specific inhibitory receptors are prevented from attacking self-cells by becoming hyporesponsive, while those that do express self-specific inhibitory receptors are inhibited from attacking self-cells through engagement of these cells' self-MHC class I.

Fig. 5 shows a schematic representation of classical NK-cell education.

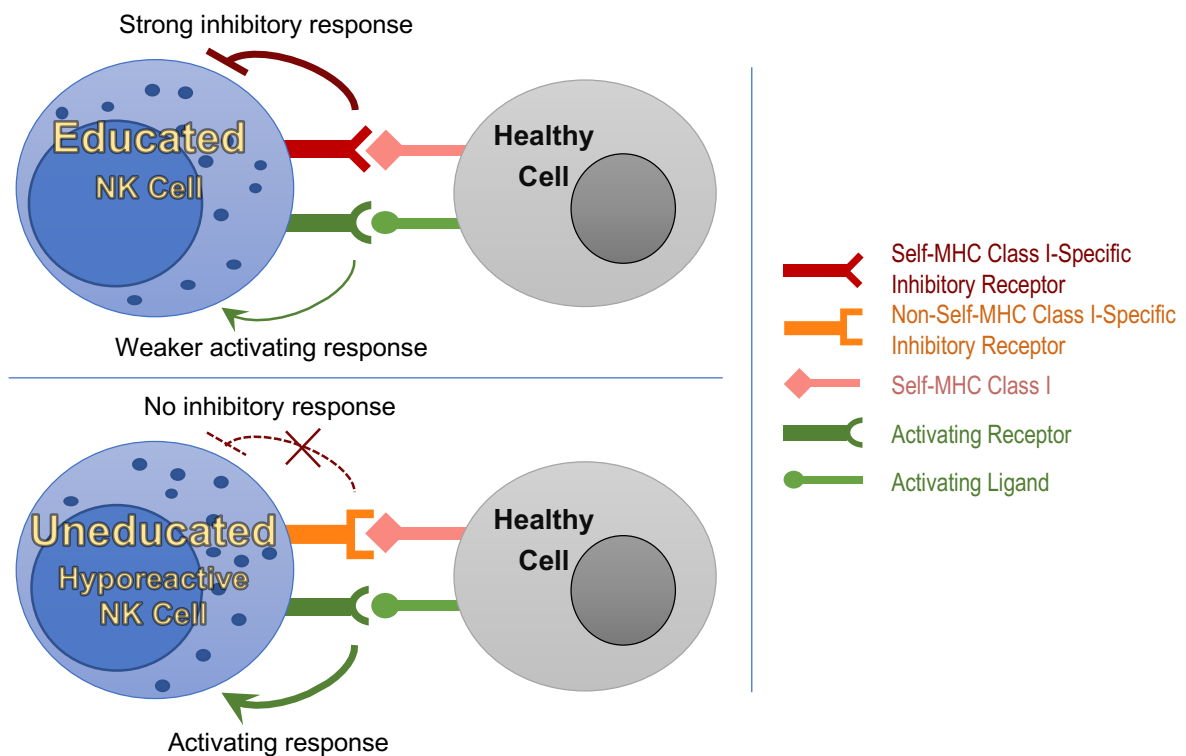


Fig. 5: Schematic representation of classical NK-cell education. NK-cell education relies on engagement of self-specific inhibitory receptors, mainly KIRs, by their cognate ligands. Author's illustration.

Despite the hyporesponsiveness of unlicensed NK cells particularly in the missing-self setting, unlicensed NK cells are not functionally incompetent. For instance, they have been shown to display enhanced effector functions in response to cytokines and in inflammatory microenvironments, including some infections like *Listeria* and MCMV in mice (134),(138),(139), which suggests that NK-cell education is a dynamic process and that the strict distinction between licensed and unlicensed cells may only apply in steady-state conditions. A study by Elliott *et al.* in 2010, in which unlicensed murine NK

Introduction

cells from an MHC class I-deficient environment became licensed upon transfer to an MHC class I-sufficient host, further supports this notion (140).

The process of education is postulated to begin during NK-cell development, enhanced proliferation having been shown in bone marrow-derived NK cells that express a self-MHC class I-specific inhibitory receptor compared with those that do not (134).

1.4.2 NK-Cell Education by Non-Classical MHC

Licensing, or classical education, depends on the recognition of classical HLA class I by KIRs, as indicated above. However, evidence is mounting that inhibitory receptors for non-classical MHC molecules also contribute. Crucially, CD94/NKG2A, via recognition of HLA-E, has been implicated in human NK-cell education, and education via CD94/NKG2A has been shown to be able to compensate whenever there is lack of KIR-mediated licensing (111),(112),(141),(142).

1.4.3 Comparative Analyses of Licensed vs Unlicensed NK Cells

So far, comparative analyses of licensed *versus* (vs) unlicensed NK cells, particularly in humans, have yielded limited results, including regarding phenotypic differences. One of the few examples of phenotypic differences between licensed and unlicensed NK cells is the higher expression of the adhesion molecule and activating receptor DNAX Accessory Molecule (DNAM)-1 by educated compared with uneducated NK cells (143). DNAM-1, together with LFA-1, a protein important in granule polarisation, has been postulated to be important for the augmented degranulation responses observed in educated compared with uneducated NK cells (143).

Notably, grB, one of the main cytotoxic mediators expressed by NK cells, has been highlighted in a recent study comparing licensed and unlicensed NK cells (144). In this study, Goodridge *et al.* demonstrate a positive correlation between NK-cell licensing and grB expression, showing accumulation of grB in educated NK cells in a transcription-independent manner. They also implicate restructuring of the endolysosomal compartment, which may also provide an explanation for the heightened degranulative and cytotoxic potential of licensed NK cells.

DNAM-1 and grB represent some of the few examples of molecules found to be differentially expressed between educated and uneducated NK cells, but the precise intracellular mechanism of NK-cell licensing remains elusive. Nonetheless, several models have been proposed to attempt an explanation: the 'arming/stimulatory licensing', 'disarming/inhibitory licensing', 'rheostat/tuning' and 'confining', as well as the '*cis*-interaction' and '*trans*-interaction' models.

1.4.4 NK-Cell Education – Different Models

1.4.4.1 *The Arming/Stimulatory Licensing and Disarming/Inhibitory Licensing Models*

The arming model suggests that from the pool of unresponsive NK cells only those that express a self-specific inhibitory receptor become responsive/armed, while those that do not express one remain hyporesponsive (145). In this model, downstream signalling from an inhibitory receptor is, by itself,

Introduction

sufficient for an NK cell to be licensed and for functional potential to be induced, as evidenced by abolition of licensing when such a receptor's ITIM is mutated (134). The disarming model, on the other hand, suggests that cells that were potentially responsive lose function; tonic, unopposed activation via stimulatory NK receptors leading to the hyporesponsiveness observed in unlicensed NK cells (145). Evidence supporting the disarming model comes mainly from murine studies that have observed NK-cell tolerance patterns after transplantation of mixtures of cells expressing cell-surface MHC and cells not expressing cell-surface MHC into irradiated mice (146),(147).

1.4.4.2 The Rheostat/Tuning Model

The rheostat model states that NK-cell education is not a 'yes-or-no' phenomenon, but that it occurs in a quantitative manner, depending on the level of inhibitory input a given NK cell receives, both based on the strength of inhibitory receptor:ligand binding and the number of self-specific inhibitory receptors the NK cell expresses (141),(148),(149). According to this model, which was developed from mouse studies, more inhibitory input results in a higher level of functionality, exemplified by increased degranulation and IFN- γ production in experimental settings (148). The rheostat model provides a possible means of reconciling the arming and disarming models, suggesting that NK-cell responsiveness is 'tuned up' or 'tuned down', as put by Brodin *et al.* in 2009, depending on the net inhibitory input received during development and also during states of immune system activation (148).

1.4.4.3 The Confining Model

Not a separate model *per se*, the confining model focuses on the localisation of activating and inhibitory receptors with regard to the cell-surface membrane and the cytoskeleton, suggesting a spatial aspect to NK-cell education (135). Educated and hyporesponsive NK cells appear to display different receptor dynamics. In hyporesponsive NK cells, activating receptors have been shown to be confined to the NK cell's actin meshwork and to demonstrate slower diffusion rates, while inhibitory receptors are less confined (150),(151). In educated NK cells, on the other hand, activating receptors, located within cell-surface membrane lipid rafts that are advantageous for signalling, have been shown to display faster diffusion rates, while inhibitory receptors are more restricted, implying an enhanced functional responsiveness (150),(151).

1.4.4.4 The Cis-Interaction and Trans-Interaction Models

Also not a separate model *per se*, the *cis*-interaction/*trans*-interaction models attempt to address the mechanistic issue of whether educating receptor-ligand interactions occur between an inhibitory NK-cell receptor on one NK cell and its ligand on another cell (*trans*), whether they occur on the same cell (*cis*) or whether both types of interaction are important (152). Chalifour *et al.* show that NK cells in transgenic mice expressing a variant of the MHC class I-specific inhibitory receptor Ly49A that can only be inhibited by MHC class I in *trans* but that cannot engage MHC class I in *cis* are not educated (153). Conversely, Elliott *et al.* demonstrate that NK cells from MHC class I-deficient mice become licensed when adoptively transferred into MHC class I-sufficient recipients, indicating that a *trans* interaction is sufficient for education (140). Though seemingly inconsistent, these disparate results could be interpreted as indicating that both mechanisms play a role in NK-cell education, possibly in a context-dependent manner. In fact, Boudreau *et al.* have shown in adoptive transfer experiments of human NK

Introduction

cells in transgenic mice that both mechanisms appear to play a role in the education of KIR⁺ NK cells (154). They postulate that *cis*-interactions may have more of a role in maintaining education while *trans*-interactions may be more important in increasing NK-cell reactivity (154).

1.4.5 NK-Cell Education – Clinical Relevance

The importance of NK-cell education for NK-cell functionality is evident. However, the real relevance of understanding this process better lies in its potential utilisation for translational medicine. Several studies, including in mice, have hinted at the differential importance of licensed and unlicensed NK cells in various disease settings, but more studies are required to access the full potential of the process, particularly in the move from murine models to human diseases.

For example, Tay *et al.* described in 1995 that NK cells from mice with defective MHC class I expression, so hyporesponsive NK cells in the education model, were still able to mount effective antiviral responses, possibly through cytokine release (155), and Fernandez *et al.* showed in 2005 that murine NK cells not expressing self-MHC class I-specific inhibitory receptors became hyporesponsive to stimulation with MHC-reduced target cells but not to infection with *Listeria* (138). Educated human NK cells, on the other hand, have been shown to demonstrate greater activation than unlicensed cells in response to anti-HIV-1 antibodies *in vitro* (156).

Educated and uneducated NK cells may thus play differential roles in the control of viral infections, suggesting that exploitation of these differences may be beneficial in the development of antiviral therapies.

NK-cell education also plays a role in anti-tumour responses. For instance, in the classical missing-self response, licensed NK cells recognise and kill tumour cells that have downregulated self-MHC class I (57). However, artificial augmentation of unlicensed NK cells in particular has proven beneficial in an anti-tumour response where the classical missing-self response was ineffective: Tarek *et al.* showed in 2012 that neuroblastoma-cell lines that had not downregulated HLA class I were preferentially killed by unlicensed NK cells after pre-treatment with an antibody that induced ADCC, the so-called ‘missing KIR ligand’ benefit (157).

Studies like those discussed above help to highlight the critical importance of gaining a broader understanding of the mechanisms that underlie NK-cell licensing, as this can inform approaches of how best to utilise NK cells clinically and therapeutically, particularly in anti-tumour and antiviral therapies. Finding and studying phenotypic differences between educated and uneducated cells, like the study of grH here, provide important steps towards this goal.

Having described NK-cell education, the discussion now turns to granzymes and grH in particular, since grH, in the context of NK-cell education, is the focus of this study.

1.5 Granzymes

1.5.1 Overview and Functions

Granzymes, *granule-associated enzymes* (158), are serine proteases that are found mainly in the cytolytic granules of cytotoxic lymphocytes and that are highly conserved between different species (159),(160). They are critical for NK-cell function, being some of their main cytotoxic mediators (161),(162). To a large extent, granzymes rely on the pore-forming protein perforin for delivery into target cells (163),(164),(165) (**Fig. 6**). GrA and grB are stored as zymogens (pro-proteins) that need to be cleaved prior to activation, in order to prevent death of the cells carrying them (166),(167). Perforin activity, on the other hand, appears to be dependent on calcium and a neutral pH, perforin being non-toxic to its host cell due to the acidic pH within secretory lysosomes, as well as due to additional inhibition by C-terminal glycosylation (168),(169),(170).

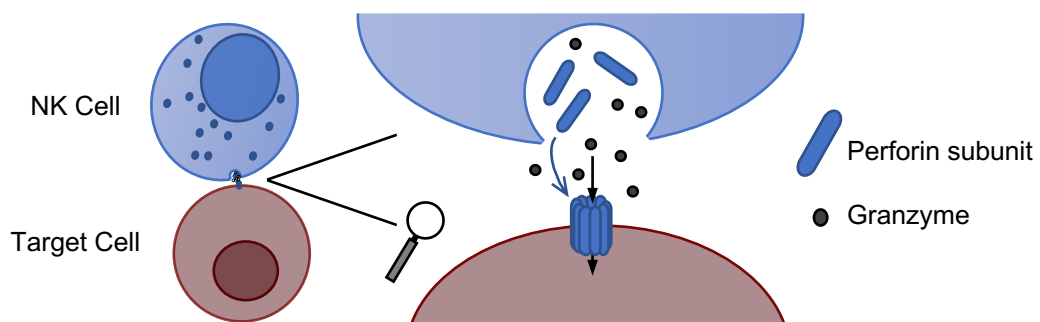


Fig. 6: Schematic representation of granzyme delivery into target cells. After target-cell recognition by the NK cell and trafficking of its cytotoxic granules to the immunological synapse, the granules fuse with the presynaptic membrane and release their contents. Then, perforin forms a pore in the postsynaptic membrane, allowing, for instance, granzymes to diffuse into the target cell and induce apoptosis. Adapted (simplified) by permission from Springer Nature Customer Service Centre GmbH: *Nature Reviews Immunology: Perforin and granzymes: function, dysfunction and human pathology*, Voskoboinik I, Whisstock JC, Trapani JA, 2015 (from Fig. 1d) (162) <https://www.nature.com/articles/nri3839>, accessed 09/09/2019.

Of the five human granzymes A, B, H, K and M, grB and grA are the best studied. As reviewed by, among others, Susanto *et al.* (161) and Voskoboinik *et al.* (162), the canonical role of granzymes in target-cell cytotoxicity has actually only been demonstrated uncontroversially for grB and grA. GrB has been shown to induce rapid target-cell apoptosis, predominantly via cleavage of BH3-interacting domain death agonist (Bid), which in turn leads to mitochondrial disruption; rather than via direct activation of caspases; and the process is inhibitable by B-cell lymphoma 2 (BCL-2) (171). GrA, on the other hand, has been shown to induce athetosis, a non-apoptotic form of cell death (161),(162). As an ‘asp-ase’, grB has been shown to preferentially cleave after aspartic acid or glutamic acid residues (172), while grA, a tryptase, preferentially cleaves after arginine or lysine residues (173),(174).

Although grH (see section 1.5.4), grK and grM have also been described to have cytotoxic functions, the results have been more contentious (161),(162).

In addition to their cytotoxic functions, different roles of granzymes are emerging, including immunomodulatory, extracellular matrix remodelling and direct antiviral ones. For example, grA has been shown to induce proinflammatory cytokine release from target cells (175), grB and grA have been implicated in causing detachment of target cells from surrounding structures (176),(177), and, among other direct antiviral actions, grH has been shown to inhibit hepatitis B virus replication by directly cleaving the hepatitis B virus protein HBx (178).

1.5.2 Granzyme Expression by Lymphocytes

Granzymes are predominantly found in cytotoxic lymphocytes. Among NK cells, resting mature NK cells have been shown to constitutively express grA, grB, grH and grM – though, perhaps surprisingly, grB expression has occasionally been described as being very low to undetectable – while grK is restricted to the CD56^{bright} NK-cell subset (179),(180),(181),(182). Circulating CD8⁺ T cells, on the other hand, express grB and grA to a lower extent than NK cells do, levels in their CD4⁺ counterparts being even lower (179). GrH, too, has been demonstrated to be expressed by resting CD8⁺ and CD4⁺ T cells, also to a lower extent than by NK cells, but, in contrast to grB, its expression by these cells has been shown to be poorly inducible by IL-2 or phytohaemagglutinin (182),(183). Expression of grK by T cells has also been demonstrated, the extent varying between the precise type of T cell, while grM expression by T cells has been shown to be inducible only after prolonged culture (180),(181),(184).

1.5.3 Genomic Organisation of Granzymes and Comparison between GrB and GrH

The five human granzymes have considerable structural and functional overlap with the ten murine granzymes A, B, C, D, E, F, G, M, K and N, and both families are grouped into three clusters on separate chromosomes (160),(161),(185),(186) (*GZM* = *granzyme* gene):

- Granzyme A cluster
 - o Humans, chromosome 5: *GZMA* and *K*
 - o Mice, chromosome 13: *GZMA* and *K*
- Granzyme B cluster
 - o Humans, chromosome 14: *GZMB* and *H*
 - o Mice, chromosome 14: *GZMB*, *C*, *D*, *E*, *F*, *G* and *N*
- Granzyme M cluster
 - o Humans, chromosome 19: *GZMM*
 - o Mice, chromosome 10: *GZMM*

This inter-species comparison is important as all human granzymes, with the notable exception of grH, have murine orthologues (187). GrH shares 71% amino acid identity with human grB and 55% with human cathepsin G, another serine protease encoded by a gene that resides on chromosome 14 (187). The *GZMH* gene is postulated to have arisen from interlocus recombination between the ancestral *GZMB* and *H* genes and to have diverged from *CTSG* (the cathepsin G gene) ~21 million years ago, before mammalian radiation, while the rodent lineage diverged from the primate lineage before granzymes C-G had evolved (187). On the one hand, this indicates that human grH is unlikely to have evolved from rodent granzymes C-G. On the other hand, however, this also indicates that grH, having evolved relatively recently, must have an important role; one that is unlikely to overlap entirely with that of grB and one that is worth studying. **Fig. 7** shows an alignment of the open reading frames (ORFs) of *GZMH* and *GZMB* transcript variants 1 (other transcript variants arise as a result of alternative splicing) to give an indication of the sequence similarity between the two genes (188).

1.6 Aims of this Thesis

Before expounding upon the aims of this thesis, it is important to provide the rationale behind examining grH in the context of NK-cell education, as well as its expression patterns and its functions. Any steps towards creating a more complete understanding of NK-cell licensing are important, given the significance of this process for NK-cell biology and, ultimately, for the clinical utilisation of NK cells, thus making NK-cell education a valuable and valid subject to study. GrH was chosen as the focus of this investigation due to its high degree of sequence and structural identity with grB, which has already been linked with NK-cell education. In light of the crucial role of granzymes in NK-cell function, this suggested link between NK-cell licensing and grB expression is a powerful one and an investigation into whether other granzymes play a role in this critical process is needed. In light of the aforementioned high degree of sequence and structural identity between grB and grH, grH is a likely candidate to also be implicated in NK-cell licensing. Given the limited knowledge available regarding grH and its function, as well as the potential for further study of NK-cell education, an examination of the possible role of grH in NK-cell licensing was the logical and critical next step.

Preliminary experiments performed by Prof. Dr M. Uhrberg's group, Institute of Transplantation Diagnostics and Cell Therapeutics (ITZ), University Hospital Düsseldorf, Germany, in cooperation with Prof. Dr L. Walter's group, Primate Genetics Laboratory, German Primate Center, Göttingen, Germany, showed that, indeed, mRNA levels of *GZMH*, but not of other granzymes, including *GZMB*, were higher in licensed than unlicensed NK cells. The main aim of the present study was to confirm and then to robustly establish this putative link between NK-cell education and grH expression at the protein level using different inhibitory receptors to determine education status. GrB was aimed to be examined for comparison, and reasons for any potential discrepancies with the literature were aimed to be explored experimentally. An effective antibody to stain for grH first needed to be found to be able to establish an optimised staining protocol for flow cytometry. In view of the limited evidence regarding grH expression patterns in general, these were aimed to be examined among different populations of lymphocytes, prior to establishing the link between education and grH protein expression. Furthermore, given the more mature status of KIR-expressing NK cells (which include licensed NK cells) compared with receptor-negative NK cells, this study also set out to examine grH expression by NK cells of different maturities and stages of development. These phenotypic analyses were aimed to be supplemented by examination of potential correlations between expression of grH and other proteins potentially correlated with NK-cell licensing.

Since most of the published studies have used recombinant grH for examination of the function of grH, the present study aimed to use more physiological whole-cell approaches for examination of its function, particularly using primary NK cells. These were to be stimulated via target cells and soluble mediators, or their survival examined when starving them of important cell-culture components such as serum.

Moreover, due to the need for cell fixation and permeabilisation prior to staining for the intracellular grH protein, it is not currently possible to perform functional studies on primary NK cells sorted, eg via fluorescence-activated cell sorting (FACS), based on grH-positivity or negativity. Therefore, a further goal was to overexpress grH in cells that hardly express it, to create a clean system for its study.

Ultimately, it is the author's intention that this study contribute to our common understanding both of specific properties of grH as well as of the mechanisms of NK-cell education.

2 Materials and Methods

2.1 Materials

2.1.1 Dyes Used for Flow Cytometry

Table 3: Antibodies.

Antibody Target	Fluorochrome	Clone	Isotype	Company	Catalogue #
BCL-2	PE	100	IgG1	BioLegend	658707
CD3	BV785 TM	OKT3	IgG2a	BioLegend	317330
	BV605 TM	UCHT1	IgG1	BioLegend	300460
	APC/Cy7	UCHT1	IgG1	BioLegend	300426
	PE/Cy5	UCHT1	IgG1	BioLegend	300410
	PE/Cy7	UCHT1	IgG1	BioLegend	300420
	FITC	UCHT1	IgG1	BioLegend	300406
CD8a	AlexaFluor®700	HIT8a	IgG1	BioLegend	300920
CD11c	FITC	3.9	IgG1	BioLegend	301604
CD16	FITC	3G8	IgG1	BioLegend	302006
CD56	PE/Dazzle TM 594	HCD56	IgG1	BioLegend	318348
	APC/Cy7	HCD56	IgG1	BioLegend	318332
	PE	HCD56	IgG1	BioLegend	318306
	PE/Cy7	HCD56	IgG1	BioLegend	318318
CD57	Pacific Blue TM	HCD57	IgM	BioLegend	322316
CD62L	PE/Cy7	DREG-56	IgG1	BioLegend	304822
CD107a	BV785 TM	H4A3	IgG1	BioLegend	328644
	APC/Cy7	H4A3	IgG1	BioLegend	328630
KIR2DL1 (CD158a)	FITC	143211	IgG1	R&D Systems	FAB1844F
	APC	143211	IgG1	R&D Systems	FAB1844A
KIR2DL1/S1 (CD158a,h)	VioBlue	11PB6	IgG1	Miltenyi Biotec	130-095-233
KIR2DL1/S1/S3/S5 (CD158a,h,g)	FITC	HP-MA4	IgG2b	BioLegend	339504
KIR2DL2/L3/S2 (CD158b1,b2,j)	PC5.5	GL183	IgG1	Beckman Coulter	A66900
	PE	DX27	IgG2a	BioLegend	312606
	FITC	DX27	IgG2a	BioLegend	312604
	PE/Cy7	DX27	IgG2a	BioLegend	312610
KIR3DL1 (CD158e1)	PE/Cy7	DX9	IgG1	BioLegend	312720
	AlexaFluor®700	DX9	IgG1	BioLegend	312712
NKG2A (CD159a)	PE	Z199	IgG2b	Beckman Coulter	IM3291U
	APC	Z199	IgG2b	Beckman Coulter	A60797
	PC7	Z199	IgG2b	Beckman Coulter	B10246
NKG2C (CD159c)	PE	134591	IgG1	R&D Systems	FAB138P
	APC	134591	IgG1	R&D Systems	FAB138A
DNAM-1 (CD226)	PE	11A8	IgG1	BioLegend	338306
Granzyme A	FITC	CB9	IgG1	BioLegend	507204
Granzyme B	Pacific Blue TM	GB11	IgG1	BioLegend	515408
	PE	GB11	IgG1	BD Pharmingen TM	561142
Granzyme H	Biotinylated (no fluorochrome)	Polyclonal	Goat IgG	R&D Systems	BAF1377
	Unconjugated	3G10F4	IgG2a	Sino Biological	10348-MM02
Granzyme K	PE	24C3	IgG1	ImmunoTools	21144054
IFN- γ	PE/Cy7	B27	IgG1	BioLegend	506518
KLRG1	APC/Fire TM 750	SA231A2	IgG2a	BioLegend	367718

TNF- α	APC/Cy7	MAb11	IgG1	BioLegend	502944
	PE/Dazzle™594	MAb11	IgG1	BioLegend	502946
Biotin	VioGreen	Bio3-18E7	IgG1	Miltenyi Biotec	130-097-022
	VioGreen	Bio3-18E7	IgG1	Miltenyi Biotec	130-113-297

Isotype: mouse, unless otherwise stated.

Table 4: Non-antibody dyes.

Substance	Fluorochrome	Company	Catalogue #
Streptavidin	APC/Cy7	BioLegend	405208
Annexin V	FITC	BioLegend	640906
eBioscience™ Fixable Viability Dye eFluor™ 780	eFluor™ 780	Invitrogen™	65-0865-14
Propidium Iodide Solution	/	BioLegend	421301
Tag-it Violet™ Proliferation and Cell Tracking Dye	/	BioLegend	425101

2.1.2 Cell Culture

Table 5: Reagents used in cell culture.

Substance	Company
RPMI-1640 (+ 25 mM HEPES, + L-Glutamine), (s.-f.)	Lonza
Dulbecco's Modified Eagle Medium (DMEM) (1x) High Glucose (+ 4.5 g/L D-Glucose, L-Glutamine, + Pyruvate)	Gibco
DMEM (1x) + GlutaMAX™-I (+ 4.5 g/L D-Glucose, + Pyruvate)	Gibco
Alpha Minimum Essential Medium (MEM) without L-Glutamine (s.-f.)	Lonza
Iscove's Modified Dulbecco's Medium (IMDM) (s.-f.)	SIGMA®
Dulbecco's Phosphate-Buffered Saline (DPBS) (1x) (no Calcium Chloride, no Magnesium Chloride)	Gibco
Foetal Bovine Serum (FBS) (s.-f.)	Gibco
Foetal Bovine Serum, (FBS) (h.-i.)	Gibco
Human Serum, from human male AB plasma, USA origin (s.-f.)	SIGMA®
Horse Serum (s.-f.)	Gibco
Albumin Fraction V, protease-free (BSA)	ROTH
Penicillin Streptomycin (10,000 U/ml Penicillin, 10,000 µg/ml Streptomycin), sterile	Gibco
Gentamicin Reagent Solution (50 mg/ml)	Gibco
L-Glutamine 200 mM 100×, sterile	Gibco
PROLEUKIN® S (IL-2) (Aldesleukin), 1.1 mg (18×10 ⁶ IU)/ml	NOVARTIS
Human IL-15, premium grade, 50 µg/ml	Miltenyi Biotec
Rituximab (MabThera®), stock: 10 mg/ml	Roche

s.-f. = sterile-filtered, h.-i. = heat-inactivated

Composition of the Main Cell-Culture Media Used and of Staining Buffer

Standard Medium

RPMI-1640
10% (v/v) FBS (s.-f.)
100 U/ml penicillin
100 µg/ml streptomycin
(Standard medium forms the basis of several other media used here).

NK-Cell Medium

Standard medium
5% (v/v) human serum (s.-f.)
+/- 1000 U/ml IL-2 (as stated in the text)

NK-92 Medium

Alpha MEM
12.5% (v/v) FBS (s.-f.)
12.5% (v/v) horse serum (s.-f.)
2 mM L-Glutamine
200 U/ml IL-2

K562 Medium

DMEM (1x) high glucose
10% (v/v) FBS (s.-f.)
50 µg/ml gentamicin reagent solution

Materials and Methods

HEK293T and HT1080 Medium
 DMEM (1x) + GlutaMAX™-I
 10% (v/v) FBS (h.-i.)
 100 U/ml penicillin
 100 µg/ml streptomycin

2nd HEK293T Medium

IMDM
 10% (v/v) FBS (h.-i.)
 100 U/ml penicillin
 100 µg/ml streptomycin
 2 mM L-Glutamine

Cryopreservation Medium

Standard medium
 45% (v/v) FBS (s.-f.)
 10% (v/v) DMSO

Staining Buffer

DPBS
 0.5% (w/v) BSA
 2mM EDTA (pH 8.0)

2.1.3 Other Reagents

Table 6: Other reagents.

Substance	Company
Biocoll Separating Solution, Density 1.077 g/ml	Biochrom
Lysis Buffer pH 7,4 (Isotonic Ammonium Chloride Solution)	Central Pharmacy, University Hospital Düsseldorf (UKD), Germany
Dimethyl Sulfoxide (DMSO)	ChemCruz®
Brefeldin A Solution (1,000×), diluted to 1x in PBS prior to use	BioLegend
Monensin Solution (1,000×), diluted to 1x in PBS prior to use	BioLegend
Fixation Buffer (contains 4% paraformaldehyde)	BioLegend
Intracellular Staining Perm Wash Buffer (10×), diluted to 1x in Aqua ad iniectionis prior to use	BioLegend
Trypan Blue Solution	SIGMA®
TRIZOL® Reagent	Ambion®
Annexin V Binding Buffer	BioLegend
RetroNectin® (Recombinant Human Fibronectin Fragment)	TaKaRa
Protamine phosphate, 1 µg/µl	SIGMA®
Polyethylenimine, branched (PEI)	SIGMA®
VersaComp Antibody Capture Bead Kit, 1×10 ⁷ particles/ml	Beckman Coulter
Ethylenediamine Tetraacetic Acid (EDTA) Disodium Salt Dihydrate	ROTH
Distilled Water (Aqua dest.)	Central Pharmacy, UKD
Ampuwa® Spüllösung 1000 ml Plastipur Aqua ad iniectionis	Fresenius Kabi
Trypsin – EDTA Solution 1x, sterile	SIGMA®

2.1.4 Reagents Used for Molecular Biology

Table 7: Restriction enzymes and other enzymes.

Enzyme	Company	Catalogue #
XhoI 10 U/µl	Thermo Scientific™	ER0691
XhoI 10 U/µl	Invitrogen™	15231012
EcoRI 10 U/µl	Invitrogen™	15202-021
Calf Intestinal Alkaline Phosphatase 1 U/µl	Invitrogen™	18009-027
T4 DNA Ligase 1 U/µl	Thermo Scientific™	EL0016
50× Advantage® 2 Polymerase Mix	Clontech	S1798
HotStarTaq® DNA Polymerase 5 U/µl	QIAGEN	1007837
M-MLV Reverse Transcriptase 200 U/µl	Promega	M170A
PacI 10 U/µl	New England BioLabs®	R0547S
MluI 10 U/µl	Invitrogen™	15432016
ClaI 10 U/µl	Invitrogen™	15416050
RNase-free DNase Set	QIAGEN	79254

Table 8: Other reagents.

Substance	Company
Deoxynucleoside triphosphate (dNTP) mixture, 10 mM	PEQLAB
Oligo(dT) ₁₅ Primers, 500 µg/ml	Promega
Rnasin® Plus Rnase Inhibitor, 40 U/µl	Promega
Perfect™ 100 bp DNA Ladder, 125 µg (0.125 µg/µl)	EUR _x ®
Perfect™ Plus 1 kb DNA Ladder, 100 µg (0.1 µg/µl)	EUR _x ®
UltraPure™ Agarose, electrophoresis grade	Invitrogen™
Roti®-Phenol/Chloroform/Isoamyl Alcohol	ROTH
Nuclease-Free Water	QIAGEN
TRIS PUFFERAN® ≥99.3%, Buffer Grade	ROTH
Boric Acid ≥99.8%, p.a., ACS, ISO	ROTH
2-Mercaptoethanol 50 mM	Gibco
Ethidium Bromide Solution 1% (10 mg/ml)	ROTH
Ethanol ≥99.5%	ROTH
Ethanol ≥70%	VWR™
Sodium Chloride (NaCl)	ROTH
Glycerol, for molecular biology, minimum 99%	SIGMA®
Xylene Cyanol FF	SIGMA®
Bromophenol Blue	SIGMA®
S.O.C. Medium	Invitrogen™
LB Broth Base (Lennox L Broth Base) (for preparation add 20.0 g to 1000 ml distilled water, autoclave at 121°C for 15 minutes)	Invitrogen™
LB Agar (Lennox L Agar) (for preparation add 32.0 g to 1000 ml distilled water, autoclave at 121°C for 15 minutes)	Invitrogen™
Ampicillin Sodium Salt	SIGMA®

*Composition of Buffers and Loading Dye***TBE Buffer (10×)**

107.8 g tris-pufferan
 55.0 g boric acid
 8.2 g EDTA
 To 1000 ml: Aqua dest.
 (Diluted to 1x in Aqua dest. prior to use.)

Loading Dye

1 spatula tip of xylene cyanol FF
 1 spatula tip of bromophenol blue
 15 ml glycerol
 35 ml Aqua dest.

TE Buffer

Aqua dest.
 10 mM tris-pufferan
 1 mM EDTA

Materials and Methods

2.1.5 Cells Used

2.1.5.1 Primary Cells and Ethical Clearance

Human peripheral-blood mononuclear cells (PBMCs) were isolated (section 2.2.1) from whole blood of healthy volunteers or from buffy coats, by-products of whole-blood donations that were kindly provided by the blood donation centre at the ITZ (head of department: Dr J. Fischer). Human cord-blood mononuclear cells (CBMCs) were isolated from cord blood, kindly provided by the José Carreras Cord Blood Bank at the ITZ (head of department: Prof. Dr G. Kögler). Frozen PBMCs from donors who harbour an NKG2C expansion, defined as $\geq 9.25\%$ of CD56^{dim} NK cells being NKG2C⁺ according to Manser *et al.*, 2019 (119), were kindly provided by Dr A. Manser at the ITZ. NK cells expanded from PBMCs according to a protocol published by Fujisaki *et al.* in 2009 (195) were kindly provided by Dr M. Hejazi at the ITZ.

Written consent had been obtained from the donors prior to blood or cord blood donation in accordance with the Declaration of Helsinki, and this study was approved by the ethics committee of the faculty of medicine at the Heinrich Heine University (HHU) Düsseldorf, Germany (study reference 6155R).

2.1.5.2 Cell Lines

Table 9: Cell lines.

Cell Line	Description	Source
K562	HLA class I-deficient chronic myeloid leukaemia suspension-cell line from a 52-year-old woman in blast crisis, which, inducing the missing-self response, acts as a good NK-cell target (196),(197).	Kind gift from Prof. Dr C. Watzl, Leibniz Research Centre for the Working Environment and Human Factors, Dortmund, Germany
NK-92	Cytotoxic suspension NK-cell line from a 50-year-old man with large granular lymphocytic non-Hodgkin lymphoma (peripheral blood) (198).	Kind gift from Prof. Dr T. Tonn, Experimental Transfusion Medicine, Dresden, Germany
HEK293T	Highly transfectable adherent cell line from human embryonic kidney cells, transformed with adenovirus type 5 DNA fragments. Allows, due to stable expression of the simian virus 40 (SV40) large T antigen, replication of retroviral vectors carrying the SV40 origin of replication. (199),(200),(201).	German Collection of Microorganisms and Cell Cultures GmbH (DSMZ), Braunschweig, Germany
HT1080	Adherent fibrosarcoma-cell line from a 35-year-old man (202).	DSMZ

2.1.5.3 Bacterial Strains

Table 10: Bacterial strains. *Escherichia (E.) coli* One Shot™ TOP10 chemically competent cells were kindly provided by Prof. Dr H. Hanenberg and Dr C. Wiek at the Department of Otorhinolaryngology, Head and Neck Surgery, HHU Düsseldorf, Germany, and *E. coli* SURE electrocompetent cells were kindly provided by Dr HI Trompeter, ITZ.

Type	Strain	Genotype	Company
Chemically competent <i>E. coli</i>	One Shot™ TOP10	F- mcrA Δ (mrr-hsdRMS-mcrBC) Φ 80lacZ Δ M15 Δ lacX74 recA1 araD139 Δ (araleu)7697 galU galK rpsL (StrR) endA1 nupG	Invitrogen™
Electro-competent <i>E. coli</i>	SURE	e14 ⁻ (McrA ⁻) Δ (mcrCB-hsdSMR-mrr)171 endA1 gyrA96 thi-1 supE44 relA1 lac recB recJ sbcC umuC::Tn5 (Kan ^r) uvrC [F' proAB lacI ^q Δ M15 Tn10 (Tet ^r)]	Stratagene™

2.1.6 Primers Used in but not Designed within this Study

Table 11: Primers for HLA-C1/C2 typing. Kindly provided by Ms N. Scherenschlich, ITZ.

Primer	Sequence 5' to 3'	Tm	Ref.
Forward (NK2)	GTTGTAGTAGCCGCGCAGG	59	(203)
Forward (NK1)	GTTGTAGTAGCCGCGCAGT	58	(203)
Reverse	CGCCGCGAGTCCRAGAGG	60	(203)

Ref. = reference. Tm = calculated primer melting temperature in °C.

Table 12: Primers for KIR typing. Kindly provided by Ms N. Scherenschlich, ITZ.

KIR	Forward Primer (5' to 3')	Tm	Reverse Primer (5' to 3')	Tm	Ref.
KIR2DL1	ACTCACTCCCCCTATCAG G	56	AGGGCCCAGAGGAAAGTCA	59	(87)
KIR2DL1			AGGGCCCAGAGGAAAGTT	57	(87)
KIR2DL2	CCATGATGGGGTCTCCAA A	55	GCCCTGCAGAGAACCTACA	58	(77)
KIR2DL3	CCTTCATCGCTGGTGCTG	57	CAGGAGACAACCTTTGGATCA	53	(77)
KIR2DL5	TGCCTCGAGGAGGACAT	56	GGTCTGACCACTCATAGGGT	57	(204)
KIR3LD1	TACAAAGAAGACAGAATC CACA	53	TAGGTCCCTGCAAGGGCAA	60	(87)
KIR3DL1	TCCCATCTTCCATGGCAG AT	57			(87)
KIR3DL2	CGGTCCTTGATGCCTGT	58	GACCACACGCAGGGCAG	59	(77)
KIR2DS1	TCTCCATCAGTCGCATGA A/G	55	AGGGCCCAGAGGAAAGTT	57	(77)
KIR2DS2	TGCACAGAGAGGGGAAG TA	56	CACGCTCTCTCCTGCCAA	58	(77)
KIR2DS3	TCACTCCCCCTATCAGTTT	53	GCATCTGTAGGTTCCCTCCT	54	(87)
KIR2DS4	CTGGCCCTCCCAGGTCA	60	GGAATGTTCCGTTGATGC	52	(87)
KIR2DS5	AGAGAGGGGACGTTTAAC C	53	TCCGTGGGTGGCAGGGT	63	(87)
KIR3DS1	GGCAGAATATTCCAGGAG G	53	AGGGGTCCTTAGAGATCCA	55	(87)

Ref. = reference. Tm = calculated primer melting temperature in °C.

Table 13: Primers for sequencing the inserts of vectors p2CL6I2EGwo and p2CL7IPcowo. Kindly provided by Prof. Dr H. Hanenberg and Dr C. Wiek at the Department of Otorhinolaryngology, Head and Neck Surgery, HHU Düsseldorf, Germany.

Primer	Sequence 5' to 3'	Tm
Forward	GGACCTGAAATGACCCTGCG	59
Reverse	CTAGGAATGCTCGTCAAGAAG	54

Tm = calculated primer melting temperature in °C.

2.1.7 Vectors

Lentiviral vectors, helper plasmids, and the design template for shRNA construction were kindly provided by Prof. Dr H. Hanenberg and Dr C. Wiek, Department of Otorhinolaryngology, Head and Neck Surgery, HHU Düsseldorf.

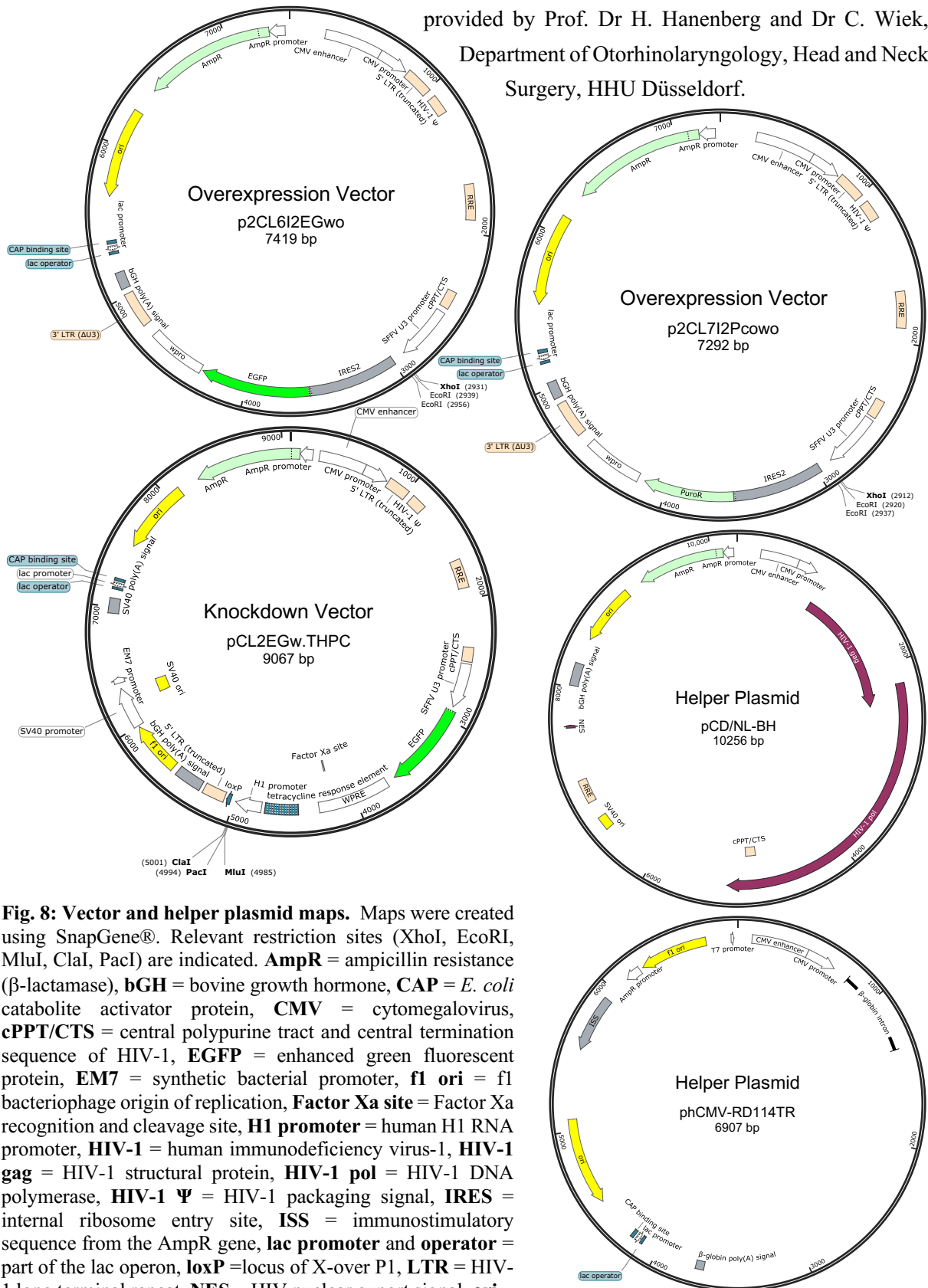


Fig. 8: Vector and helper plasmid maps. Maps were created using SnapGene®. Relevant restriction sites (XhoI, EcoRI, MluI, ClaI, PacI) are indicated. **AmpR** = ampicillin resistance (β -lactamase), **bGH** = bovine growth hormone, **CAP** = *E. coli* catabolite activator protein, **CMV** = cytomegalovirus, **cPPT/CTS** = central polypurine tract and central termination sequence of HIV-1, **EGFP** = enhanced green fluorescent protein, **EM7** = synthetic bacterial promoter, **f1 ori** = f1 bacteriophage origin of replication, **Factor Xa site** = Factor Xa recognition and cleavage site, **H1 promoter** = human H1 RNA promoter, **HIV-1** = human immunodeficiency virus-1, **HIV-1 gag** = HIV-1 structural protein, **HIV-1 pol** = HIV-1 DNA polymerase, **HIV-1 Ψ** = HIV-1 packaging signal, **IRES** = internal ribosome entry site, **ISS** = immunostimulatory sequence from the AmpR gene, **lac promoter** and **operator** = part of the lac operon, **loxP** = locus of X-over P1, **LTR** = HIV-1 long terminal repeat, **NES** = HIV nuclear export signal, **ori** = high-copy-number origin of replication, **poly(A) signal** = polyadenylation signal, **PuroR** = puromycin resistance, **RRE** = HIV-1 Rev response element, **SFFV U3** = spleen focus forming virus U3, **SV40 ori** = SV40 origin of replication, **T7 promoter**: promoter from bacteriophage T7 RNA polymerase, **WPRE** = woodchuck hepatitis virus posttranscriptional regulatory element, **wpro** = modified WPRE.

2.1.10 Devices and Software

Table 16: Devices.

Device and Model	Company
Flow cytometer: CytoFLEX	Beckman Coulter Inc., USA
Cell Sorter: MoFlo™ XDP	Beckman Coulter Inc., USA
Centrifuge Rotina 46 R	Andreas Hettich GmbH & Co. KG, Germany
Centrifuge 5415 D	Eppendorf AG, Germany
Centrifuge 5417 R	Eppendorf AG, Germany
CO ₂ incubator: APT.line™ Series CB	BINDER GmbH, Germany
Standard incubator: Series B	BINDER GmbH, Germany
Workbench: Safe 2020	Thermo Scientific™ by Thermo Fisher Scientific, USA
Workbench: MSC 12	Jouan SA by Thermo Fisher Scientific, USA
Fume cupboard: Always Safe	Vinitex Laboratoriuminrichtungen BV, The Netherlands
Shaking block heater: Thermomixer comfort	Eppendorf AG, Germany
Water bath: 1003	GFL Gesellschaft für Labortechnik mbH, Germany
Microscope: Wilovert S	Helmut Hund GmbH, Germany
Shaking incubator: 3020	GFL Gesellschaft für Labortechnik mbH, Germany
Flat Bed Shaker: Certomat® MO	B. BRAUN Melsungen AG, Germany
Incubation Hood: Certomat® H	B. BRAUN Melsungen AG, Germany
Vortex mixer: Reax top	Heidolph Instruments GmbH & Co. KG, Germany
Spectrophotometer: NanoDrop™ 2000	Thermo Scientific™ by Thermo Fisher Scientific, USA
Electrophoresis power supply: PowerPac™ 300	BIO-RAD Laboratories, Inc., USA
Gel-electrophoresis chamber and UV-transmissible gel trays: PerfectBlue™ horizontal midi and maxi gel systems	PEQLAB Biotechnologie GmbH, now VWR™ International, USA
Gel imaging (UV): Quantum ST4	Vilber Lourmat Deutschland GmbH, Germany
Precision balance: 440-47	KERN & SOHN GmbH, Germany
Electroporator: Gene Pulser® II Electroporation System	BIO-RAD Laboratories, Inc., USA
Automated haematology analyser: CELL-DYN Ruby	Abbott, Abbott Park, USA
Thermal cycler: GeneAmp® PCR System 9700	Applied Biosystems by Thermo Fisher Scientific, USA
pH meter: HI 9321	Hanna Instruments Deutschland GmbH, Germany
PCR-plate heat sealer: 4titude heat sealer	4titude® Limited, United Kingdom
Cell-Counting Chamber: Neubauer improved counting chamber	Paul Marienfeld GmbH & Co. KG, Germany

Table 17: Software.

Category	Programme	Company/ Creator
Flow-cytometry data acquisition	CytExpert 2.2	Beckman Coulter
Flow-cytometry data analysis	Kaluza Analysis Software 2.1	Beckman Coulter
Cell sorting	Summit 5.2	Beckman Coulter
Tabulation of data	Excel for Mac Version 16.27	Microsoft
Graphical representation and statistical analysis	Prism 8 for macOS	GraphPad Software
Plasmid editing	ApE– A plasmid Editor v2.0.53c	M. Wayne Davis
Plasmid editing	SnapGene® Version 5.1.0	GSL Biotech LLC
Sequence comparison	BLAST®	National Library of Medicine

v = version.

2.2 Methods

Unless otherwise stated, washing cells with DPBS, cell-culture medium, staining buffer or 1x Perm Wash Buffer involved filling up the tube containing the cells with the fluid at hand, centrifuging it at 380×g for 10 minutes (min) with brake at 4°C, discarding the supernatant and resuspending the cells in the appropriate fluid. Pelleting, unless otherwise stated, involved the same centrifugation settings.

2.2.1 Isolation of Mononuclear Cells

Isolation of mononuclear cells (MCs) from peripheral blood (PB) or cord blood (CB) was performed via density gradient centrifugation using a separating solution with a density of 1.077 g/ml. Erythrocytes and granulocytes have a higher buoyant density than MCs, which in turn have a higher density than plasma and platelets. Thus, when blood is layered onto the separating solution and centrifuged, erythrocytes and granulocytes form a sediment at the bottom of the tube, while MCs remain in a distinct layer at the interphase between the separating solution and plasma, from which they are harvested (205).

Isolation of PBMCs or CBMCs was performed no later than 24 hours (h) after blood collection. After blood collection, an automated full blood count was first performed using a CELL-DYN Ruby device to ensure that the blood components were within the normal range (using the device's reference ranges). The samples were then diluted 1:1 with sterile DPBS, 35 ml of this were carefully layered onto 15 ml of Biocoll Separating Solution in a 50 ml screw-cap conical centrifuge tube and centrifuged (870×g, 20 min, no brake, 21°C). The MCs were then carefully removed from the interphase layer and washed with DPBS. The cell pellet was then resuspended in 20 ml of cold (4°C) isotonic ammonium chloride solution and incubated for 10 min at room temperature (RT) to induce erythrolysis in case of sample impurity. The MCs were then washed twice with DPBS and resuspended in the appropriate fluid, either for immediate further use or for cryopreservation. Prior to the last wash step, the cells were counted manually using a counting chamber (see below) or automatically using a CELL-DYN Ruby device.

2.2.2 Counting Cells Using a Counting Chamber

20 µl of a cell suspension mixed with 20 µl of trypan blue solution were applied to a Neubauer counting chamber (depth: 0.1 mm, area: 1 mm² per large square). The number of live (not stained blue) and/or dead (stained blue, as trypan blue can only enter cells that have lost their membrane integrity (206)) cells was counted and the concentration of the original cell suspension determined as follows:

$$\text{Concentration (\# of Cells/ml)} = \frac{\text{\# of Cells Counted}}{\text{\# of Large Squares} \times \text{Dilution}} \times 10^4.$$

The factor 10⁴ is used to obtain the volume of interest (1 ml) from the volume per large square (0.1 µl). # = Number.

2.2.3 Cryopreservation of Cells

To prevent the formation of damaging crystals within cells during freezing, cells were frozen in dimethyl sulfoxide (DMSO)-containing medium, keeping the time taken to complete the freezing process (as well as later the thawing process) to a minimum due to toxicity of DMSO at RT (207). After pelleting, cells were resuspended in cold (4°C) cryopreservation medium without DMSO at a maximum concentration of 1×10⁷ cells/ml. 500 µl aliquots of the cell suspensions were transferred to 2 ml freezing tubes to each

Materials and Methods

of which 500 µl of cryopreservation medium supplemented with 20% (v/v) DMSO had been added, to make a final concentration of 10% (v/v) DMSO. The tubes were placed on ice, immediately transferred to -80°C for initial freezing and eventually moved to -196°C (liquid nitrogen) for long-term storage.

2.2.4 Thawing Cells

Cell-containing freezing tubes were briefly warmed in a 37°C water bath, just enough for the cell clump to detach from the walls and bottom of the tubes. The clumps were then quickly transferred to 15 ml screw cap conical centrifuge tubes containing ≥10 ml of pre-warmed cell-culture medium, staining buffer or DPBS, depending on the protocol that was to follow, and pelleted at 21°C. The cell pellet was washed again with and resuspended in the appropriate fluid at the appropriate concentration.

2.2.5 Culture of Cell Lines

Cell lines were cultured in the appropriate medium (section 2.1.2) at 37°C, 5% CO₂. K562 and NK-92 cells were cultured in non-treated cell-culture plates or tissue-culture flasks for suspension cells, depending on cell numbers to allow for target concentrations of 3×10^5 /ml (K562) and $2-2.5 \times 10^5$ /ml (NK-92), unless otherwise stated, and fed, through the addition of fresh medium, twice or three times a week.

2.2.6 Flow Cytometry and Fluorescence-Activated Cell Sorting

2.2.6.1 Principles

Flow cytometers analyse light emitted by cells or particles after their excitation by a laser (208). Fluid-suspended, fluorescently labelled cells are passed through a laser beam in a single-cell stream. The specific wavelengths of light emitted by the label after excitation, as well as the visible light scattered by the cells passing through the beam are measured (208). Forward scatter (FSC) correlates with cell size and side scatter (SSC) with cell granularity (208). Thus, specific labelling allows examination of particular cell characteristics. Most frequently, fluorochrome-conjugated antibodies are used for labelling because of their specificity for a particular target. Other labels include fluorescent reporter genes transduced into cells, cell-tracking dyes, dead cell markers like propidium iodide (PI) that bind to DNA after loss of membrane integrity, or annexin V that binds to phosphatidylserine (PS) (209).

Fluorescence-activated cell sorting (FACS) operates on a similar principle, but instead of merely being analysed, cells can be physically separated according to their optical properties (208). Based on their fluorescence, individual cells are manoeuvred into single droplets to which a positive or negative charge is applied (208). This charge allows droplets to be deflected and sorted into collection tubes (208).

2.2.6.2 Cell Staining

Antibodies already conjugated with fluorochromes or biotin were used. The exception was the unconjugated anti-grH monoclonal antibody (mAb) clone 3G10F4 by Sino Biological, which was conjugated manually with phycoerythrin (PE) using the R-Phycoerythrin Conjugation Kit by abcam according to the manufacturer's instructions. Success of the conjugation was tested using the VersaComp Antibody Capture Bead Kit by Beckman Coulter according to the manufacturer's instructions. The selection of a suitable anti-grH antibody is demonstrated in section 3.4.

Materials and Methods

2.2.6.2.1 Cell Surface Staining

Prior to staining, cells were washed with staining buffer or cell-culture medium, the BSA and FBS these fluids contain reducing non-specific antibody binding, and EDTA in staining buffer reducing cell clumping, EDTA being a metal ion chelator (particularly of Ca^{2+}) (210). After resuspension in 100 μl staining buffer or culture medium, $0.1\text{-}1\times 10^6$ cells were transferred to 5 ml flow-cytometry tubes. Within one experiment, either staining buffer or culture medium was used for all samples to ensure consistency. Fluorochrome-conjugated antibodies specific for the cell-surface antigens of interest were then added and incubated for 20 min at 4°C . The samples were then washed with DPBS, resuspended in 100 μl DPBS and either analysed immediately using Beckman Coulter's CytoFLEX flow cytometer, or stained intracellularly first. As soon as fluorochrome-conjugated antibodies had been added, the samples were protected from light, especially UV light, to prevent photobleaching.

2.2.6.2.2 Intracellular Staining

After cell-surface staining (or after washing cells once with DPBS if no cell-surface staining was carried out), cells were resuspended in 250 μl Fixation Buffer (which contains 4% paraformaldehyde), and incubated at 4°C for 20 min. Then, they were washed with 1x Perm Wash Buffer to permeabilise cells. For direct staining, fluorochrome-conjugated antibodies specific for intracellular targets (in this study: grH, grB, grA, grK, IFN- γ , TNF- α and BCL-2) were then added and incubated for 30 min at 4°C . The samples were again washed with 1x Perm Wash Buffer, then with DPBS and analysed using multicolour flow cytometry. Indirect staining for grH was performed as follows: after the first wash with 1x Perm Wash Buffer, biotinylated anti-grH antibody was added in addition to all other antibodies used and incubated for 30 min at 4°C . The samples were then washed again with 1x Perm Wash Buffer. Anti-biotin-VioGreen or streptavidin-APC/Cy7 was then added and incubated for 30 min at 4°C . The samples were washed again with 1x Perm Wash Buffer and then with DPBS, prior to flow cytometrical analysis. Antibodies specific for other intracellular antigens were able to be added at the same time as the primary biotinylated anti-grH antibody, yielding sufficiently clear signals (data not shown).

2.2.7 Functional Assays

2.2.7.1 Soluble Mediator-Induced NK-Cell Stimulation

The impact of soluble mediator-induced NK-cell stimulation on grH and grB expression was examined. PBMCs from donors with no known NKG2C expansion were cultured in medium supplemented with IL-2 and IL-15. PBMCs from donors with a known NKG2C expansion were cultured in medium with IL-15 and the anti-CD20 mAb rituximab, to induce ADCC in adaptive NKG2C⁺ NK cells, due to their poor response to cytokines alone. To this end, thawed or freshly isolated PBMCs were resuspended in NK-cell medium supplemented with either 1000 U/ml IL-2 or 10 ng/ml IL-15 or both, or with 1 $\mu\text{g}/\text{ml}$ Rituximab and 10 ng/ml IL-15, or with nothing at all, at cell concentrations of $0.5\text{-}1\times 10^6/\text{ml}$ (day 0), aliquots of $0.5\text{-}1\times 10^6$ cells having been stained and analysed using flow cytometry. The cell suspensions were incubated in non-treated 24-well plates at 37°C , 5% CO_2 , for 7 days. Depending on cell density, 150-500 μl of fresh medium supplemented with the appropriate soluble mediators were added on days 2 and 4. The cells were again stained and analysed on days 1, 3 and 7.

2.2.7.2 *Degranulation and Cytokine-Production Assay*

Target cell-induced activation is a common way to study NK-cell function. In this context, cell-surface CD107a expression is used as a marker of NK-cell activation and degranulation (211),(212). CD107a lines the luminal surface of cytolytic granule membranes in resting NK and other cytotoxic cells; thus, upon NK-cell activation and fusion of cytolytic granules with the plasma membrane, CD107a becomes exposed and detectable at the cell surface (211),(212).

Here, PBMCs (= effector cells) were thawed and resuspended in NK-cell medium without IL-2 at a concentration of 1×10^6 /ml, and, to aid recovery from the freezing/thawing process, cultured overnight (16 h) at 37°C, 5% CO₂, in a non-treated 6-well plate. After overnight culture, the PBMCs were harvested, washed with DPBS (790×g, 7 min, brake, 21°C) and resuspended in NK-cell medium without IL-2 at a concentration of 1×10^7 /ml. At the same time, K562 target cells were counted and the required volume to achieve an effector:target ratio of 10:1 was washed with DPBS (790×g, 7 min, brake, 21°C) and also resuspended in NK-cell medium without IL-2 at a concentration of 1×10^7 /ml.

The PBMCs and K562 cells were transferred to a U-bottom 96-well plate at an effector:target ratio of 10:1, using 1×10^6 effector cells and 1×10^5 target cells per well. 1×10^6 effector cells only were placed into a control well for determination of spontaneous degranulation and cytokine production. All wells were filled up to 200 µl using NK-cell medium without IL-2. Fluorochrome-conjugated anti-CD107a antibody was then added to each well, after which the plate was protected from light. It was then gently centrifuged (55×g, 3 min, brake, 21°C) to maximise cell-to-cell contact. The cells were incubated for an initial 15 min at 37°C, 5% CO₂, at which point monensin and brefeldin A were added to all wells, including to the *no target* controls. Monensin and brefeldin A, being intracellular transport inhibitors, lead to cytokine accumulation within cytokine-producing cells, thus facilitating their staining (213),(214),(215). The cells were then incubated for a further 4 h 45 min, after which they were transferred to individual 5 ml flow-cytometry tubes, stained using fluorochrome-conjugated antibodies, including intracellular staining for TNF-α and IFN-γ, and analysed flow cytometrically.

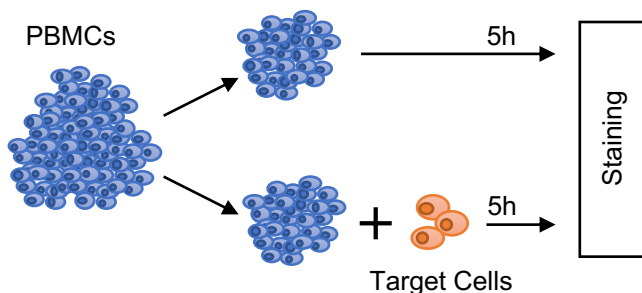


Fig. 10: Schematic representation of the degranulation and cytokine-production assay. Blue ovoids: PBMCs, orange ovoids: K562 target cells. Author's illustration.

The specific change, ie the change due to co-incubation with target cells, in the percentage of effector cells positive for CD107a, IFN-γ or TNF-α, was calculated as follows:

Specific Change (% points)

$$= \% \text{ Marker}^+ \text{ Effector Cells}_{\text{With Target}} - \% \text{ Marker}^+ \text{ Effector Cells}_{\text{No Target}}$$

The same assay was also performed with transduced NK-92 cells. Since these cells were already in long-term cell culture, the assay was commenced on day 1 of the protocol described above, omitting the overnight culture step. Furthermore, effector:target ratios of 1:1, 0.2:1 and 0.1:1 were employed, using 5×10^5 , 2×10^5 and 1×10^5 effector cells respectively.

2.2.7.3 Cytotoxicity Assay

Another way of studying NK-cell function is to look at the killing of target cells pre-labelled with a cell-tracking dye. Cell-tracking dyes generally require intracellular processing to become fluorescent, and therefore stain live cells (216). The dye used here was Tag-it Violet™ (BioLegend), which, unlike the more commonly used carboxyfluorescein succinimidyl ester, is compatible in flow cytometrical analysis with fluorescent molecules detected by the fluorescein isocyanate (FITC) channel, like enhanced green fluorescent protein (EGFP) (216),(217),(218),(219). After the assay, dead target cells are additionally stained with a dead cell marker such as PI, which binds to DNA of cells that have lost their membrane integrity, and which therefore stains dead cells (220). Those cells that are tracking dye⁺/PI⁺ (so Tag-it Violet™⁺/PI⁺ here) are presumed to have died during the assay.

The following protocol was adapted from the official Tag-it Violet™ (BioLegend) protocol (217). K562 target cells were counted, the required volume taken out of culture, pelleted at 21°C, resuspended in the 5 µM Tag-it Violet™ working solution at a concentration of 1×10⁷/ml, and incubated for 20 min at 37°C, protected from light. Then, they were washed with K562 medium at 21°C, resuspended in pre-warmed NK-92 medium at a concentration of 1×10⁷/ml and incubated at RT for 10 min. NK-92 effector cells were also counted, the required volume taken out of culture, pelleted at 21°C, and resuspended in pre-warmed NK-92 medium at a concentration of 1×10⁷/ml. The NK-92 and Tag-it Violet™-labelled K562 cells were transferred to a U-bottom 96-well plate at effector:target ratios of 10:1, 5:1, 1:1 and 0.2:1, using 5×10⁵, 5×10⁵, 3×10⁵ and 1×10⁵ effector cells respectively. 3×10⁵ Tag-it Violet™-labelled K562 cells were placed into a separate well without any effector cells for determination of spontaneous lysis. 3×10⁵ unlabelled K562 cells were also placed into a separate well, also without any effector cells, to aid later identification of Tag-it Violet™-positive cells flow cytometrically (data not shown). All wells were then filled up to 200 µl using NK-92 medium. The cells were incubated at 37°C, 5% CO₂, for 5 h. Afterwards, the cells were harvested, transferred to 5 ml flow-cytometry tubes, washed with staining buffer at 21°C, and resuspended in 100 µl staining buffer. Then, PI was added to each sample, incubated at 4°C for 2 min, and the samples were immediately analysed using flow cytometry. As described above, target cells that were Tag-it Violet™⁺/PI⁺ were taken to have died in the assay. Specific lysis (death) of target cells, ie due to effector cells, was calculated as follows:

$$\text{Specific Lysis (\% points)} = \text{Lysis With Effector (\%)} - \text{Lysis Without Effector (\%)}$$

2.2.7.4 Serum-Starvation Assay and Apoptosis

Survival and apoptosis of NK cells, as another functional indicator, can be measured flow cytometrically by staining cells with annexin V and dead cell markers, including fixable viability dyes, which irreversibly bind dead cells. Annexin V⁺/dead cell marker⁻ cells are considered to be early apoptotic, while annexin V⁺/dead cell marker⁺ are considered late apoptotic (209) (see also section 3.11.2)).

For induction of apoptosis in PBMCs a serum-starvation assay was performed. On day 0, thawed PBMCs were resuspended in FBS-containing standard medium at a concentration of 1×10⁶/ml. They were transferred to a non-treated 6-well plate and cultured overnight (16 h) at 37°C, 5% CO₂, to aid recovery from the freezing/thawing process, an aliquot of 1×10⁶ of the cells having been stained and analysed flow cytometrically. On day 1, the cells were counted, washed twice with DPBS, and resuspended either in standard medium without FBS (ie RPMI-1640 with 100 U/ml penicillin and 100

Materials and Methods

$\mu\text{g/ml}$ streptomycin), or in FBS-containing standard medium as a control, both at a concentration of $1 \times 10^6/\text{ml}$, placed into non-treated 6-well plates and cultured at 37°C , 5% CO_2 , for a further two days, an aliquot of 1×10^6 cells having again been stained and analysed. The cells were stained and analysed again on days 2 and 3. Staining was performed as follows: after cell-surface staining (section 2.2.6.2.1), the cells were resuspended in 1 ml DPBS. Then, 1 μl of eBioscience™ Fixable Viability Dye eFluor™ 780 was added to each sample, the samples vortexed immediately, and incubated at 4°C for 30 min. The samples were then washed twice with staining buffer and resuspended in 100 μl Annexin V Binding Buffer. Then, 5 μl of FITC-Annexin V were added to each sample and incubated for 15 min at RT. The samples were then washed once with 1 ml Annexin V binding buffer and once with 2 ml DPBS, after which intracellular staining (section 2.2.6.2.2) followed. All staining was performed protected from light. To ensure the staining protocol worked, it was tested prior to the serum-starvation assay on thawed PBMC samples that were either stained straight after thawing or, as a positive control, had been heated to 65°C for 1 min to induce cell death (data not shown).

2.2.7.5 NK-Cell Expansion and GrH Expression

NK cells expanded according to a protocol by Fujisaki *et al.* (195) were kindly provided by Dr M. Hejazi at the ITZ and examined by this study's author for grH (and grB) expression (flow cytometric analysis after staining) to see whether expression changed with NK-cell expansion. In brief, NK cells isolated from PBMCs had been expanded by her for 7-14 days using K562 target cells transduced with membrane-bound versions of IL-15 and 4-1BB ligand, the latter being a molecule mainly expressed by antigen-presenting cells for co-stimulation of T cells (221). The cells were provided before and after expansion for staining.

2.2.8 Nucleic Acid Purification and cDNA Generation

2.2.8.1 DNA Purification from Blood

DNA was purified from blood by means of the QIAamp® DNA Blood Mini Kit by QIAGEN using spin technology according to the manufacturer's instructions. Samples were eluted in 200 μl elution buffer at the end and stored at -20°C until further use.

2.2.8.2 RNA Purification from Thawed PBMCs

Total RNA was purified from thawed PBMCs by means of the RNeasy® Mini Kit by QIAGEN using spin technology according to the manufacturer's instructions. Cell lysates were always homogenised using QIAshredder spin columns by QIAGEN and the optional DNase digestion was always performed. Samples were eluted in 50 μl RNase-free water at the end. The RNA concentration was measured spectrophotometrically, and the samples were stored at -20°C until further use.

DNA and RNA concentrations and purity were measured using the NanoDrop™ 2000 spectrophotometer. Ratios of absorbance at 260 nm and 280 nm (260/280) of ~ 1.8 for DNA and ~ 2.0 for RNA were considered reasonably pure.

Materials and Methods

2.2.8.3 RNA Purification from Fixed and Permeabilised PBMCs

RNA purification from fixed and permeabilised PBMCs was attempted using the RNA isolation protocol from *MARIS: Method for Analyzing RNA following Intracellular Sorting* by Hrvatin *et al.* (222), including the use of the RecoverAll™ Total Nucleic Acid Isolation Kit by Ambion®. To test whether the RNA purification had worked, cDNA was synthesised from the extracted RNA as described in section 2.2.8.4, and the presence or absence of KIR2DL2 and KIR2DL3, one of which would definitely be expressed, was examined as described in section 2.2.10.3. Neither KIR yielded a band on gel electrophoresis, however, so this method of RNA extraction was abandoned.

2.2.8.4 cDNA Synthesis

Complementary DNA (cDNA) was synthesised from RNA using Moloney Murine Leukaemia Virus (M-MLV) reverse transcriptase and oligo(dT) primers.

The following were added to a sterile, RNase-free, 0.5 ml microcentrifuge tube, incubated at 70°C for 5 min to melt secondary structures within the RNA templates, then placed onto ice immediately:

Oligo(dT) ₁₅ Primers (500 µg/ml)	0.5 µg
RNA	2 µg
Nuclease-free H ₂ O	to 12.5 µl

Then, the following were added and incubated at 42°C for 60 min and at 70°C for 10 min:

M-MLV Reverse Transcriptase 5x Buffer	4 µl
dNTP mixture, 10 mM	2 µl
RNasin® Plus RNase Inhibitor, 40 U/µl	0.5 µl
M-MLV Reverse Transcriptase	1 µl

cDNA concentration was measured spectrophotometrically, and the samples stored at -20°C until further use.

2.2.9 Agarose Gel Electrophoresis

Agarose gel electrophoresis was used to distinguish DNA fragments based on size and charge. Agarose added to 1x Tris/Borate/EDTA (TBE) buffer at the appropriate percentage (w/v) (as stated in the relevant sections) was boiled until dissolved and stained with 30 µg ethidium bromide per 100 ml 1x TBE buffer for visualisation of DNA. After solidification of the gel and transfer to a TBE buffer-filled electrophoresis chamber, 40-200 ng DNA, 2 µl loading dye and Tris/EDTA (TE) buffer to 10 µl were carefully loaded into wells within the gel. Unless otherwise stated, the loading dye contained both xylene cyanol and bromophenol blue. Depending on the expected size of the DNA fragment, either a 100-base pair (bp) or a 1-kilobase (kb) DNA ladder was used as a size marker. A 90-180 mA current was then applied to the chamber applied for 30-120 min, after which a UV photograph was taken of the gel.

2.2.10 HLA and KIR Typing

2.2.10.1 PCR-SSP-Based HLA-C Typing

To determine whether a donor expressed HLA-C1, HLA-C2 or both, HLA-C1/C2 typing was performed by means of a polymerase chain reaction (PCR) using sequence-specific primers (SSP). PCRs are used to exponentially amplify a target DNA sequence. In brief, a sample containing a DNA template is heated

Materials and Methods

to denature the double-stranded DNA. It is then cooled to allow specific primers to anneal to the 5' ends of the target sequence on the sense and antisense strands, allowing a thermostable DNA polymerase (eg Taq polymerase from the thermophilic bacterium *Thermus aquaticus*) to replicate the target sequence. Through repetition of these steps the newly synthesised DNA also becomes a template, eventually leading to exponential amplification of the target DNA fragment. (223)

The SSPs used here differ with regard to a single base at their 3' end to distinguish between *HLA-C1* and *C2*, not aligning with the template and not allowing amplification thereof unless the correct base is present. The presence or absence of an amplified product is tested electrophoretically, here using a 2% (w/v) agarose gel, loading dye containing xylene cyanol only, and a 100 bp DNA ladder as a size marker. The template used here was DNA isolated from blood (section 2.2.8.1). Reactions were set up in 0.2 ml PCR wells, using primers as published by Frohn *et al.*, 1998 (203) (see also **Table 11**), as follows:

DNA template	40-50 ng
dNTP mixture 10 mM	1 µl
Forward primer 10 µM	1 µl
Reverse primer NK1 or NK2 10 µl	1 µl
HotStarTaq® DNA Polymerase 5 U/µl	0.125 µl
10× PCR Buffer	2.5 µl
Nuclease-free H ₂ O	to 25 µl

The PCR plate was then placed in a thermocycler using the PCR programme shown in **Fig. 11**.

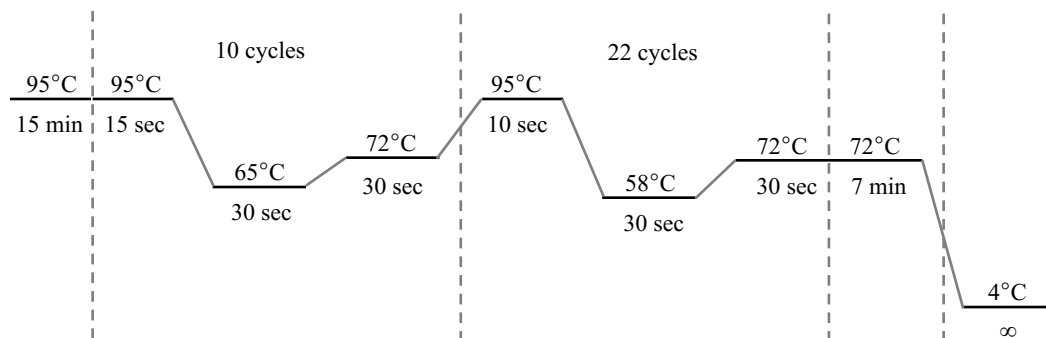


Fig. 11: The PCR programme used for HLA-C1/C2 typing. Adapted from Journal of Immunological Methods, 218, Frohn C, Schlenke P, Ebel B, Dannenberg C, Bein G, Kirchner H: DNA typing for natural killer cell inhibiting HLA-Cq groups NK1 and NK2 by PCR-SSP, 155-160, with permission from Elsevier (203).

2.2.10.2 HLA-Bw4/-Bw6 Typing

HLA-Bw4/-Bw6 typing on DNA isolated as described in section 2.2.8.1 was kindly performed by Dr J. Enczmann and colleagues at the HLA laboratory at the ITZ. In brief, using the Luminex® 100 System, target DNA was amplified by them using biotinylated group-specific primers for a given *HLA* locus. The DNA was then denatured to allow hybridisation to complementary DNA bound to labelled detection microbeads, which were analysed flow cytometrically (224).

2.2.10.3 KIR Typing

KIR typing by means of a PCR-SSP-based method, using DNA purified as described in section 2.2.8.1, was kindly performed by Dr A. Manser and Ms N. Scherenschlich at the ITZ. Primers were used as published by Uhrberg *et al.*, 1997 (77), Vilches *et al.*, 2000 (204), and Uhrberg *et al.*, 2002 (87) (also see **Table 12**). For electrophoretic visualisation of the PCR products, 1-1.5% (w/v) agarose gels and a loading dye containing bromophenol blue only were used.

2.2.11 GrH and grB Overexpression and Preparation for Knockdown of grH and grB

To overexpress a protein in a cell of interest, the open reading frame (ORF) of a particular gene can be cloned into a lentiviral, ie retroviral, vector system. After transduction of the cell of interest, stable, long-term expression of the foreign gene is achieved through lentiviral integration into the host-cell genome (225). Conversely, to knock down a gene of interest, DNA sequences that encode short hairpin RNA (shRNA) directed against this gene can be cloned into the vector, shRNA being able to induce gene silencing in mammalian cells in a sequence-specific manner (226).

Thus, for modulation of grH and grB expression in cells of interest, *GZMH*- and *GZMB* ORFs amplified from cDNA, as well as DNA encoding shRNA directed against *GZMH* and *GZMB*, were separately cloned into vectors. The overexpression vectors used here were p2CL6I2EGwo (7419 bp), and p2CL7IPcowo (7292 bp). They contain an internal ribosome entry site (IRES), which allows the simultaneous translation of a gene of interest and a reporter or selection gene from a single transcript (227),(228),(229),(230): p2CL6I2EGwo encodes EGFP and p2CL7IPcowo encodes puromycin resistance. The expression of viral genes in both vectors is controlled by a CMV promoter, while gene expression via the IRES is controlled by a spleen focus forming virus U3 (SFFV U3) promoter.

The knockdown vector used here was pCL2Egw.THPC (9067 bp). Viral proteins in this vector are also under the control of a CMV promoter and the vector also encodes EGFP controlled by an SFFV U3 promoter. However, an IRES is not required. The human H1 promoter controls shRNA transcription here, which directs RNA polymerase III necessary for shRNA expression (231),(226).

All three vectors encode an ampicillin resistance gene to help select for plasmid-containing bacteria on/in ampicillin-containing agar/-medium after transformation of bacteria.

2.2.11.1 Vector Preparation

The inserts of interest were directionally cloned into the vectors by means of digestion by restriction endonucleases and subsequent ligation of the sticky ends. For this, sticky ends first had to be generated in the vectors.

2.2.11.1.1 Restriction Enzyme Digestion

XhoI and EcoRI were chosen for digestion of p2CL6I2EGwo and p2CL7IPcowo, which both contain one XhoI restriction site upstream of two EcoRI sites. The XhoI and EcoRI digestions were performed in separate steps: first XhoI digestion, confirming the success gel electrophoretically on a 0.4% (w/v) agarose gel with a 1 kb DNA ladder size marker (data not shown), then purification and precipitation (see section 2.2.11.1.2) with resuspension of the samples in 30 μ l TE buffer, then EcoRI digestion and, again, purification and precipitation, with resuspension in 265 μ l TE buffer.

pCL2Egw.THPC contains a PacI restriction site between an MluI- and a ClaI restriction site. ClaI and MluI were chosen for vector and insert digestion and the resulting loss of the PacI restriction site was used to confirm the presence of an insert. The ClaI and MluI digestions were performed in a single step, followed by purification and precipitation and resuspension in 50 μ l TE buffer.

The digestion reactions were performed in 1.5 ml microcentrifuge tubes at 37°C for \geq 1.5 h, as follows:

Table 18: Stepwise XhoI- and EcoRI digestion of p2CL6I2EGwo and p2CL7IPcowo:

	XhoI	EcoRI
Vector	12 µg	12 µg
XhoI 10 U/µl	3.6 µl	
EcoRI 10 U/µl		3.6 µl
10× Buffer R	5 µl	
10× RE_{ACT}® 3 Buffer		5 µl
Nuclease-free H₂O	to 50 µl	to 50 µl

Table 19: Combined MluI- and ClaI digestion of pCL2Egw.THPC:

Vector (2 µg/µl)	5 µl
ClaI 10 U/µl	4 µl
MluI 10 U/µl	4 µl
10× RE_{ACT}® 3 Buffer	10 µl
Nuclease-free H₂O	81 µl

2.2.11.1.2 Purification – Using Phenol/Chloroform/Isoamyl Alcohol Extraction – and Precipitation

For purification and precipitation of the vectors after digestion, 1 volume of phenol/chloroform/isoamyl alcohol was added to each sample, mixed vigorously and centrifuged (15700×g, 10 min, brake, RT). Then, the upper aqueous phase was carefully transferred to a new 1.5 ml microcentrifuge tube. Then, a 1/20 volume of 5 M (moles/l) NaCl and 3 volumes of ≥99.5% ethanol were added, mixed thoroughly and left to rest at RT for 10 min for precipitation of the DNA. Then, the samples were again centrifuged (15700×g, 10 min, brake RT) and the supernatant discarded. 3 volumes of 70% ethanol were added, the samples gently swirled to mix, and centrifuged (15700×g, 5 min, brake RT). The supernatant was carefully discarded, and the previous step repeated with 3 volumes of ≥99.5% ethanol. After discarding the supernatant, the DNA pellets were carefully dried on a heat block at 68°C. The pellets were then dissolved in the appropriate volumes of TE buffer at 68°C and then frozen at -20°C until further use.

2.2.11.1.3 Dephosphorylation

Next, the 5' ends of the digested vectors were dephosphorylated.

The following reagents were added to a 1.5 ml microcentrifuge tube and incubated at 37°C for 45 min:

Vector (50-200 ng/µl)	1 µg
Calf Intestinal Alkaline Phosphatase 1 U/µl	1 µl
10× Dephosphorylation Buffer	3 µl
Nuclease-free H ₂ O	to 30 µl

After dephosphorylation, the vectors were purified and precipitated as described in section 2.2.11.1.2, dissolved in TE buffer to achieve a concentration of 200 ng/µl (overexpression vectors) or 500 ng/µl (knockdown vector) and stored at -20°C until ligation with the inserts (see section 2.2.11.3).

2.2.11.2 Insert Preparation

2.2.11.2.1 GZMH and GZMB Insert Preparation for Overexpression

2.2.11.2.1.1 Primer Design

For insert generation, total RNA was first extracted from a PBMC sample, as described in section 2.2.8.2. From this, cDNA was synthesised as described in section 2.2.8.4, and primers were designed to specifically amplify the sequence from start codon ATG to stop codon TAA of the *GZMH* and *GZMB* coding sequences, ie the *GZMH* and *B* ORFs (**Table 20**) using cDNA as a template. The primers contained restriction enzyme sites (XhoI and EcoRI) for directional cloning of the ORFs into the vectors. Furthermore, part of the Kozak consensus sequence was included for more efficient translation (232), and so-called ‘on-end’ bases were added to the 5' ends of the primers to increase the efficiency of later

digestion of the PCR products. Primer lengths were adjusted to keep the melting temperatures (T_m), as calculated by the software ApE, roughly consistent between the different primers. The published coding sequence of *GZMH* transcript variant 1 (accession number: NM_033423.4) and *GZMB* transcript variant 1 (accession number NM_004131.5), both of which encode the full-length protein (unlike other available transcript variants), were used as reference sequences (188). The *GZMH* ORF has a length of 741 bp and the *GZMB* ORF a length of 744 bp. Using the National Center for Biotechnology Information (NCBI) software BLAST®, specificity of the primers was confirmed.

Table 20: *GZMH*- and *GZMB*-specific primers.

Primer	Restriction Enzyme	Sequence (5' to 3')	T_m
<i>GZMH</i> Forward Primer	XhoI	<i>ctggcacctcgaggccg</i> ccATGCAGCCATTCCCTCCTCCTGTTGGCCTTTCTTCTG	71°C
<i>GZMH</i> Reverse Primer	EcoRI	<i>ctgaacgaattc</i> TTAGAGGCGCTTCATTGTTCTCTTTATCCAGGGC	66°C
<i>GZMB</i> Forward Primer	XhoI	<i>ctggcacctcgaggccg</i> ccATGCAACCAATCCCTGCTTCTGCTGGCCTTCC	70°C
<i>GZMB</i> Reverse Primer	EcoRI	<i>ctgaacgaattc</i> TTAGTAGCGTTTCATGGTTTCTTTATCCAGTGTACAAAGC	65°C

Template-specific sequence: capitalised; restriction sites: green; Kozak sequence: purple; on-end bases: italicised. T_m = melting temperature of the template-specific sequences of the primers.

The primers, as well as the shRNA oligonucleotides in section 2.2.11.2.2, were ordered as high-performance liquid chromatography (HPLC)-purified products (biomers.net GmbH, Germany). Upon receipt, the primers were reconstituted in TE buffer at a concentration of 10 pmol/ μ l (= 10 μ M).

2.2.11.2.1.2 PCR-Mediated Amplification of *GZMH* and *B* ORFs

The proofreading Advantage® 2 Polymerase Mix (Clontech) was used for PCR-mediated amplification of the *GZMH* and *B* ORFS. The reagents were added to 0.2 ml PCR wells as follows:

cDNA Template (250 ng/ μ l)	0.5 μ l
dNTP mixture, 10 mM	1 μ l
Forward Primer, 10 μ M	1 μ l
Reverse Primer, 10 μ M	1 μ l
50 \times Advantage 2 Polymerase Mix	1 μ l
10 \times Advantage 2 PCR Buffer	5 μ l
Nuclease-Free H ₂ O	40.5 μ l

The PCR programme used is shown in **Fig. 12**. It was adapted from the manufacturer's protocol based on the calculated primer melting temperatures depicted in **Table 20**.

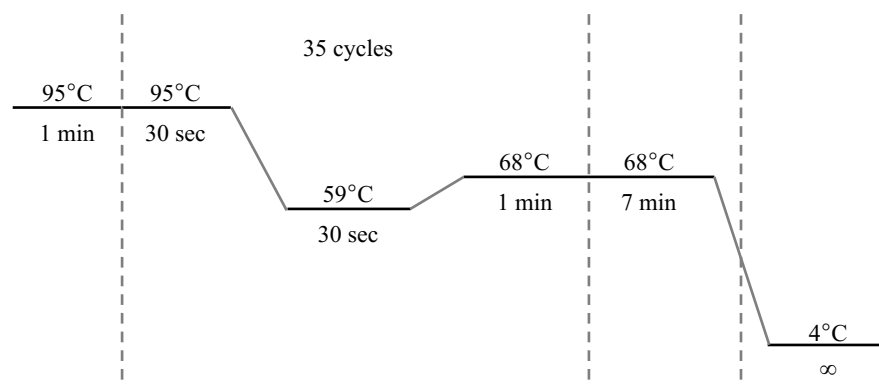


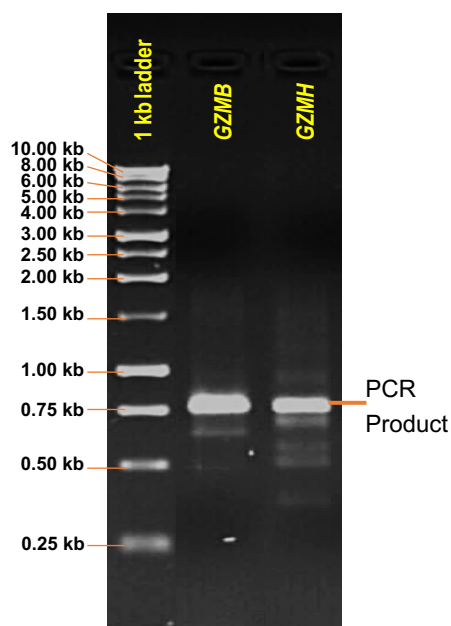
Fig. 12: The PCR programme used for *GZMH* and *B* ORF amplification.

Materials and Methods

Success of the PCR was confirmed by means of gel electrophoresis using a 1% (w/v) agarose gel and a 1 kb DNA ladder as a size marker (**Fig. 13**). Including the XhoI and EcoRI restriction sites as well as the Kozak consensus sequence and on-end bases, the final PCR products had expected lengths of 772 bp (*GZMH*) and 775 bp (*GZMB*).

Fig. 13: Gel electrophoresis of *GZMH*- and *-B* ORF PCR products. Size markers are indicated.

The PCR products (from now on termed ‘inserts’) were purified and precipitated as described in section 2.2.11.1.2, and dissolved in 50 μ l TE buffer. The DNA concentration was estimated electrophoretically, using a 0.5% (w/v) agarose gel and a 1 kb DNA ladder as a size marker and concentration reference (data not shown), prior to restriction enzyme-mediated digestion. The inserts were frozen at -20°C until further use.



2.2.11.2.1.3 Restriction Enzyme-Mediated Digestion of the Inserts

The inserts were then digested as follows (within a 1.5 ml microcentrifuge tube) to match the vectors:

Table 21: XhoI and EcoRI digestion of *GZMH* and *GZMB* inserts.

Insert ~8 ng/μl	40 μ l
XhoI 10 U/μl	3 μ l
EcoRI 10 U/μl	3 μ l
10\times RE_{ACT}[®] 2 Buffer	7 μ l
Nuclease-free H₂O	17 μ l

The digestion was carried out overnight (16 h) at 37°C . The inserts were then purified and precipitated as described in 2.2.11.1.2; dissolving them in 10 μ l of TE buffer at the end to make a concentration of ~ 32 ng/ μ l, as per the amount used for digestion. They were then frozen at -20°C until further use.

2.2.11.2.2 *GZMH* and *B* shRNA Insert Preparation for Knockdown – Oligonucleotide Design and Annealing

shRNA oligonucleotides were designed based on the design template shown in **Fig. 9**, using the target sequence of published or commercially available shRNAs that target the coding sequence of *GZMH* and *GZMB*, and to include a 5' phosphate group. A sense and an antisense strand were designed, the annealing of which resulted in the generation of the sticky ends (MluI and ClaI) appropriate for directional cloning into the vector. The final oligonucleotides are shown in **Table 22**.

After receipt, the ordered oligonucleotides were reconstituted in TE buffer to 100 pmol/ μ l (~ 2 μ g/ μ l). Then, they were annealed: 10 μ l of each sense oligonucleotide and 10 μ l of the respective antisense oligonucleotide were added to 80 μ l of TE buffer in a 1.5 ml microcentrifuge tube, placed on a 95°C heat block for 5 min and then left to slowly cool to RT. The annealed oligonucleotides are henceforth referred to as ‘inserts’. The final concentrations after annealing were ~ 400 ng/ μ l per insert.

Table 22: The sequences of the final *GZMH* and *GZMB* shRNAs.

<i>GZM</i> target	shRNA name	shRNA sequence (5' to 3') (as DNA)	Name of published shRNA	Ref.
<i>H</i>	<i>GZMH_6819_</i> Sense	<u>cgcg</u> tccccGGCATCCTAGTGAGAAAGGACT <u>ttcaa</u> <u>gaga</u> AGTCCTTTCTCACTAGGATGCC <u>tttt</u> ggaaat	TRCN000 0006819	(233) (SIGMA®)
	<i>GZMH_6819_</i> AntiSense	<u>cgatttcc</u> aaaaGGCATCCTAGTGAGAAAGGACT <u>t</u> <u>ctcttgaa</u> AGTCCTTTCTCACTAGGATGCC <u>gggga</u>	TRCN000 0006819	
	<i>GZMH_6820_</i> Sense	<u>cgcg</u> tccccGGTTATGTCTCAATGAGCACTT <u>ttcaa</u> <u>gaga</u> AAGTGCTCATTGAGACATAACC <u>tttt</u> ggaaat	TRCN000 0006820	
	<i>GZMH_6820_</i> AntiSense	<u>cgatttcc</u> aaaaGGTTATGTCTCAATGAGCACTT <u>tc</u> <u>tcttgaa</u> AAGTGCTCATTGAGACATAACC <u>gggga</u>	TRCN000 0006820	
	<i>GZMH_35611</i> 1_Sense	<u>cgcg</u> tccccACGTCTCTCCATGGCAATTACT <u>ttcaag</u> <u>aga</u> GTAATTGCCATGGAAGAGACGT <u>tttt</u> ggaaat	TRCN000 0356111	
	<i>GZMH_35611</i> 1_AntiSense	<u>cgatttcc</u> aaaaACGTCTCTCCATGGCAATTACT <u>tct</u> <u>cttgaa</u> GTAATTGCCATGGAAGAGACGT <u>gggga</u>	TRCN000 0356111	
<i>B</i>	<i>GZMB_6445_</i> Sense	<u>cgcg</u> tccccCGAATCTGACTTACGCCATTAT <u>ttcaaga</u> <u>ga</u> TAATGGCGTAAGTCAGATTTCG <u>tttt</u> ggaaat	TRCN000 0006445	(234), (235)
	<i>GZMB_6445_</i> AntiSense	<u>cgatttcc</u> aaaaCGAATCTGACTTACGCCATTAT <u>tctc</u> <u>ttgaa</u> TAATGGCGTAAGTCAGATTTCG <u>gggga</u>	TRCN000 0006445	

shRNA-encoding sequence: capitalised; loop: purple; stop signal: orange; the bases that will make up the sticky ends: green for MluI and red for ClaI; sequences derived from published shRNAs: underlined. Ref. = Reference.

2.2.11.3 Vector and Insert Ligation

Ligation of vectors and inserts for both overexpression and knockdown vectors was performed overnight (16 h) at 16°C using 1 µl of T4 DNA Ligase (1 U/µl) and 0.5 µl of 10× T4 DNA Ligase Buffer in a total reaction volume of 5 µl. The amounts and volumes of the vectors and inserts, however, differed—

- GrH and grB overexpression: for optimum ligation efficiency and to account for inefficiently digested inserts, a stoichiometric ratio of 1:5 (vector:insert) was applied; thus 100 ng vector (~100 ng/µl) and 50 ng insert (~30 ng/µl) were used.
- *GZMH* and *GZMB* knockdown: for optimum ligation efficiency, a stoichiometric ratio of 1:2 (vector:insert) was applied; for ease of handling, 200 ng vector (~140 ng/µl) and 4 ng insert (~400 ng/µl, diluted to 4 ng/µl using nuclease-free H₂O) were used.

A ligation control using nuclease-free H₂O instead of an insert was included for each vector.

After ligation, the plasmid samples were stored at -20°C until transformation of chemically competent cells. The grH and grB overexpression plasmids are henceforth referred to as p2CL6I2EGwo×*GZMH*, p2CL6I2EGwo×*GZMB*, p2CL7IPcowo×*GZMH* and p2CL7IPcowo×*GZMB*.

2.2.11.4 Transformation of Bacteria, Mini- and Maxipreparation

2.2.11.4.1 Transformation of Chemically Competent Cells Prior to Minipreparation

Amplification of the plasmids, for both overexpression and knockdown, was achieved through bacterial transformation and replication via minipreparation. First, chemically competent cells needed to be transformed. For this, aliquots of One Shot® TOP10 Competent Cells (*E. coli*) were thawed on ice. Then, 2.5 µl of each ligation reaction as well as 2.5 µl of the no insert ligation control were separately added to individual 40 µl aliquots of the cell suspensions and incubated on ice for 20 min. A 42°C heat shock was then applied for exactly 45 seconds, after which the samples were placed on ice immediately. 250 µl of pre-warmed S.O.C. medium was then added and incubated for 45 min on a shaking block

Materials and Methods

heater at 37°C, 600 revolutions per minute (rpm). Each sample was then spread onto separate, labelled sterile petri dishes (94-mm diameter) containing LB agar supplemented with 100 µg/ml ampicillin (LB-amp) and incubated at 37°C overnight (16 h). As expected, there was far less colony growth from bacteria transformed with the ligation control than from bacteria with the vector/insert samples.

2.2.11.4.2 Minipreparation for Plasmid DNA Purification

After overnight incubation, sterile petri dishes (35-mm diameter) containing ~2.5 ml of LB-amp medium were inoculated with individual bacterial colonies and again incubated overnight (16 h) at 37°C, 110 rpm. For the overexpression plasmids, 12 dishes were inoculated per vector/insert combination, and for the knockdown plasmids, 6 dishes were inoculated per vector/insert combination. The next day, the bacterial suspensions were transferred to 2 ml microcentrifuge tubes. Plasmid DNA was purified using the NucleoSpin® Plasmid kit by MACHEREY-NAGEL, according to the manufacturer's protocol, with the following modifications: after initial cell harvest, the bacterial suspensions were centrifuged for 1 min at 6000×g, the optional washing step with buffer AW was omitted, and DNA was eluted in 50 µl TE buffer. DNA concentration and purity were measured spectrophotometrically.

2.2.11.4.3 Test Digestion and Sequencing

To reveal which vectors contained the correct inserts, a test digestion on aliquots of the samples from section 2.2.11.4.2 was performed. For p2CL6I2EGwo×*GZMH*, p2CL6I2EGwo×*GZMB*, p2CL7IPcowo×*GZMH* and p2CL7IPcowo×*GZMB*, a double digestion with XhoI and EcoRI was done. For the knock-down plasmids (including an undigested vector without insert as a positive control), digestion using PacI was performed, loss of the PacI site confirming presence of an insert, and an MluI digestion to confirm that there were no multiple inserts. The digestions were performed at 37°C for 1.5-2 h, as follows:

Table 23: Test digestion of overexpression plasmids.

Plasmid DNA	200-500 ng (2 µl)
XhoI 10 U/µl	0.3 µl
EcoRI 10 U/µl	0.3 µl
10× RE_{ACT}® 2 Buffer	1 µl
Nuclease-Free H₂O	6.4 µl

Table 25: Test digestion of knockdown plasmids using MluI:

Plasmid or Vector DNA	1.2-1.8 µg (6 µl)
MluI 10 U/µl	0.3 µl
10× RE_{ACT}® 3 Buffer	1 µl
Nuclease-Free H₂O	2.7 µl

Table 24: Test digestion of knockdown plasmids using PacI:

Plasmid or Vector DNA	100-150 ng (0.5 µl)
PacI 10 U/µl	0.1 µl
10× NEBuffer 1	1 µl
Nuclease-Free H₂O	8.4 µl

The results were visualised electrophoretically on 0.8% (w/v) (overexpression) and 0.4% (w/v) (knockdown) agarose gels using a 1 kb DNA ladder as a size marker (data not shown).

Of those overexpression plasmids that contained inserts of the correct length (seven of p2CL6I2EGwo×*GZMH*, five of p2CL6I2EGwo×*GZMB*, five of p2CL7IPcowo×*GZMH* and nine of p2CL7IPcowo×*GZMB*), aliquots of five per vector (p2CL6I2EGwo and p2CL7IPcowo) / insert (*GZMH* and *GZMB*) combination were sent for Sanger sequencing (236) at Microsynth AG, Switzerland. The primers used for sequencing are shown in **Table 13**. Of those, the inserts of two of p2CL6I2EGwo×*GZMH* and one of p2CL7IPcowo×*GZMH* had the correct sequence when compared to the ORF of *GZMH* transcript variant 1. No *GZMB* inserts had the correct sequence, but the inserts of four of p2CL6I2EGwo×*GZMB* and three of p2CL7IPcowo×*GZMB* had the near-correct sequence when

compared to the ORF of *GZMB* transcript variant 1: all *GZMB* inserts had CAA at codon 48 instead of CGA (the latter being found in the sequence of *GZMB* transcript variant 1 with accession number NM_004131.5), which results in an amino acid change from arginine (R) to glutamine (Q). All clones, including the above-named and those with multiple other errors contained this change. Since, however, this change has been described in the literature and has been shown to result in a functional protein (237),(238),(239) (see section 4.4 for more detail), one of the clones with the otherwise correct sequence was chosen for overexpression of grB. Thus, one of each combination that contained the correct or near-correct insert sequence was chosen for maxipreparation.

For the knockdown vector + insert samples, one of each vector/shRNA combination (pCL2Egw.THPC × *GZMH*_6819_Sense/Antisense, pCL2Egw.THPC × *GZMH*_6820_Sense/Antisense, pCL2Egw.THPC × *GZMH*_356111_Sense/Antisense and pCL2Egw.THPC × *GZMB*_6445_Sense/Antisense) of those not cut by PacI and not containing multiple inserts was chosen for maxipreparation.

The samples from section 2.2.11.4.2 that had been selected based on test digestion and sequencing in this section were stored at -20°C until electroporation.

2.2.11.4.4 Electroporation Prior to Maxipreparation

Maxipreparation was performed to generate sufficient amounts of pure plasmid DNA for transfection of cells. First, electrocompetent *E. coli* were transformed by electroporation. For this, 40 µl aliquots of electrocompetent *E. coli* SURE cells were thawed on ice. 0.5 µl of the chosen plasmid samples were added to individual 40 µl aliquots of the bacterial suspensions, carefully mixed and transferred to pre-cooled sterile 2 mm cuvettes. Electroporation was performed on the Gene Pulser® II Electroporation System (BIO-RAD) using the following settings: 2500 V, 200 Ohms, 25 µF. The bacteria were then immediately added to 1 ml ampicillin-free LB medium in a 1.5 ml microcentrifuge tube and incubated at 37°C for 30 min to allow for expression of ampicillin resistance (β -lactamase) in transfected *E. coli*.

2.2.11.4.5 Maxipreparation

For maxipreparation, individual flasks containing 200 ml LB-amp medium were inoculated with 10 µl of each of the bacterial suspensions from 2.2.11.4.4 and incubated overnight (16 h) at 37°C, 250 rpm. The bacterial suspensions were then used for maxipreparation by means of the NucleoBond® Xtra Maxi kit (MACHEREY-NAGEL), according to the manufacturer's instructions. The resulting DNA pellet was dissolved in 500 µl TE buffer at 68°C. After cooling, DNA concentrations and purity were measured spectrophotometrically. A test digestion was performed on an aliquot of each sample to ensure that inserts of the correct length and thus, with very high probability, the correct inserts, were still present. The remainder of each sample was frozen at -20°C until transfection.

The digestion reactions were performed in 1.5 ml microcentrifuge tubes at 37°C for ≥ 1.5 h, as follows:

Table 26: Test digestion of overexpression plasmids with inserts.

Plasmid DNA 2 µg/µl	2 µg
XhoI 10 U/µl	0.5 µl
EcoRI 10 U/µl	0.5 µl
10× RE_{ACT}® 2 Buffer	1 µl
Nuclease-Free H₂O	7.5 µl

Table 27: Test digestion of knockdown plasmids with inserts.

Plasmid DNA 1.5-3 µg/µl	3 µg
MluI 10 U/µl	0.5 µl
ClaI 10 U/µl	0.5 µl
10× RE_{ACT}® 3 Buffer	1 µl
Nuclease-Free H₂O	to 10 µl

Gel electrophoresis, using a 0.6% (w/v) agarose gel for the overexpression vectors with a 1 kb DNA ladder as a size marker (**Fig. 14a**) and a 1.5% (w/v) agarose gel for the knockdown vector with 1 kb and

Materials and Methods

100 bp DNA ladders as size markers (data not shown), confirmed that the final vectors still contained inserts of the correct length. The digested inserts, which also contained sticky ends from restriction enzyme digestion, had expected lengths of 753 bp (*GZMH*), 756 bp (*GZMB*) and 73 bp (shRNA). Schematic representations of the final vectors containing the inserts are shown in **Fig. 14b-d**, and schematic representations of the cloning sites in **Fig. 14e-f**.

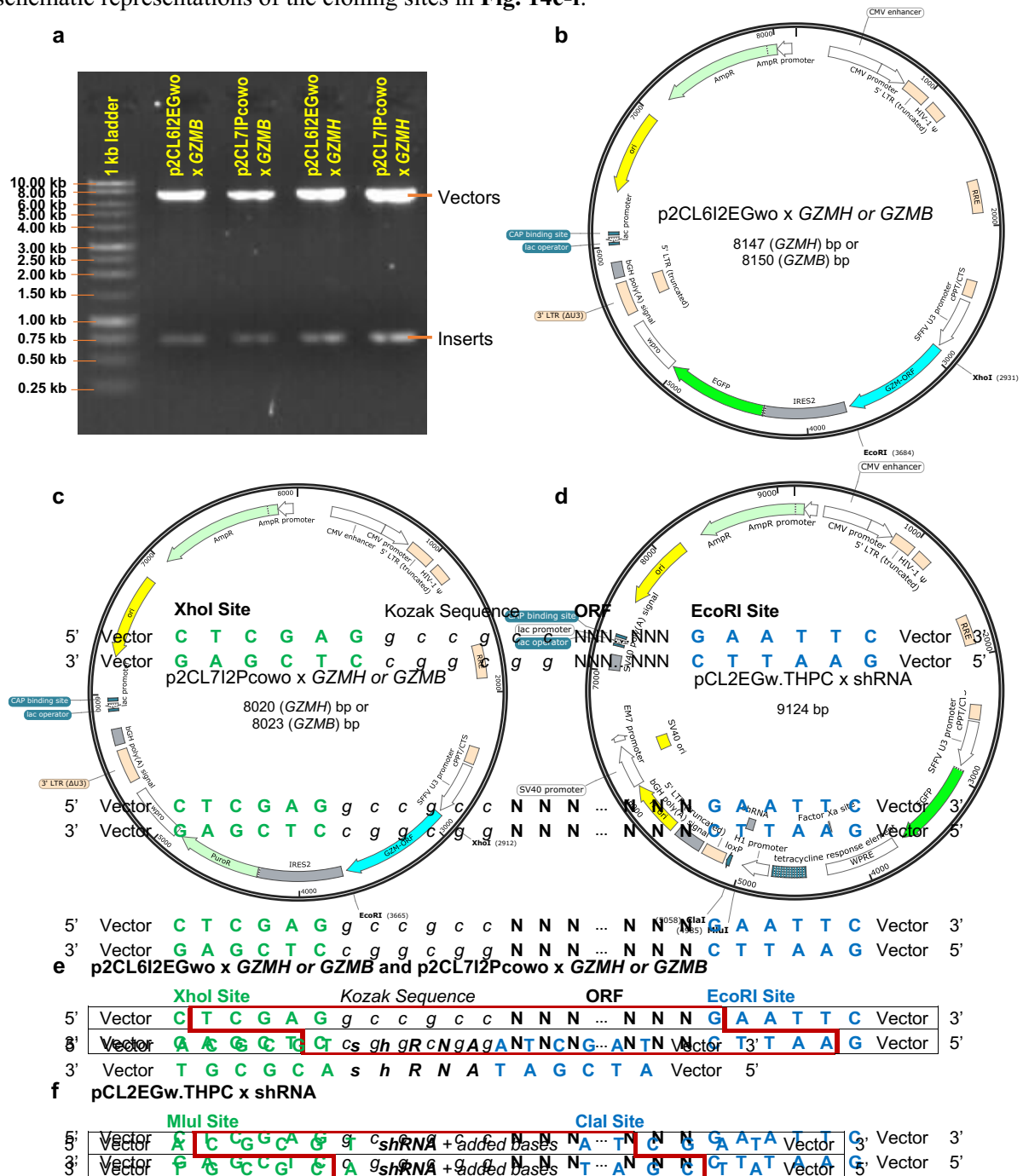


Fig. 14: Gel electrophoresis of the products of test digestion of insert-containing overexpression vectors after maxipreparation, and maps and schematic representations of insert-containing vectors. **a:** gel electrophoresis of p2CL6I2EGwo×*GZMH* or *GZMB* and p2CL7I2Pcowo×*GZMH* or *GZMB* after test digestion. Size markers are indicated, as well as which bands correspond to the vectors and which to the inserts. **b, c** and **d:** maps of p2CL6I2EGwo×*GZMH* or *GZMB* (**b**), p2CL7I2Pcowo×*GZMH* or *GZMB* (**c**) and pCL2EGw.THPC ×shRNA (**d**), with inserts indicated in turquoise. ‘GZM’ = both *GZMH* and *GZMB*, shRNA = all four shRNAs listed in **Table 22**. The restriction sites used for cloning (EcoRI and XhoI (**b** and **c**) and MluI and ClaI (**d**)) are indicated. Abbreviations: see **Fig. 8**. Maps were created using SnapGene®. **e** and **f:** schematic representation of the inserts (enclosed in red) within the overexpression (**e**) and knockdown (**f**) vectors. **e:** XhoI and EcoRI sites are indicated, as is the Kozak consensus sequence. The ORF is represented by the generic nucleotide N. **f:** MluI and ClaI sites are indicated. See **Fig. 9** and **Table 22** for what ‘shRNA + added bases’ means.

2.2.11.5 *Transduction of Cell Lines and Primary NK Cells*

Although inserts (*GZMH* and *GZMB* ORFs or shRNA) were cloned into all three vectors, only the overexpression vector p2CL6I2EGwo was used for infectious viral particle production and cell transduction in the end, the other two being kept for future use. p2CL7IPcowo and pCL2Egw.THPC are thus not referred to again. p2CL6I2EGwo, a replication-defective human immunodeficiency virus (HIV)-1-based vector, requires helper plasmids for progeny production as a measure of increasing biosafety. pCD/NL-BH, which encodes genes necessary for virus packaging (225), was used for this purpose. Furthermore, p2CL6I2EGwo was pseudotyped (provided with foreign viral envelope proteins) using phCMV-RD114/TR, a plasmid that contains a modified version of the feline endogenous retrovirus envelope glycoprotein (240). During initial trials in this study, vesicular stomatitis virus glycoprotein (pczVSV-G) (241) and a modified version of gibbon ape leukaemia virus glycoprotein (pcoGaLVTM) (242) were also used for pseudotyping, but they yielded much lower cell transduction efficiencies than phCMV-RD114/TR (maps and data not shown) and are thus not referred to again.

2.2.11.5.1 *Transfection of HEK293T Cells and Virus Harvest*

The highly transfectable adherent cell line HEK293T was used for the production of infectious viral particles for eventual transduction of cells of interest. On the day before transfection, 6×10^6 HEK293T cells were seeded onto cell-culture dishes (10-cm diameter). On the day of transfection, 6 μg of p2CL6I2EGwo \times *GZMH*, p2CL6I2EGwo \times *GZMB* or p2CL6I2EGwo without insert ('empty vector'), 6 μg of pCD/NL-BH and 6 μg of phCMV-RD114/TR were pre-incubated for 20 min at RT with 45 μg of polyethylenimine (PEI) transfection reagent in a total of 2 ml cell-culture medium (DMEM (1 \times) + GlutaMAXTM-I) without any supplemented serum or antibiotics. After pre-incubation, the plasmid and PEI-containing medium was added to the HEK293T cells, from which the old medium had been removed and replaced with 4 ml of DMEM (1 \times) + GlutaMAXTM-I supplemented with additives such that overall, the HEK293T medium contained 10% (v/v) h.-i. FBS, 100 U/ml penicillin and 100 $\mu\text{g}/\text{ml}$ streptomycin. After overnight incubation at 37°C, 5% CO₂, all cell-culture medium was carefully removed from the HEK293T cells and replaced with 10 ml of IMDM supplemented with 10% (v/v) h.-i. FBS, 100 U/ml penicillin, 100 $\mu\text{g}/\text{ml}$ streptomycin and 2 mM L-glutamine.

2.2.11.5.2 *Virus Harvest and Transduction of the Cells of Interest*

After a further 24 h of incubation at 37°C, 5% CO₂, the virus supernatant was harvested and filtered using a 0.45 μm filter to remove any cells that had been inadvertently harvested. It was either transferred straight to freezing tubes for storage at -80°C prior to transduction of cell lines, or concentrated (centrifugation at 10,000 \times g, 1 h 45 min, brake, 4°C, then resuspension in 200 μl of the appropriate cell-culture medium) prior to transfer to freezing tubes for storage at -80°C before transduction of primary cells. For transduction, the virus supernatant was completely thawed at RT and utilised without any further steps.

2.2.11.5.2.1 *HT1080 Titre*

Transduction of HT1080 cells was performed to determine the titre of the infectious viral particles. For this, 3.5×10^4 HT1080 cells were seeded into each well of a tissue culture-treated 6-well plate in 2 ml of DMEM (1x) + GlutaMAXTM-I supplemented with 10% (v/v) h.-i. FBS, 100 U/ml penicillin and 100 $\mu\text{g}/\text{ml}$ streptomycin, and incubated overnight (16 h) at 37°C, 5% CO₂. Then, serial dilutions (10^0 , 10^{-1} ,

Materials and Methods

10^{-2} , 10^{-3} , 10^{-4} , 10^{-5}) of thawed, unconcentrated virus supernatant were made in the above-described medium and 1 ml of each dilution was added to a correspondingly labelled well of HT1080 cells. A medium-only control was included. 10 µg/ml protamine phosphate were then added to each well to increase transduction efficiency. The cells were incubated at 37°C, 5% CO₂, for 72 h, carefully removing the medium and replacing it with 3 ml of fresh medium after the initial 24 h.

To harvest the HT1080 cells, the medium was completely removed, and the wells were rinsed with 500 µl sterile DPBS. After removal of the DPBS, 250 µl Trypsin-EDTA were added to each well and incubated (37°C, 5% CO₂) until the cells had detached. The reaction was quenched using 250 µl of the above-described medium, and the cell suspensions were transferred to 5 ml flow-cytometry tubes. They were washed twice with DPBS (307×g, 10 min, brake, 21°C) to remove any residual virus supernatant and to change their biosafety level from 2 to 1. After resuspension in 500 µl DPBS with 0.5 µl propidium iodide, EGFP expression was analysed flow cytometrically. The results were used to calculate the number of transduction units (TU)/ml according to the following equation, the final TU/ml being calculated as a mean of the TU/ml from the linear part of the vector dose-response curve (243),(244):

$$TU/ml = \text{Number of Cells Used} \times \frac{\% \text{ of Cells EGFP}^+}{100\%} \times \text{Dilution}$$

The HT1080 titres yielded numbers of TU/ml with similar orders of magnitude for the unconcentrated virus supernatants of p2CL6I2EGwo×GZMH, p2CL6I2EGwo×GZMB and of the empty vector (TU/ml: 3.58×10^4 , 3.54×10^4 and 4.16×10^4 respectively) (data not shown). The supernatants were thus expected to produce similar transduction efficiencies, so the same volumes of virus supernatant of each sample were used for cell transduction.

2.2.11.5.2.2 Transduction of Cell Lines (NK-92 and K562)

To aid co-localisation of cells and viral particles and thus enhance transduction efficiencies, non-treated 6 or 12-well plates were coated for at least 2 h at 37°C (or overnight at 4°C) with 1.5 ml (6-well plates) or 1 ml (12-well plates) of 10 µg/ml of recombinant fibronectin fragment (RetroNectin®) in DPBS. Just prior to transduction, the excess RetroNectin® was removed and the wells rinsed with 1 ml of the appropriate cell-culture medium (NK-92 or K562 medium). Then, 1.5 ml of thawed, unconcentrated virus supernatant, 2.5×10^5 cells, 10 µg/ml protamine phosphate and a volume of the appropriate cell-culture medium to make a total of 2 ml were added to each well, using 12-well plates when only transducing 2×10^5 cells (NK-92) and 6-well plates when transducing 5×10^5 cells (K562). A *no virus*-control was also included. The plates were swirled gently to mix, incubated at 37°C, 5% CO₂, for 72 h, carefully adding 4 ml (6-well plate) or 2 ml (12-well plate) of fresh medium of the appropriate kind to each well after the initial 24 h. After the 72 h, the cells were harvested, counted and washed twice with DPBS (307×g, 10 min, brake, 21°C) to remove any residual virus supernatant and to change their biosafety level from 2 to 1. The cells were then resuspended and placed into cell culture at 37°C, 5% CO₂, as described in section 2.2.5. To quantify the success of the transduction, aliquots of the cells were analysed for EGFP expression using flow cytometry without any further staining. Staining for grH and grB and subsequent flow cytometrical analysis were also performed.

2.2.11.5.2.3 Transduction of Primary Cells

Primary NK cells expanded by Dr M. Hejazi (ITZ) according to Fujisaki *et al.*'s protocol (195) (also see section 2.2.7.5) were kindly provided by her for transduction by this study's author. For transduction,

Materials and Methods

non-treated 6-well plates were coated with RetroNectin®, as described in section 2.2.11.5.2.2. Then, 0.5 ml of thawed, concentrated virus supernatant, 5×10^5 expanded primary NK cells, 10 µg/ml protamine phosphate and NK-cell medium with IL-2 to make a total volume of 2.5 ml were added to each well. A *no virus*-control was also included. The plates were swirled gently to mix, incubated at 37°C, 5% CO₂ for 72 h, carefully adding 3 ml of fresh NK medium to each well after the initial 24 h. After the 72 h, the cells were harvested and washed as described in section 2.2.11.5.2.2. They were then resuspended in NK-cell medium with IL-2 at a concentration of 5×10^5 cells/ml and taken into cell culture at 37°C, 5% CO₂ in non-treated cell-culture plates or suspension cell-culture bottles, depending on cell numbers. Transduction success was evaluated and staining for grH and grB performed as for the transduced cell lines. The transduced primary cells were discarded after flow cytometrical analysis.

2.2.11.5.3 Sorting of Transduced Cell Lines

Once steady growth of the transduced cell lines had been established, EGFP⁺ cells were enriched through FACS. The cells were first counted, pelleted at 21°C, resuspended at a maximum of 5×10^7 /ml in 300 µl of the appropriate cell-culture medium, and transferred to sterile 5 ml flow-cytometry tubes via a 30 µm sterile filter. Using Beckman Coulter's MoFlo™ XDP cell sorter they were sorted, kindly performed by Dipl. Ing. K. Raba at the ITZ, into new sterile 5 ml flow-cytometry tubes that had been coated with the appropriate cell-culture medium overnight. After sorting, only EGFP⁺ cells were kept, washed with DPBS at 21°C, resuspended and placed into cell culture at 37°C, 5% CO₂, as described in 2.2.5.

2.2.11.5.4 Determination of Daily Growth Rate and Adjusted Number of Dead Cells

The transduced NK-92 cells were placed into prolonged cell culture, counted and fed twice or three times a week, as described in section 2.2.5. A counting chamber was used to count both live and dead cells. The daily growth rate on a particular day was calculated using the following equation:

$$\text{Growth Rate on Day } y = \frac{\text{Total Number of Live Cells on Day } y}{\text{Total Number of Live Cells on Day } x} (\text{Day } y - \text{Day } x)$$

The number of cells that had died between counting events, adjusted for growth rate, (# Dead) was calculated using the following equation:

$$\# \text{ Dead} = \frac{\text{Total Number of Dead Cells on Day } y - \text{Total Number of Dead Cells on Day } x}{\text{Daily Growth Rate on Day } y}$$

Serial flow cytometrical measurements, to assess the stability of EGFP expression, were also performed.

2.2.11.5.5 IL-2 Withdrawal Assay

In order to assess whether overexpression of grH provides NK-92 cells with a survival advantage, EGFP⁺ grH or empty vector-transduced NK-92 cells were thawed and placed into culture with NK-92 medium at a concentration of 1×10^6 /ml. On day 1 post-thawing, they were counted and fed to a concentration of 5×10^5 /ml. On day 3 post-thawing, they were counted, split into two equal-sized populations per sample: one population was fed to a concentration of 2×10^5 /ml with 'standard' NK-92 medium containing IL-2, while the other population was fed to the same concentration with NK-92 medium without IL-2. On day 7, the cells were counted again, and were fed to a concentration of 2×10^5 /ml using medium with or without IL-2, as before. On day 10, they were counted one final time. The daily growth rate and adjusted number of cells that had died were calculated for each day.

2.2.11.5.6 RNA Deep Sequencing (RNA-Seq)

In order to establish the transcriptomes of transduced NK-92 cells, the cells were prepared as follows: 1.25×10^5 each of non-transduced and EGFP⁺ transduced NK-92 cells that had been enriched by means of FACS were pelleted, resuspended in 320 μ l TRIzol® Reagent and transferred to a 2 ml freezing tube. The samples were then immediately frozen at -80°C prior to RNA-Seq. This is also the approach used by Prof. Dr M. Uhrberg's group at the ITZ to prepare licensed, unlicensed and adaptive peripheral blood NK cells, as well as NK cells expanded according to Fujisaki et al.'s protocol, for RNA-Seq, to all of which this study refers (see sections 3.1, 3.7 and 3.9.2.2). RNA-Seq itself was kindly performed by Prof. Dr L. Walter's group at the Primate Genetics Laboratory: in brief, after extraction of total RNA via phase separation using TRIzol® Reagent and chloroform, RNA was reverse transcribed and cDNA libraries were established, indexed and sequenced using the HiSeq 4000 System by Illumina. Sequence reads were demultiplexed, mapped to the human reference genome GRCh38 (245) using the STAR software (246), and read counts for individual genes calculated using the featureCounts package (247). Normalised count values for each gene were calculated using the DESeq2 package (248).

2.2.12 Statistics

Statistical analysis was performed using the software Prism 8 for macOS by GraphPad.

When comparing two groups, a paired t test was used when the groups were matched, and an unpaired t test when they were not. When comparing three or more matched groups, a repeated measures (RM) one-way analysis of variance (ANOVA) or, if any values were missing, a mixed-effects analysis, was used (an ordinary one-way ANOVA for three or more unmatched groups was not necessary in this study). When comparing two or more matched groups that were affected by two variables, a RM two-way ANOVA was used. One and two-way ANOVAs as well as mixed-effects analyses were followed by multiple comparisons tests: Tukey's test when comparing the mean of every sample to the mean of every other sample, and Sidak's test when comparing selected pairs of sample means.

p values were defined as follows: $p \geq 0.05 \triangleq$ not significant (ns), $p < 0.05 \triangleq$ * (significant), $p < 0.01 \triangleq$ ** (very significant), $p < 0.001 \triangleq$ *** (extremely significant), $p < 0.0001 \triangleq$ **** (extremely significant).

2.2.13 General Statements

In this manuscript, a superscripted '+' indicates positivity and a superscripted '-' negativity. When specific values are stated, a data set mean is referred to or, if the sample size (n) was 1, the single value is referred to, including for flow cytometry plots. Whenever a sample is stated to have been stained for certain proteins, this was followed by flow cytometrical analysis. Furthermore, unless otherwise stated, 'expression of a protein of interest' is used in this report as shorthand for the percentage of a particular cell population that is positive for that protein. Finally, only inhibitory KIRs and CD94/NKG2A (henceforth referred to as NKG2A) are examined as inducers of education, so the terms *education* and *licensing* are used interchangeably here, *licensing* being restricted to MHC-dependent education.

Unless explicitly stated otherwise, all experimental steps and analyses were performed by this study's author.

3 Results

3.1 NK-Cell Licensing and *GZMH* mRNA Levels – Transcriptome Data

In preliminary experiments, Prof. Dr M. Uhrberg's group at the ITZ and Prof. Dr L. Walter's group at the Primate Genetics Laboratory in Göttingen established transcriptomes of licensed and unlicensed NK cells. In brief, human PB CD56^{dim} NK cells were sorted into licensed and unlicensed groups via FACS based on expression of KIRs and NKG2A, and these cells' transcriptomes established through RNA-Seq. The raw data was kindly provided to and then analysed as below by this study's author. Licensed NK cells were defined as expressing a self-HLA class I-specific inhibitory KIR (KIR2DL3 in HLA-C1/C1 donors or KIR2DL1 in HLA-C2/C2 donors) but no other KIRs or NKG2A ('KIR^{Lic}') or expressing NKG2A but no KIRs ('NKG2A sp' (single-positive)), while unlicensed ones were defined as expressing a non-self-HLA class I-specific inhibitory KIR but no other inhibitory KIR or NKG2A ('KIR^{Unlic}') or neither a self-specific inhibitory KIR nor NKG2A ('DN' (double-negative)) NK cells. The data revealed that of the granzymes, grH was the only one of which there were significantly more transcripts in licensed than unlicensed NK cells, regardless of whether licensing had occurred via a KIR (KIR^{Lic}) or NKG2A (NKG2A sp) and regardless of whether the licensed cells were compared to KIR^{Unlic} or DN cells (mean number in DN: 845, NKG2A sp: 1561, KIR^{Lic}: 1863, KIR^{Unlic}: 950) (**Fig. 15**). On the other hand, and consistent with Goodridge *et al.* (144), there were no significant differences for *GZMB*, despite the high degree of sequence homology between the *GZMH* and *GZMB* genes. For *GZMA*, though there were significantly more transcripts in KIR^{Lic} (mean: 2502) than KIR^{Unlic} (mean: 2243) cells, the difference was much smaller than for *GZMH*, and there were no significant differences between KIR^{Lic} and DN cells, or NKG2A sp and KIR^{Unlic} or DN cells. Furthermore, the repeated measures (RM) one-way analysis of variance (ANOVA) showed no overall significance for *GZMA*, while it did for *GZMH*. Finally, the number of *GZMK* transcripts was highest in NKG2A sp NK cells (significantly so) but did not show a predilection for licensed cells *per se*. For *GZMM* there were also no significant differences.

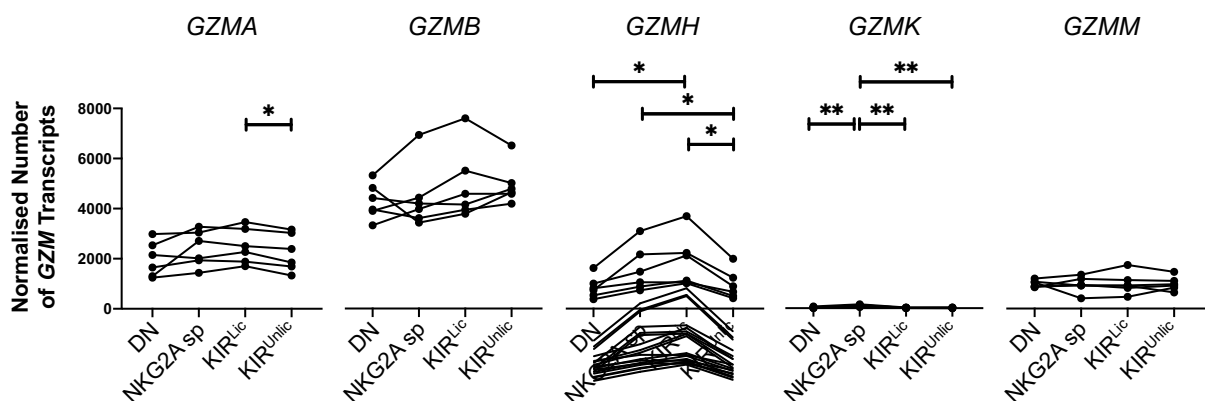


Fig. 15: There are significantly more transcripts of *GZMH* but not of *GZMA*, *B*, *K* or *M* in licensed than unlicensed NK cells. Transcriptome establishment and abbreviations: see text. DN and KIR^{Unlic} = unlicensed, NKG2A sp and KIR^{Lic} = licensed. n = 6. Significance testing was performed using a RM one-way ANOVA for each *GZM* followed by Tukey's test. For clarity, only (but all) significant results of Tukey's test are displayed. Overall significance levels of the ANOVAs: *GZMA*: ns, *GZMB*: ns, *GZMH*: **, *GZMK*: ***, *GZMM*: ns.

These data establish a likely link between NK-cell licensing and *GZMH* mRNA levels, a questionable link for *GZMA*, and no link for *GZMB*, *GZMK* or *GZMM*. Given the tremendous importance of NK-cell licensing for NK-cell biology, as well as the sparse knowledge available on grH, a deeper investigation of this likely link between NK-cell licensing and grH expression is essential, especially at the protein level, as well of grH function and expression patterns more generally, setting the stage for this study.

3.2 Donor Characteristics

Peripheral and cord blood was used to study expression of grH by NK cells. **Table 28** shows the donor characteristics, particularly with regard to *KIR* genotype (for reference, see **Table 1** and **Table 29**) and HLA-C1/C2 and HLA-Bw4/Bw6 status, as determined by KIR, HLA-C1/C2 and HLA-Bw4/Bw6-typing. **Table 29** shows additional *KIR* genotypes that did not match those cited in **Table 1**.

Table 28: Characteristics of blood donors.

Donor	<i>KIR</i> Haplotype	<i>KIR</i> Genotype	HLA-C1/-C2 Status	# of Bw4 Epitopes	NKG2C Expansion
PB1	A/A	1	C1/C1	1	
PB2	Bx	4	C1/C1	0	
PB3	A/A	1	C1/C1	0	
PB4	A/A	1	C1/C1	0	
PB5	Bx	34	C1/C1	2	
PB6	A/A	1	C1/C1	1	
PB7	Bx	4	C1/C1	1	
PB8	Bx	*42	C1/C1	1	
PB9	Bx	12	C1/C1	1	
PB10	A/A	1	C1/C1	0	
PB11	Bx	*41	C1/C1	1	
PB12	A/A	1	C1/C1		
PB13	A/A	1	C1/C1		
PB14	A/A	1	C1/C1		
PB15	A/A	1	C1/C1		
PB16	A/A	1	C1/C1		
PB17	A/A	1	C1/C1		
PB18	A/A	1	C1/C1		
PB19	A/A	1	C1/C1		
PB20	Bx	*46	C1/C2	3	
PB21	A/A	1	C1/C2	2	
PB22	Bx	*43	C1/C2	0	
PB23	Bx	2	C1/C2	3	
PB24	A/A	1	C1/C2	1	
PB25	A/A	1	C1/C2		
PB26	A/A	1	C1/C2		
PB27	A/A	1	C2/C2	1	
PB28	A/A	1	C2/C2	3	Yes
PB29	A/A	1	C2/C2		
PB30	Bx	2	C2/C2		
PB31	Bx	2	C2/C2		
PB32	A/A	1	C2/C2		
PB33	Bx	2	C2/C2		
PB34					Yes
PB35					Yes
PB36	Bx	4			
PB39			C1/C1		
PB40			C1/C2		
PB41			C1/C1		Yes
CB1	Bx	4	C1/C1		
CB2	Bx	*42	C1/C1		
CB3	Bx	*44	C1/C1		
CB4	A/A	1	C1/C1		
CB4	Bx	5	C1/C2		
CB6	Bx	*45	C1/C2		

PB = peripheral-blood donor, CB = cord-blood donor, # = number, Bw4 = HLA-Bw4, blank = unknown.

Table 29: Additional *KIR* genotypes found in the donors in this study. Naming of *KIR* genotypes was arbitrary.

Haplotype	Genotype	2DL1	2DL2	2DL3	2DL4	2DL5	3DL1	3DL2	3DL3	2DS1	2DS2	2DS3	2DS4	2DS5	3DS1
Bx	*41														
Bx	*42														
Bx	*43														
Bx	*44														
Bx	*45														
Bx	*46														

Bx = either hetero- or homozygous for group B haplotypes. Grey = *KIR* gene present, white = *KIR* gene absent.

3.3 General Gating Strategy

Since flow cytometry was one of the main methods used in this study, an overview of the general gating strategy employed is provided (**Fig. 16**). After staining of PBMCs and flow cytometrical data acquisition, compensation to correct for spectral overlap of fluorochromes was performed manually

Results

using Beckman Coulter's Kaluza Analysis Software. Lymphocytes within PBMCs or CBMCs were identified based on forward scatter (size) and side scatter (granularity). Cells counted individually by the flow cytometer (singlets) were focused on, excluding doublets by their larger area but similar height compared with singlets. NK cells were identified by CD56-positivity and CD3-negativity, and CD56^{dim} and CD56^{bright} NK cells could be distinguished. Gating on further markers was performed using clearly negative populations as a guide and keeping gates as consistent as possible between different samples. For ease of reading, the 'Lymphocytes/Singlets' gate is henceforth referred to as 'Lymphocytes'.

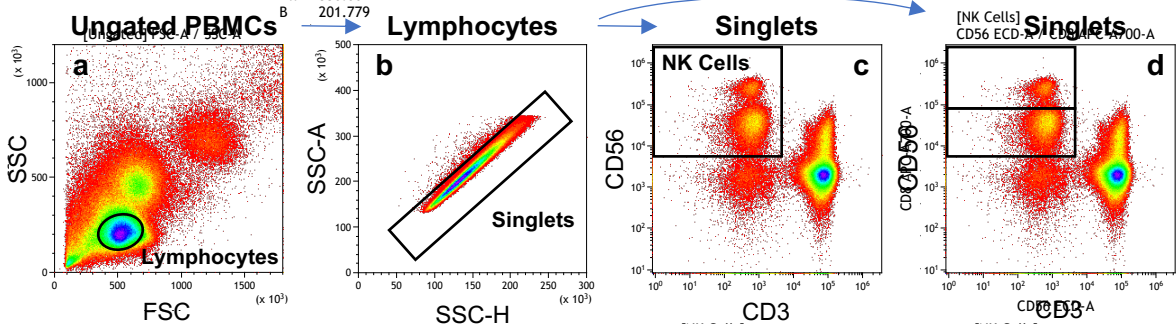


Fig. 16: Representative flow cytometry plots to show gating of antibody-labelled PBMCs. A gate was first set on lymphocytes (a), then singlets (b), then NK cells (CD56⁺CD3⁻) (c), dividing them (d) into CD56^{dim} (bottom gate) and CD56^{bright} (top gate) where appropriate. FSC = forward scatter, SSC = side scatter, A = area, H = height.

3.4 GrH Antibody Selection

For staining of grH for flow cytometry, a suitable antibody first needed to be found (Fig. 17), since flow cytometry data for grH expression was not readily available in the literature, with no information on anti-grH antibodies used in flow cytometry. So, thawed PBMCs were stained for CD56 and CD3, and different methods of staining for grH (or grB for comparison) were tested. First, the anti-grH monoclonal antibody (mAb) clone 3G10F4 (Sino Biological), conjugated manually with phycoerythrin (PE), was tested. It yielded no acceptable distinguishability between positive and negative populations (Fig. 17a) despite successful conjugation, as had been confirmed through staining of antibody capture beads (data not shown). A biotinylated polyclonal anti-grH antibody (R&D Systems) for primary and anti-biotin-VioGreen (Miltenyi Biotec) for secondary staining produced far superior results (Fig. 17b). Secondary staining using anti-biotin-VioGreen also led to far better distinguishability between positive and negative populations than using streptavidin-APC/Cy7, the latter yielding a signal too strong for signal compensation to be possible (Fig. 17c). Staining for grH using the biotinylated antibody and anti-biotin yielded population morphologies similar to those observed when staining for grB using the anti-grB mAb GB11 (Fig. 17d), which provided an internal control of the plausibility of the staining method.

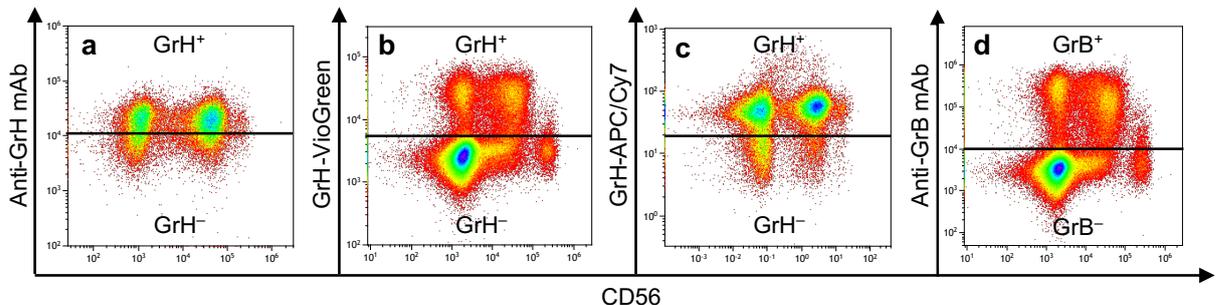


Fig. 17: Representative flow cytometry plots to show superiority of using biotinylated polyclonal anti-grH with secondary anti-biotin-VioGreen for grH staining compared with other methods; grB staining is shown for comparison. Staining and flow cytometrical analysis were performed as described in the text. GrH⁺ and GrH⁻ (a-c) and GrB⁺ and GrB⁻ (d) populations within lymphocytes were identified. a: PE-conjugated mAb. b: polyclonal anti-grH + anti-biotin-VioGreen. c: polyclonal anti-grH + streptavidin-APC/Cy7. d: anti-grB mAb.

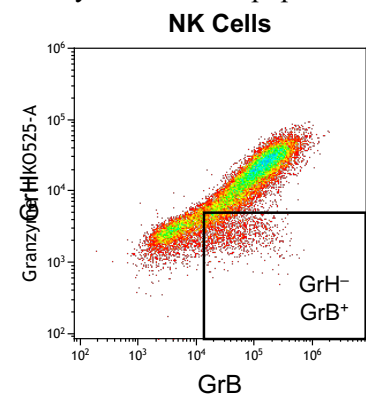
Results

Of note, Miltenyi Biotec assure that their anti-biotin antibodies do not bind to free biotin in cell-culture media (249), ensuring specificity.

Next, an optimum grH staining protocol, described in section 2.2.6.2.2, was established. In brief, adding the secondary antibody only after the primary antibody had been incubated for 30 minutes and washed, was far superior to adding the primary and secondary antibodies simultaneously or adding the secondary antibody 15 minutes after the primary antibody without a wash step in between (data not shown).

As grH and grB are structurally very similar, determination of the specificity of the anti-grH antibody with regard to grB was important. For this purpose, grH and grB-staining of NK cells was compared (**Fig. 18**). For staining of grB, the anti-grB mAb clone GB11 was again used, and is throughout this study. As expected, there was a large degree of overlap between cells positive for grH and for grB, which was most likely due to expression of both granzymes by NK cells but may have been due to lack of antibody specificity. A population negative for grH but positive for grB could be observed however, indicating that most of this overlap came from expression of both granzymes by the same cell population rather than lack of specificity of the anti-grH antibody. The anti-grH antibody, despite being polyclonal, was thus deemed satisfactory.

Fig. 18: Representative flow cytometry plot confirming specificity of anti-grH with regard to grB. Thawed PBMCs stained for CD56, CD3, grH and grB were analysed flow cytometrically. NK cells are shown. The square gate shows a grH⁺ grB⁺ population within NK cells.



3.5 GrH and GrB Expression by Lymphocytes

Before attempting to confirm the mRNA data displayed in **Fig. 15**, it was important to first examine grH expression by different lymphocyte subtypes, both from PB and from CB.

3.5.1 GrH and GrB Expression by NK Cells, NK-Like T Cells, T Cells and Non-NK/Non-T Cells

So far, studies assessing grH expression by different cell types have focused mainly on western blotting and PCR-based analyses (183),(189),(190),(191),(192), whole-cell flow cytometry-based approaches somewhat lacking, except for one brief mention of flow cytometrical examination of peripheral-blood NK-cell grH expression (178). Having established an effective staining protocol for grH (section 3.4), this study therefore employed flow cytometry to examine grH expression by different lymphocyte subtypes and compared it with grB. For this purpose, thawed PBMCs were stained for CD56, CD3, CD8 and grH or grB. Within lymphocytes, grH or grB expression by NK cells (CD56⁺CD3⁻), NK-like T cells (CD56⁺CD3⁺), CD8⁺ cytotoxic T cells (CD56⁻CD3⁺CD8⁺), CD4⁺ T cells (here: CD56⁻CD3⁺CD8⁻), and non-NK/non-T lymphocytes (CD56⁻CD3⁻) (eg B cells) was examined. As **Fig. 19** shows, CD56 was the main factor in determining grH and grB expression, higher grH and grB expression being observed when CD56 was present in a lymphocyte. Both grH and grB expression were highest in NK cells (grH⁺: 76.8%, grB⁺: 89.6%), significantly higher than in the other main cytotoxic lymphocyte type CD8⁺ T cells (grH⁺: 30.5%, grB⁺: 36.1%). The second highest expression was observed in NK-like T cells (grH⁺: 56.7%, grB⁺: 69.6%), though the differences in grH expression between NK-like T cells and both NK cells and CD8⁺ T cells lacked statistical significance. GrH and grB expression by NK cells, NK-like T cells and CD8⁺ T cells was significantly higher than by both CD4⁺ T cells (grH⁺: 9.39%, grB⁺: 16.7%) and CD56⁻

Results

CD3⁻ lymphocytes (grH⁺: 9.49%, grB⁺: 12.4%), showing that both granzymes are predominantly found in cytotoxic lymphocytes. GrB expression overall appeared to be higher than grH expression.

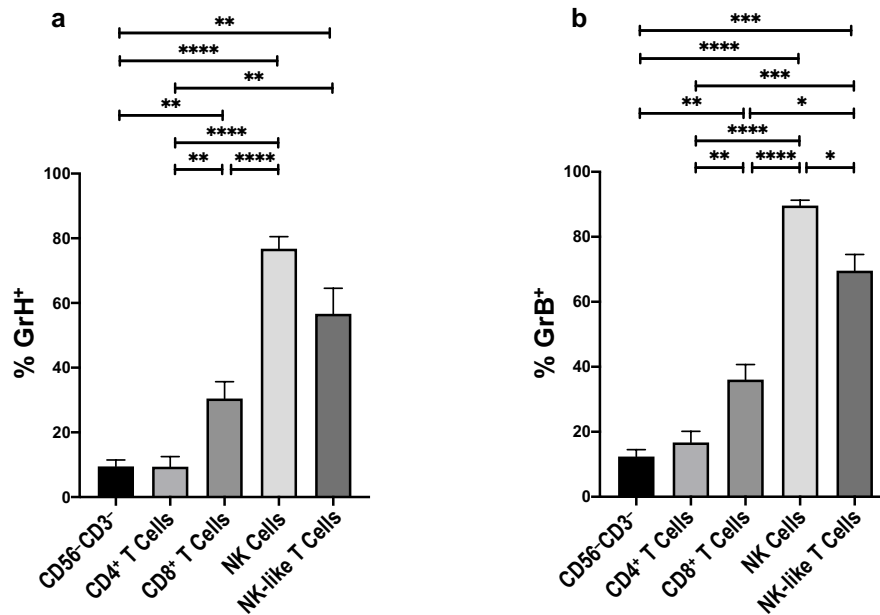


Fig. 19: GrH expression is higher in cytotoxic than non-cytotoxic lymphocytes, and, of those, significantly higher in NK cells than CD8⁺ T cells. Thawed PBMCs were stained and analysed as described in the text. The percentage of NK cells (CD56⁺CD3⁻), NK-like T cells (CD56⁺CD3⁺), CD8⁺ T cells (CD56⁻CD3⁺CD8⁺), CD4⁺ T cells (CD56⁻CD3⁺CD8⁻), and non-NK/non-T lymphocytes (CD56⁻CD3⁻) that were grH⁺ (a) or grB⁺ (b) was determined. n = 9. Bars represent the data set means and the standard error or the mean (SEM). For significance testing a RM one-way ANOVA was used for both plots, followed by Tukey's test, of which, for clarity, only (but all) significant results are displayed. The overall level of significance of the ANOVAs was **** for both plots.

3.5.2 GrH and GrB Expression by CD56^{dim} and CD56^{bright} NK Cells

Next, grH expression by NK cells was looked at in more detail by comparing CD56^{dim} with CD56^{bright} NK cells, examining grB for comparison. Thawed PBMCs were stained for CD56, CD3, grH and grB, and grH and grB expression by CD56^{dim} and CD56^{bright} NK cells was analysed. As **Fig. 20a** shows, grH expression by CD56^{dim} NK cells (80.5%) was significantly higher than by CD56^{bright} NK cells (11.4%), showing that grH is almost exclusively expressed by the more mature CD56^{dim} subtype. A similar result was observed for grB (92.0% (dim) vs 28.3% (bright)) (**Fig. 20b**). Direct comparison of grH and grB revealed that CD56^{dim} NK-cell expression of grB (92.0%) was significantly higher than of grH (80.5%) (**Fig. 20c**). Of note, the transcriptome data described in section 3.1 showed that *GZMH* mRNA levels were higher in CD56^{dim} than CD56^{bright} NK cells (data not shown), corroborating the findings here.

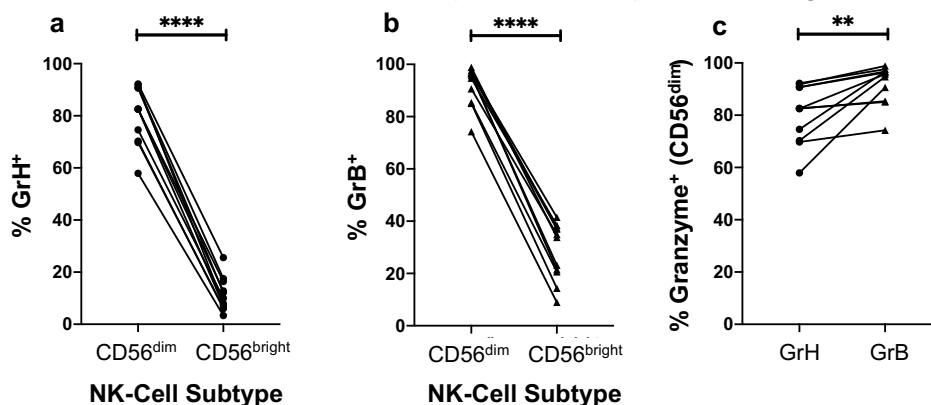


Fig. 20: GrH expression by CD56^{dim} NK cells is significantly higher than by CD56^{bright} NK cells. Thawed PBMCs were stained and analysed as described in the text. a and b: the percentage of CD56^{dim} vs CD56^{bright} NK cells that are grH⁺ (a) or grB⁺ (b). c: the percentage of CD56^{dim} NK cells that are grH⁺ vs grB⁺. n = 11. For significance testing, a paired t test was used for each plot.

Results

3.5.3 GrH Expression by PB and CB-Derived CD56^{dim} NK Cells

Having compared grH expression by PB-derived CD56^{dim} and CD56^{bright} NK cells, grH expression by CD56^{dim} and CD56^{bright} NK cells derived from PB were compared with those from CB, given the lower maturity of CB than PB-derived NK cells. Thawed PBMCs and CBMCs were stained for CD56, CD3 and grH or grB, and grH or grB expression by CD56^{dim} and CD56^{bright} NK cells was analysed.

Interestingly, grH expression by PB-derived CD56^{dim} NK cells (80.5%) was significantly higher than by CB-derived CD56^{dim} NK cells (63.3%) (**Fig. 21a**). GrH expression by CD56^{bright} NK cells was not significantly different between PB and CB (11.4% (PB) vs 8.84% (CB)) (**Fig. 21b**). GrB expression by PB-derived CD56^{dim} NK cells (92.0%) was also significantly higher than by CB-derived CD56^{dim} NK cells (68.9%) (**Fig. 21c**). These results lend weight to the assumption of a lower maturity of CB-derived NK cells compared with PB-derived NK cells, possibly associated with a lower effector potential.

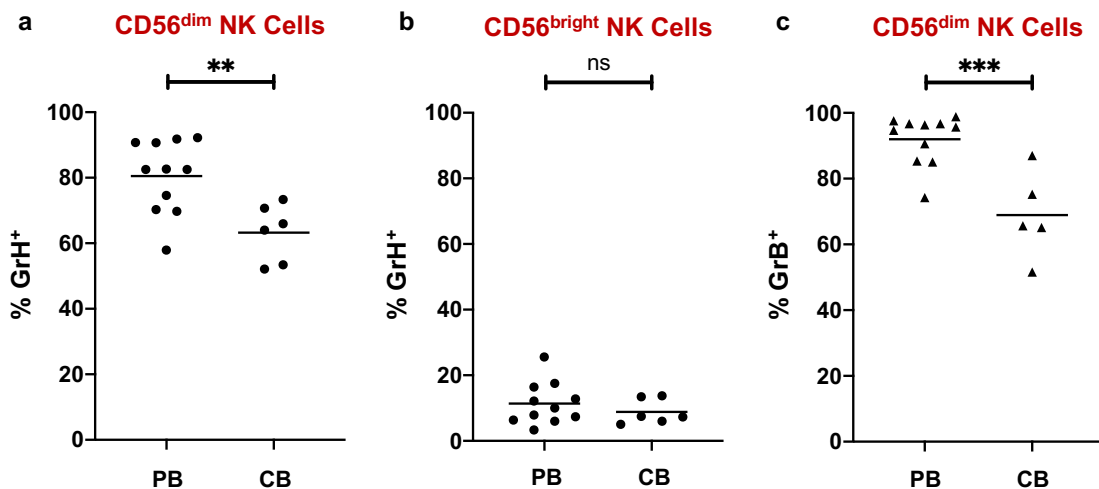


Fig. 21: GrH expression is significantly higher in PB than CB-derived CD56^{dim} NK cells. Thawed PBMCs and CBMCs were stained and analysed as described in the text. GrH expression as a percentage of CD56^{dim} (a) and CD56^{bright} (b) PB and CB-derived NK cells positive for it is shown, as well as grB expression by CD56^{dim} NK cells (c). n (PB) = 11, n (CB, grH) = 6. n (CB, grB) = 5. Individual data points with data set means (horizontal bars) are shown. Significance testing was performed using an unpaired t test for each plot.

3.6 NK-Cell Education and GrH Expression; GrB for Comparison

As suggested by the transcriptome data that led to this closer examination of grH in the context of NK-cell education, *GZMH*, but not *GZMB*, mRNA levels are higher in licensed than unlicensed NK cells. The confirmation of this link at the protein level forms a crucial pillar of this study and, having analysed grH expression by different lymphocyte and NK-cell subtypes, can finally be addressed.

3.6.1 Staining Strategy and Receptor-Based Definition of NK-Cell Populations

PBMC samples were categorised based on their donors' *KIR* genotypes and HLA-C1/C2 (henceforth referred to as C1/C2) as well as HLA-Bw4 (henceforth referred to as Bw4) statuses (**Table 28**), to be able to identify licensed and unlicensed NK cells and examine these for grH expression. Since KIR2DL3, KIR2DL1 and KIR3DL1 (henceforth referred to as 2DL3, 2DL1 and 3DL1 respectively) are the main inhibitory KIRs encoded by group A *KIR* haplotypes, and since CD94/NKG2A (henceforth referred to as NKG2A) is a ubiquitously expressed, crucial inhibitory NK-cell receptor also involved in NK-cell education, these receptors were chosen to enable a reliable determination of education status.

Results

As described in section 1.4, interaction between an NK-cell inhibitory receptor and its cognate self-ligand, mainly self-HLA class I, leads to NK-cell licensing. The receptor-ligand pairs of interest here are thus 2DL3-C1, 2DL1-C2, 3DL1-Bw4 and NKG2A-HLA-E. Therefore, for example, 2DL3⁺ NK cells are licensed in C1/C1 donors but not in C2/C2 donors, while it is the other way around for 2DL1⁺ NK cells. Inhibitory KIR⁻/NKG2A⁻ ('double-negative', DN) NK cells were considered to be unlicensed, regardless of C1/C2/Bw4 status.

For the cleanest possible analyses, single receptor type-positive (sp) NK cells were examined, but populations positive for two (dp) or three receptors (tp) were also analysed for comparison. Due to the lower number of KIRs on group *A* KIR haplotypes compared with group *B* haplotypes, which permits simultaneous staining of nearly all KIRs expressed, samples from group *A* KIR haplotype-homozygous donors were used wherever possible. A further reason for preferentially choosing such samples was that the antibodies used to stain for 2DL3, clones GL183 and DX27, also recognise 2DL2 and 2DS2, which are not expressed by group *A/A* KIR haplotype donors and thus cannot be stained for. However, to obtain larger sample sizes, donors expressing one or two group *B* haplotypes were also included occasionally. Therefore, to analyse granzyme expression by licensed and unlicensed NK cells, thawed PBMCs were stained for CD56, CD3, 2DL2/3/S2, 2DL1, 3DL1, NKG2A and grH or grB and analysed using flow cytometry. Receptor-positive populations within CD56^{dim} NK cells were identified to define DN, sp, dp and tp NK-cell populations, which were in turn analysed for granzyme-positivity.

3.6.2 Correlation between NK-Cell Licensing and GrH Expression

As **Fig. 22**, **Fig. 23** and **Fig. 24** show, NK-cell licensing strongly correlated with higher expression, at the protein level, of grH, confirming the transcriptome data displayed in **Fig. 15**.

In samples from group *A/A* KIR haplotype (*KIR* genotype 1) donors, grH expression by licensed CD56^{dim} NK was significantly higher than by unlicensed NK cells. This was the case for samples with all three C1/C2 statuses (C1/C1: **Fig. 22c-e**, C1/C2: **Fig. 22f-h** and C2/C2: **Fig. 22i-k**), when comparing self-specific with non-self-specific inhibitory KIR sp NK cells, but also when comparing the former with DN cells (which are unlicensed in all three C1/C2 statuses)–

- C1/C1, licensed 2DL3 sp vs unlicensed 2DL1 sp vs DN, grH⁺: 85.9% vs 61.5% vs 57.5%
- C1/C2, licensed 2DL3 sp vs licensed 2DL1 sp vs DN, grH⁺: 80.0% vs 89.8% vs 49.6%
- C2/C2, licensed 2DL1 sp vs unlicensed 2DL3 sp vs DN, grH⁺: 90.1% vs 57.8% vs 49.1%

There was no significant difference in grH expression between non-self-specific inhibitory KIR sp and DN cells. Furthermore, the difference in grH expression between 2DL3 sp and 2DL1 sp NK cells in C1/C2 donors was also non-significant, but, notably, grH expression by 2DL1 sp NK cells among these samples was somewhat higher than by 2DL3 sp NK cells, possibly indicating a role for differences in the strength of inhibitory receptor:ligand interactions.

To aid visualisation of the data just described, representative flow cytometry plots (**Fig. 22a** and **b**) are also shown. They not only give a visual depiction of the higher percentage of licensed compared with unlicensed NK cells that are grH⁺, but they also show that licensed grH⁺ NK cells were *more* positive for grH, ie expressed higher levels of it per cell, than unlicensed grH⁺ NK cells, as demonstrated by a higher grH mean fluorescence intensity (MFI). Though the MFI data for the other samples included in the analyses are not shown, they displayed the same trend, which was in line with the percentage data.

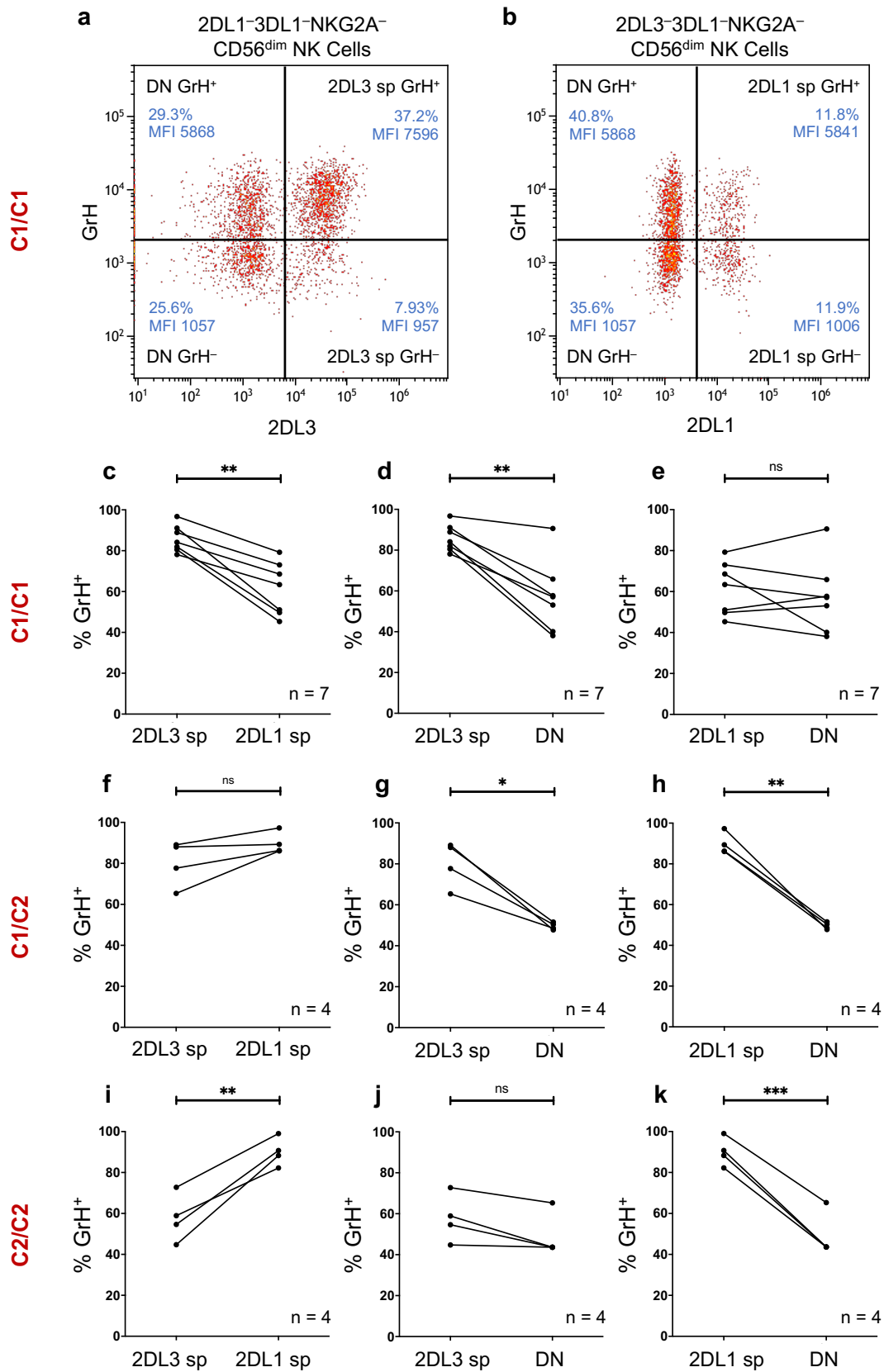


Fig. 22: NK-cell licensing via C1 and C2-specific KIRs correlates strongly and highly significantly with grH expression. Thawed PBMCs from group *A/A* *KIR* haplotype (*KIR* genotype 1) donors were stained and analysed as described in the text. **a** and **b**: representative flow cytometry plots showing grH expression by licensed (2DL3 sp) and unlicensed (2DL1 sp and DN) NK cells in a C1/C1 donor. **c-k**: percentage of licensed and unlicensed NK cells that were grH⁺. HLA statuses: C1/C1 (**a-e**), C1/C2 (**f-h**), C2/C2 (**i-k**). **c-k**: Significance testing for each plot was performed using a paired t test.

Results

The correlation between licensing and grH expression was so strong that it held true even when samples from KIR group *B* haplotype donors, in whom the licensed populations were less stringently definable, were included in addition to samples from group *A/A* KIR haplotype donors, the resulting larger sample size leading to even higher levels of significance (**Fig. 23**). Notably, inclusion of such samples led to a small but significant difference in grH expression between 2DL2/3/S2 ‘sp’ and DN NK cells in C2/C2 samples (**Fig. 23h**), possibly due to the variable genetic background and inclusion of 2DL2⁺ cells, which bind to C2 epitopes with weaker – though still functionally relevant, particularly for licensing – avidity (see **Table 2**).

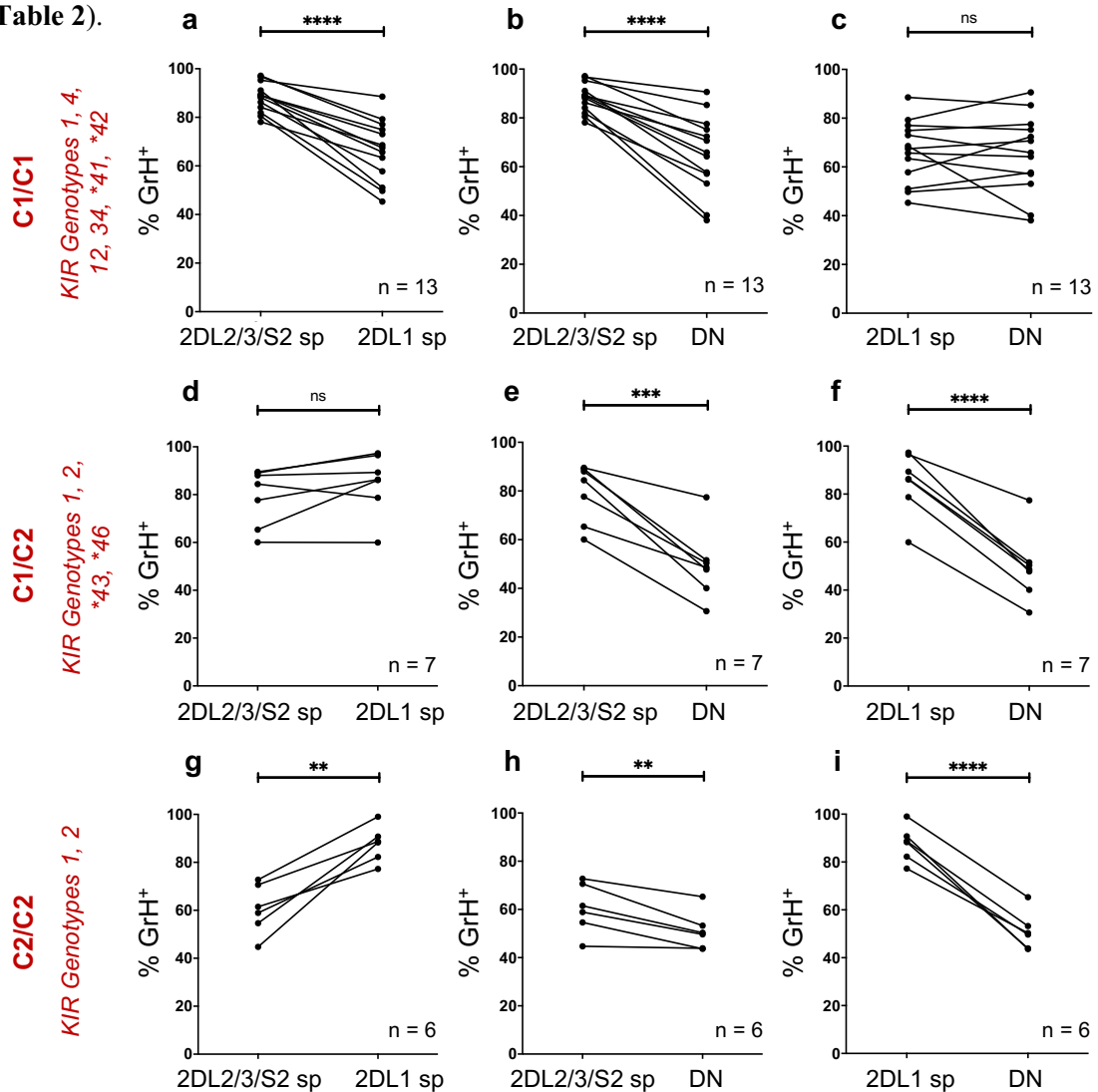


Fig. 23: The correlation between NK-cell licensing via C1- and C2-specific KIRs and grH is also evident when samples from group *Bx* KIR haplotype donors are included in the analysis in addition to samples from group *A/A* KIR haplotype donors. The figure was created and contains information presented and analysed in the same way as **Fig. 22c-k**. **a-c:** C1/C1, **d-f:** C1/C2, **g-i:** C2/C2. KIR genotypes are indicated.

Fig. 24 shows that education via 3DL1 in Bw4⁺ donors (**Fig. 24a**) and via NKG2A in donors with any C1/C2 or Bw4/Bw6 status (**Fig. 24c**) also strongly correlated with grH expression, the differences being highly significant (grH⁺ 3DL1 sp vs DN from Bw4⁺ donors: 90.4% vs 43.7%; grH⁺ NKG2A sp vs DN: 75.0% vs 52.7%). When 3DL1 had no cognate ligand, as in Bw4⁻Bw6⁺ donors, the difference in grH expression between 3DL1 sp and DN NK cells was not significant (**Fig. 24b**), in line with the results for 2DL3 sp or 2DL1 sp NK cells when 2DL3 or 2DL1 have no cognate ligand, as in C2/C2 or C1/C1 donors respectively (**Fig. 22** and **Fig. 23**). However, to be able to make any definitive statements

Results

about this phenomenon, particularly since there appeared to be a trend towards higher grH expression in 3DL1 sp (82.5%) than DN (68.5%) cells in these donors, the sample size needs to be increased.

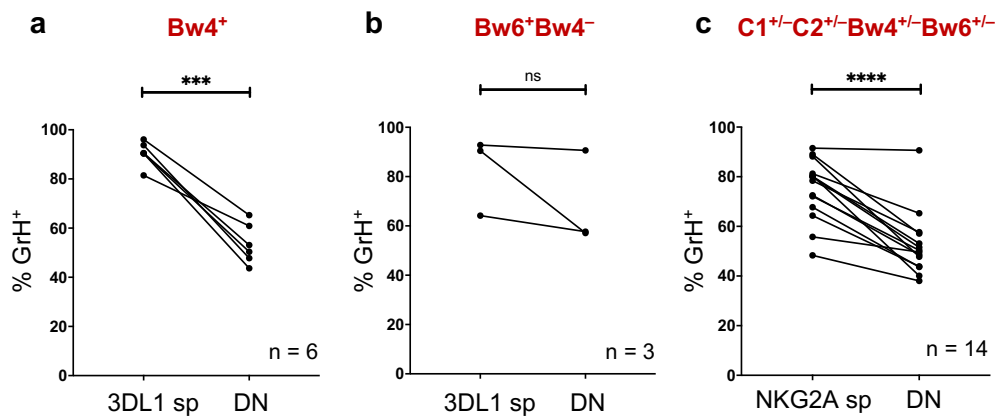


Fig. 24: NK-cell licensing via 3DL1 and NKG2A also correlates strongly and highly significantly with grH expression. Data were acquired and are displayed as in Fig. 22c-k. **a:** HLA-Bw4⁺, 3DL1 sp NK cells = licensed; **b:** Bw6⁺Bw4⁻, 3DL1 sp NK cells = unlicensed; **c:** all C1/C2/Bw4/Bw6 combinations, NKG2A sp NK cells = licensed. All plots: DN NK cells = unlicensed. Only group *AA* samples are shown. The *n* is displayed within each plot, individual data points, and significance testing for each plot was performed using a paired t test.

The influence of the presence of more than one self-specific inhibitory receptor on grH expression is shown in the next section.

3.6.3 GrH Expression by NK Cells Expressing more than one Type of Receptor

To test whether grH expression by licensed NK cells is affected by the number of different types of inhibitory receptors present, CD56^{dim} NK cells expressing one, two or three of a self-specific inhibitory KIR, a non-self-specific inhibitory KIR, and NKG2A were compared for grH expression.

The data revealed that the presence of and therefore licensing via a self-specific inhibitory KIR (2DL3 in C1/C1 donors, 2DL3 or 2DL1 in C1/C2 donors, and 2DL1 in C2/C2 donors) led to highest grH expression (higher than in NK cells expressing NKG2A only, see below), regardless of whether or not a non-self-specific inhibitory KIR or NKG2A was also present. For instance, in samples from C1/C1 donors (**Fig. 25a**) there were no significant differences in grH expression between NK cells expressing 2DL3 only (85.9%), 2DL3 plus 2DL1 (88.2%), 2DL3 plus NKG2A (89.6%), or 2DL3 plus 2DL1 plus NKG2A (88.0%). This phenomenon was reproducible in C2/C2 donors for 2DL1 (2DL1 sp grH⁺: 81.4%, 2DL3⁺2DL1⁺: 81.4%, 2DL1⁺NKG2A⁺: 78.4%, 2DL3⁺2DL1⁺NKG2A⁺: 79.8%) (**Fig. 25c**). Furthermore, whether only one or more than one type of self-specific inhibitory KIR was expressed did not significantly affect grH expression, as in the case of 2DL3⁺2DL1⁺ compared with 2DL3 sp or 2DL1 sp NK cells in C1/C2 donors (2DL3 sp grH⁺: 80.0%, 2DL1 sp: 89.8%, 2DL3⁺2DL1⁺: 93.8%) (**Fig. 25b**). Of note, 2DL1 appeared to have a stronger effect than 2DL3: in C1/C2 samples grH expression by NK cells licensed via 2DL1 was higher than by NK cells licensed via 2DL3 (though not significantly so) (**Fig. 25b**). This may be due to differences in ligand-binding affinities between 2DL3 and 2DL1.

As an internal control, the licensing role of NKG2A shown in **Fig. 24** is corroborated by grH expression by unlicensed NK cells expressing a non-self-specific inhibitory KIR only (2DL1 sp cells in C1/C1 donors (61.5%) (**Fig. 25a**) and 2DL3 sp cells in C2/C2 donors (44.5%) (**Fig. 25c**) being significantly lower than by licensed NKG2A sp cells (grH⁺ in NKG2A sp in C1/C1: 78.7%, in C2/C2: 55.2%).

Results

As alluded to above, in samples from all three C1/C2 backgrounds, grH expression by NK cells expressing a self-specific inhibitory KIR (and thus licensed via this KIR), regardless of whether the KIR was expressed alone or with a non-self-specific inhibitory KIR and/or with NKG2A, was higher than by NK cells expressing NKG2A and no self-specific inhibitory KIR (and thus licensed via NKG2A), regardless of whether NKG2A was expressed alone or together with a non-self-specific inhibitory KIR. Though not always significant, the trend was present for donors with all three C1/C2 statuses: present but non-significant for C1/C1 donors (**Fig. 25a**) and 2DL3 sp cells in C1/C2 donors (**Fig. 25b**), and present and significant for most comparisons in C1/C2 (**Fig. 25b**) and C2/C2 donors (**Fig. 25c**).

Mean grH expression was as follows:

- C1/C1 grH⁺: NKG2A sp: 78.7%, 2DL3 sp: 85.9%, 2DL3⁺NKG2A⁺: 89.6%, 2DL1⁺NKG2A⁺: 76.6%, 2DL3⁺2DL1⁺: 88.2%, 2DL3⁺2DL1⁺NKG2A⁺: 88.0%
- C1/C2 grH⁺: NKG2A sp: 78.2%, 2DL3 sp: 80.0%, 2DL1 sp: 89.8%, 2DL3⁺NKG2A⁺: 92.2%, 2DL1⁺NKG2A⁺: 93.4%, 2DL3⁺2DL1⁺: 93.8%, 2DL3⁺2DL1⁺NKG2A⁺: 93.6%
- C2/C2 grH⁺: NKG2A sp: 55.2%, 2DL1 sp: 81.4%, 2DL3⁺NKG2A⁺: 65.5%, 2DL1⁺NKG2A⁺: 78.4%, 2DL3⁺2DL1⁺: 81.44%, 2DL3⁺2DL1⁺NKG2A⁺: 79.8%

The difference in grH expression between NK cells licensed via a KIR vs via NKG2A was again more pronounced in NK cells licensed via 2DL1 than via 2DL3.

The data indicate that KIRs likely have a stronger licensing effect than NKG2A does.

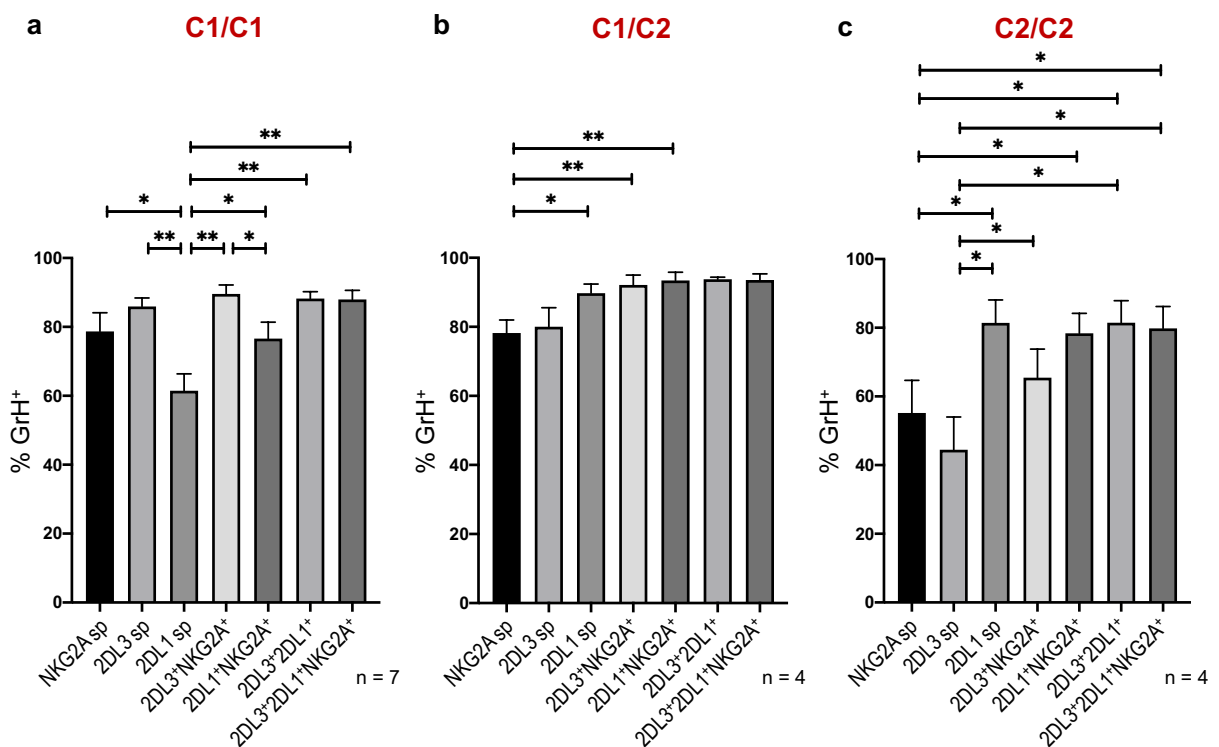


Fig. 25: There is no significant difference in grH expression between CD56^{dim} NK cells expressing one type of self-specific inhibitory KIR only and CD56^{dim} NK cells expressing a self-specific inhibitory KIR plus a non-self-specific inhibitory KIR or NKG2A. Staining of thawed PBMCs from C1/C1 (a), C1/C2 (b) and C2/C2 (c) group *A/A* KIR haplotype donors, identification of DN, sp, dp and tp populations and measurement of grH expression were performed as described in section 3.6.1. Bars represent the data set means and the SEM, each bar showing an NK-cell population with the indicated receptor status. Significance testing was performed using a RM one-way ANOVA followed by Tukey's test, of which only (but all) significant results are displayed. The overall levels of significance of the ANOVAs were *** (a), * (b) and ** (c).

Notably, the lack of significance in some of the described differences may be due to potential type II errors being committed when using ANOVAs and post hoc multiple comparisons tests, rather than due to the lack of an actual biological difference, indicating the importance of taking trends into account, too.

Results

3.6.4 NK-Cell Licensing and GrB Expression

Unlike grH, where a correlation between NK-cell licensing and grH expression is a new finding, the structurally very similar grB has been implicated in licensing in the literature (144). Neither Goodridge *et al.* (144) nor this study (**Fig. 15**) show a correlation between licensing and *GZMB* mRNA levels, but Goodridge *et al.* do show a potential correlation between licensing and grB protein expression. To study this somewhat baffling discrepancy further, this study examined grB in the same manner as grH.

When examining grB expression as a percentage of licensed and unlicensed cells positive for it, the data did not show a clear correlation between it and NK-cell licensing (**Fig. 26a-e**), in line with the transcriptome data. There were no significant differences in grB expression between self-specific inhibitory KIR sp and non-self-specific inhibitory KIR sp NK cells in either C1/C1 (**Fig. 26c**), C1/C2 (**Fig. 26d**) or C2/C2 (**Fig. 26e**) donors. However, grB expression by both self-specific inhibitory KIR sp and non-self-specific inhibitory KIR sp NK cells was significantly higher than by DN cells, suggesting that the presence of any inhibitory KIR, rather than a self-specific inhibitory KIR, was the determining factor for grB expression. The mean numbers of grB expression were as follows:

- C1/C1, licensed 2DL3 sp vs unlicensed 2DL1 sp vs DN, grB⁺: 92.8% vs 96.9% vs 79.4%
- C1/C2, licensed 2DL3 sp vs licensed 2DL1 sp vs DN, grB⁺: 91.2% vs 98.6% vs 69.8%
- C2/C2, licensed 2DL1 sp vs unlicensed 2DL3 sp vs DN, grB⁺: 99.3% vs 89.6% vs 86.1%.

Of note, in C1/C2 donors, grB expression was significantly higher in 2DL1 sp than in 2DL3 sp NK cells, and, though not statistically significant, the trend in C2/C2 donors suggests that grB expression was higher in 2DL1 sp than 2DL3 sp NK cells. These results indicate that ligand binding avidities, and thus potentially licensing, may, in fact, play some role, too, though less pronounced than for grH expression, necessitating an examination of grB MFI.

When examining grB expressing as MFI rather than as a percentage (**Fig. 26f-h**), a correlation between grB expression and licensing is seen. While countering the transcriptome data in **Fig. 15**, this is in line with Goodridge *et al.*. The grB MFI of licensed NK cells was significantly higher than that of unlicensed NK cells in samples from all three C1/C2 backgrounds (C1/C1: **Fig. 26f**, C1/C2: **Fig. 26g**, C2/C2: **Fig. 26h**), mirroring the data for grH. Though the difference between 2DL3 sp and DN cells in C1/C1 donors was non-significant (**Fig. 26f**), the trend held true, as well, and this lack of significance was likely due to one artefactual sample. The mean grB MFIs were as follows:

- C1/C1, licensed 2DL3 sp vs unlicensed 2DL1 sp vs DN, MFI of grB⁺: 84962 vs 44882 vs 60733
- C1/C2, licensed 2DL3 sp vs licensed 2DL1 sp vs DN, MFI of grB⁺: 88230 vs 94105 vs 50531
- C2/C2, licensed 2DL1 sp vs unlicensed 2DL3 sp vs DN, MFI of grB⁺: 64102 vs 29833 vs 25355.

Of note, when comparing NK cells licensed via 2DL3 with those licensed via 2DL1 in C1/C2 donors (**Fig. 26g**), those licensed via 2DL1 had a significantly higher grB MFI than those licensed via 2DL3, mirroring the trend seen for grH and adding to the argument of a role for differences in the strength of inhibitory receptor:ligand interactions. There was no significant difference in grB MFI between NK cells expressing a non-self-specific inhibitory KIR and DN NK cells in samples from C1/C1 and C2/C2 donors, again mirroring the grH data.

Importantly, a firm conclusion regarding the putative correlation between NK-cell licensing and grB expression cannot, however, be made without addressing the discrepancy between the transcriptome data (**Fig. 15**) and the protein data (**Fig. 26f-h**). This discrepancy is addressed in section 3.12.

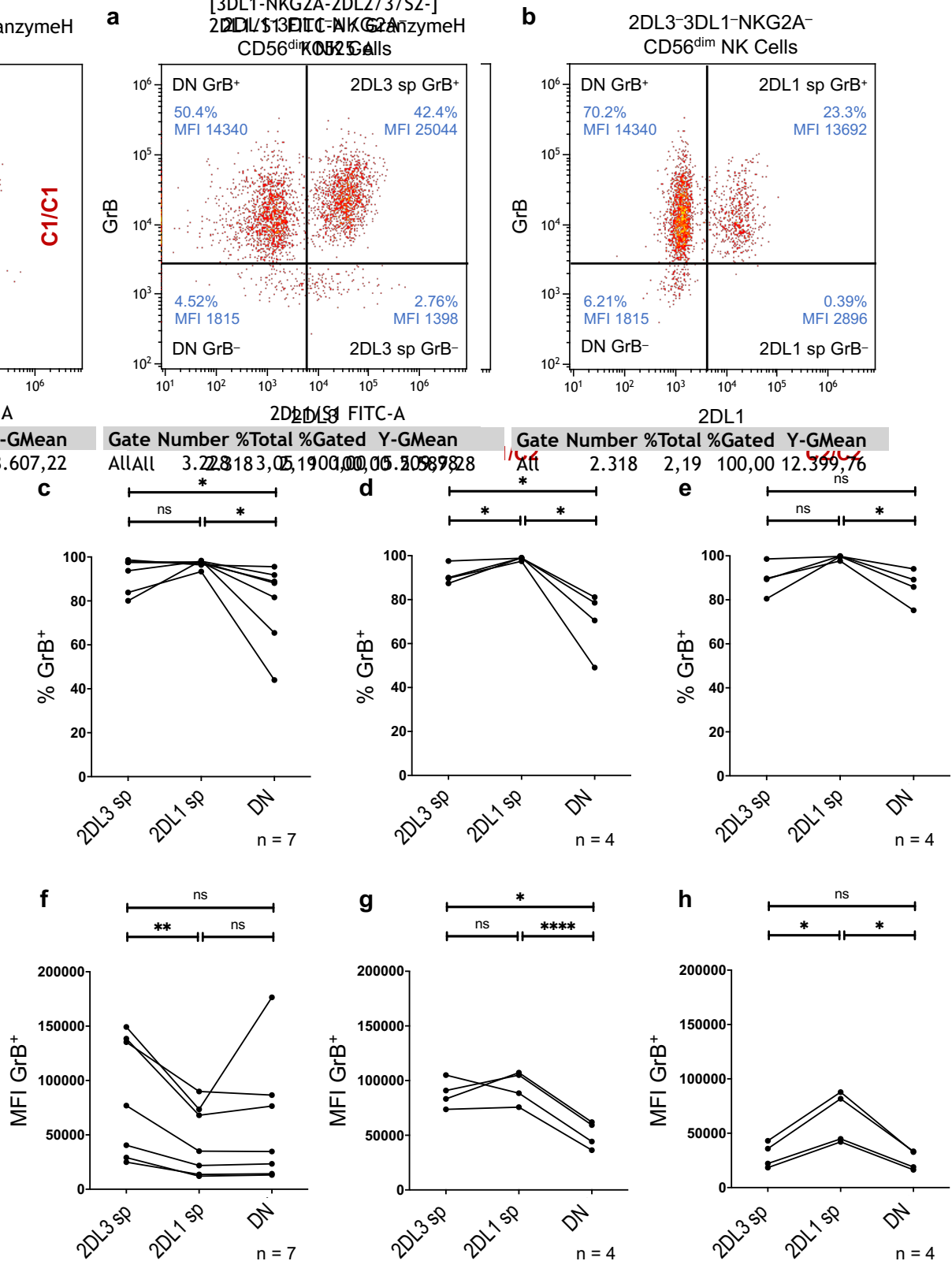


Fig. 26: NK-cell licensing via HLA-C-specific KIRs correlates with grB expression when measured as MFI but not clearly when measured as a percentage of cells positive for grB. The data were acquired in the same way as in Fig. 22, except that grB rather than grH expression was measured, and not only percentage but also MFI was included. Only samples from group *A/A* *KIR* haplotype donors are shown. **a** and **b**: representative flow cytometry plots showing grB expression by licensed (2DL3 sp) and unlicensed (2DL1 sp and DN) NK cells in a C1/C1 donor. **c-h**: grB expression as a percentage of cells positive for it (**c-e**) and as MFI (**f-h**). HLA statuses: C1/C1 (**a-c** and **f**), C1/C2 (**d** and **g**), C2/C2 (**e** and **h**). For ease of comparison between percentage (**c-e**) and MFI (**f-h**) data, the data is displayed differently than the grH data in Fig. 22 and Fig. 23, but to allow for comparisons with the grH data and to reduce the risk of type II errors being committed, significance testing for each plot was deliberately performed using paired t tests between all samples in one plot, rather than using a one-way ANOVA.

3.6.5 NK-Cell Licensing and GrA and GrK Expression

Next, it was important to examine grA expression with regard to NK-cell licensing, given the unclear transcriptome results displayed in **Fig. 15**. As shown in **Fig. 27**, there was no clear correlation between NK-cell licensing and grA expression at the protein level in C1/C1 donors, both in terms of the percentage of cells positive for grA and grA MFI. Regarding the percentage data, the main factor appeared to be the presence of an inhibitory KIR, regardless of its being self-specific or non-self-specific: grA expression by KIR sp NK cells was significantly higher than by DN NK cells (grA⁺ 2DL3 sp: 95.6%, 2DL1 sp: 97.7%, DN: 78.4%). The MFI data showed grA expression to be lowest, and significantly so, in non-self-specific inhibitory KIR (2DL1) sp NK cells (MFI: 14621), both compared to self-specific inhibitory KIR (2DL3) sp (MFI: 18243) and DN (MFI: 16048) NK cells. Both results suggest that there is no correlation between NK-cell licensing and grA expression.

Since there was no correlation between grA expression and NK-cell licensing in C1/C1 donors, C1/C2 and C2/C2 donors were not examined, as grA was not the main focus of this study.

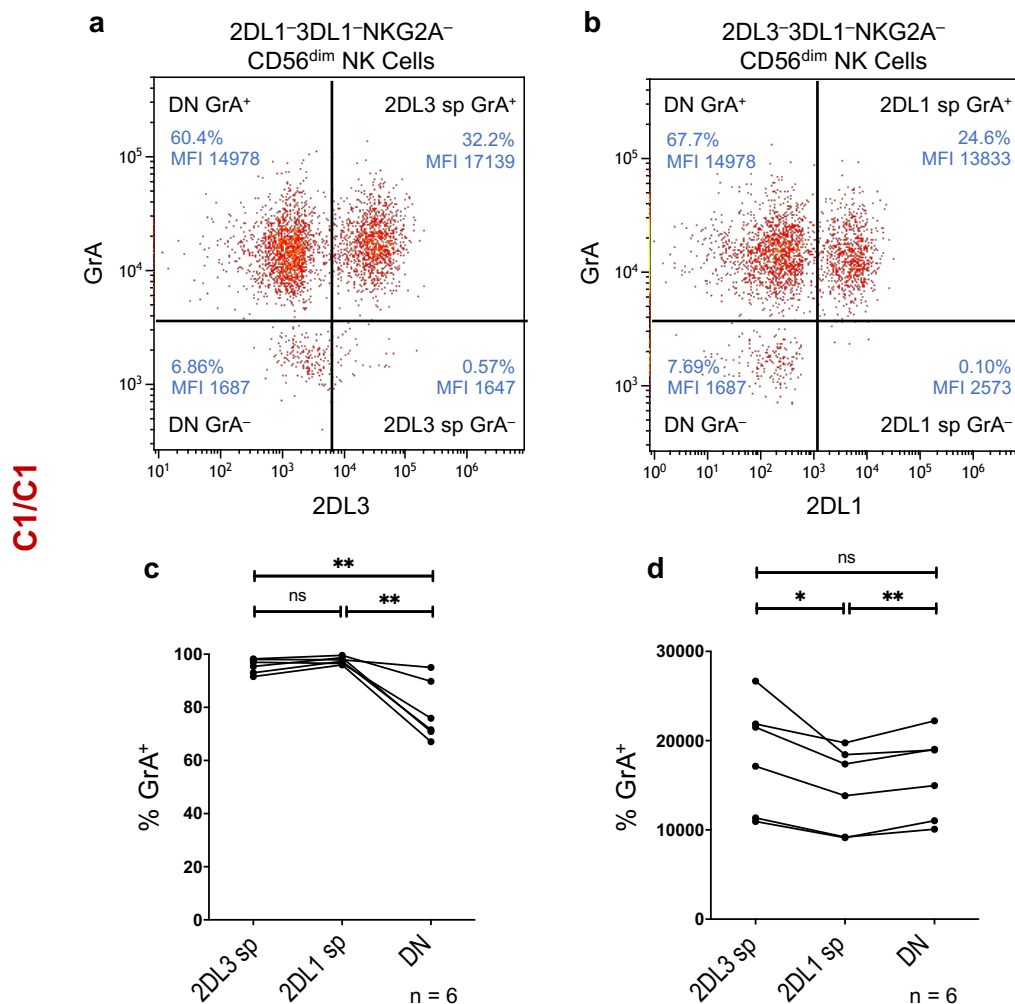


Fig. 27: NK-cell licensing via HLA-C-specific KIRs does not correlate with grA expression. The data were acquired in the same way as in **Fig. 26**, except that grA rather than grB was measured. HLA-C type is indicated. Only samples from C1/C1 group *A/A* *KIR* haplotype donors are shown. For the same reasons as in **Fig. 26**, significance testing for each plot was performed using paired t tests between all samples in one plot, rather than using a one-way ANOVA.

The expression of grK by licensed and unlicensed NK cells was also examined, but since grK is mainly expressed by CD56^{bright} NK cells, analysis of grK expression by licensed and unlicensed CD56^{dim} NK

Results

cells yielded cell numbers too low for any meaningful analyses to be conducted, so only representative flow cytometry plots rather than graphs are shown in **Fig. 28**. No significant correlation between NK-cell licensing and grK expression was expected in any case, since the transcriptome data in **Fig. 15** had not shown any convincing correlation between NK-cell licensing and *GZMK* mRNA levels. Therefore, grK will not be referred to again.

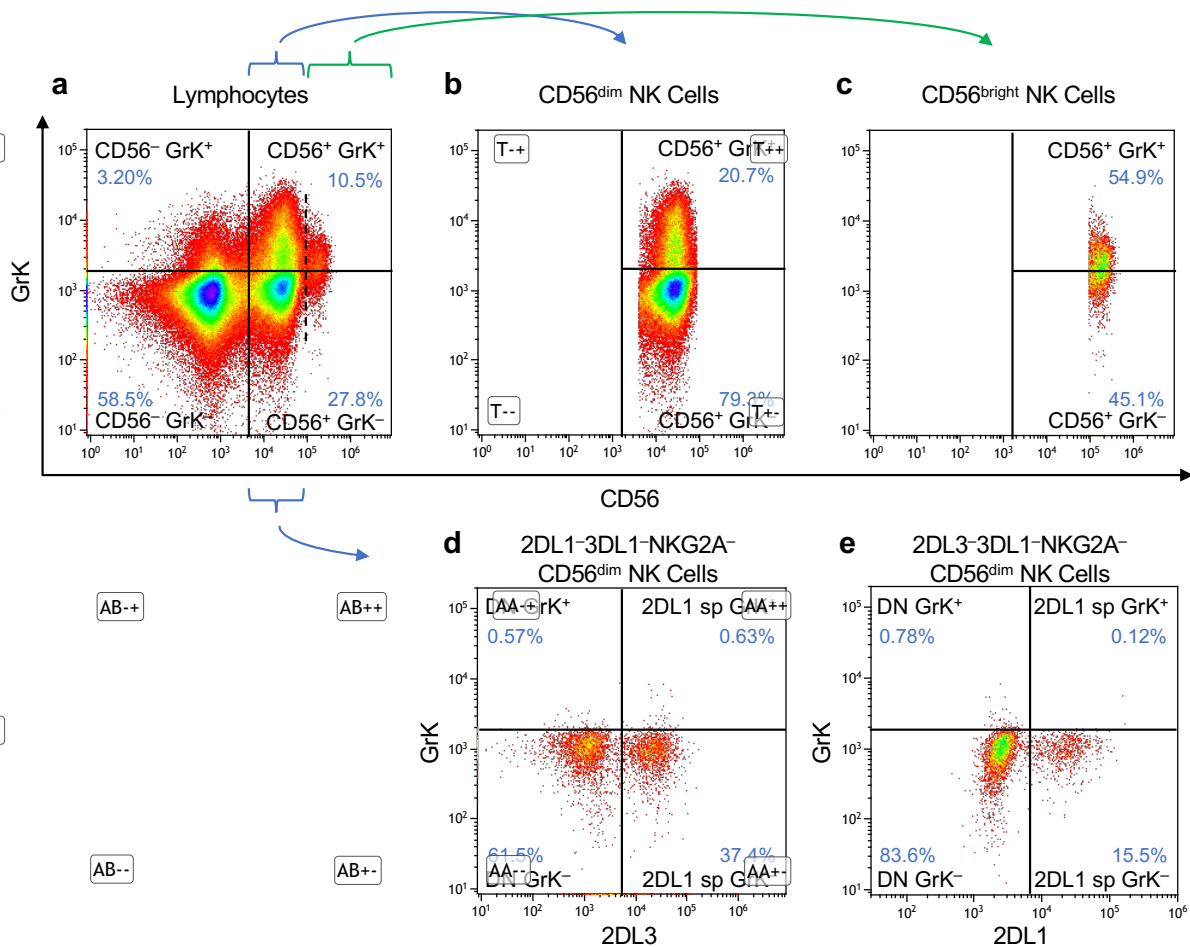


Fig. 28: GrK expression by CD56^{bright} NK cells is higher than by CD56^{dim} NK cells and grK expression by licensed and unlicensed CD56^{dim} NK cells is too low for meaningful analyses about any potential correlation between NK-cell licensing and grK protein expression to be conducted. Representative flow cytometry plots from a C1/C1 group *A/A* *KIR* haplotype donor are shown. Thawed PBMCs were stained and analysed in the same way as in **Fig. 27**, except that grK rather than grA was measured.

3.6.6 GrH Expression by Licensed NK Cells in CB

Next, grH expression by licensed and unlicensed NK cells derived from CB was examined to elucidate whether the correlation between licensing and grH expression is apparent already in the less mature CB-derived NK cells. So, thawed CBMCs from C1/C1, group *A/A* or *Bx* *KIR* haplotype donors were stained and analysed like PBMCs in **Fig. 22**. Samples from donors with group *Bx* *KIR* haplotypes were included to increase the sample size. This strategy was deemed acceptable, since for PB almost the same results were found when only examining *A/A* donors as when also including *Bx* donors (**Fig. 22** and **Fig. 23**). One CB sample had *KIR* genotype *44, which only encodes 2DL2 and not 2DL3; therefore, 2DL2 sp rather than 2DL3 sp NK cells were licensed in this donor. As stated in section 3.6.1, the antibody used to stain 2DL3 also stains 2DL2 (and 2DS2), allowing for inclusion of this sample in the analysis. Interestingly, despite the differences in overall grH expression between PB and CB shown in **Fig. 21**, in CB, grH expression by licensed 2DL2/3 sp NK cells (76.0%) was significantly higher than by

Results

unlicensed 2DL1 sp NK cells (58.4%) and also significantly higher than by DN NK cells (50.3%) (**Fig. 29**), this trend being very comparable to PB. Also like in PB, there was no significant difference in grH expression between unlicensed 2DL1 sp NK cells and DN NK cells.

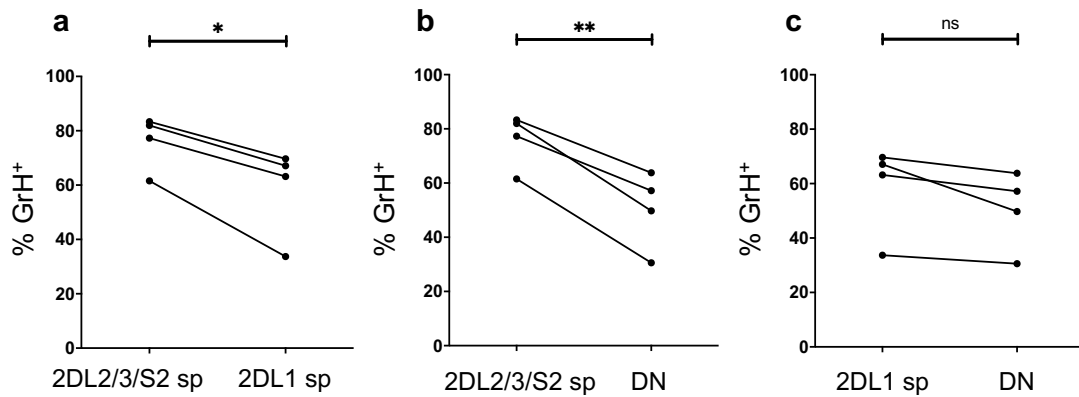


Fig. 29: NK-cell licensing in cord blood, too, correlates with grH expression. Thawed CBMCs from C1/C1 donors with *KIR* genotypes 1, 4, *42 and *44 were stained and analysed as described in the text (see **Table 1** and **Table 29** for a key to the *KIR* genotypes). 2DL2/3 sp NK cells were licensed and 2DL1 sp as well as DN NK cells were unlicensed. **a:** 2DL2/3/S2 sp vs 2DL1 sp, **b:** 2DL2/3/S2 sp vs DN, **c:** 2DL1 sp vs DN. n = 4. Individual data points are shown. Significance testing was performed using a paired t test for each plot.

3.7 NK-Cell Maturity and GrH Expression

As just shown in the previous section, the highest expression of grH and, less clearly, grB, among the mature KIR-expressing NK-cell subset was found in self-specific inhibitory KIR⁺ (ie licensed) NK cells. Furthermore, as shown in section 3.5.2, grH expression was significantly higher in the more mature CD56^{dim} NK cells compared with the less mature CD56^{bright} NK cells. Therefore, in order to firmly establish that NK-cell maturity *per se* in addition to the type of inhibitory receptor expressed influences grH expression, grH expression by CD56^{dim} NK cells was examined with regard to the marker of NK-cell maturation and terminal differentiation CD57.

For this, thawed PBMCs were stained for CD56, CD3, CD57 and grH or grB, and analysed flow cytometrically. GrH (and for comparison grB) expression by terminally differentiated CD57⁺CD56^{dim} NK cells and non-terminally differentiated CD57⁻CD56^{dim} NK cells was then analysed, regardless of KIR and NKG2A expression (and thus regardless of licensing status). Notwithstanding this, the majority of CD57⁺CD56^{dim} NK cells are known to express inhibitory KIRs, however (36). Three of the donors had an NKG2C expansion and thus included adaptive NK cells (see below) and three of them did not. The results however showed the same trend in all six donors, validating the inclusion of all donors. As **Fig. 30a** and **b** show, both grH and grB expression were significantly higher in terminally differentiated CD57⁺CD56^{dim} (grH⁺: 89.3%, grB⁺: 95.4%) than in less mature CD57⁻CD56^{dim} NK cells (grH⁺: 54.2%, grB⁺: 69.9%), indicating that NK-cell maturity *per se* does impact grH (and grB) expression.

Next, to examine whether the effects on grH expression of licensing and CD57 expression were independent of one another, thawed PBMCs from C1/C1, group A/A *KIR* haplotype donors were stained for CD56, CD3, 2DL3, 2DL1, 3DL1, NKG2A, CD57 and grH, and analysed flow cytometrically for grH expression by licensed 2DL3 sp and unlicensed 2DL1 sp CD57⁻ and CD57⁺ CD56^{dim} NK cells. Indeed, as **Fig. 30c** shows, though not always statistically significant, NK-cell licensing and CD57-positivity independently correlated with higher grH expression: grH expression by both licensed and unlicensed CD57⁺ NK cells (2DL3 sp CD57⁺ grH⁺: 84.1%; 2DL1 sp CD57⁺ grH⁺: 56.7%) was higher

Results

than by licensed or unlicensed CD57⁻ NK cells (2DL3 sp CD57⁻ grH⁺; 69.3%, 2DL1 sp CD57⁻ grH⁺: 39.1%), and grH expression by both CD57⁻ and CD57⁺ NK cells was higher when the cells were licensed (2DL3 sp CD57⁻ grH⁺: 69.3%; 2DL3 sp CD57⁺ grH⁺: 84.1%) than when unlicensed (2DL1 sp CD57⁻ grH⁺: 39.1%; 2DL1 sp CD57⁺ grH⁺: 56.7%). Licensed CD57⁺ NK cells have the highest grH expression, and the effect of licensing on grH expression was higher than that of CD57 expression, as licensed CD57⁻ NK cells displayed higher grH expression than unlicensed CD57⁺ NK cells.

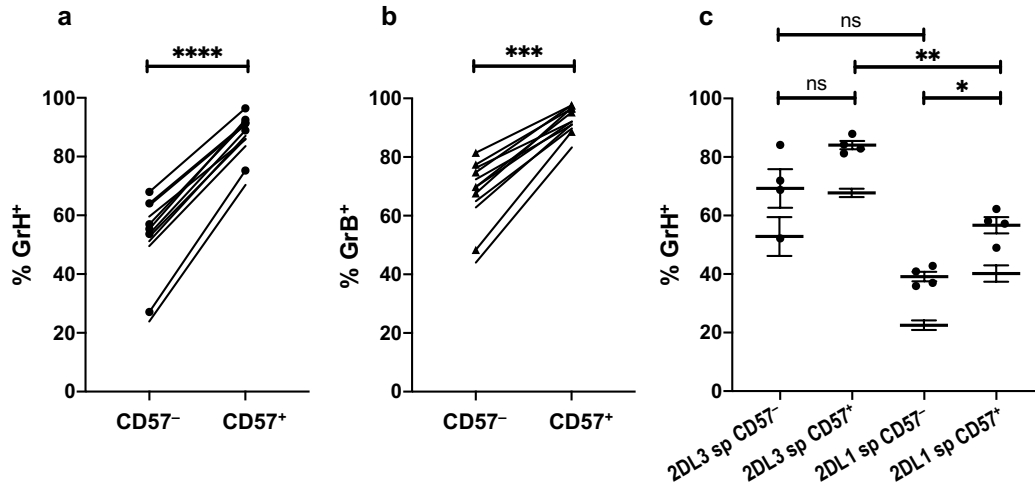


Fig. 30: GrH expression is significantly higher in CD57⁺CD56^{dim} than in less mature CD57⁻CD56^{dim} NK cells and NK-cell licensing and CD57-positivity independently correlate with higher grH expression. Thawed PBMCs were stained and analysed as described in the text. **a** and **b**: the percentage of CD57⁺ or CD57⁻ CD56^{dim} NK cells that are grH⁺ (**a**) or grB⁺ (**b**). $n = 6$. Significance testing was performed using a paired t test for both plots. **c**: The percentage of licensed 2DL3 sp and unlicensed 2DL1 sp CD57⁻ and CD57⁺ CD56^{dim} NK cells that are grH⁺. $n = 4$. Significance testing was performed using a RM one-way ANOVA followed by Sidak's test comparing 2DL3 sp CD57⁻ with 2DL3 CD57⁺, 2DL1 sp CD57⁻ with 2DL1 sp CD57⁺, 2DL3 sp CD57⁻ with 2DL1 sp CD57⁻, and 2DL3 sp CD57⁺ with 2DL1 sp CD57⁺ populations. The overall level of significance of the ANOVA was **.

Next, adaptive NKG2C⁺CD56^{dim} NK cells from donors with an NKG2C expansion, defined as $\geq 9.25\%$ of CD56^{dim} NK cells being NKG2C-positive according to Manser *et al.*, 2019 (119), were examined. These cells, which occur in response to HCMV infection, are known to possess memory-like functionality and express self-specific KIRs and CD57 but not NKG2A, and are thought to be a highly mature NK-cell subset (see section 1.3.3). The majority of these cells express self-specific inhibitory KIRs (26),(119), and are thus assumed to be licensed. To analyse such cells, thawed PBMC samples from donors with a known NKG2C expansion (kindly provided by Dr A. Manser at the ITZ) were stained for CD56, CD3, CD57, NKG2C, NKG2A and grH as well as grB for comparison, and analysed flow cytometrically. The donors' CMV status was unknown but assumed to be positive. Within CD56^{dim} NK cells, cell populations were defined as follows and their grH and grB expression analysed:

A: CD57⁻NKG2C⁻NKG2A⁻: non-terminally differentiated non-adaptive (licensing status unclear)

B: CD57⁺NKG2C⁻NKG2A⁻: terminally differentiated non-adaptive (licensing status unclear)

C: CD57⁻NKG2C⁺NKG2A⁻: early adaptive (assumed to be licensed)

D: CD57⁺NKG2C⁺NKG2A⁻: terminally differentiated adaptive (assumed to be licensed)

GrH expression by populations **B** (83.1%), **C** (95.6%) and **D** (97.3%) was significantly higher than by population **A** (48.5%) (**Fig. 31a**), indicating that the presence of either CD57 or NKG2C was sufficient for an increase in grH expression. Though not statistically significant, maximum grH expression was observed in the two NKG2C⁺ populations regardless of CD57 expression, indicating that NKG2C had a larger effect than CD57. The data were very similar for grB (population **A**: 67.0%, **B**: 90.0%, **C**: 97.7% and **D**: 98.6% (**Fig. 31b**)), though the difference between populations **A** and **B** was not significant.

Results

GrH expression by NKG2C⁺NKG2A⁻ NK cells (both CD57⁺ and CD57⁻ combined) (96.9%) was then compared to grH expression by NK cells licensed via self-specific inhibitory KIRs (86.4%) in samples not known to have an NKG2C expansion, and found to be significantly higher (**Fig. 31c**). It was, in fact, so high that no significant difference between grH (97.3%) and grB (98.6%) expression in terminally differentiated, adaptive CD56^{dim} NK cells could be detected (**Fig. 31d**), in contrast to the significantly higher grB expression in CD56^{dim} NK cells from donors with no known NKG2C expansion (**Fig. 20**). The trends shown in **Fig. 31a, b and c** (granzyme expression as a percentage of granzyme⁺ NK cells) were the same when examining granzyme expression as MFI (data not shown), corroborating the findings. For even more robust conclusions to be drawn, however, the sample size should be increased. The MFIs of grH and grB expression were not compared as this would have been futile given the different fluorochromes (VioGreen and PE respectively) that were used to stain for the two granzymes.

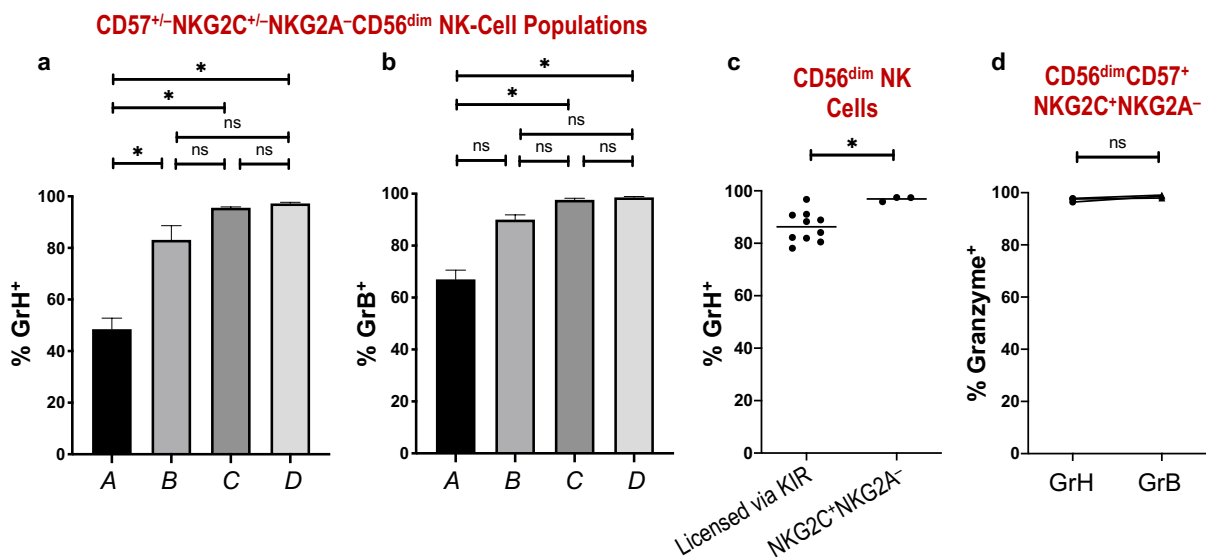


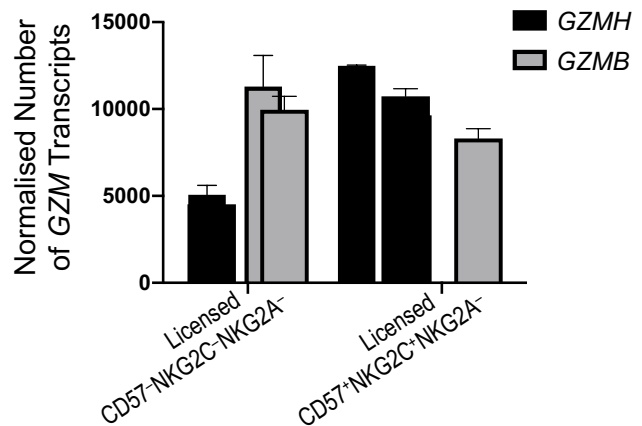
Fig. 31: GrH expression by adaptive NK cells from donors with an NKG2C expansion is significantly higher than by non-adaptive NK cells. Plots **a, b, c** (‘NKG2C⁺NKG2A⁻’) and **d**: thawed PBMCs from healthy donors with an NKG2C expansion were stained and analysed as described in the text. **c** (‘Licensed via KIR’): grH expression data from **Fig. 22** was used: grH⁺ expression by 2DL3 sp NK cells from C1/C1 donors and by 2DL1 sp cells from C2/C2 donors (all group A/A *KIR* haplotype). **a** and **b**: grH (**a**) and grB (**b**) expression by populations A (CD57⁺NKG2C⁻), B (CD57⁺NKG2C⁻), C (CD57⁺NKG2C⁺) and D (CD57⁺NKG2C⁺) within NKG2A⁻CD56^{dim} NK cells as a percentage of cells positive for grH or grB. n = 3. Bars represent the data set means and the SEM. Significance testing was performed using a RM one-way ANOVA followed by Tukey’s test. The overall levels of significance of the ANOVAs were ** (**a**) and * (**b**). **c**: grH expression by NK cells licensed via self-specific inhibitory KIRs vs grH expression by NKG2C⁺NKG2A⁻CD56^{dim} NK cells (both CD57⁺ and CD57⁻ combined). n (‘Licensed via KIR’) = 10; n (‘NKG2C⁺NKG2A⁻’) = 3. Individual data points with data set means (horizontal bars) are shown. **d**: grH vs grB expression by CD56^{dim}CD57⁺NKG2C⁺NKG2A⁻ NK cells. n = 3. **c** and **d**: Significance testing was performed using an unpaired (**c**) or paired (**d**) t test.

Next, expression of grH by terminally differentiated adaptive vs non-adaptive NK cells was examined at the mRNA level. For this, RNA-Seq of licensed (2DL1 sp or 2DL3 sp, depending on the donor’s HLA-C status) terminally differentiated adaptive CD57⁺NKG2C⁺NKG2A⁻ vs licensed non-terminally differentiated non-adaptive CD57⁻NKG2C⁻NKG2A⁻ NK cells was performed by Prof. Dr M. Uhrberg’s and Prof. Dr L. Walter’s groups and the raw data kindly provided to and analysed as below by this study’s author. The results reveal that the number of *GZMH* transcripts was higher in licensed adaptive (mean: 10734) than in licensed non-adaptive (4522) NK cells (**Fig. 32**), mirroring the protein data (**Fig. 31c**). In contrast, however, though grB protein expression was also highest in terminally differentiated adaptive NK cells (**Fig. 31b**), *GZMB* transcript numbers were lower in terminally differentiated adaptive (8306) than non-terminally differentiated non-adaptive NK cells (9952) (**Fig. 32**). Furthermore, while

Results

the protein data showed no significant difference between grH and grB expression by terminally differentiated adaptive NK cells, the transcriptome data showed that the number of *GZMH* transcripts was higher than that of *GZMB* transcripts in terminally differentiated adaptive NK cells (10734 vs 8306 respectively). A possible explanation for these discrepancies is that there is post-transcriptional (or post-translational) regulation that may lead to differential mRNA and protein levels of the two granzymes. More likely however, and also indicated by the discrepancy between the flow cytometry data displayed in **Fig. 26** and the transcriptome data in **Fig. 15** with regard to grB expression by licensed vs unlicensed NK cells, the anti-grB antibody may not be specific for grB but also recognise grH, thus causing a difference in mRNA and detected protein levels. This is addressed in more detail in section 3.12.

Fig. 32: The normalised number of *GZMH* transcripts in licensed terminally differentiated adaptive $CD57^+NKG2C^+NKG2A^-$ NK cells is higher than in licensed non-terminally differentiated non-adaptive $CD57^-NKG2C^-NKG2A^-$ NK cells, while the opposite is observed for *GZMB*. Transcriptomes were established as described in the text. $n = 2$, so no significance testing was performed. Bars represent the data set means and the SEM.



3.8 Correlation between Expression of GrH, CD57, KLRG1, CD11c and DNAM-1

The expression patterns of grH at rest, as described above, particularly the link with NK-cell licensing, are a crucial factor when studying the potential role of grH. Even more important for elucidating this role are functional studies. Since grH is an intracellular protein, however, staining for it necessitates cell fixation and permeabilisation and thus makes functional analyses of cells sorted according to grH-positivity impossible. In order to further characterise grH⁺ and grH⁻ licensed and unlicensed NK cells, more phenotypic analyses were first conducted in an attempt to circumvent the need for sorting cells into grH⁺ and grH⁻ ones through finding a potential extracellular proxy for grH expression.

To this end, grH⁺ expression was examined in relation to four other cell-surface proteins: CD57, KLRG1, CD11c and DNAM-1. CD57 was chosen because this study had already shown its expression to be associated with that of grH (**Fig. 30**). DNAM-1 was chosen because of the published association with NK-cell licensing (143). KLRG1 and CD11c were chosen because, in addition to the results already described, the aforementioned RNA-Seq data of licensed vs unlicensed NK cells established by Prof. Uhrberg and Prof. Walter had also revealed that mRNA levels of *KLRG1* and *ITGAX* (CD11c gene name (250)) were lower in licensed than unlicensed NK cells (unpublished data, mentioned here with permission). Also, expression of KLRG1 and CD57 have been shown to negatively correlate (251). KLRG1 (killer-cell lectin-like receptor G1) is an inhibitory receptor that binds classic members of the cadherin family important for cell-to-cell adhesion (252). It has been shown to be expressed by NK cells and highly differentiated T cells and has often been linked with cell senescence (252), with KLRG1⁺ NK cells having been demonstrated to exhibit reduced effector functions (253),(254). CD11c is part of the integrin family and mainly expressed by dendritic cells, but also by NK cells, monocytes and subsets of B and T cells, and has functions in cell adhesion and conjugation events (44),(255),(256),(257),(258). So, thawed PBMCs from C1/C1, group A/A *KIR* haplotype donors were stained for CD56, CD3, 2DL3, 2DL1, 3DL1, NKG2A and grH, as well as for CD57, KLRG1, CD11c or DNAM-1 and analysed flow

Results

cytometrically. GrH⁺ and grH⁻ licensed 2DL3 sp and unlicensed 2DL1 sp CD56^{dim} NK cells were then identified and the percentage of these cells that were positive for CD57, KLRG1, CD11c or DNAM-1 was established (**Fig. 33**). The data showed that grH-positivity correlated with higher expression of CD57 (significantly so for 2DL1 sp cells), CD11c (significantly so for 2DL3 sp cells) and DNAM-1, while it correlated with lower expression of KLRG1, significantly so in the unlicensed setting (2DL3 sp grH⁻ vs grH⁺ CD57⁺: 55.6% vs 72.3%, 2DL1 sp grH⁻ vs grH⁺ CD57⁺: 44.9% vs 60.0%; 2DL3 sp grH⁻ vs grH⁺ CD11c⁺: 50.6% vs 67.1%, 2DL1 sp grH⁻ vs grH⁺ CD11c⁺: 87.3% vs 87.4%; 2DL3 sp grH⁻ vs grH⁺ DNAM-1⁺: 79.5% vs 96.0%, 2DL1 sp grH⁻ vs grH⁺ DNAM-1⁺: 94.2% vs 96.3%; 2DL3 sp grH⁻ vs grH⁺ KLRG1⁺: 62.0% vs 50.8%; 2DL1 sp grH⁻ vs grH⁺ KLRG1⁺: 86.1% vs 69.0%). Furthermore, in both the grH⁻ and grH⁺ populations KLRG1 and CD11c expression was higher in unlicensed than licensed NK cells (non-significantly so for KLRG1, significantly so for CD11c in the grH⁺ population), as would be expected from the transcriptome data. CD57 expression, on the other hand, was non-significantly higher in licensed than unlicensed NK cells in both grH⁻ and grH⁺ populations. For DNAM-1 it was not clear at the percentage level, but at the MFI level DNAM-1 expression was non-significantly higher in licensed than unlicensed NK cells (data not shown), in line with the literature (143). When combining grH⁻ and grH⁺ populations to examine the association between licensing and expression of CD57, KLRG1, CD11c and DNAM-1, the results showed the same trends as just described (data not shown). CD11c expression being higher in grH⁺ than grH⁻ NK cells, while being higher in unlicensed than licensed NK cells is interesting, given that grH expression is higher in licensed NK cells.

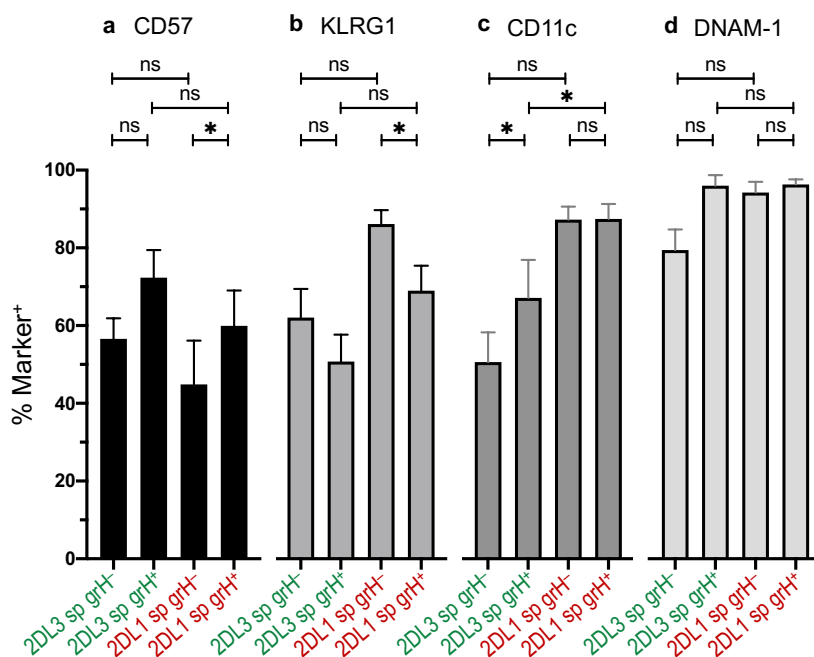


Fig. 33: GrH expression by licensed and unlicensed NK cells correlates positively with CD57, CD11c and DNAM-1 expression and negatively with KLRG1 expression. Thawed PBMCs were stained and analysed as described in the text. n (a, b and c) = 4, n (d) = 3. Bars represent the data set means and the SEM. Significance testing was performed using a RM one-way ANOVA for each plot followed by Sidak's test comparing 2DL3 sp grH⁻ with 2DL3 sp grH⁺, 2DL1 sp grH⁻ with 2DL1 sp grH⁺, 2DL3 sp grH⁻ with 2DL1 sp grH⁻ and 2DL3 sp grH⁺ with 2DL1 sp grH⁺ populations. The overall levels of significance of the ANOVAs were ns (a), ** (b), * (c) and ns (d).

The results for CD57 and KLRG1 displayed almost opposing trends, which was not as observable for the other two proteins. Therefore, to look for the abovementioned proxy of grH expression, CD57 and KLRG1 were examined to see whether they can be used to allow for indirect functional analyses of cells presumed to be positive or negative for grH, which would circumvent the difficulties associated with intracellular staining. PBMCs from C1/C1 group *A/A* *KIR* haplotype donors were thus stained for CD56, CD3, 2DL3, 2DL1, 3DL1, NKG2A, grH and CD57 and KLRG1 simultaneously. This time, licensed (2DL3 sp) and unlicensed (2DL1 sp) CD56^{dim} CD57^{+/+} KLRG1^{+/+} NK cells were identified, and the percentage of these cells that was grH⁺ was established (**Fig. 34a**). The data revealed that grH expression was highest in licensed CD57⁺ KLRG1⁻ (84.4%) and lowest in unlicensed CD57⁻ KLRG1⁺ (25.0%)

Results

CD56^{dim} NK cells. The difference between the two was statistically significant. Some of the differences in grH expression between other populations were also statistically significant but are not detailed further because the difference between licensed CD57⁺KLRG1⁻ and unlicensed CD57⁻KLRG1⁺ cells was the most pronounced. As expected, grH expression by licensed NK cells was higher than by unlicensed NK cells for each CD57^{+/+}-KLRG1^{+/+} pair. While this difference was only significant in the CD57⁻KLRG1⁺ population (grH⁺ 2DL3 sp: 62.1%, 2DL1 sp: 25.0%), it is expected to become significant for the other pairs as well with an increase in sample size.

Though the data in **Fig. 34a** indicate that mainly grH⁺ cells may be identified by focusing on licensed CD57⁺KLRG1⁻ CD56^{dim} NK cells, and that mainly grH⁻ cells may be identified by focusing on unlicensed CD57⁻KLRG1⁺ ones, licensing status and CD57 and KLRG1-positivity and negativity are shown not to be absolute markers of grH expression, even when combined. Therefore, using them as such would result in considerable impurity of grH⁺ and grH⁻ populations, necessitating a different approach. One possibility of defining almost pure grH⁺ and grH⁻ populations was overexpression of the protein in cells that inherently express very little of it – an approach used in section 3.10.

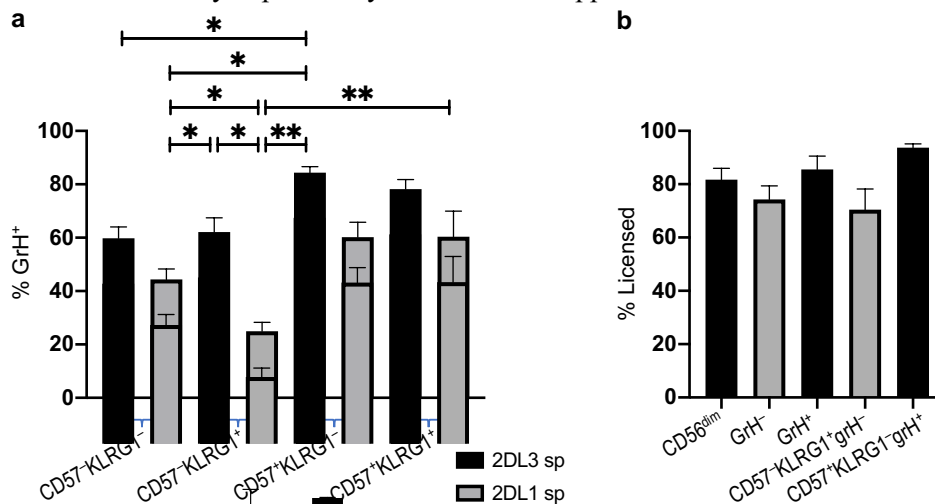


Fig. 34: GrH expression is highest in licensed CD57⁺KLRG1⁻, lowest in unlicensed CD57⁻KLRG1⁺CD56^{dim} NK cells, and grH, CD57 and KLRG1 can be used to predict whether or not an NK cell is licensed. Thawed PBMCs from C1/C1, group *A/A* *KIR* haplotype donors were stained and analysed as described in the text. **a**: % grH⁺ cells among 2DL3 sp or 2DL1 sp CD57⁻KLRG1⁻, CD57⁻KLRG1⁺, CD57⁺KLRG1⁻ and CD57⁺KLRG1⁺ CD56^{dim} NK cells. **b**: % licensed cells (all cells that expressed 2DL3 and/or NKG2A and/or 3DL1 in Bw4⁺ donors) among all CD56^{dim} NK cells, or among grH⁻, grH⁺, CD57⁻KLRG1⁺grH⁻ or CD57⁺KLRG1⁻grH⁺ CD56^{dim} NK cells. **a** and **b**: n = 3. Significance testing was performed using a RM one-way ANOVA for each plot, followed by Tukey's test, of which for clarity, only (but all) significant results are displayed; in **b**, there were no significant differences among the comparisons. The overall levels of significance of the ANOVAs were * (**a**) and ns (**b**).

Next, it was examined whether expression of grH, with or without CD57 positivity and KLRG1, negativity could allow for any predictions to be made about licensing status. For this purpose, using the samples from **Fig. 34a**, the percentage of cells that were licensed (all cells that expressed 2DL3 and/or NKG2A and/or 3DL1 in Bw4⁺ donors (single and multiple receptor-positive, regardless of non-specific inhibitory KIR expression)) was determined among CD56^{dim} NK cells, CD56^{dim}grH⁻, CD56^{dim}grH⁺, CD56^{dim}CD57⁻KLRG1⁺grH⁻ and CD56^{dim}CD57⁺KLRG1⁻grH⁺ NK cells (**Fig. 34b**). The latter two populations were chosen because of the results from **Fig. 34a**. All cells not included among the licensed cells (all DN, all 2DL1 sp, all 3DL1 sp in Bw4⁻ donors and all 2DL1/3DL1 dp cells in Bw4⁻ donors) were considered unlicensed. The data revealed that while there were more licensed than unlicensed cells in all of the examined populations, the highest percentages of licensed cells, though non-significantly so, were among grH⁺ NK cells (85.6%) and, even higher, among CD57⁺KLRG1⁻grH⁺ NK cells (93.7%).

Results

This means that grH expression can be used as a marker to predict a cell's licensing status, and that an even more robust prediction can be made when also looking at CD57 and KLRG1 in addition to grH.

3.9 Functional Analyses of Primary NK Cells with Regard to GrH Expression

3.9.1 Soluble Mediator-Induced NK-Cell Stimulation

Prior to overexpression of grH, several functional analyses of primary cells that did not require sorting of the cells into pure grH⁺ and grH⁻ populations were performed.

First, the effect of soluble mediator-induced NK-cell stimulation on grH expression was assessed and compared with grB. Since most studies have focused on non-NK lymphocytes or even non-lymphocytes when studying this effect, it was important to examine it in NK cells specifically. IL-2 and IL-15 were chosen for their known stimulatory and, in the case of IL-15, pro-survival, actions on NK cells. Freshly isolated or thawed PBMCs were cultured in NK-cell medium supplemented with either IL-2, IL-15, both or neither for seven days and analysed for the below-discussed characteristics on days 0, 1, 3 and 7. As a note on methodology, the clear distinction between CD56^{dim} and CD56^{bright} NK cells disappeared with prolonged stimulation (data not shown), so in the following analyses NK-cell gating always encompassed both CD56^{dim} and CD56^{bright} NK cells, including in the comparison between licensed and unlicensed cells, in order to keep the gating consistent throughout the assay.

First, the proportion of NK cells (CD56⁺CD3⁻) among lymphocytes was examined to ensure that the stimulation did target NK cells. For this, PBMCs were stained for CD56 and CD3. As **Fig. 35** shows, an initial decrease in the proportion of NK cells among lymphocytes (day 0: 5.91%; day 3 IL-2: 2.80%, IL-15: 1.90%, IL-2/IL-15: 2.13%) was followed by an eventual surge on day 7 (day 7 IL-2: 13.2%, IL-15: 18.7%, IL-2/IL-15: 14.0%) in all three cytokine conditions, but not in the no cytokine-condition (day 3: 5.72%, day 7: 4.62%). This indicates that IL-2 and IL-15 did act on NK cells, and that the changes observed were due to the cytokines added. Thus, given the known NK-cell stimulatory roles of IL-2 and IL-15 and this experiment taking place in cell culture, NK-cell stimulation can be assumed to have occurred. Absolute cell numbers were not examined, so no conclusions can be drawn about any potential net expansion.

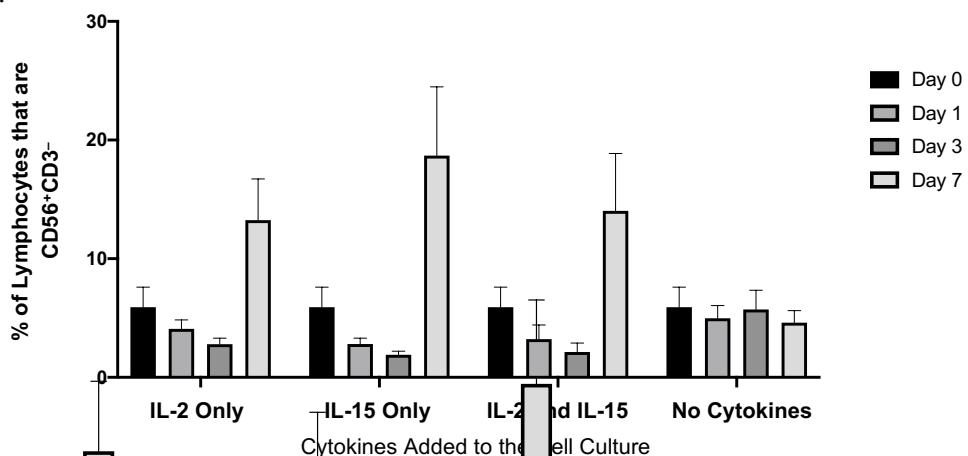


Fig. 35: IL-2 and IL-15-mediated stimulation over 7 days leads to an initial decrease followed by a surge in the proportion of NK cells (CD56⁺CD3⁻) among lymphocytes. Freshly isolated PBMCs were cultured for 7 days as described in the text, stained and analysed on days 0 (straight after isolation from peripheral blood), 1, 3 and 7, as also described in the text. Within the lymphocyte gate, CD56⁺CD3⁻ cells were identified. Bars represent the data set means and the SEM. n = 2, so no significance testing was performed.

Results

Next, NK cells were examined for expression of grH (or grB for comparison) on days 0, 1, 3 and 7 of stimulation with IL-2, IL-15 or both. Cells were stained for CD56, CD3 and grH or grB (grB on days 0, 3 and 7 only), and grH⁺ or grB⁺ NK cells identified. As **Fig. 36** shows, there was a drastic decrease in grH expression by NK cells in all three conditions. Significances were only calculated for stimulation with both IL-2 and IL-15 due to a larger sample size in this condition. The decrease in grH expression in this setting was highly significant, particularly between days 0 and 7 (mean grH⁺ day 0: 51.9%, day 1: 32.9%, day 3: 36.0%, day 7: 4.68%). By comparison, there was no significant change in NK-cell grB expression (mean grB⁺ day 0: 86.0%, day 3: 93.0% day 7: 99.0%); if anything, there was an increase.

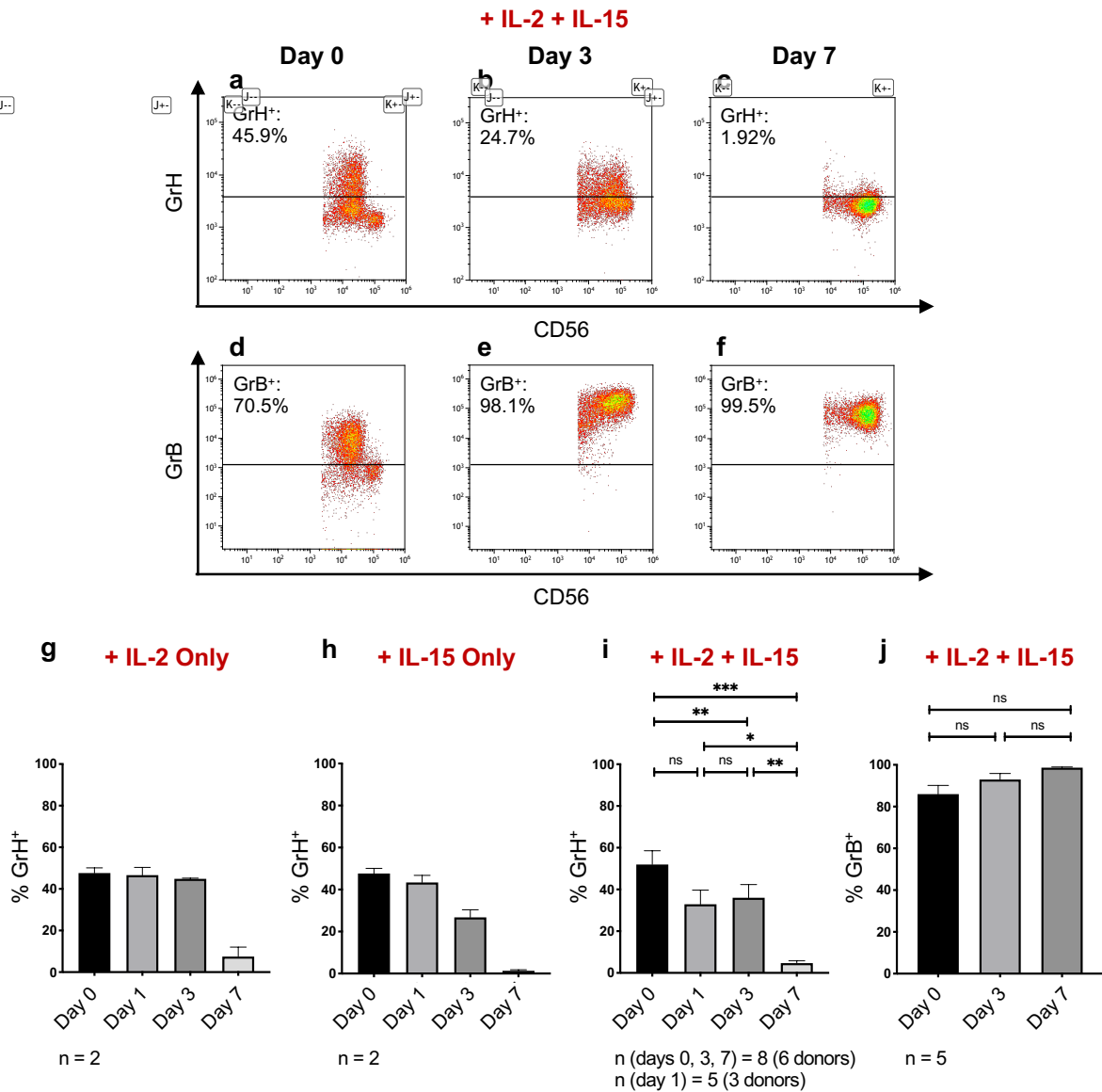


Fig. 36: GrH expression by NK cells decreases drastically with 7-day stimulation with IL-2- and/or IL-15, while grB expression does not. Thawed (a-f), fresh (g and h) or thawed and fresh (i and j) PBMCs were cultured for 7 days in NK-cell medium supplemented with IL-2 (g), IL-15 (h) or both (a-f, i and j), and stained and analysed as described in the text. a-f: representative flow cytometry plots focusing on days 0, 3 and 7 to show a more visual representation of the decrease in grH expression. n = 1. g-i: the percentage of NK cells that are grH⁺. j: the percentage of NK cells that are grB⁺. g-j: the n is displayed within the plots. Bars represent the data set means and the SEM. i: significance testing was performed using a mixed-effects analysis followed by Tukey's test. j: significance testing was performed using a RM one-way ANOVA followed by Tukey's test. The overall levels of significance of the mixed-effects analysis (i) was ****, and of the ANOVA (j) was ns.

The data displayed within **Fig. 36i** can be dissected further by examining grH expression by licensed vs unlicensed NK cells. For this, fresh and thawed PBMCs from C1/C1 group A/A *KIR* genotype donors

Results

were stimulated with IL-2 and IL-15 and stained and analysed on days 0, 1, 3 and 7, as before. After staining for CD56, CD3, 2DL3, 2DL1, 3DL1, NKG2A and grH, grH expression (as a percentage of cells positive for it) by licensed 2DL3 sp and unlicensed 2DL1 sp NK cells determined.

As **Fig. 37** shows, there was a steady and significant decrease in grH expression by licensed 2DL3 sp NK cells (day 0: 66.5%; day 1: 37.3%; day 3: 22.7%; day 7: 6.94%) and a slight, though non-significant, decrease in grH expression by unlicensed 2DL1 sp NK cells (day 0: 25.9%; day 1: 22.3%; day 3: 29.3%; day 7: 11.4%). The significant difference in grH expression between licensed and unlicensed NK cells on day 0 (the phenomenon known from **Fig. 22** and **Fig. 23**) disappeared after only one day of culture. The data suggest that though the predominant part of the decrease in NK-cell grH expression following cytokine-mediated stimulation came from licensed cells, unlicensed NK cells were also able to respond to the stimulus and contributed to the observed decrease in grH expression.

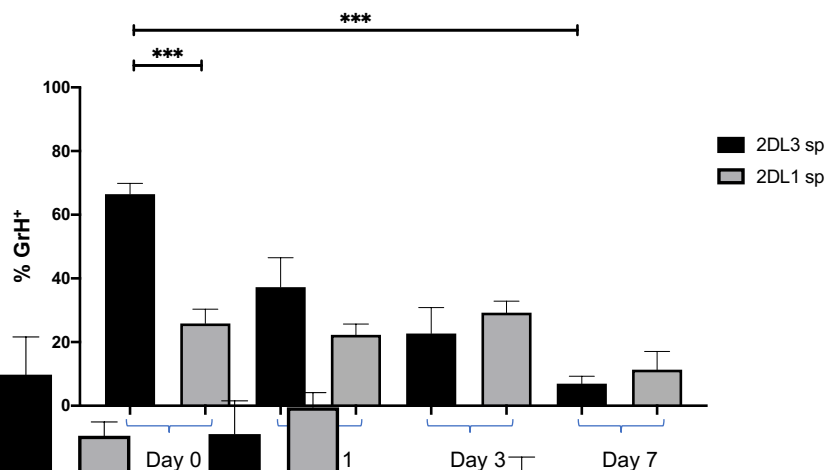


Fig. 37: GrH expression by licensed as well as unlicensed NK cells decreases with seven-day stimulation with IL-2 and IL-15, the decrease observed in licensed NK cells being steady and highly significant. PBMCs were cultured, stained and analysed as described in the text. $n = 5$ (3 donors). Bars represent the data set means and the SEM. Significance testing was performed using a mixed-effects analysis followed by Sidak's test comparing 2DL3 sp populations with 2DL1 sp for each day, and 2DL3 sp or 2DL1 sp on each day with 2DL3 sp or 2DL1 sp respectively on every other day. For clarity, only (but all) significant results of Sidak's test are displayed. The overall level of significance of the mixed-effects analysis was ***.

As demonstrated in section 3.7, the NK-cell population with the highest grH expression were terminally differentiated adaptive NK cells from donors with an NKG2C expansion. It was therefore important to establish whether stimulation of these cells also leads to a decrease in grH expression. Due to their reduced responsiveness to cytokines, adaptive NK cells were stimulated with the anti-CD20 antibody rituximab to induce ADCC, and supplemented with IL-15 to aid survival. So, thawed PBMCs from donors with an NKG2C expansion (again kindly provided by Dr A. Manser, ITZ) were cultured in NK-cell medium supplemented with rituximab and IL-15 for seven days, and stained and analysed flow cytometrically on days 0, 1, 3 and 7, as before. Staining for CD56, CD3, CD57, NKG2C, NKG2A and grH or grB for comparison was performed and grH or grB expression by terminally differentiated adaptive ($CD56^+CD3^-CD57^+NKG2C^+NKG2A^-$) and non-terminally differentiated non-adaptive ($CD56^+CD3^-CD57^-NKG2C^-NKG2A^-$) NK cells determined. As in section 3.7, $CD57^+NKG2C^+NKG2A^-$ cells were assumed to be licensed, while KIR expression and licensing status of $CD57^-NKG2C^-NKG2A^-$ was unclear; the latter population was included only as a comparative entity. Indeed, stimulation with rituximab and IL-15 led to a significant and much more drastic reduction in grH expression by terminally differentiated adaptive (day 0: 97.2%, day 1: 92.3%, day 3: 91.3%, day 7:

Results

10.5%) than by non-terminally differentiated non-adaptive NK cells (day 0: 44.6%, day 1: 43.5%, day 3: 47.9%, day 7: 4.70%). By contrast, no significant change in grB expression was observed in either population (adaptive day 0: 98.5%, day 1: 100%, day 3: 99.9%, day 7: 100%; non-adaptive day 0: 61.5%, day 1: 97.3%, day 3: 86.7%, day 7: 99.7%) (**Fig. 38**). GrH and B expression were examined as a percentage of cells positive for grH or B rather than as MFI, because the MFI of all cell populations as well as overall cell sizes increased with stimulation, making the MFI data incomparable between different days (data not shown).

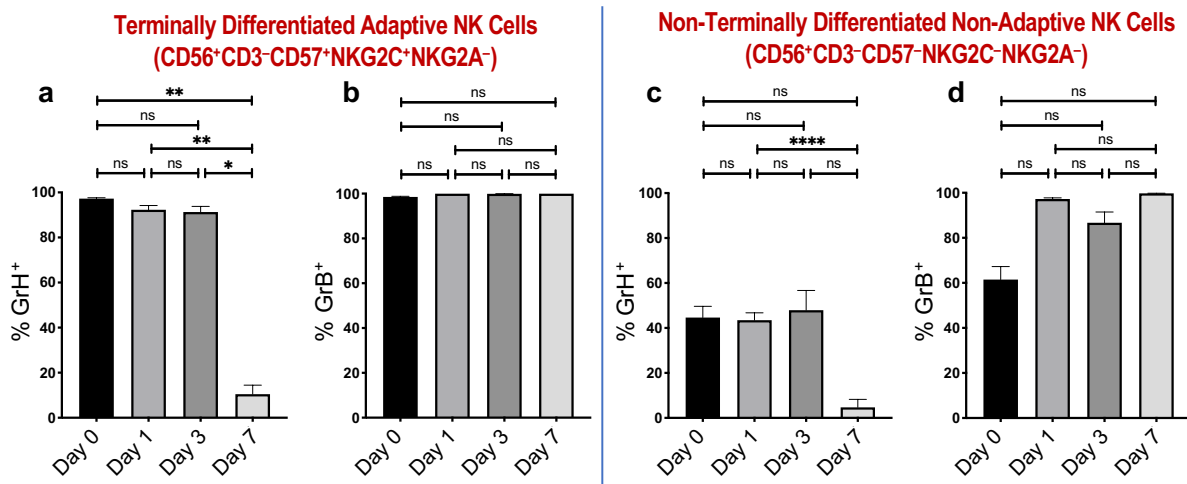


Fig. 38: Stimulation of terminally differentiated adaptive NK cells with rituximab and IL-15 leads to a drastic and very significant decrease in grH but not grB expression. Thawed PBMCs from donors with an NKG2C expansion were cultured, stained and analysed as described in the text. **a** and **c**: the percentage of cells that are grH⁺; **b** and **d**: the percentage of cells that are grB⁺. **a** and **b**: terminally differentiated adaptive NK cells; **c** and **d**: non-terminally differentiated non-adaptive NK cells. n = 3. Bars represent the data set means and the SEM. Significance testing was performed using a RM one-way ANOVA for each plot, followed by Tukey's test. The overall levels of significance of the ANOVAs were ** (**a**), * (**b**), ns (**c**) and ns (**d**).

3.9.2 Target Cell-Mediated NK-Cell Stimulation

3.9.2.1 A Degranulation and Cytokine-Production Assay

After the above analysis of the effect of soluble mediator-induced stimulation, NK cells were co-cultured with HLA class I-deficient K562 target cells to induce a missing-self response and examine the influence of target cell-mediated stimulation on grH expression. For this, thawed PBMCs from C1/C1, group A/A *KIR* haplotype donors were cultured overnight in NK-cell medium with no cytokine supplements to aid recovery from the freezing/thawing process. They were then cultured for 5 hours either with or without target cells at an effector:target-cell ratio of 10:1. They were stained for CD56, CD3, 2DL3, 2DL1, 3DL1, NKG2A, grH, grB, CD107a, IFN- γ and TNF- α , and analysed flow cytometrically; both straight after thawing and after culture with or without target cells. Cell-surface CD107a was used as a marker of degranulation, and intracellular IFN- γ and TNF- α as measures of cytokine production. CD56^{dim} NK cells were examined for receptor, grH, grB, CD107a, IFN- γ and TNF- α -positivity or negativity. Since this assay only included 5 hours of stimulation (total length 21 hours), the distinction between CD56^{dim} and CD56^{bright} NK cells was maintained, allowing the following analyses to focus on CD56^{dim} NK cells. As before, 2DL3 sp CD56^{dim} NK cells were licensed and 2DL1 sp CD56^{dim} NK cells unlicensed.

First, a significant increase in cell-surface expression of CD107a (mean: 9.06% to 51.3%) and intracellular expression of IFN- γ (3.21% to 25.5%) and TNF- α (3.03% to 19.5%) by CD56^{dim} NK from 'no target' to 'target' confirmed that the assay had worked (**Fig. 39**). Licensed 2DL3 sp CD56^{dim} NK

Results

cells showed a more pronounced response to target cell-mediated stimulation than unlicensed 2DL1 sp CD56^{dim} NK cells, as shown by a significantly larger specific increase (Δ) in CD107a (mean Δ (%) licensed vs unlicensed: 43.5 vs 18.2), IFN- γ (Δ (%) licensed vs unlicensed: 25.2 vs 7.43) and TNF- α (Δ (%) licensed vs unlicensed: 16.9 vs 5.04) expression (see section 2.2.7.2 for how the specific change (Δ) was calculated). However, the fact that unlicensed NK cells displayed a specific increase in the three markers at all shows that they, too, were activated. As will be remarked upon in the discussion, this is most likely to be an indirect effect.

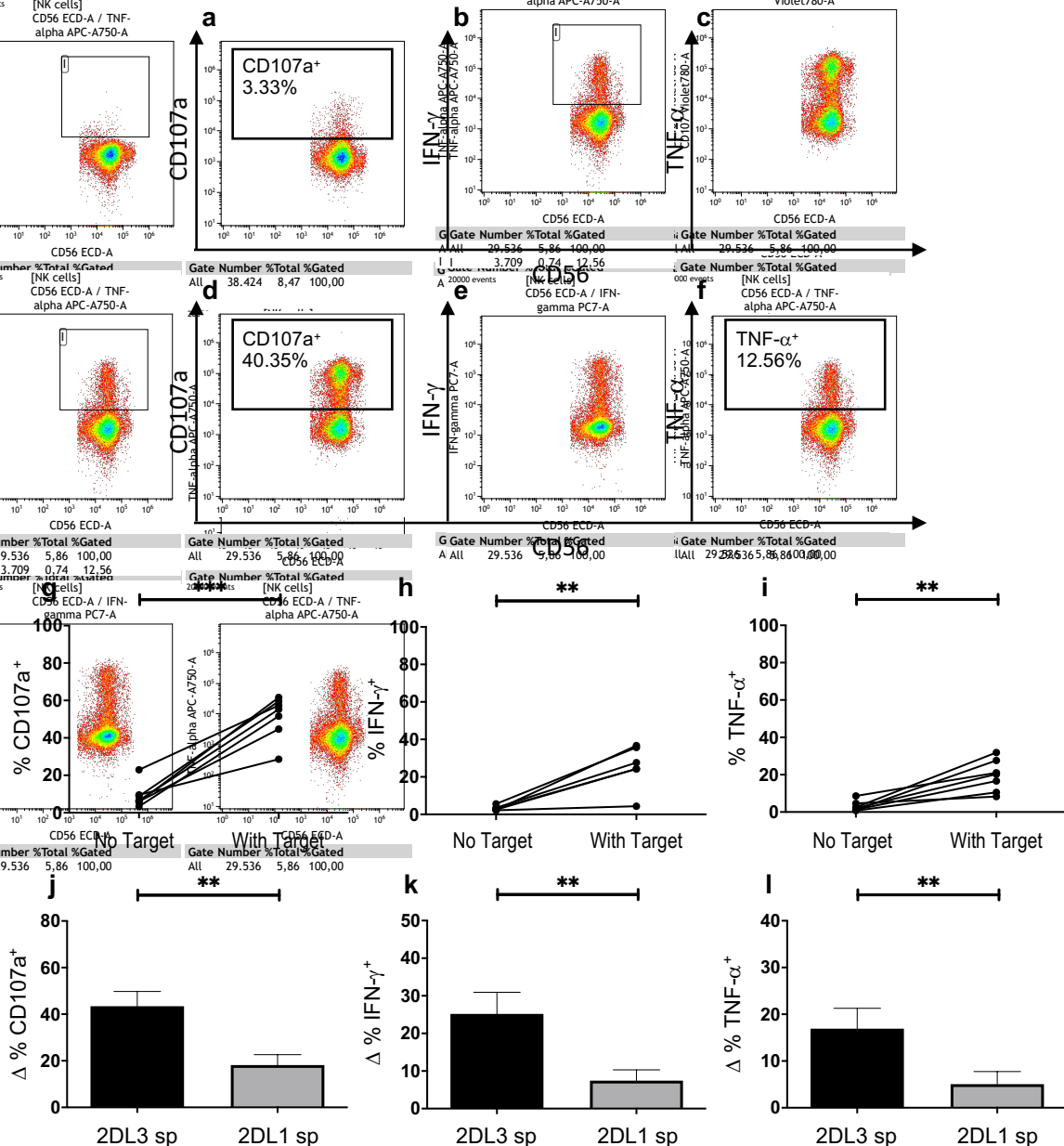


Fig. 39: Co-culture of PBMCs with K562 target cells leads to increases in expression of CD107a, IFN- γ and TNF- α by CD56^{dim} NK cells, more so in licensed than unlicensed NK cells. PBMCs were treated and analysed as described in the text. **a-f:** representative flow cytometry plots to give a more visual representation of the increase in CD107a, IFN- γ and TNF- α in CD56^{dim} NK cells ($n = 1$). **g-i:** the percentage of CD56^{dim} NK cells positive for CD107a (**g**), IFN- γ (**h**) or TNF- α (**i**). **j-l:** the specific change (Δ) in percentage points in licensed or unlicensed CD56^{dim} NK cells positive for CD107a (**j**), IFN- γ (**k**) or TNF- α (**l**) between cultures with target and cultures without target; positive Δ = increase. **g, i, j, l:** $n = 7$; **h, k:** $n = 6$. Significance testing was performed using a paired t test for each plot. **g-i:** individual data points are shown. **j-l:** bars represent the data set means and the SEM.

Results

Having established that the assay worked, grH expression by CD56^{dim} NK cells (as a percentage of cells positive for grH) straight after thawing and after culture without or with target was examined, and compared to grB, to determine whether and how short-term stimulation via target cells affects it.

As **Fig. 40** shows, grH expression by CD56^{dim} NK cells cultured with target cells (38.6%) was very significantly lower than by CD56^{dim} NK cultured without target cells (53.7%) and those stained straight after thawing (56.9%) (**Fig. 40a**), which parallels the decrease in grH expression following soluble mediator-induced stimulation. This decrease following co-culture with target cells was observed both in licensed (grH⁺ straight after thawing: 72.4%; without target: 70.5%; with target: 52.8%) (**Fig. 40b**) and unlicensed (grH⁺ straight after thawing: 42.1%; without target: 45.7%; with target: 35.8%) (**Fig. 40c**) NK cells, though more significantly so in the licensed population. In contrast, there was no decrease at all (if anything, a slight increase again) in grB expression by CD56^{dim} NK cells (grB⁺ straight after thawing: 86.1%; without target: 88.8%; with target: 89.3%) (**Fig. 40d**).

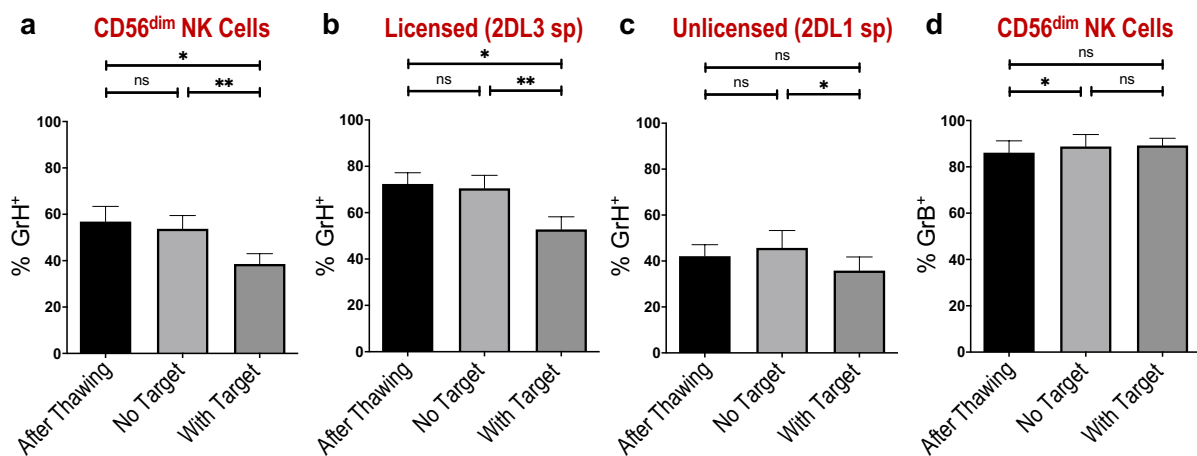


Fig. 40: Co-culture with K562 target cells leads to a significant decrease in expression of grH by CD56^{dim} NK cells (both in licensed and unlicensed NK cells), but not in expression of grB. PBMCs were treated as described in the text. GrH (**a**) and grB (**d**) expression by CD56^{dim} NK cells, and grH expression by licensed 2DL3 sp (**b**) and unlicensed 2DL1 sp (**c**) CD56^{dim} NK cells as a percentage of cells positive for grH or grB was determined straight after thawing of PBMCs, after culture without target and after culture with target. n = 6. Bars represent the data set means and the SEM. Significance testing was performed using a RM one-way ANOVA for each plot, followed by Tukey's test.

Next, grH⁻ and grH⁺ CD56^{dim} NK cells were compared for the specific change (Δ) in CD107a, IFN- γ and TNF- α to see whether there was any difference between the two populations. Interestingly, the specific increase in all three markers was significantly larger in grH⁻ than grH⁺ CD56^{dim} NK cells (Δ (%) in grH⁻ vs grH⁺ cells of CD107a: 50.7 vs 29.1; IFN- γ : 29.8 vs 11.2; TNF- α : 23.0 vs 7.43) (**Fig. 41a-c**). When dissecting this data further and looking at licensed 2DL3 sp and unlicensed 2DL1 sp CD56^{dim} NK cells, the specific increase in all three parameters was larger in grH⁻ than grH⁺ cells both within the licensed (Δ (%) in grH⁻ vs grH⁺ cells of CD107a: 53.0 vs 32.4; IFN- γ : 35.5 vs 14.2; TNF- α : 24.3 vs 9.28) (**Fig. 41d-f**) and unlicensed (Δ (%) in grH⁻ vs grH⁺ cells of CD107a: 23.9 vs 9.31; IFN- γ : 10.5 vs 1.78; TNF- α : 8.00 vs 1.31) (**Fig. 41g-i**) populations. These results were significant for all parameters in both licensed and unlicensed NK cells except for TNF- α in unlicensed cells, the trend being the same as in licensed cells and as for the other parameters, however.

A potential explanation may be grH exhaustion: those cells that show increased cell-surface CD107a and intracellular cytokine expression may have released their grH stores during activation without them then being replenished. Subsequent staining and flow cytometrical analysis then reveal only the activation markers, grH no longer being detectable.

Results

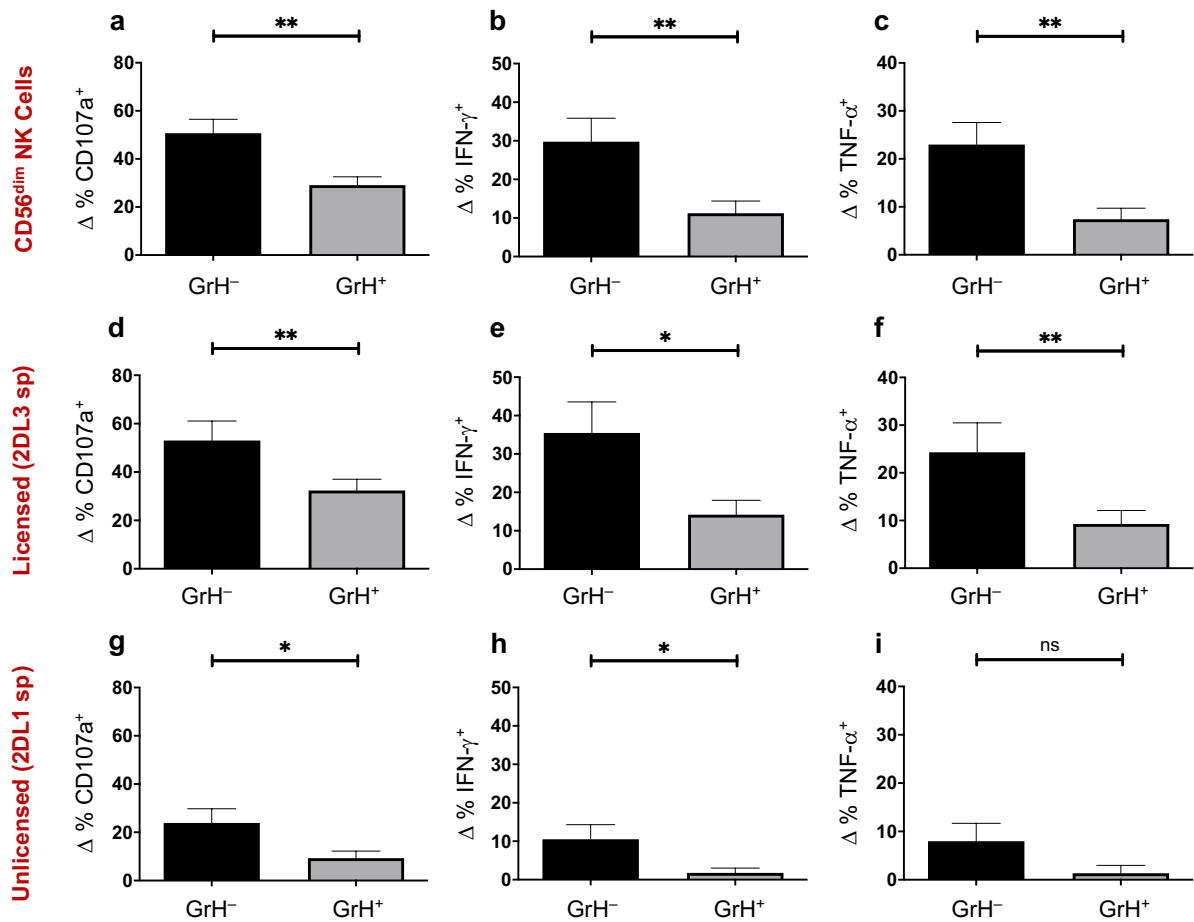


Fig. 41: Following co-culture with K562 target cells, the specific change in CD107a, IFN- γ and TNF- α is greater in grH⁻ than grH⁺ CD56^{dim} NK cells, both in licensed and unlicensed CD56^{dim} NK cells. PBMCs were treated and analysed as described in the text. A positive specific change (Δ) signifies an increase. **a-c:** Δ (%) in CD107a (**a**), IFN- γ (**b**) and TNF- α (**c**) in grH⁻ vs grH⁺ CD56^{dim} NK cells. **d-f:** Δ (%) in CD107a (**d**), IFN- γ (**e**) and TNF- α (**f**) in grH⁻ vs grH⁺ licensed 2DL3 sp CD56^{dim} NK cells. **g-i:** Δ (%) in CD107a (**g**), IFN- γ (**h**) and TNF- α (**i**) in grH⁻ vs grH⁺ unlicensed 2DL1 sp CD56^{dim} NK cells. n (**a, c, d, f, g, i**) = 7; n (**b, e, h**) = 6. Bars represent the data set means and the SEM. Significance testing was performed using a paired t test for each plot.

By comparison, there was no significant difference in the specific increase in CD107a, IFN- γ and TNF- α in grB⁻ vs grB⁺ CD56^{dim} NK cells; if anything, though not statistically significantly so, there was a slightly smaller specific increase in the three markers in grB⁻ than grB⁺ CD56^{dim} NK cells (Δ (%) in grB⁻ vs grB⁺ cells of CD107a: 31.2 vs 38.1; IFN- γ : 15.7 vs 20.9; TNF- α : 11.6 vs 15.3) (**Fig. 42**). This may mean that in contrast to grH, grB stores may be replenished upon degranulation or, alternatively, may be so high to begin with that exhaustion is less likely to happen.

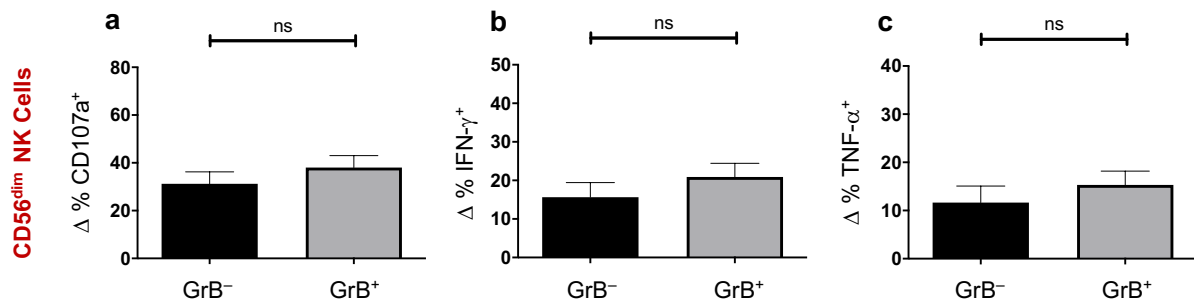


Fig. 42: Following co-culture with K562 target cells, there was no significant difference in the specific change in CD107a, IFN- γ and TNF- α between grB⁻ and grB⁺ CD56^{dim} NK cells. The experimental setup was as described in **Fig. 41**. The Δ (%) in CD107a (**a**), IFN- γ (**b**) and TNF- α (**c**) in grB⁻ and grB⁺ CD56^{dim} NK cells is displayed. n (**a** and **c**) = 7, n (**b**) = 6. Bars represent the data set means and the SEM. Significance testing was performed using a paired t test for each plot.

3.9.2.2 GrH Expression by NK Cells Expanded according to Fujisaki *et al.*'s protocol

In order to test the effect of yet another stimulatory protocol on grH expression, grH expression by primary NK cells (day 0) was compared to that by NK cells expanded according to a protocol published by Fujisaki *et al.* in 2009 (195). The non-expanded (day 0) and expanded (day 7-14) cells were kindly provided by Dr M. Hejazi at the at the ITZ. On day 0 and after expansion the provided cells were stained for CD56, CD3 and grH or grB and analysed, both by this study's author. GrH or grB expression by NK cells (both CD56^{dim} and CD56^{bright}, as the distinction again disappeared with stimulation) as a percentage of CD56⁺CD3⁻ cells positive for the granzyme in question was determined.

As can be seen in **Fig. 43a** and **b**, grH expression by NK cells decreased drastically and significantly with expansion from a mean of 77.1% to a mean of 3.41%. There also appeared to be a slight, though far smaller, decrease in grB expression from a mean of 89.6% to a mean of 84.9%, though the sample size is too small to draw a definitive conclusion (**Fig. 43c**).

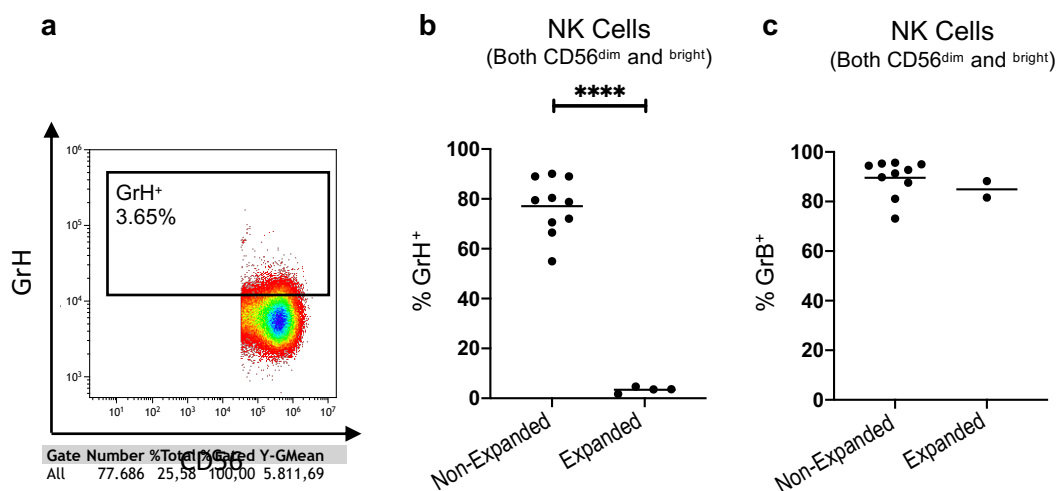


Fig. 43: Expansion of primary NK cells according to Fujisaki *et al.* (195) leads to a drastic decrease in grH expression. GrB is shown for comparison. Thawed PBMCs were stained and analysed as described in the text, before and after expansion. **a**: representative flow cytometry plot of expanded NK cells to show grH expression. **b** and **c**: the percentage of non-expanded and expanded NK cells that are grH⁺ (**b**) or grB⁺ (**c**). n (non-expanded) = 10, n (expanded) = 4 (grH) and 2 (grB). Individual data points are shown, bars represent data set means. Significance testing was performed using an unpaired t test for plot **b**; no significance testing was performed for plot **c** due to the small sample size.

On the mRNA level (transcriptome established through RNA-Seq of non-expanded and expanded CD56⁺CD3⁻ NK cells by Dr Hejazi, Prof. Uhrberg and Prof. Walter, and the raw data kindly provided to and analysed by this study's author, as before), this decrease in grH protein expression was paralleled by a drastic and significant decrease in *GZMH* transcript numbers with expansion (mean non-expanded: 1466, vs expanded: 418) (**Fig. 44a**), indicating a possible downregulation of *GZMH* at the gene level. The data for grB was not as clear: though some samples also appeared to show downregulation of *GZMB* mRNA, *GZMB* transcript numbers remained much higher even than initial *GZMH* transcript numbers (mean non-expanded: 5660, vs expanded: 6325) (**Fig. 44b**). Interestingly and contrasting particularly with *GZMH*, transcript numbers of *GZMA* increased significantly with NK-cell expansion, so the data for *GZMA* is also shown (mean non-expanded: 3194, vs expanded: 15977) (**Fig. 44c**). No confirmation of this increase in *GZMA* mRNA was performed at the protein level, but the demonstrated increase does corroborate the finding of differential regulation of granzyme expression by NK cells.

To further study the potentially differential granzyme expression upon NK-cell stimulation, transcriptomes of the cells stimulated with IL-2 and IL-15 or rituximab and IL-15 (section 3.9.1) as well as of those stimulated with non-transduced K562 cells (section 3.9.2.1) should be established.

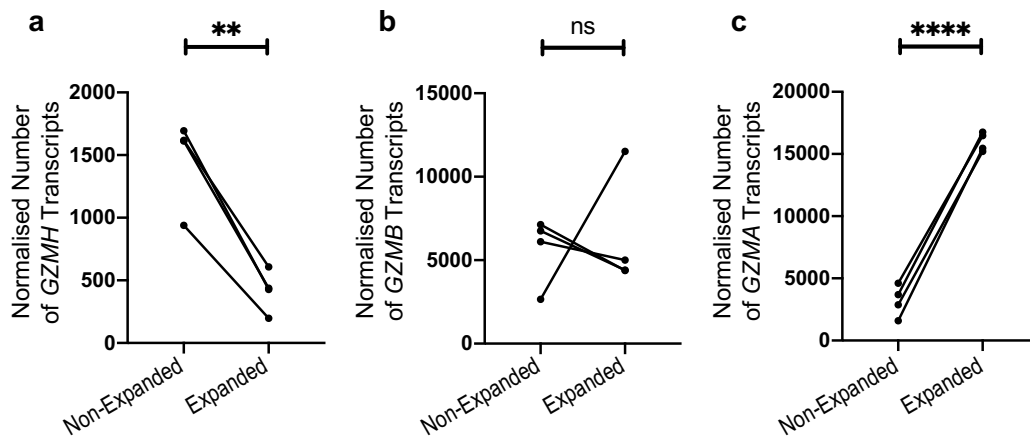


Fig. 44: The normalised number of *GZMH* transcripts in NK cells decreases drastically upon stimulation using Fujisaki *et al.*'s protocol. *GZMB* and *GZMA* are shown for comparison. Transcriptomes were established as described in the text. $n = 4$. Significance testing was performed using a paired t test for each plot, as the samples were matched.

3.10 Overexpression of GrH in NK-92 Cells and Primary NK Cells

3.10.1 Overexpression in NK-92 Cells

3.10.1.1 The Overexpression Process, Cell Sorting and RNA-Seq

This section now addresses overexpression of grH in cells that express very little of it, as has been alluded to before. The rationale for attempting overexpression of grH lies in this granzyme's intracellular location. Because of this, as mentioned before, a pure population of *live* cells that all express grH cannot be established by conventional means like cell sorting. The study of potential differences between grH⁺ and grH⁻ cells is further complicated by the difficulty in establishing transcriptomes of these cells, due to modification of RNA and cross-linking of RNA with proteins upon cell fixation (259) for subsequent permeabilisation. Though RNA extraction from such cells was attempted in this study using a published protocol (222), this was unsuccessful (data not shown). As an alternative approach, grH was overexpressed in cells with little or no inherent grH expression as a way of establishing reasonably pure grH⁺ and grH⁻ populations for study. The NK-cell line NK-92, which, as shown in **Fig. 45d** and **e**, expresses very little grH, was chosen for this purpose.

The NK-92 cells were transduced using virus supernatant of the EGFP-encoding p2CL6I2EGwo × *GZMH* ('NK-92 + GrH') and of the empty vector ('NK-92 + Empty Vector'), or, as a further control, were not transduced at all ('NK-92 No Vector'). Transduction success was confirmed by flow cytometrical analysis of EGFP (via the FITC channel) and, after staining for grH, grH expression.

The gating strategy for identifying EGFP⁺ and grH⁺ NK-92 cells is shown in **Fig. 45**. Analysis on day 4 after transduction revealed that, within the singlets gate, 38.7% of grH-transduced NK-92 and 41.4% of empty vector-transduced NK-92 cells were EGFP⁺, while only 3.64% of non-transduced NK-92 cells were EGFP⁺, the latter representing non-specific staining (**Table 30**). 57.1% of EGFP⁺ grH-transduced NK-92 cells were grH⁺, while only 7.12% of EGFP⁺ empty vector-transduced NK-92 cells were grH⁺ and 6.96% of EGFP⁺ non-transduced NK-92 cells were grH⁺. These results indicate that transduction both worked and was specific. As shown qualitatively in **Fig. 45c**, higher EGFP expression correlated with higher grH expression.

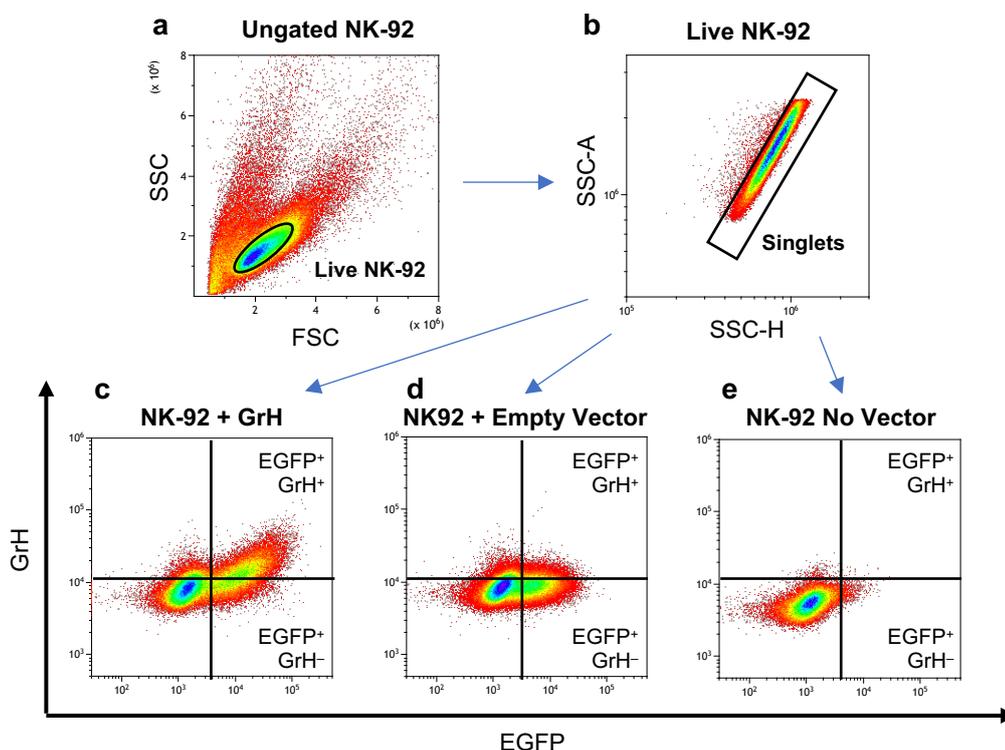


Fig. 45: Transduction of NK-92 cells with grH or empty vector was successful. Representative flow cytometry plots of transduced and non-transduced ('no vector') NK-92 cells stained for grH. **a:** gating on NK-92 cells that were alive prior to staining. **b:** gating on singlets. **c:** grH, **d:** empty vector, and **e:** non-transduced NK-92 cells.

Table 30: The percentage of NK-92 cells transduced with grH (a) or empty vector (b) or not transduced (c) that were EGFP⁺ and the percentage of EGFP⁺ NK-92 cells that stained positive with anti-grH. n = 1.

	a: NK-92 + GrH	b: NK-92 + Empty vector	c: NK-92 No Vector
Singlets that were EGFP ⁺	38.7%	41.4%	3.64%
EGFP ⁺ singlets that stained positive with anti-grH	57.1%	7.12%	6.96%

Once steady cell growth had been re-established following transduction, EGFP⁺ cells were enriched via FACS (**Fig. 46**) (kindly performed by Dipl. Ing. K. Raba at the ITZ). On the sorting platform of the MoFlo™ XDP cell sorter the FITC-channel (for EGFP) was plotted against the PE-channel (after gating on singlets) to enable exclusion of highly autofluorescent cells. Only highly EGFP⁺ singlets were selected (gate R3 in **Fig. 46a** and **b**) to yield maximally grH-expressing cells. EGFP⁻ cells were identified for reference (gate R4) but discarded. After sorting, the cells were placed into long-term cell culture again by this study's author using NK-92 medium as described in section 2.2.5.

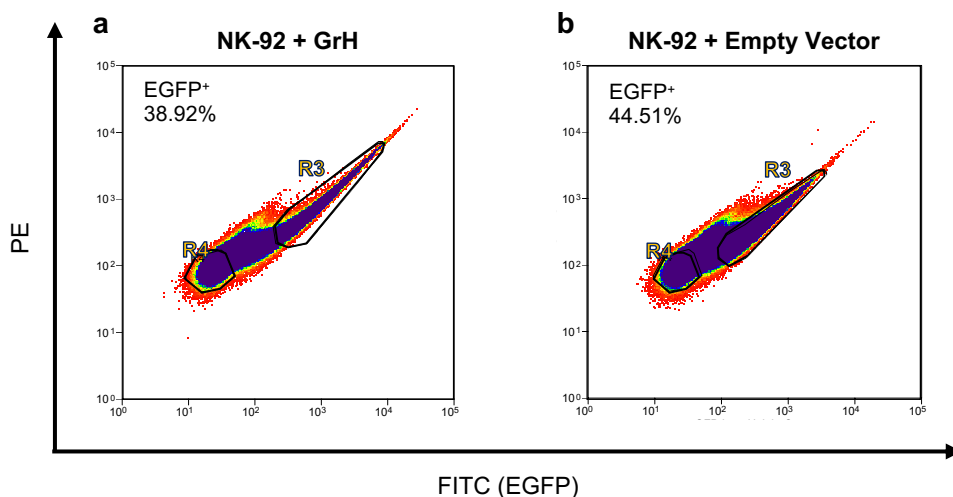


Fig. 46: FACS plots to show the gating employed for the sorting of EGFP⁺ transduced NK-92 cells. Only singlets were included for EGFP-gating. **a:** empty vector-transduced NK-92. **b:** grH-transduced NK-92. R3 gate = EGFP⁺, R4 gate = EGFP⁻.

Results

The cells (both pre- and post-sorting) were monitored for EGFP expression over time using flow cytometry without additional staining (**Fig. 47**). An initial increase in EGFP expression by unsorted transduced NK-92 cells was observed (EGFP⁺ NK-92 + GrH: 35.8% to 43.3%; NK-92 + Empty Vector: 40.2% to 49.2%), and EGFP expression by sorted transduced NK-92 cells remained stable for several weeks (EGFP⁺ NK-92 + GrH: 91.8% to 91.5%; NK-92 + Empty Vector: 90.8% to 96.0%). Therefore, the sorted cells were able to be used for functional assays at different time points without the risk of non-comparability. As a control, non-transduced NK-92 cells displayed no relevant EGFP-positivity.

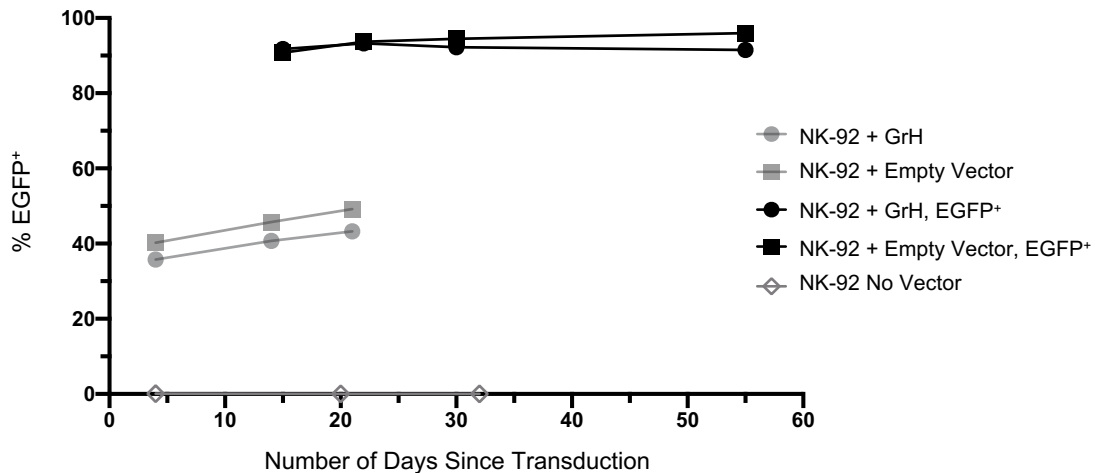


Fig. 47: EGFP expression by transduced NK-92 remains stable over several weeks. GrH, empty vector and non-transduced ('NK-92 No Vector') NK-92 cells were flow cytometrically analysed for EGFP expression at the indicated time points. Individual data points are shown. EGFP⁺ = cells sorted based on EGFP-positivity.

Next, RNA-Seq of the sorted, EGFP⁺ transduced NK-92 cells was performed (kindly carried out by Prof. Walter and colleagues after preparation of the cells for RNA-Seq by this study's author), to reveal whether expression of any other genes had changed notably in response to grH overexpression. The obtained data was analysed by this study's author.

No global gene expression changes could be detected (data not shown) and, particularly with regard to grB, this confirmed the specificity of grH overexpression. Far more *GZMH* transcripts were found in grH-transduced (normalised number of transcripts (#): 2162) than in empty vector-transduced (#: 611) or non-transduced (#: 702) NK-92 cells (**Fig. 48**). *GZMB* transcripts are shown for comparison; their number in non-transduced NK-92 cells was much higher than that of *GZMH* transcripts and did not increase between non-transduced (#: 6210) or empty vector-transduced (#: 3446) and grH-transduced (#: 3321) cells (**Fig. 48**), confirming specificity of grH-overexpression (in fact, they decreased somewhat). Furthermore, it is clear from this high number of grB transcripts in NK-92 cells that it would have been futile to attempt overexpression of grB as a potential control.

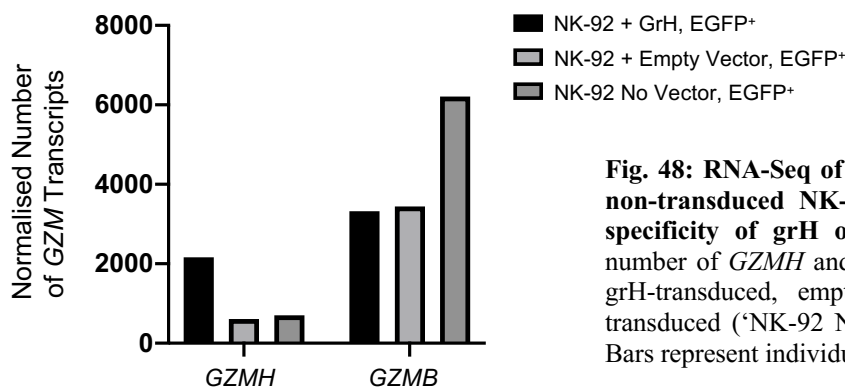


Fig. 48: RNA-Seq of sorted EGFP⁺ transduced and non-transduced NK-92 cells revealed success and specificity of grH overexpression. The normalised number of *GZMH* and *GZMB* transcripts is shown for grH-transduced, empty vector-transduced and non-transduced ('NK-92 No Vector') NK-92 cells. n = 1. Bars represent individual data points.

Results

3.10.1.2 Functional Analyses of Transduced NK-92 Cells

3.10.1.2.1 Degranulation and Cytokine-Production Assay

To establish whether overexpression of grH has a functional impact on NK-92 cells, as an indication of the function of grH –focusing particularly on grH’s putative cytotoxic role–, the response of the sorted transduced NK-92 cells to HLA class I-deficient K562 target cells was examined. The cytotoxic response of NK-92 cells to K562 cells is well-established (198). Changes in expression of CD107a, IFN- γ and TNF- α by NK-92 cells following stimulation by K562 cells appear to be less pronounced, though this differs between different studies (260),(261). Both responses were therefore examined here.

A degranulation and cytokine-production assay was first performed, co-culturing grH-transduced and empty vector-transduced NK-92 cells with K562 target cells for 5 hours and determining the specific increase in expression of cell-surface CD107a and intracellular IFN- γ and TNF- α by NK-92 cells as a result of co-culture, as in section 3.9.2.1. Trials with different effector:target-cell ratios revealed that a ratio of 1:1 yielded the clearest results (data not shown). Cells were stained for CD107a, IFN- γ and TNF- α and analysed flow cytometrically. The percentage of CD107a⁺, IFN- γ ⁺ and TNF- α ⁺ EGFP⁺ singlets were identified. There was no specific increase (see section 2.2.7.2 for the calculation) in IFN- γ and TNF- α expression by either of the NK-92 samples (data not shown). A small specific increase in CD107a expression was observed, which was slightly larger in grH-transduced (mean: 6.07%) than empty vector-transduced NK-92 cells (mean: 3.91%), though non-significantly so (Fig. 49).

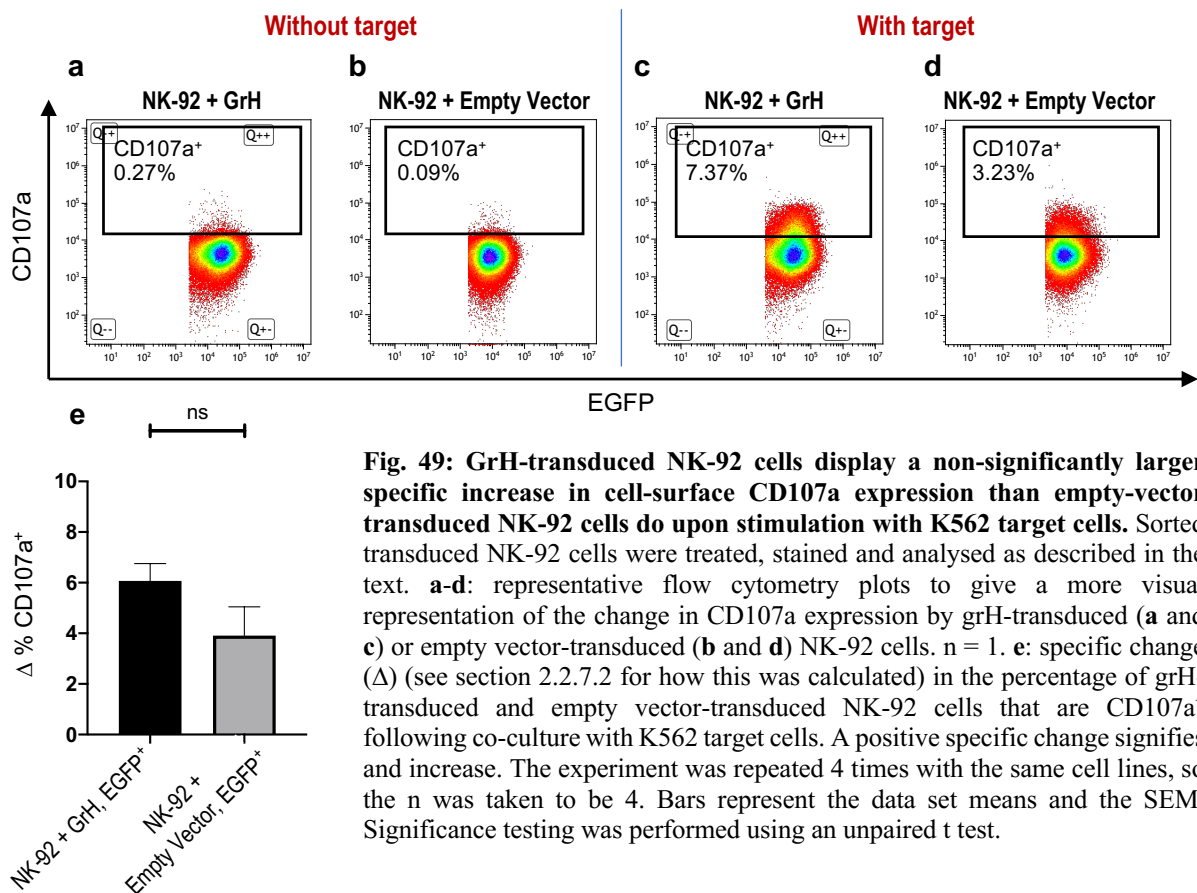


Fig. 49: GrH-transduced NK-92 cells display a non-significantly larger specific increase in cell-surface CD107a expression than empty-vector transduced NK-92 cells do upon stimulation with K562 target cells. Sorted transduced NK-92 cells were treated, stained and analysed as described in the text. **a-d**: representative flow cytometry plots to give a more visual representation of the change in CD107a expression by grH-transduced (**a** and **c**) or empty vector-transduced (**b** and **d**) NK-92 cells. $n = 1$. **e**: specific change (Δ) (see section 2.2.7.2 for how this was calculated) in the percentage of grH-transduced and empty vector-transduced NK-92 cells that are CD107a⁺ following co-culture with K562 target cells. A positive specific change signifies an increase. The experiment was repeated 4 times with the same cell lines, so the n was taken to be 4. Bars represent the data set means and the SEM. Significance testing was performed using an unpaired t test.

These results must be viewed with care, as the specific increase in CD107a expression was very low overall, in line with those studies that show only small if any changes (e.g. (260)). It was much lower than for primary NK cells in section 3.9.2.1. The degranulation and cytokine-production assay, at least in this study, was thus not satisfactory for studying the function of NK-92 cells. The slight difference

Results

between grH and empty vector-transduced NK-92 cells may, therefore, not represent a true difference, as also suggested by the lack of significance of the result. Partly for this reason, as well as because no certain conclusions regarding a protein's cytotoxic potential can be drawn without looking at its effects on target cells, the data do not give any clarity with regard to the presence or absence of a cytotoxic role of grH. Therefore, a cytotoxicity assay, again using K562 cells as target cells, was performed.

3.10.1.2.2 Cytotoxicity Assay

For the cytotoxicity assay, K562 target cells were pre-labelled with Tag-it Violet™ to stain live cells. After 5-hour co-culture of either sorted EGFP⁺ grH-transduced, sorted EGFP⁺ empty vector-transduced, or non-transduced NK-92 effector cells with these pre-labelled K562 target cells at different effector:target-cell ratios, the samples were stained with propidium iodide (PI) and analysed flow cytometrically to identify those target cells that had died or been killed during the assay (Tag-it Violet™⁺/PI⁺). Specific lysis was calculated as described in section 2.2.7.3.

Importantly, there was no significant difference in the specific lysis of target cells between grH-transduced, empty vector-transduced and non-transduced NK-92 cells (**Fig. 50**). This provides strong evidence against a cytotoxic role of grH in a whole-cell setting.

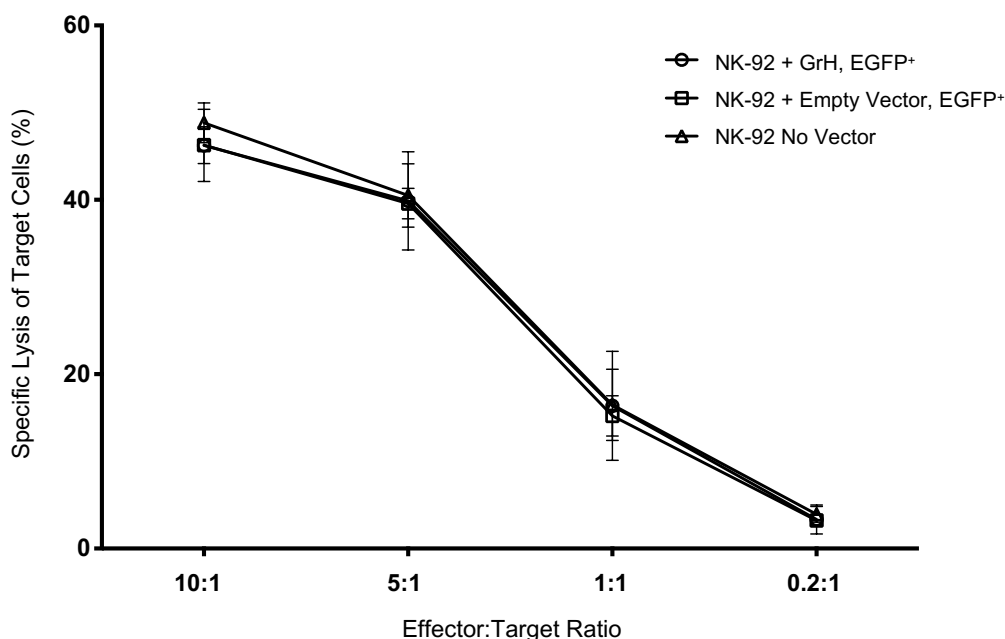


Fig. 50: There is no difference between grH, empty vector and non-transduced NK-92 cells in K562 target-cell cytotoxicity. The assay was performed 3 times with the same cell lines, so the n was taken to be 3. Points and bars represent the data set means and the SEM. Lack of significance was determined using a RM two-way ANOVA, followed by Tukey's test.

3.10.1.2.3 Growth and Death Rates of Transduced and Non-Transduced NK-92 Cells

Since no difference in cytotoxicity between the different NK-92 samples was detected, an alternative role of grH was sought. The question arose whether grH may have an impact on the survival of the cells that express it. To examine this, transduced NK-92 cells were monitored until day 58 after transduction to determine daily growth rate as well as the number of cells, adjusted for growth rate, that had died between counting events (see section 2.2.11.5.4 for the calculations). The effect on cell growth and death of withdrawal of IL-2, to potentiate any differences between the samples, was also examined.

There was no significant difference in growth rate or death between grH-transduced and empty vector-transduced NK-92 cells, though the trend suggests that fewer grH (mean: 1.26×10^6) than empty vector-

Results

transduced NK-92 cells (mean: 1.92×10^6) had died at each counting event (**Fig. 51a** and **b**). Withdrawal of IL-2, as expected, led to a decrease in growth and an increase in death of *both* samples but not to any apparent differences in growth *between* the two samples (**Fig. 51c** and **d**). However, again, fewer grH than empty vector-transduced NK-92 cells died, both with and without IL-2 (adjusted number of dead cells on day 11 *NO IL-2*: 1.20×10^6 (grH) vs 1.82×10^6 (empty vector)). The results of the IL-2 withdrawal assay need to be interpreted with care, however, as $n = 1$.

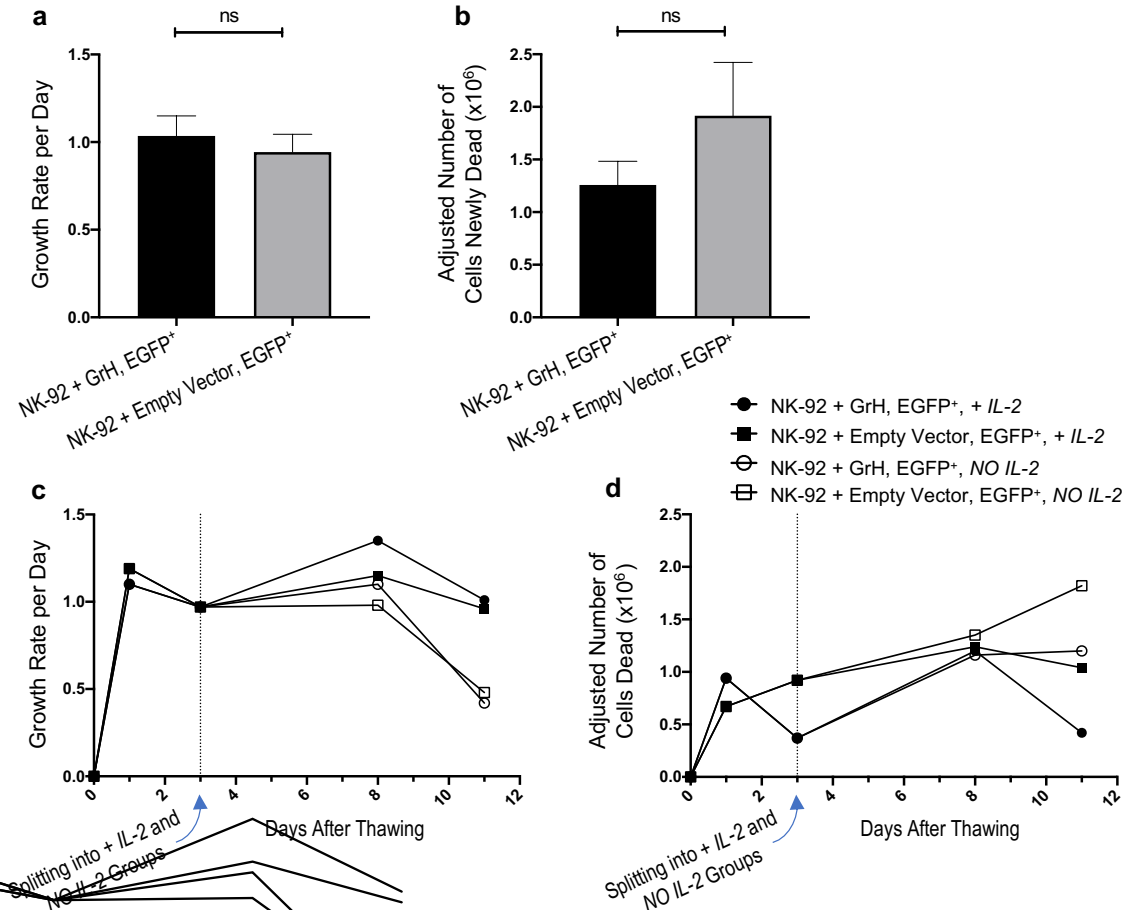


Fig. 51: There was no difference in cell growth between grH and empty vector-transduced NK-92 cells, both under normal cell-culture conditions and following IL-2 withdrawal, but slightly, though non-significantly, fewer grH than empty vector-transduced NK-92 cells died. **a** and **b**: live and dead grH and empty vector-transduced NK-92 cells were counted, using a counting chamber, until day 58 after transduction, the growth rates per day and the number of cells that died between counting events, adjusted for growth rate, calculated for each counting event, and displayed as one column per category per sample. Bars represent the data set means and the SEM. Significance testing was performed using an unpaired t test for each plot. $n \triangleq$ number of counting events per sample; **a**: $n = 17$; **b**: $n = 11$. **c** and **d**: IL-2 withdrawal: thawed grH and empty vector-transduced NK-92 cells were cultured in NK-92 medium and split into '+ IL-2' and 'NO IL-2' groups on day 3. Growth rates and adjusted numbers of dead cells were determined as in **a** and **b**. Each data point = one counting event, so $n = 1$.

3.10.2 Overexpression in Primary NK Cells

The results from **Fig. 51** suggest that grH, though not appearing to have a role in aiding cell growth, may play a part in aiding cell survival. To test this further, overexpression of grH was attempted in primary NK cells that had been expanded according to Fujisaki *et al.* (195) by and kindly provided by Dr M. Hejazi (ITZ) for transduction by this study's author. Given these cells' drastic downregulation of grH expression (**Fig. 43**, **Fig. 44**), they were predicted to represent good targets for grH overexpression. Unfortunately, however, despite several attempts, transduction of these cells (for protocol: see section 2.2.11.5.2.3) yielded transduction efficiencies too low (data not shown) for any meaningful functional analyses. The potential role of grH in NK-cell survival therefore had to be examined differently.

3.11 Examination of GrH with Regard to Cell Survival and Apoptosis

3.11.1 Correlation between Expression of GrH and BCL-2 and Licensing

To further test the hypothesis that grH may be linked with NK-cell survival, primary NK cells were examined for anti-apoptotic and apoptotic markers at rest and in a serum-starvation assay.

First, a possible correlation between expression of grH and of the anti-apoptotic protein BCL-2 was examined in resting NK cells. For this, thawed PBMCs from group *A/A KIR* haplotype, C1-homozygous donors were stained for CD56, CD3, 2DL3, 2LD1, 3DL1, NKG2A, grH and BCL-2, and analysed flow cytometrically. BCL-2 expression (both as a percentage and as MFI) by licensed 2DL3 sp and unlicensed 2DL1 sp CD56^{dim} NK cells was examined. Then, BCL-2 expression by grH⁻ and grH⁺ CD56^{dim} NK cells, as well as by grH⁻ and grH⁺ 2DL3 sp and 2DL1 sp CD56^{dim} NK cells, was analysed, as was grH expression by BCL-2⁻ and BCL-2⁺ CD56^{dim} NK cells, and by 2DL3 sp and 2DL1 sp BCL-2⁻ and BCL-2⁺ CD56^{dim} NK cells.

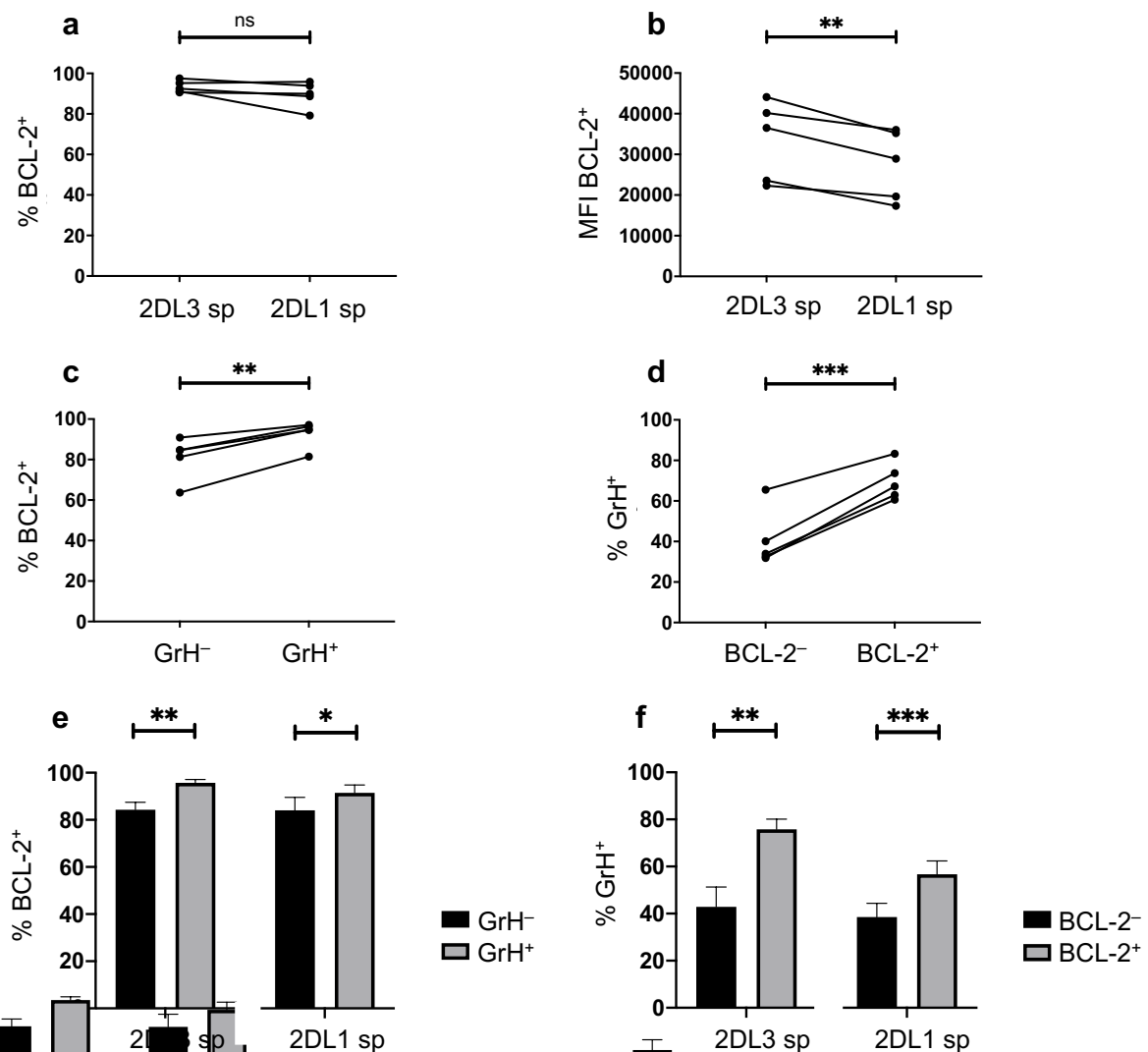


Fig. 52: BCL-2 expression is higher in licensed than unlicensed NK cells and there is a positive correlation between expression of grH and BCL-2 by CD56^{dim} NK cells. Thawed PBMCs were stained and analysed as described in the text. **a** and **b**: BCL-2 expression by licensed 2DL3 sp and unlicensed 2DL1 sp CD56^{dim} NK cells as a percentage (**a**) and as MFI (**b**). **c** and **e**: BCL-2 expression (as a percentage of cells positive for it) by grH⁻ and grH⁺ CD56^{dim} NK cells (**c**) and by licensed 2DL3 sp and unlicensed 2DL1 sp grH⁻ and grH⁺ CD56^{dim} NK cells (**e**). **d** and **f**: GrH expression by BCL-2⁻ and BCL-2⁺ CD56^{dim} NK cells (**d**) and by 2DL3 sp and 2DL1 sp BCL-2⁻ and BCL-2⁺ CD56^{dim} NK cells (**f**). *n* = 5. Significance testing for all comparisons of two data sets was performed using a paired t test. **e** and **f**: Bars represent the data set means and the SEM.

Results

Interestingly, licensing correlated with BCL-2 expression: though not significantly higher in licensed than unlicensed NK cells when examined as a percentage of cells positive for it (2DL3 sp BCL-2⁺: 93.4%, vs 2DL1 sp: 89.5%) (**Fig. 52a**), BCL-2 expression was significantly higher in licensed than unlicensed NK cells when examined as MFI (2DL3 sp: 33335, vs 2DL1 sp: 27438) (**Fig. 52b**). This clarifies the findings of Felices *et al.* (53), who showed BCL-2 expression to be higher in KIR⁺ than KIR⁻ resting NK cells, which the present study now shows to be likely due to a licensing effect. Furthermore, a positive correlation between grH and BCL-2 expression was found. BCL-2 expression by grH⁺ CD56^{dim} NK cells (BCL-2⁺: 92.9%) was significantly higher than by grH⁻ CD56^{dim} NK cells (81.0%) (**Fig. 52c**). The correlation held true in reverse, as well, grH expression by BCL-2⁺ CD56^{dim} NK cells (grH⁺: 69.5%) being significantly higher than by BCL-2⁻ CD56^{dim} NK cells (40.8%) (**Fig. 52d**). Both findings were reproducible in licensed as well as in unlicensed CD56^{dim} NK cells (BCL-2⁺ in licensed grH⁺ vs grH⁻ cells: 95.7% vs 84.3%, in unlicensed grH⁺ vs grH⁻ cells: 91.5% vs 84.1%; grH⁺ in licensed BCL-2⁺ vs BCL-2⁻ cells: 75.8% vs 42.9%, in unlicensed BCL-2⁺ vs BCL-2⁻ cells: 56.7% vs 38.5%) (**Fig. 52e and f**).

These findings suggest that grH expression does indeed correlate positively with NK-cell survival at some level.

3.11.2 Serum-Starvation Assay

In order to examine the potential role of grH in NK-cell survival with respect to apoptosis in a functional setting, apoptosis was induced in PBMCs through serum starvation. Apoptotic cells can be detected flow cytometrically using annexin V, a protein that preferentially binds phosphatidylserine (PS), and which can be used to label apoptotic cells. In healthy cells, PS is predominantly located on the inner leaflet of the plasma membrane, but is translocated to the cell surface in early apoptosis, where it can be identified using fluorochrome-conjugated annexin V (262). This translocation of PS also occurs in later-stage apoptotic, as well as necrotic, cells, so in order to distinguish between early apoptotic and late apoptotic or necrotic cells, cells can be labelled with dead cell markers that can only bind in significant amounts if cells have lost their membrane integrity (262). Thus, early apoptotic cells are annexin V⁺/dead cell marker⁻, while late apoptotic cells are annexin V⁺/dead cell marker⁺ (220),(262). Fixable viability dyes (FVDs) are dead cell markers that irreversibly bind to dead cells, allowing cells to be fixed and permeabilised for intracellular staining (263).

For the assay, thawed PBMCs were placed into overnight culture in standard cell-culture medium (see section 2.1.2 for its composition) to aid recovery from the freezing and thawing process, after which they were starved of serum for a further two days. Samples were stained with a FVD and annexin V, as well as for CD56, CD3, grH and BCL-2, and analysed flow cytometrically straight after thawing (day 0), after overnight culture (day 1), after one day of starvation (day 2) and after two days of starvation (day 3). GrH, BCL-2, annexin V and FVD-positivity or negativity within CD56^{dim} NK cells within the lymphocyte gate were established, to examine live and early apoptotic NK cells.

As expected from gating on the lymphocyte 'live' gate, throughout the assay the majority of cells were alive (FVD⁻AnnexinV⁻) prior to fixation (eg day 0: 86.6%). However, a small (non-significant) decrease in the percentage of FVD⁻AnnexinV⁻ NK cells was observed on day 3 (day 3: 64.9%), with a small (non-significant) increase in the percentage of early apoptotic NK cells (FVD⁻AnnexinV⁺) in parallel

Results

(day 0: 2.29%, day 3: 3.93%) (**Fig. 53a** and **b**). This indicates that apoptosis, though only to a small degree, had indeed been induced by the assay.

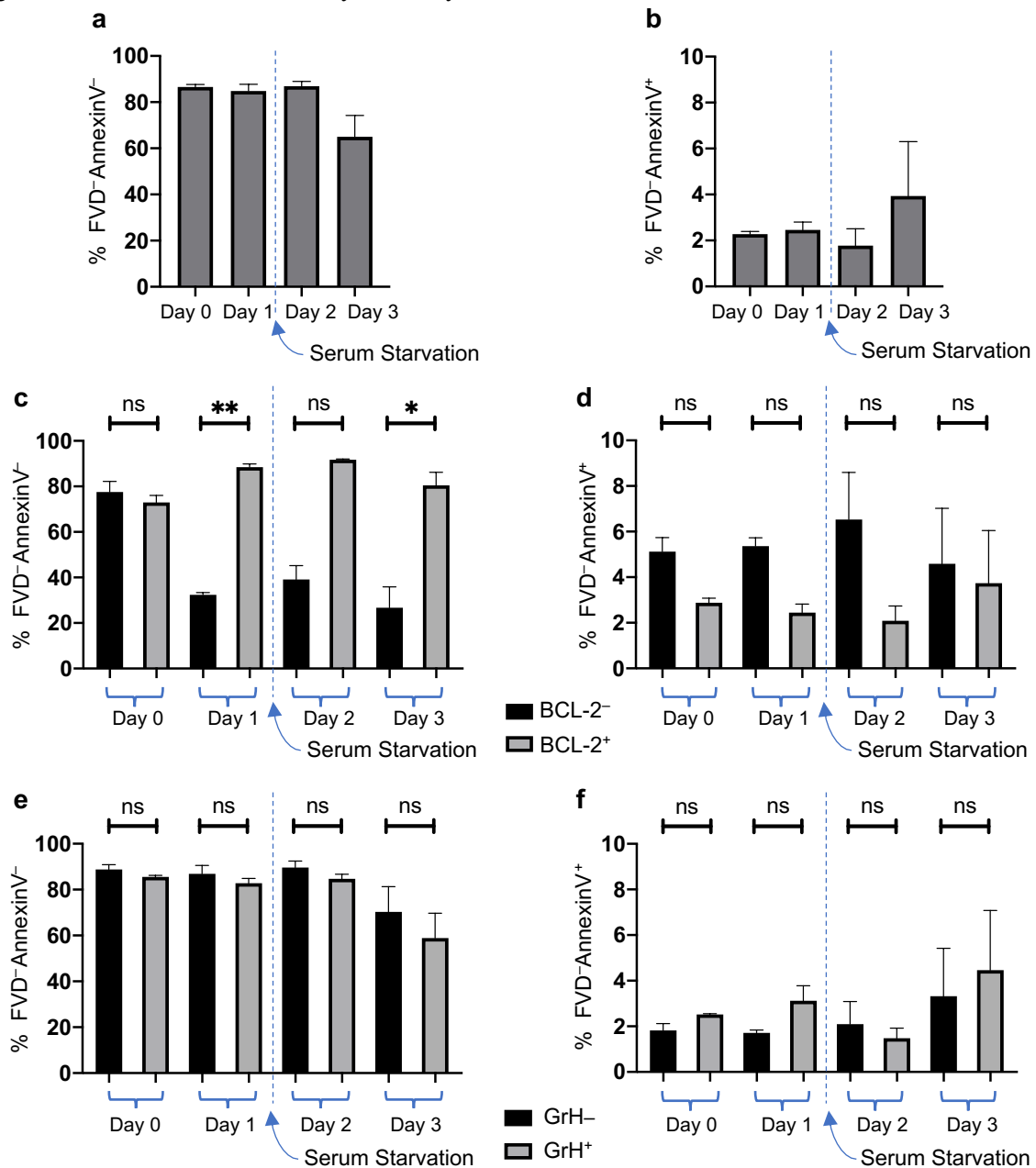


Fig. 53: During serum starvation, BCL-2, but not grH, expression correlates inversely with early apoptotic markers. Thawed PBMCs were treated, stained and analysed as described in the text. **a** and **b**: The percentage of CD56^{dim} NK cells that were alive (FVD⁻AnnexinV⁻) (**a**) or early apoptotic (FVD⁻AnnexinV⁺) (**b**) prior to staining. Significance testing was performed using a RM one-way ANOVA for each plot, followed by Tukey's test, all results of which were non-significant (not displayed for clarity). **c** and **d**: The percentage of BCL-2⁻ or BCL-2⁺ CD56^{dim} NK cells that were alive (**c**) or early apoptotic (**d**). **e** and **f**: The percentage of grH⁻ or grH⁺ CD56^{dim} NK cells that were alive (**e**) or early apoptotic (**f**). Significance testing in **c-f** was performed using a RM one-way ANOVA for each plot followed by Sidak's test, all results of which are displayed. All plots: n = 3. Bars represent the data set means and the SEM.

The percentage of BCL-2⁻ CD56^{dim} NK cells that were alive (FVD⁻AnnexinV⁻) beyond day 0 was shown to be significantly lower than that of BCL-2⁺ CD56^{dim} NK cells (BCL-2⁻ vs BCL-2⁺ cells that were FVD⁻AnnexinV⁻ on eg day 3: 25.67% vs 80.44%) (**Fig. 53c**), while, though only a small and non-significant difference was observed, the results were the other way around for early apoptotic (FVD⁻AnnexinV⁺) NK cells (BCL-2⁻ vs BCL-2⁺ cells that were FVD⁻AnnexinV⁺ on eg day 3: 4.58% vs 3.74%) (**Fig. 53d**). This serves as an internal control given that BCL-2 is an anti-apoptotic marker.

Results

Somewhat unexpectedly, the percentage of grH⁻ CD56^{dim} NK cells that were alive was non-significantly and slightly larger than that of grH⁺ CD56^{dim} NK cells, and this difference increased with prolonged culture (grH⁻ vs grH⁺ cells that were FVD⁻AnnexinV⁻ on day 0: 88.8% vs 85.5%, on day 3: 70.3% vs 58.9%). It was the other way around for early apoptotic markers, even if the difference increased only minimally with prolonged culture (grH⁻ vs grH⁺ cells that were FVD⁻AnnexinV⁺ on day 0: 1.82% vs 2.52%, on day 3: 3.32% vs 4.46%) (**Fig. 53e** and **f**). While at first glance this appears to violate the notion that grH may be associated with host-cell survival, the differences between grH⁻ and grH⁺ cells increasing with prolonged culture could indicate that grH may be important for host-cell survival at steady state but that its importance decreases in the presence of pro-apoptotic stimuli. On the other hand, given that the differences observed were all non-significant, care must be taken not to overestimate the robustness of the conclusions that can be drawn from this assay.

3.12 GrH and GrB Overexpression in K562 Cells to Test Antibody Specificity

As a final endeavour and as alluded to before, specificity of the anti-grB antibody GB11 was tested. As discussed above, there are discrepancies between the transcriptome data shown in sections 3.1 and 3.7 and some of the protein data shown in sections 3.6.4 and 3.7, as well as selected literature, with regard to grB expression in some circumstances. To reiterate, there was a clear correlation between NK-cell licensing and grB expression (as MFI) (**Fig. 26**), which parallels the licensing data for grH (**Fig. 22** and **Fig. 23**) and is consistent with the literature (144), but at odds with the transcriptome data shown in **Fig. 15**. Furthermore, the data displayed in **Fig. 31** showed no difference between expression of grH and grB (at the protein level) by terminally differentiated, adaptive CD56^{dim} NK cells, whereas the transcriptome data suggested expression of *GZMH* mRNA to be higher than that of *GZMB* mRNA (**Fig. 32**).

While protein levels, as assessed by flow cytometry, may not fully parallel mRNA levels due to post-transcriptional or post-translational regulation (264), it was nonetheless essential to assess whether the observed results could be due to anything other than a true measurement of grB protein levels. Given the high degree of structural identity between grH and grB, the possibility of the anti-grB mAb GB11 antibody cross-reacting with grH was examined. To study this, pure cell populations that express either one or the other granzyme but not both needed to be used and were established through separate overexpression of grH or grB in cells that ordinarily express little of either. Here, K562 cells were used for this purpose. They are known to express only low to medium levels of granzymes (265) and were thus good candidates for overexpression of these proteins.

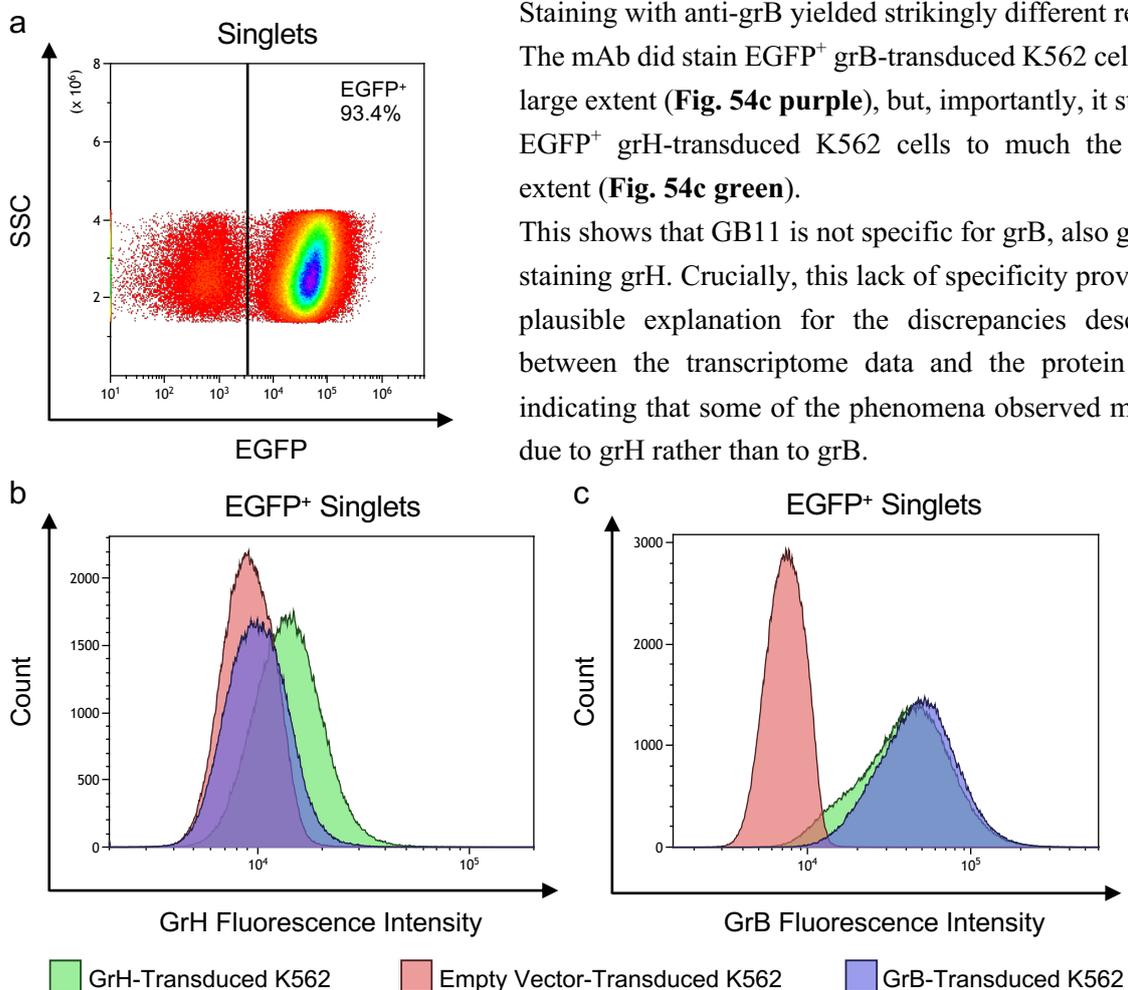
Overexpression of grH and grB in K562 cells was achieved via the same lentiviral vector system as for NK-92 cells (see also section 2.2.11), using virus supernatant of the EGFP-encoding p2CL6I2EGwo × *GZMH*, of the empty vector and this time also of p2CL6I2EGwo × *GZMB*.

Transduction success was confirmed by flow cytometrical analysis, which revealed substantial EGFP-positivity (data not shown). Once stable growth of the transduced cells had been re-established following transduction, EGFP⁺ populations were enriched via FACS (again kindly performed by Dipl. Ing. K. Raba at the ITZ), stained for grH and grB using the polyclonal anti-grH antibody and the GB11 mAb respectively and analysed flow cytometrically. GrH-transduced, empty vector-transduced and grB-transduced K562 cells all were >90% EGFP⁺ after FACS (**Fig. 54a**), confirming that FACS-mediated enrichment had worked. Staining of empty vector-transduced K562 with anti-grH (**Fig. 54b red**) or anti-

Results

grB (**Fig. 54c red**) did not yield any substantial positivity, verifying this sample's usefulness as a control, and also confirming the low expression of grH and grB by K562 cells.

As expected, staining of grH-transduced K562 cells with anti-grH gave a positive result (**Fig. 54b green**), though with lower intensity than might have been expected. This may have been due to the antibody used being quite old at this late stage of this study: because of the polyclonality of the antibody, a new lot number may have meant slightly different staining properties, so the same lot number as for the previous experiments was used (lot: ILD013061), meaning that the antibody vial had been open for several months, possibly resulting in some loss of sensitivity. A downregulation of grH with prolonged culture as a possible cause of this relatively low staining intensity is unlikely, given the large extent to which the anti-grB antibody stained grH (see next). The specificity of the anti-grH antibody was not compromised, however: despite the considerable structural overlap between grH and grB, staining of grB-transduced K562 with anti-grH did not produce a considerable positive result (**Fig. 54b purple**). This once more confirms the antibody's specificity despite its polyclonality.



Staining with anti-grB yielded strikingly different results. The mAb did stain EGFP⁺ grB-transduced K562 cells to a large extent (**Fig. 54c purple**), but, importantly, it stained EGFP⁺ grH-transduced K562 cells to much the same extent (**Fig. 54c green**).

This shows that GB11 is not specific for grB, also greatly staining grH. Crucially, this lack of specificity provides a plausible explanation for the discrepancies described between the transcriptome data and the protein data, indicating that some of the phenomena observed may be due to grH rather than to grB.

Fig. 54: The anti-grB mAb GB11 stains grH to a similar extent as it does grB. FACS-sorted grH-transduced, empty vector-transduced and grB-transduced K562 cells were stained with anti-grH or anti-grB and analysed flow cytometrically. As for transduced NK-92 cells (section 3.10.1), gates were set on live cells, then on singlets. **a**: representative flow cytometry plot of singlets to show EGFP-positivity of FACS-sorted transduced K562 cells, using empty vector-transduced K562 cells as an example. GrH-transduced and grB-transduced K562 cells showed the same order of magnitude of EGFP-positivity (data not shown). **b** and **c**: flow cytometry histograms, gated on EGFP⁺ cells, of grH-transduced, empty vector-transduced and grB-transduced K562 cells stained with the polyclonal anti-grH (**b**) or the anti-grB mAb GB11 (**c**), showing fluorescence intensity. $n = 1$.

4 Discussion

As before, since only inhibitory KIRs and NKG2A are looked at as inducers of education, the terms *education* and *licensing* are used interchangeably here. HLA-C1/C2 will continue to be referred to as C1/C2, HLA-Bw4 as Bw4, KIR2DL3 as 2DL3, KIR2DL1 as 2DL1, KIR3DL1 as 3DL1 (etc.), and CD94/NKG2A as NKG2A. To note, the chronology of this discussion does not fully parallel the order of the experiments as described in section 3: in order to be able to explain or substantiate certain phenomena found here, some experiments that were not conducted in order need to be analysed together.

4.1 The Positive Correlation between NK-Cell Education and GrH Expression

4.1.1 A Novel Temporal and Developmental Model of NK-Cell Licensing

NK-cell education is not yet fully understood. This study shows that expression of grH, a granzyme and thus one of the classic NK-cell effector molecules, is positively correlated, and highly significantly so, with NK-cell licensing via the expression of a self-specific inhibitory receptor. This is the case for licensing via 2DL3 and 2DL1 in the respective HLA-C1/C2 backgrounds, via 3DL1 in Bw4⁺ backgrounds and via NKG2A. The correlation between NK-cell education and grH expression at the protein level is established in this study, and, particularly when taken in concert with the link demonstrated at the mRNA level as part of the preliminary experiments shown in **Fig. 15**, is highly robust. No clear link was found between NK-cell licensing and the expression of grA and grK (**Fig. 27**, **Fig. 28**), with only a tenuous one established for grB (see below). GrH expression, on the other hand, correlated so well with the type of inhibitory receptor that was expressed, increasing in an almost stepwise fashion between different NK-cell populations, that it can be used to formulate a temporal and developmental model of NK-cell licensing, intricately linked with NK-cell maturation (**Fig. 55**). The next paragraphs describe how **Fig. 55** was arrived at, as well as some of its implications.

When focusing on inhibitory receptor status, the highest grH expression levels were consistently found in CD56^{dim} NK cells licensed via a self-specific inhibitory KIR (**Fig. 22**, **Fig. 23**, **Fig. 24**, **Fig. 25**). The lowest levels among CD56^{dim} NK cells were found in receptor-negative populations as well as in those expressing a non-self-specific inhibitory KIR only, while the lowest levels overall were found in the less mature CD56^{bright} NK cells (**Fig. 20**). NKG2A⁺KIR⁻ and NKG2A⁺/non-self-specific inhibitory KIR⁺ CD56^{dim} NK cells expressed grH at an intermediate level (**Fig. 24**, **Fig. 25**). When also examining NK-cell characteristics other than inhibitory receptor expression, however, the highest levels of grH expression overall were found in terminally differentiated adaptive (CD57⁺NKG2C⁺NKG2A⁻) NK cells from donors with a (presumed to be CMV-associated) NKG2C expansion (**Fig. 31**).

Most simply put, the model proposes five main steps of licensing/maturity status based on grH expression: CD56^{bright} < unlicensed < licensed via NKG2A < licensed via KIR < adaptive NK cells.

GrH expression also positively correlated with expression of the differentiation marker CD57 in samples from donors with or without an NKG2C expansion (**Fig. 30**, **Fig. 31**), which indicates that grH expression is related not just to NK-cell licensing but also to maturity *per se*, particularly when taken in concert with grH expression by CD56^{dim} NK cells being significantly higher than by the less mature CD56^{bright} NK cells. NK-cell licensing and CD57-positivity independently correlated with higher grH

expression, though licensing was the dominant process, licensed $CD57^-$ NK cells showing higher grH expression than unlicensed $CD57^+$ ones. Within licensed and unlicensed NK cells, $CD57$ expression, as a proxy for maturation, then led to a further progressive increase in grH expression. Interestingly, the finding that even in the unlicensed NK cell population there were differences in grH expression by $CD57^-$ vs $CD57^+$ cells indicates that unlicensed NK cells, too, in addition to licensed ones, may show functional maturation in some circumstances, in line with their having been shown (though so far mainly in mice) to display enhanced effector functions under certain conditions (139),(155).

The expression of grH being highest in terminally differentiated adaptive NK cells suggests that these cells may embody not just a highly differentiated subset of NK cells (27),(36),(121), but also the endpoint of NK-cell licensing and functional competence, which would be in line with the highly mature, memory-like phenotype (27),(31) that has been ascribed to them. Particularly when taken in concert with the drastic reduction in grH expression upon NK-cell stimulation (see later), this suggests that those NK cells that are the most mature and cycle the least accumulate the highest levels of grH, with more cycling ($NGK2A^+ > KIR^+ > CD57^+NGK2C^+NGK2A^-$) translating to lower grH levels.

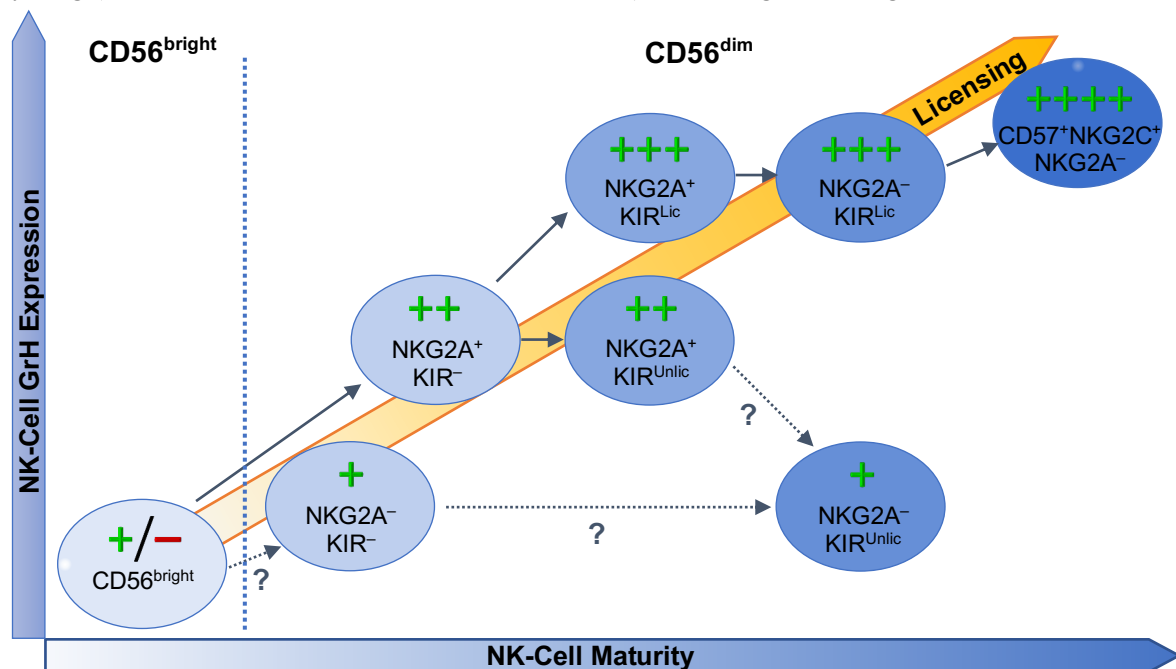


Fig. 55: Temporal and developmental model of NK-cell licensing as determined by grH expression; NK-cell maturity is also included as a factor. The ovoids represent NK cells, $CD56^{bright}$ to the left of the dashed blue line and $CD56^{dim}$ to its right. The respective receptor and/or $CD57$ -expression status is written within the ovoids. For clarity, the effect of $CD57$ expression on grH expression is not explicitly shown (except for $CD57^+NGK2C^+NGK2A^-$ cells), but regardless of receptor status, $CD57$ -positivity correlated with greater grH expression. KIR^{Unlic} = non self-specific inhibitory KIR-single-positive, KIR^{Lic} = self-specific inhibitory KIR-single-positive, $+/-$ to $++++$ = relative level of grH expression, ? = developmental process not clear. Author's illustration.

The reader is also referred back to the different stages of NK-cell development shown in **Fig. 1** in section 1.2. **Fig. 55** shown here is not only in line with a more detailed progression from Stage 4 ($CD56^{bright}$ NK cells) to Stage 5 ($CD56^{dim}$ NK cells) in **Fig. 1** (31), but, importantly, also provides evidence for the – to date – putative development from Stage 5 to Stage 6 (memory NK cells).

The author proposes that, given the robust positive correlation between NK-cell education and grH expression, the latter can be used as a marker of the former, independently of whether *KIR* genotype and HLA-C type are known. Its robustness as a marker is increased when also taking $CD57$ -positivity and *KLR1*-negativity (see later) into account (**Fig. 34**).

Discussion

4.1.2 The Number of Self-Specific Inhibitory KIRs and GrH Expression

Notably, the number of different self-specific inhibitory KIRs expressed by an NK cell did not influence the level of grH expression, as long as at least one type of self-specific inhibitory KIR was expressed (**Fig. 25**). However, the strength of the interaction between a self-specific inhibitory KIR and its cognate ligand likely plays a role in determining grH levels: though the results were non-significant, more 2DL1 sp than 2DL3 sp NK cells were grH⁺ in samples from C1/C2 donors (**Fig. 22, Fig. 25**), conceivably due to the interaction between 2DL1 and C1 being stronger than between 2DL3 and C2 (95).

4.1.3 GrH Expression in Cord Blood-Derived NK Cells, and the Novel Licensing Model

This study also shows grH expression to be significantly lower in CB-derived (ie developmentally less mature) compared with PB-derived CD56^{dim} NK cells (**Fig. 21**). Even in CB, however, grH expression was significantly higher in licensed than in unlicensed NK cells, though at lower levels overall than in peripheral blood (**Fig. 29**). These data fit nicely into and also provide further evidence in support of the model shown in **Fig. 55**, and they too indicate that maturation adds an additional layer to grH regulation.

4.1.4 Effect of Non-Discrimination between 2DL3 and 2DL2

A point that must be addressed is the slightly but significantly higher expression of grH by 2DL2/3/S2-‘single’-positive than receptor-negative NK cells in samples from C2/C2 donors when samples from group *B* *KIR* haplotype-expressing donors are included in addition to group *A* *KIR* haplotype-homozygous donors (**Fig. 23h**). When using the antibody clones GL183 and DX27 to stain for 2DL3, as was done here, 2DL2 and 2DLS2 are also stained for when expressed (as is the case for many donors with group *Bx* but not group *A/A* *KIR* haplotypes), since GL183 and DX27 do not discriminate between 2DL3, 2DL2 and 2DS2. Importantly, 2DL2 also recognises some C2-allotypes, particularly Cw*0501, Cw*0202 and Cw*0401 (96). It is very possible that the donors in this study with group *Bx* *KIR* haplotypes also expressed these allotypes, which would thus have led to licensing of 2DL2-positive NK cells, offering an explanation of the higher grH expression by cells stained with GL183 or DX27. Therefore, in order to be able to examine even purer populations of licensed and unlicensed NK cells and to eliminate this uncertainty, high-resolution HLA-C typing could be performed in the future.

4.2 GrB Expression, NK-Cell Licensing and Lack of Antibody Specificity

4.2.1 Antibody Non-Specificity and the Putative Link between Licensing and GrB Expression

This study is the first to link grH to NK-cell licensing, after the more well-studied grB was recently correlated with the process by Goodridge *et al.* (144). The present study did not detect a clear link between NK-cell licensing and grB expression as a percentage of cells positive for it, the presence of an inhibitory KIR *per se* rather than the presence of a self-specific inhibitory KIR appearing to be the main determinant of grB expression levels (**Fig. 26**). It did detect a correlation between NK-cell licensing and the MFI of grB (**Fig. 26**), in line with the literature, but this correlation is proposed here to be a likely artefact. Importantly, both the *GZMB* mRNA levels shown in **Fig. 15**, as well as *GZMB* mRNA levels examined by Goodridge *et al.* (144), were not higher in educated than uneducated NK cells, whereas

Discussion

protein levels (as MFI) were, as described above. While it is true that protein levels may not fully parallel mRNA levels due to post-transcriptional or post-translational regulation (264), which Goodridge *et al.* suggest is the main reason for the observed discrepancies between the transcriptome and protein data (144), the present study proposes a different explanation. Both this study and Goodridge *et al.* used the anti-grB mAb GB11 for flow cytometrical analysis of grB expression at the protein level. However, as shown in section 3.12, GB11 was not specific for grB, also binding grH to a very similar extent. The lack of specificity of GB11 now suggests that grB protein levels may, in fact, have been measured incorrectly at times. It stands to reason that the differences in GB11-mediated staining in licensed vs unlicensed NK cells were actually due to differences in grH and not grB expression, as *GZMH*, unlike *GZMB*, did display marked differences in mRNA levels between the two cell populations (**Fig. 15**). A further striking example of grB protein levels probably not being measured accurately by GB11 was the present study's finding that both grH and grB expression *at the protein level* was highest in terminally differentiated adaptive NK cells (**Fig. 31**), and that though this finding was mirrored at the mRNA level for *GZMH*, *GZMB* transcript numbers were actually lower in terminally differentiated adaptive than non-terminally differentiated non-adaptive NK cells (**Fig. 32**).

These data therefore call into question the putative correlation between NK-cell licensing and grB expression and implicate grH instead. Rather than NK-cell licensing, the main factor that determines grB expression is likely to be NK-cell maturity, given that the presence of an inhibitory KIR *per se* – as a marker of NK-cell maturity – rather than by the presence of a self-specific inhibitory KIR – as a marker of licensing – was the main determinant of grB expression levels when examining them as the percentage of cells positive for grB, as described above.

Just like expression of grH, expression of grB was also heavily influenced by NK-cell maturity regardless of KIR expression, being higher, for instance, in CD56^{dim} than CD56^{bright} NK cells (**Fig. 20**), in PB-derived than CB-derived NK cells (**Fig. 21**), and in CD57⁺ than CD57⁻ NK cells (**Fig. 30**). Nevertheless, grH expression appeared to be affected somewhat more by NK-cell maturity than expression of grB was, the difference in grB expression between the more mature NK-cell subset and the less mature NK-cell subset in each comparison always being somewhat less pronounced than for grH, as overall grB levels tended to be higher.

4.2.2 Further Implications of the Lack of GB11-Specificity

Returning to antibody specificity, the lack of specificity of GB11 has implications for the study of grB in cells that also express grH. Problems arise particularly in settings where grH expression is higher than 'usual', as differentiation between grH and grB through staining with GB11 alone becomes impossible. Arguably, when there is known to be no or very little grH expression, like in grB-transduced K562 cells, GB11 might be considered acceptable for detecting grB. However, since there is always some expression of grH in resting NK cells and since regulation of expression of grH and grB can be highly disparate, as discussed below, making differentiation between grH and grB paramount, the cross-reactivity of GB11 with grH should always be taken into account in order to avoid misleading results. The author therefore suggests that if use of GB11 cannot be avoided, staining for grH should always be included as well, as was done in this study. If staining for grB is considerably more pronounced than for grH, the result regarding staining for grB may be genuine and in any case, grH expression can be differentiated from it through the grH-specific antibody. However, if staining for grH is equal to or only

Discussion

somewhat more pronounced than that for grB, further analyses, for instance using different anti-grB antibody clones or transcriptome analyses, should be conducted to determine actual grB levels.

In this study, only GB11 was used. Therefore, to improve the accuracy and robustness of future analyses, anti-grB antibody clones that have been shown not to display any substantial cross-reactivity with grH should be used. An example of such a clone is 2C5 (182), though it would first need to be tested for use in flow cytometry, having been mainly used in western blot and ELISA-based studies to date (182).

Undeniably, the result that GB11 stains grH in addition to grB is highly significant not only in the context of NK-cell licensing, where the role of granzymes is being redefined by this study, but also for other parts of the NK-cell and granzyme fields. GB11, a common commercially available antibody clone, is now at least the second anti-grB antibody clone to have been attested considerable cross-reactivity with grH, the anti-grB mAb GB7 being another one (182). GB11 has been used extensively in the study of grB, including for examination of grB expression levels in tumour-infiltrating NK cells and their resulting effector functions (266). If GB11 has in fact been identifying grH in addition to or even instead of grB, this may require the conclusions drawn in such studies to be revisited, like the conclusion regarding the correlation between NK-cell licensing and grB expression is revisited here, and imparts a whole new level of importance on the study of grH.

4.3 The Polyclonal Anti-GrH Antibody

Following the discussion of the anti-grB antibody in the preceding section, this section now takes a closer look at the polyclonal anti-grH antibody used in this study. Using a polyclonal antibody has some disadvantages but also advantages compared with mAbs. With regard to target specificity, using a mAb to stain for any cellular protein is often preferable to using a polyclonal antibody, which has a higher likelihood of cross-reacting with other targets (267). Furthermore, as polyclonal antibodies are produced *in vivo*, their specificity may differ between different batches (267). Nevertheless, polyclonal antibodies are often more sensitive than mAbs, as they recognise more than one epitope of a target and are thus not as prone to reduced target recognition upon target-epitope changes as mAbs are (267).

The polyclonal anti-grH antibody used here was deemed suitable for use in this study, as it produced far more clearly distinguishable positive and negative populations than the anti-grH mAb tested (**Fig. 17**), and as it was specific for grH when compared with grB. Its specificity was tested in several ways, including through staining grB-transduced K562 cells, which only produced a minimal positive result (**Fig. 54**). As sections 3.12 and 4.2 show, even a mAb is not always specific for its target and thus not inherently better than a rigorously tested polyclonal one, therefore the polyclonality of the anti-grH antibody alone is not a contraindication to its use. Notwithstanding this, however, when the polyclonal anti-grH antibody was used to stain grH-transduced K562 cells, a relatively large population thereof remained negative (**Fig. 54**). Despite the antibody supposedly being highly sensitive for its target (given its polyclonality), there is therefore scope for finding one with even higher sensitivity. The obtained results may have been due to the antibody used being quite old at the late stage of the study at which this experiment was performed: because of the polyclonality of the antibody, a new lot number may have meant slightly different staining properties, so the same lot number as for the previous experiments was used, meaning that the antibody vial had been open for several months, possibly resulting in some

Discussion

loss of sensitivity. A downregulation of grH with prolonged culture as a possible cause of this relatively low staining intensity is unlikely, given the large extent to which the anti-grB antibody stained grH.

To recapitulate, the polyclonal anti-grH antibody was shown here to be specific for its target, but its sensitivity was suboptimal. Its use in this study was legitimate, but for future studies, finding an at least equally specific but more sensitive antibody may be desirable. Particularly for reproducibility of experiments, a mAb is preferable to a polyclonal one.

4.4 A Single Base Change in the *GZMB* Insert Sequence

Having discussed antibody specificities, which were determined in part through staining of granzyme-overexpressing cell lines, a discussion of the sequences of the inserts used for this overexpression is now necessary, particularly of the *GZMB* insert, despite its not being directly relevant to the study of grH. Sequencing of *GZMH* and *GZMB* inserts after cloning them into the overexpression vector revealed that two *GZMH* inserts had the correct sequence and three had multiple errors, but all five *GZMB* inserts had CAA at codon 48 instead of CGA (four clones with an otherwise correct sequence and one clone with multiple other errors), CGA being found in the reference sequence of *GZMB* transcript variant 1 (accession number NM_004131.5) (188). This CGA to CAA change resulted in an amino acid change from arginine (R) to glutamine (Q). There are several possible reasons for this single-base change. It could either have been present in the genome of the cells from which total RNA for cDNA synthesis was extracted or been due to an error in cDNA synthesis in turn, or due to a very early error in the PCR used to generate the inserts. Given that this Q48R single-nucleotide polymorphism has been described in the literature (237), the former, ie presence of the change in the host-cell genome, is the most likely.

Q48 has been shown to be in linkage disequilibrium with a proline residue at position 88 (P88) and a tyrosine at position 245 (Y245) (QPY), while R48 on the other hand has been shown to be in linkage disequilibrium with an alanine at position 88 (A88) and a histidine at position 245 (H245) (RAH) (237). The insert sequences also encoded P88 and Y245, confirming the presence of the common QPY allele in the inserts, this allele being known to result in a functional protein (237),(238),(239). The NCBI sequence used for reference encodes R48, P88 and Y245 (188) and based on the cited literature could thus represent a rare *GZMB* allele. Since the QPY allele results in a functional protein, use of the vector containing the insert in question was perfectly adequate for grB overexpression. If, however, in future studies functional analyses need to be performed on cells in which the QPY grB variant has been overexpressed, it may be prudent to generate an overexpression vector containing an insert that encodes the RAH variant and overexpress this, as well. This way, the two grB variants will be able to be compared and potential artefactual functional differences that are due to the grB variant used, as well as possible differences in the strengths of antibodies binding to these variants, may be identified.

4.5 GrH and GrB Expression by Different Types of Lymphocytes

This discussion can now finally return to the study of grH. Having discussed the main finding of this study (the correlation between NK-cell licensing and grH expression), it is important to also discuss grH expression by different types of lymphocytes, which was also examined here (**Fig. 19**).

Discussion

The highest expression of grH among lymphocytes was found in NK cells, and in T cells to a lower extent, consistent with the literature (182). To the author's knowledge, this study is the first, however, to specifically show that grH is also expressed by NK-like T cells, here defined by CD56-positivity and CD3-positivity. GrH expression by lymphocytes, as demonstrated in the present study, and as illustrated in **Fig. 56**, was as follows (in descending order): NK cells, NK-like T cells, CD8⁺ T cells, CD4⁺ T cells, non-NK/non-T lymphocytes. As expected, grH is thus preferentially expressed by cytotoxic lymphocytes, chiefly by those expressing CD56. The pattern was mirrored by grB expression, though always at somewhat higher overall levels than grH. For instance, grB expression by CD56^{dim} NK

cells was found here to be significantly higher than that of grH (**Fig. 20**), in contrast to what has previously been shown (182). The result found here is substantiated by the transcriptome data displayed in **Fig. 15**, which clearly show that at the mRNA level, too, *GZMH* expression by NK cells was lower than that of *GZMB* expression. This study therefore provides an update on the difference between grH and grB expression by resting NK cells. Despite the slight differences in expression *levels* when comparing grH and grB directly, the highly parallel expression *patterns* indicate very similar regulatory mechanisms of grH and grB expression at rest. Given their structural similarity, this is to be expected. However, their regulation becomes highly disparate upon stimulation (see next section).

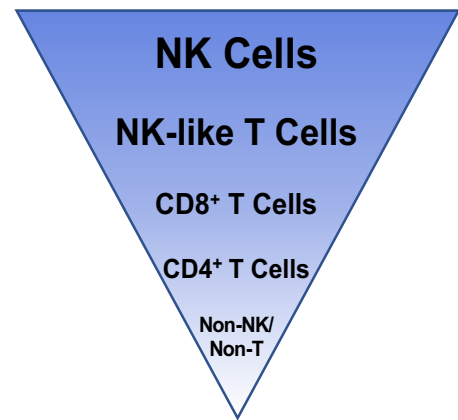


Fig. 56: GrH expression is highest in NK cells. Different types of lymphocytes are shown according to grH expression levels, in decreasing order. Author's illustration.

4.6 NK-Cell Stimulation and GrH Expression, as well as GrB for Comparison

4.6.1 Decreases in Expression of GrH but not GrB upon NK-Cell Stimulation

In contrast to the highly parallel expression patterns between grH and grB at rest, stimulation of PBMCs, both soluble mediator (cytokines and/or rituximab) and target cell-induced, led to a significant and sometimes drastic reduction in NK-cell grH but not grB expression, as demonstrated in **Fig. 36**, **Fig. 38**, **Fig. 40** and **Fig. 43**. On the contrary, grB expression not only did not decrease, but in fact increased slightly with stimulation. This, unlike the patterns at rest, indicates differences in the regulation of grH and grB expression upon stimulation, which is remarkable when considering the striking structural similarity between grH and grB, and indicates that the regulatory mechanisms governing expression of the two proteins must be extraordinarily precise.

Differential regulation of the two granzymes has also been shown in the literature. Most studies have, however, focused on cells other than NK cells. For instance, stimulation of CBMCs and of mast cells via calcium ionophores or IgE-receptor cross-linking has been shown to lead to a decrease in grH levels but an increase in grB levels in these cell populations – both at the mRNA and protein level (268). GrH expression by *in vitro*-expanded human T cells has been shown to decrease at the transcriptional level following stimulation via IL-15 (269), while phytohaemagglutinin-mediated stimulation of CD4⁺ and CD8⁺ T cells has been shown to lead to induction of grB to a greater extent than grH (182). Only parts of a study by Sedelies *et al.* examined NK cells: steady or slightly decreased grH expression and an increase in grB expression by NK cells was demonstrated after four-day stimulation with IL-2 (182). The difference in magnitude of the decrease in grH between Sedelies *et al.* and the present study is likely

Discussion

due to Sedelies *et al.* using a different anti-grH antibody (a mAb made by Sedelies *et al.* themselves, which was not commercially available at the time the present study was conducted) than the present study, as well as western blotting rather than flow cytometry to detect grH (182).

The present study now provides robust evidence that stimulation of NK cells, in addition to the cell types described in the literature, leads to reductions in grH but not grB levels. A possible explanation is grH exhaustion: located in the endolysosomal compartment, grH, like grB, is likely to be excreted upon NK-cell activation. However, while grB expression remains high, suggesting that the *GZMB* gene continues to be transcribed, with continuing production of *GZMB* mRNA, *GZMH* transcription may cease. In fact, as evidence of this theory, examination of the transcriptome of primary NK cells expanded according to a protocol by Fujisaki *et al.* (195) revealed a drastic reduction in the number of *GZMH* transcripts between non-expanded and expanded cells, while the data were less clear for *GZMB* (**Fig. 44**). Given the structural similarity between grH and grB, differential regulation at the gene level is also conceptually more likely than active sequestration of grH but not grB. Interestingly and contrasting particularly with *GZMH*, transcript numbers of *GZMA* increased drastically with NK-cell expansion, which also corroborates the finding of differential regulation of granzyme expression by NK cells.

To further study the likely disparate regulation of granzyme expression, particularly grH and grB, upon NK-cell stimulation, transcriptomes of NK cells stimulated with IL-2 and IL-15 or rituximab and IL-15 (section 3.9.1) as well as of those stimulated with non-transduced K562 cells (section 3.9.2.1) could be established in the future and compared with the transcriptomes of unstimulated cells.

A possible reason for the putative grH exhaustion is that grH expression could be part of an NK-cell regulatory mechanism, decreases in grH expression occurring upon NK-cell activation, potentially to prevent excess NK-cell activity and autoreactivity (see also section 4.9).

4.6.2 CD107a and Cytokine Expression in GrH⁻ vs GrH⁺ NK Cells Upon Stimulation with Target

Target cell-induced stimulation not only led to reductions in grH expression but was also remarkable on another level: in a degranulation and cytokine-production assay the specific increase in NK-cell surface expression of CD107a and intracellular expression of IFN- γ and TNF- α after co-culture with HLA class I-deficient K562 target cells was significantly higher in grH⁻ than grH⁺ CD56^{dim} NK cells (**Fig. 41**). The opposite was observed for grB, the specific increase in expression of CD107a, IFN- γ and TNF- α being, though not significantly so, slightly *lower* in grB⁻ than in grB⁺ NK cells (**Fig. 42**). The result for grH⁺ and grH⁻ cells was observed both for licensed and, to a smaller degree, unlicensed NK cells. Terminally differentiated adaptive NKG2C⁺ NK cells were not examined in this assay, but given their high baseline grH expression, it would be interesting, in the future, to also examine whether after target cell-mediated stimulation of these cells, too, cell-surface CD107a expression is higher in grH⁻ cells.

In view of the higher responsiveness of licensed than unlicensed cells that was also observed in the assay (**Fig. 39**) together with the correlation of licensing with higher grH expression, the results showing that grH⁻ NK cells displayed higher responsiveness than grH⁺ NK cells may seem counterintuitive. However, they are, again, most easily explained by grH exhaustion: those cells (both licensed and unlicensed) that show increased cell-surface CD107a and intracellular cytokine expression have most likely released their grH stores during activation without them then being replenished, in contrast to grB. Additionally,

Discussion

grB levels may be so high to begin with that grB exhaustion simply does not happen. Subsequent staining and flow cytometrical analysis then reveal only the activation markers and grB, grH no longer being detectable. Again, RNA-Seq of these cells is likely to provide more clarity.

The results of the assay are noteworthy for yet another reason. Though activation of licensed NK cells in the experiment was significantly more pronounced than that of unlicensed NK cells (**Fig. 39**), some activation of unlicensed NK cells was nonetheless observed. While activation of unlicensed NK cells is unlikely to be caused by induction of a missing-self response by target cells, there are two main possibilities for this occurring in this setting: it could either have been due to stimulation by cytokines released from other cells activated by the target cells (as no external cytokines were added to the cell-culture medium) or it could have been caused by stimulatory receptors expressed by K562 cells. Indeed, unlicensed NK cells have been shown, at least in mice, to be capable of responding to cytokine-induced stimulation (139), and K562 cells have recently been shown to express ligands for activating NK-cell receptors like NKG2D (270), making both mechanisms valid hypotheses.

The degranulation and cytokine-production assay therefore not only showed that both licensed and unlicensed NK cell can be activated (directly or, in the case of unlicensed NK cells, most likely indirectly), but, more importantly, also that grH exhaustion is likely to play a role in target cell-induced stimulation as well. This strengthens the hypothesis of a possible regulatory role of grH.

Ideally, the next step would be to perform functional analyses on pure grH⁺ vs grH⁻ NK-cell populations; however, as discussed in the next section, this was not possible and alternative approaches were sought.

4.7 Correlation between GrH and CD57-Positivity and KLRG1-Negativity

Due to the need for cell fixation and permeabilisation prior to staining for grH, it is not currently possible to perform functional studies on primary NK cells sorted, eg by means of FACS, based on grH-positivity or negativity, or indeed to extract intact RNA from these populations for examination of differences in gene expression. Based on a published protocol (222), RNA extraction from fixed and permeabilised cells was, in fact, attempted in this study, but unsuccessfully so. The identification of potential markers that can reliably predict grH expression and therefore be used as a proxy for it, was thus sought. For the reasons explained in section 3.8, CD57, KLRG1, CD11c and DNAM-1 were examined for this purpose. The data revealed that grH-positivity correlated with higher expression of CD57 in both licensed and unlicensed NK cells (the result was statistically significant in unlicensed cells), CD11c in licensed cells (significantly so) and DNAM-1 in licensed cells, while it correlated with lower expression of KLRG1 in both licensed and unlicensed NK cells (significantly so in unlicensed cells) (**Fig. 33**). Furthermore, in both grH⁻ and grH⁺ populations KLRG1 and CD11c expression by unlicensed NK cells was higher than by licensed ones, as would be expected from the transcriptome data mentioned in section 3.8 that was established by Prof. Uhrberg and Prof. Walter (unpublished data, mentioned here with permission). On the other hand, CD57 expression by licensed NK cells was non-significantly higher than by unlicensed ones in both grH⁻ and grH⁺ populations, suggesting a correlation with licensing. For DNAM-1 it was not clear at the percentage level, but at the MFI level DNAM-1 expression was non-significantly higher in licensed than unlicensed NK cells, in line with the literature (143).

Of note, the results for CD11c were somewhat surprising. The combination of a) CD11c expression by licensed grH⁺ NK cells being higher than by licensed grH⁻ NK cells, b) CD11c expression by unlicensed

Discussion

NK cells being higher than by licensed ones, and c) grH expression by licensed NK cells being higher than by unlicensed NK cells, seems counterintuitive. However, given that the higher CD11c expression by grH⁺ than by grH⁻ NK cells was only observed in the licensed population and not also in the unlicensed population, these results may be due to an inherent difference between licensed and unlicensed NK cells, or the correlation with grH expression may also simply be a chance phenomenon.

Returning to the search for a proxy for grH expression, a combination of CD57 and KLRG1, expression of which showed opposing trends with regard to grH expression, was thought to have the potential to serve as such a marker. High levels of grH expression were indeed found in licensed CD57⁺KLRG1⁻CD56^{dim} NK cells and very low grH levels in unlicensed CD57⁻KLRG1⁺ cells (**Fig. 34**), which indicates that CD57 and KLRG1 in conjunction with the appropriate KIRs to mark licensing status may serve to identify mainly grH⁺ and mainly grH⁻ populations. Unfortunately, however, ‘*mainly* grH⁺’ (84.4%) and ‘*mainly* grH⁻’ (25.0%) populations are not the pure populations required for meaningful functional analyses to be possible. Thus, CD57 and KLRG1 are imperfect proxies for grH expression at best. Yet an alternative approach was thus sought by overexpressing grH in the NK-92-cell line (section 4.8.1). Interestingly, the data did show that expression of grH can be used as a predictor of an NK cell’s licensing status, as mentioned several times already, and that even more robust predictions are possible when also including CD57 positivity and KLRG1 negativity: the highest percentages of licensed NK cells (and conversely the lowest percentages of unlicensed cells) were found among CD57⁺KLRG1⁻grH⁺ NK cells.

A further point can be made here. As discussed in the preceding paragraphs, grH expression was inversely correlated with expression of KLRG1, a non-MHC-specific but self-specific inhibitory receptor, which in turn was inversely correlated with NK-cell licensing status. KLRG1 is known to bind classic members of the cadherin family (252) and has been shown to inhibit NK-cell responses to E-cadherin-transfected K562 target cells (271). Therefore, its reduced expression by licensed compared with unlicensed and grH⁺ compared with grH⁻ NK cells might contribute to licensed grH⁺ NK cells’ enhanced functional responsiveness to target cell-mediated stimulation.

4.8 Lack of GrH Cytotoxic Activity but Potential Involvement in Host-Cell Survival

4.8.1 GrH Cytotoxicity in the Literature and Lack thereof in this Study

As concluded in the previous section, using CD57, KLRG1 and KIRs for the selection of grH⁺ and grH⁻ NK cells has the main limitation of leaving considerable impurity, which may be prohibitive for the study of the function of grH. To avoid this and create clear grH⁺ and grH⁻ populations, grH was overexpressed in NK-92 cells instead. Before turning to a discussion of the *absence* of a cytotoxic role of grH found in this study through this approach, this section first lays out the current knowledge base with regard to the putative *presence* of a cytotoxic role of grH.

4.8.1.1 Review of the Literature

In contrast to studies by Fellows *et al.* (189), Hou *et al.* (190), Ewen *et al.* (191) and Wang *et al.* (183), the present study did not find substantial evidence of a cytotoxic role of grH. Independently, both

Discussion

Fellows *et al.*, 2007, (189) and Hou *et al.*, 2008, (190) suggested that *recombinant* grH induces a form of target-cell death indicative of apoptosis, as they observed chromatin condensation and DNA fragmentation. However, Fellows *et al.* described a slow (10-12 hours) caspase-independent cell death with mitochondrial depolarisation and generation of reactive oxygen species, but without the release of pro-apoptotic molecules like cytochrome c, or the cleavage of Bid or of inhibitor of caspase-activated DNase (ICAD). Hou *et al.*, on the other hand, described a more rapid cell death (2-4 hours), more similar to that induced by grB, through caspase-3 activation, cleavage of Bid (leading to mitochondrial disruption), cleavage of ICAD (leading to DNA fragmentation), and cytochrome c release.

In 2013, Ewen *et al.* (191) addressed and attempted to resolve the discrepancies between the preceding studies by expanding upon their experimental setup, including through the use of more cell lines. They confirmed Hou *et al.*'s finding of cytochrome c being released from mitochondria after target-cell treatment with grH and of recombinant grH cleaving ICAD, but they did not find substantial Bid-cleaving activity. Furthermore, they did find some caspase-3 activation, but not in all settings of grH-induced apoptosis, and therefore not as a necessary mechanism. They also implicated the pro-apoptotic proteins Bax and/or Bak as important factors in grH-induced cell death, while overexpression of the anti-apoptotic protein BCL-2 inhibited it. Finally, they showed that recombinant grH induces DNA damage as well as the release of the pro-apoptotic protein second mitochondria-derived activator of caspase/direct inhibitor of apoptosis-binding protein with low pI (Smac/DIABLO) from mitochondria, in addition to cytochrome c release. They thus confirmed the overall conclusion of the preceding studies that recombinant grH appears to induce target-cell apoptosis.

The discrepancies between the three studies just described may, at least to some extent, be due to different (and possibly higher than physiological) concentrations of grH used, as well as due to different cell lines and different mechanisms of grH delivery into target cells (using not just perforin, but also detergents or the bacterial pore-forming protein streptolysin O). However, they do invite the question of how real or at least relevant this putative cytotoxic effect of grH truly is *in vivo*. The non-physiological nature of using purified recombinant grH and the artificial modes sometimes employed to deliver this recombinant grH into target cells add to the questions regarding the conclusions drawn.

The abovementioned study by Wang *et al.* (183) also needs to be discussed in this context. Intriguingly, they described an intracellular, physiological grH inhibitor (SERPINB1), overexpression of which in target cells significantly reduced their lysis through both recombinant grH and lymphokine-activated killer (LAK) cells, thereby also implying a cytotoxic role of grH. The same reservations as mentioned in the preceding paragraph regarding the use of recombinant grH however apply here as well. Furthermore, LAK cells, as the name suggests, are activated cytotoxic lymphocytes (including NK cells) which in the cited study were generated through stimulation of PBMCs with IL-2 for four days. In light of the results of the present study, this stimulation quite likely led to a considerable reduction in grH expression by the LAK cells. While recombinant grH indeed appears to have been inhibited by SERPINB1, it is thus less clear whether SERPINB1-mediated inhibition of LAK-induced cytotoxicity truly arose from an inhibition of grH or whether a different cytotoxic mediator was targeted.

4.8.1.2 Examination of the Putative Cytotoxic Role of GrH in this Study

The question remains whether grH truly has a pro-apoptotic, cytotoxic role in more physiological settings. Since no murine orthologue of human grH has been found to date, *in vivo* studies of grH are difficult. The present study therefore used whole-cell and thus somewhat more physiological approaches

Discussion

(than using recombinant grH) to examine the function of grH, studying both primary NK cells and the NK-cell line NK-92. The latter was used for overexpression of grH to examine grH's cytotoxic potential. Because NK-92 cells are a tumour cell line and thus far removed from primary NK cells both genetically and phenotypically, care needs to be taken when extrapolating conclusions drawn from their study to the function of primary NK cells, however. Furthermore, when using cell lines to study biological processes, contamination with other potentially faster-growing cell lines or with bacteria of the genus *Mycoplasma* is a possible source of error (272),(273).

These caveats need to be addressed. The latter error source was excluded here by regular PCR-based tests for *Mycoplasma* detection (kindly performed by Ms. N. Scherenschlich using a commercially available detection kit, data not shown), which were always negative. More importantly, however, the use of NK-92 cells was deemed adequate for one critical reason: NK-92 cells are known to be cytotoxic against target cells and thus possess cellular machinery comparable to activated NK cells (198). Because of this, overexpression of grH in these cells to study its putative cytotoxic activity is a more physiological approach than utilising recombinant grH.

Therefore, grH was overexpressed in NK-92 cells and the cytotoxic activity of the grH-transduced NK-92 cells compared with that of empty vector-transduced and non-transduced NK-92 cells. If grH were truly cytotoxic at physiological concentrations, an increase in cytotoxic potential should have been observed in the grH-transduced NK-92 cells. Importantly, the present study did not find any difference at all in the killing capacity between NK-92 cells overexpressing grH and empty vector-transduced or non-transduced NK-92 cells (**Fig. 50**), which strongly argues against a significant cytotoxic role of grH in a whole-cell setting. The results displayed in **Fig. 49**, which show a slightly though non-significantly larger specific increase in cell-surface CD107a expression in grH-transduced compared with empty-vector transduced NK-92 cells upon stimulation with target cells, do not dispute this suggested lack of cytotoxicity. Firstly, this is because the specific increase in CD107a was very low overall and may not represent a true difference. Secondly, increased exocytosis, though frequently used as a marker thereof, does not necessarily equate to increased cytotoxicity, as no certain conclusions about the cytotoxic potential of an NK-cell protein can be drawn without looking at its effects on target cells.

To further strengthen the conclusions drawn here regarding the lack of a cytotoxic role of grH, overexpression of grH in primary NK cells is needed, which unfortunately was unsuccessful here. Additionally, assays that examine target-cell cytotoxicity after a longer period of co-incubation (longer than the five hours used here) of grH-overexpressing cells with target cells could be tested, as Fellows *et al.* (189) only observed grH-induced cell death after 10-12 hours.

4.8.2 Possible Involvement of GrH in Host-Cell Survival

As the present study found no evidence of grH cytotoxicity, an alternative role of grH is proposed. GrH expression by primary NK cells (both licensed and unlicensed) showed a positive correlation with that of the anti-apoptotic protein BCL-2 (**Fig. 52**) (which has been shown to be expressed by 83% of NK cells (274)), suggesting a potential role for grH in host-cell survival rather than target-cell cytotoxicity: grH may provide a survival advantage to those licensed as well as unlicensed NK cells that express it. Indeed, the correlation between grH and BCL-2 expression is plausible, as licensed NK cells, which are shown here to express higher levels of grH, are also shown here to express higher levels of BCL-2 (**Fig. 52**) and were shown in the past to be less prone to becoming apoptotic (53). Of course, the function of

Discussion

a protein within its host cell may very well be different from its function in a target cell, but since overexpression of grH in NK-92 cells did not lead to an increase in cytotoxicity, a cytotoxicity-independent role is likely, at least in some circumstances.

Further support for a potential role of grH in host-cell survival comes from an examination of the growth and death rates of grH-overexpressing compared with empty vector-transduced NK-92 cells. The growth rates were similar, which may be due to NK-92 cells being a tumour cell line and thus already displaying autonomous growth, possibly showing little responsiveness to other influences such as overexpression of a protein that is not an oncogene or tumour suppressor gene. However, grH-overexpressing NK-92 cells displayed lower death rates than empty vector-transduced NK-92 cells, both under normal culture conditions (which is as close as these cells ever come to being at steady state) and upon withdrawal of IL-2 (**Fig. 51**). The difference in death rates was non-significant, however, and a sample size of 1 was used in the IL-2-withdrawal assay, so care must be taken not to overestimate the robustness of the conclusions that can be drawn here.

In contrast and somewhat unexpectedly, survival of grH⁺ primary NK cells in a serum-starvation assay was slightly, albeit non-significantly, lower than that of grH⁻ NK cells, while the reverse was the case for early apoptosis. As depicted in **Fig. 53**, the differences increased as the assay progressed. Though on the surface appearing to violate the theory of grH being associated with host-cell survival, alternatively, grH could be important for host-cell survival at steady state, with its importance decreasing in settings of cellular stress. On the other hand, given that the differences observed were all non-significant, care must be taken not to overestimate these results either.

Despite the unexpected results from the serum-starvation assay, a positive correlation between grH expression and NK-cell survival is likely, particularly at steady state. Nevertheless, further experiments are needed to elucidate it further. For example, using more nuanced inducers of apoptosis than serum starvation and IL-2 withdrawal, eg stimulation of NK cells first with IL-2 and then with an anti-CD16 mAb to trigger activation-induced cell death (51), as well as studying larger sample sizes, may help to establish a more robust link (or lack thereof) between grH expression and NK-cell survival or apoptosis.

4.9 Direct Antiviral and GrB-Disinhibiting Roles of GrH

Regardless of whether or not it exerts cytotoxic activity, grH has been shown by multiple studies to exhibit direct, cytolysis-independent, antiviral activity. It has been demonstrated to inhibit hepatitis B virus replication by directly cleaving the hepatitis B virus protein HBx (178), and to lead to impairment in hepatitis C virus translational activity by cleavage of La, a host protein involved in RNA metabolism (275). Moreover, grH, like grB, has been shown to considerably impair adenoviral DNA replication by directly cleaving the adenoviral DNA-binding protein DBP, though at different positions than grB does (276). This direct antiviral activity is important on a further and possibly even more crucial level, as grH has been shown to also have a notable effect on grB function: by cleaving adenoviral 100K assembly protein, a viral inhibitor of grB, grH relieves inhibition of grB (276). It is possible that grH plays a role as a 'grB disinhibitor' in other contexts, as well, particularly given the striking structural similarities between the two granzymes. This theory also fits nicely with the hypothesis of grH being involved in NK-cell regulatory mechanisms. If, upon NK-cell activation, intracellular grH stores are depleted and not replenished but grH is required for optimum functioning of grB, an inherent check is placed upon grB activity (**Fig. 57**), which could help prevent autoreactivity of NK cells.

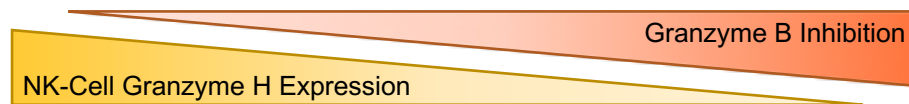


Fig. 57: GrH may act as a disinhibitor of grB. If grH is required for disinhibition of grB in NK cells, grB inhibition increases with decreasing grH expression following prolonged stimulation of NK cells, which would lead to a decrease in grB functionality. Author's illustration.

Alternatively, as suggested by Waterhouse and Trapani (277), the reduction in grH levels with NK-cell stimulation could represent a shift in focus from predominantly direct antiviral NK-cell activity, mediated by grH as well as grB, to predominantly cytotoxic NK-cell activity, mediated by grB.

4.10 Conclusions

This study is the first to link grH to NK-cell licensing. The main aim of this study, to test for and then to robustly establish a link between NK-cell licensing and grH expression at the protein level, examining grB for comparison, was fully met, as a robust positive correlation between NK-cell licensing and grH expression was found. Both grH and grB expression also positively correlated with NK-cell maturity. The observed correlation between NK-cell licensing and increased grH expression was so strong that the author proposes the use of grH expression for the formulation of a novel temporal and developmental model of NK-cell licensing and as a marker of the process. In contrast, by providing evidence of lack of specificity of a commonly used anti-grB antibody mAb (GB11), the conclusions previously drawn about a correlation between NK-cell licensing and grB expression are called into question.

Expression of both grH and grB among lymphocyte subpopulations was shown to be highest in NK cells and expression patterns of the two granzymes were found to be very similar at rest. On the other hand, stimulation of NK cells was found to lead to differential regulation of grH and grB, more dramatically so than shown in previous studies, here inducing drastic downregulation of grH but not grB expression.

Through whole-cell approaches (using grH-overexpressing NK-92 cells), which contrast with approaches using purified recombinant grH, the previously postulated cytotoxic role of grH could not be confirmed in this study. Instead, a positive correlation between grH and BCL-2 expression was found and a role of grH in host-cell survival is suggested. Furthermore, a potential regulatory rather than a mainly cytotoxic role of grH is proposed, NK-cell stimulation possibly leading to grH exhaustion, which may put a brake on potential disinhibition of the function of grB.

The data presented in this study provide substantial insight into the role and functions of grH and are an important step towards elucidating the precise intracellular processes involved in NK-cell licensing. The future steps suggested throughout this Discussion, including the use of even more functional studies, as well as more transcriptomic analyses of those functional studies, will help to further enhance the understanding already gained here of grH and its functions, as well as of NK-cell licensing as a whole. The author hopes that particularly the link between NK-cell licensing and grH expression, as well as the proposed temporal and developmental model of NK-cell licensing, will be valuable guides for the further study of the complex mechanisms involved in this process, to bring us closer to the overarching goal of exploiting NK-cell functions and functionality for more effective use in antiviral and especially anti-tumour therapies.

Bibliography

1. Kiessling R, Klein E, Wigzell H. „Natural” killer cells in the mouse. I. Cytotoxic cells with specificity for mouse Moloney leukemia cells. Specificity and distribution according to genotype. *Eur J Immunol.* 1975;5(2):112–7.
2. Kiessling R, Klein E, Pross H, Wigzell H. „Natural” killer cells in the mouse. II. Cytotoxic cells with specificity for mouse Moloney leukemia cells. Characteristics of the killer cell. *Eur J Immunol.* 1975;5(2):117–21.
3. Greenberg AH, Hudson L, Shen L, Roitt IM. Antibody-dependent Cell-mediated Cytotoxicity due to a “Null” Lymphoid Cell. *Nature New Biol.* 1973 Mar;242(117):111.
4. Freud AG, Mundy-Bosse BL, Yu J, Caligiuri MA. The Broad Spectrum of Human Natural Killer Cell Diversity. *Immunity.* 2017 Nov 21;47(5):820–33.
5. Grégoire C, Chasson L, Luci C, Tomasello E, Geissmann F, Vivier E, et al. The trafficking of natural killer cells. *Immunol Rev.* 2007;220(1):169–82.
6. Cooper MA, Fehniger TA, Caligiuri MA. The biology of human natural killer-cell subsets. *Trends Immunol.* 2001 Nov 1;22(11):633–40.
7. Robertson MJ, Ritz J. Biology and clinical relevance of human natural killer cells. *Blood.* 1990;76(12):2421–38.
8. Bukowski JF, Warner JF, Dennert G, Welsh RM. Adoptive transfer studies demonstrating the antiviral effect of natural killer cells in vivo. *J Exp Med.* 1985 Jan 1;161(1):40–52.
9. Gorelik E, Wiltrout RH, Okumura K, Habu S, Herberman RB. Role of NK cells in the control of metastatic spread and growth of tumor cells in mice. *Int J Cancer.* 1982 Jul 15;30(1):107–12.
10. Imai K, Matsuyama S, Miyake S, Suga K, Nakachi K. Natural cytotoxic activity of peripheral-blood lymphocytes and cancer incidence: an 11-year follow-up study of a general population. *The Lancet.* 2000 Nov 25;356(9244):1795–9.
11. Moffett A, Loke C. Immunology of placentation in eutherian mammals. *Nat Rev Immunol.* 2006 Aug;6(8):584.
12. Hanna J, Goldman-Wohl D, Hamani Y, Avraham I, Greenfield C, Natanson-Yaron S, et al. Decidual NK cells regulate key developmental processes at the human fetal-maternal interface. *Nat Med.* 2006 Sep;12(9):1065.
13. Robson A, Harris LK, Innes BA, Lash GE, Aljunaidy MM, Aplin JD, et al. Uterine natural killer cells initiate spiral artery remodeling in human pregnancy. *FASEB J Off Publ Fed Am Soc Exp Biol.* 2012 Dec;26(12):4876–85.
14. Hiby SE, Apps R, Sharkey AM, Farrell LE, Gardner L, Mulder A, et al. Maternal activating KIRs protect against human reproductive failure mediated by fetal HLA-C2. *J Clin Invest.* 2010 Nov 1;120(11):4102–10.
15. Russell JH, Ley TJ. Lymphocyte-Mediated Cytotoxicity. *Annu Rev Immunol.* 2002;20(1):323–70.
16. Zamai L, Ahmad M, Bennett IM, Azzoni L, Alnemri ES, Perussia B. Natural Killer (NK) Cell-mediated Cytotoxicity: Differential Use of TRAIL and Fas Ligand by Immature and Mature Primary Human NK Cells. *J Exp Med.* 1998 Dec 21;188(12):2375–80.

Bibliography

17. Wang R, Jaw JJ, Stutzman NC, Zou Z, Sun PD. Natural killer cell-produced IFN- γ and TNF- α induce target cell cytolysis through up-regulation of ICAM-1. *J Leukoc Biol.* 2012 Feb;91(2):299–309.
18. Anegón I, Cuturi MC, Trinchieri G, Perussia B. Interaction of Fc receptor (CD16) ligands induces transcription of interleukin 2 receptor (CD25) and lymphokine genes and expression of their products in human natural killer cells. *J Exp Med.* 1988 Feb 1;167(2):452–72.
19. Jewett A, Gan X-H, Lebow LT, Bonavida B. Differential secretion of TNF- α and IFN- γ by human peripheral blood-derived NK subsets and association with functional maturation. *J Clin Immunol.* 1996 Jan 1;16(1):46–54.
20. Arase H, Arase N, Saito T. Interferon gamma production by natural killer (NK) cells and NK1.1+ T cells upon NKR-P1 cross-linking. *J Exp Med.* 1996 May 1;183(5):2391–6.
21. Martín-Fontecha A, Thomsen LL, Brett S, Gerard C, Lipp M, Lanzavecchia A, et al. Induced recruitment of NK cells to lymph nodes provides IFN- γ for T H 1 priming. *Nat Immunol.* 2004 Dec;5(12):1260.
22. Mehrotra PT, Donnelly RP, Wong S, Kanegane H, Geremew A, Mostowski HS, et al. Production of IL-10 by Human Natural Killer Cells Stimulated with IL-2 and/or IL-12. *J Immunol.* 1998 Mar 15;160(6):2637–44.
23. Böttcher JP, Bonavita E, Chakravarty P, Blees H, Cabeza-Cabrerizo M, Sammicheli S, et al. NK Cells Stimulate Recruitment of cDC1 into the Tumor Microenvironment Promoting Cancer Immune Control. *Cell.* 2018 Feb 22;172(5):1022-1037.e14.
24. Gumá M, Angulo A, Vilches C, Gómez-Lozano N, Malats N, López-Botet M. Imprint of human cytomegalovirus infection on the NK cell receptor repertoire. *Blood.* 2004 Dec 1;104(12):3664–71.
25. Gumá M, Budt M, Sáez A, Brckalo T, Hengel H, Angulo A, et al. Expansion of CD94/NKG2C+ NK cells in response to human cytomegalovirus-infected fibroblasts. *Blood.* 2006 May 1;107(9):3624–31.
26. Béziat V, Liu L, Malmberg J-A, Ivarsson MA, Sohlberg E, Björklund AT, et al. NK cell responses to cytomegalovirus infection lead to stable imprints in the human KIR repertoire and involve activating KIRs. *Blood.* 2013 Jan 1;blood-2012-10-459545.
27. Foley B, Cooley S, Verneris MR, Curtsinger J, Luo X, Waller EK, et al. Human CMV-induced Memory-like NKG2C+ NK cells are Transplantable and Expand in vivo in Response to Recipient CMV Antigen. *J Immunol Baltim Md 1950.* 2012 Nov 15;189(10):5082–8.
28. Della Chiesa M, Sivori S, Carlomagno S, Moretta L, Moretta A. Activating KIRs and NKG2C in Viral Infections: Toward NK Cell Memory? *Front Immunol.* 2015;6:573.
29. Fehniger TA, Cooper MA, Nuovo GJ, Cella M, Facchetti F, Colonna M, et al. CD56bright natural killer cells are present in human lymph nodes and are activated by T cell-derived IL-2: a potential new link between adaptive and innate immunity. *Blood.* 2003 Apr 15;101(8):3052–7.
30. Moretta L. Dissecting CD56dim human NK cells. *Blood.* 2010 Nov 11;116(19):3689–91.
31. Yu J, Freud AG, Caligiuri MA. Location and cellular stages of natural killer cell development. *Trends Immunol.* 2013 Dec 1;34(12):573–82.
32. Leclercq G, Debacker V, Smedt M de, Plum J. Differential effects of interleukin-15 and interleukin-2 on differentiation of bipotential T/natural killer progenitor cells. *J Exp Med.* 1996 Aug 1;184(2):325–36.

Bibliography

33. Ranson T, Vosshenrich CAJ, Corcuff E, Richard O, Müller W, Santo JPD. IL-15 is an essential mediator of peripheral NK-cell homeostasis. *Blood*. 2003 Jun 15;101(12):4887–93.
34. Carson WE, Giri JG, Lindemann MJ, Linett ML, Ahdieh M, Paxton R, et al. Interleukin (IL) 15 is a novel cytokine that activates human natural killer cells via components of the IL-2 receptor. *J Exp Med*. 1994 Oct 1;180(4):1395–403.
35. Freud AG, Caligiuri MA. Human natural killer cell development. *Immunol Rev*. 2006 Dec;214:56–72.
36. Björkström NK, Riese P, Heuts F, Andersson S, Fauriat C, Ivarsson MA, et al. Expression patterns of NKG2A, KIR, and CD57 define a process of CD56dim NK-cell differentiation uncoupled from NK-cell education. *Blood*. 2010 Nov 11;116(19):3853–64.
37. Lanier LL, Ruitenberg JJ, Phillips JH. Functional and biochemical analysis of CD16 antigen on natural killer cells and granulocytes. *J Immunol*. 1988 Nov 15;141(10):3478–85.
38. Romee R, Foley B, Lenvik T, Wang Y, Zhang B, Ankarlo D, et al. NK cell CD16 surface expression and function is regulated by a disintegrin and metalloprotease-17 (ADAM17). *Blood*. 2013 May 2;121(18):3599–608.
39. Jacobs R, Hintzen G, Kemper A, Beul K, Kempf S, Behrens G, et al. CD56bright cells differ in their KIR repertoire and cytotoxic features from CD56dim NK cells. *Eur J Immunol*. 2001;31(10):3121–6.
40. Chattopadhyay PK, Betts MR, Price DA, Gostick E, Horton H, Roederer M, et al. The cytolytic enzymes granzyme A, granzyme B, and perforin: expression patterns, cell distribution, and their relationship to cell maturity and bright CD57 expression. *J Leukoc Biol*. 2009 Jan;85(1):88–97.
41. Loza MJ, Perussia B. Final steps of natural killer cell maturation: a model for type 1–type 2 differentiation? *Nat Immunol*. 2001 Oct;2(10):917.
42. Sivori S, Cantoni C, Parolini S, Marcenaro E, Conte R, Moretta L, et al. IL-21 induces both rapid maturation of human CD34+ cell precursors towards NK cells and acquisition of surface killer Ig-like receptors. *Eur J Immunol*. 2003;33(12):3439–47.
43. Grzywacz B, Katarina N, Sikora M, Oostendorp RA, Dzierzak EA, Blazar BR, et al. Coordinated acquisition of inhibitory and activating receptors and functional properties by developing human natural killer cells. *Blood*. 2006 Dec 1;108(12):3824–33.
44. Nagler A, Lanier LL, Cwirla S, Phillips JH. Comparative studies of human FcR3-positive and negative natural killer cells. *J Immunol*. 1989 Nov 15;143(10):3183–91.
45. Cooper MA, Fehniger TA, Turner SC, Chen KS, Ghaheri BA, Ghayur T, et al. Human natural killer cells: a unique innate immunoregulatory role for the CD56bright subset. *Blood*. 2001 May 15;97(10):3146–51.
46. Anfossi N, André P, Guia S, Falk CS, Roetynck S, Stewart CA, et al. Human NK Cell Education by Inhibitory Receptors for MHC Class I. *Immunity*. 2006 Aug 1;25(2):331–42.
47. Juelke K, Killig M, Luetke-Eversloh M, Parente E, Gruen J, Morandi B, et al. CD62L expression identifies a unique subset of polyfunctional CD56dim NK cells. *Blood*. 2010 Aug 26;116(8):1299–307.
48. Fauriat C, Long EO, Ljunggren H-G, Bryceson YT. Regulation of human NK-cell cytokine and chemokine production by target cell recognition. *Blood*. 2010 Mar 18;115(11):2167–76.

Bibliography

49. Waldmann TA. The biology of interleukin-2 and interleukin-15: implications for cancer therapy and vaccine design. *Nat Rev Immunol*. 2006 Aug;6(8):595–601.
50. Caligiuri MA, Zmuidzinas A, Manley TJ, Levine H, Smith KA, Ritz J. Functional consequences of interleukin 2 receptor expression on resting human lymphocytes. Identification of a novel natural killer cell subset with high affinity receptors. *J Exp Med*. 1990 May 1;171(5):1509–26.
51. Ortaldo JR, Mason AT, O’Shea JJ. Receptor-induced death in human natural killer cells: involvement of CD16. *J Exp Med*. 1995 Jan 1;181(1):339–44.
52. Ortaldo JR, Winkler-Pickett RT, Nagata S, Ware CF. Fas involvement in human NK cell apoptosis: lack of a requirement for CD16-mediated events. *J Leukoc Biol*. 1997;61(2):209–15.
53. Felices M, Lenvik TR, Ankarlo DEM, Foley B, Curtsinger J, Luo X, et al. Functional NK cell repertoires are maintained through IL-2R α and Fas ligand. *J Immunol Baltim Md 1950*. 2014 Apr 15;192(8):3889–97.
54. Lanier LL. Nk Cell Recognition. *Annu Rev Immunol*. 2005;23(1):225–74.
55. Vivier E, Raulet DH, Moretta A, Caligiuri MA, Zitvogel L, Lanier LL, et al. Innate or adaptive immunity? The example of natural killer cells. *Science*. 2011 Jan 7;331(6013):44–9.
56. Lanier LL, Phillips JH, Hackett J, Tutt M, Kumar V. Natural killer cells: definition of a cell type rather than a function. *J Immunol*. 1986 Nov 1;137(9):2735–9.
57. Kärre K, Ljunggren HG, Piontek G, Kiessling R. Selective rejection of H-2-deficient lymphoma variants suggests alternative immune defence strategy. *Nature*. 1986 Feb;319(6055):675.
58. Ljunggren H-G, Kärre K. In search of the ‘missing self’: MHC molecules and NK cell recognition. *Immunol Today*. 1990 Jan 1;11:237–44.
59. Bauer S, Groh V, Wu J, Steinle A, Phillips JH, Lanier LL, et al. Activation of NK Cells and T Cells by NKG2D, a Receptor for Stress-Inducible MICA. *Science*. 1999 Jul 30;285(5428):727–9.
60. Mandelboim O, Lieberman N, Lev M, Paul L, Arnon TI, Bushkin Y, et al. Recognition of haemagglutinins on virus-infected cells by NKp46 activates lysis by human NK cells. *Nature*. 2001 Feb;409(6823):1055–60.
61. Arnon TI, Lev M, Katz G, Chernobrov Y, Porgador A, Mandelboim O. Recognition of viral hemagglutinins by NKp44 but not by NKp30. *Eur J Immunol*. 2001;31(9):2680–9.
62. Sivori S, Falco M, Chiesa MD, Carlomagno S, Vitale M, Moretta L, et al. CpG and double-stranded RNA trigger human NK cells by Toll-like receptors: Induction of cytokine release and cytotoxicity against tumors and dendritic cells. *Proc Natl Acad Sci U S A*. 2004 Jul 6;101(27):10116–21.
63. Hart OM, Athie-Morales V, O’Connor GM, Gardiner CM. TLR7/8-Mediated Activation of Human NK Cells Results in Accessory Cell-Dependent IFN- γ Production. *J Immunol*. 2005 Aug 1;175(3):1636–42.
64. Morvan MG, Lanier LL. NK cells and cancer: you can teach innate cells new tricks. *Nat Rev Cancer*. 2016 Jan;16(1):7–19.
65. Moretta A, Bottino C, Vitale M, Pende D, Biassoni R, Mingari MC, et al. Receptors for Hla Class-I Molecules in Human Natural Killer Cells. *Annu Rev Immunol*. 1996;14(1):619–48.
66. Moretta L, Biassoni R, Bottino C, Mingari MC, Moretta A. Human NK-cell receptors. *Immunol Today*. 2000 Sep 1;21(9):420–2.

Bibliography

67. Marsh SGE, Parham P, Dupont B, Geraghty DE, Trowsdale J, Middleton D, et al. Killer-cell Immunoglobulin-like Receptor (KIR) Nomenclature Report, 2002. *Hum Immunol.* 2003 Jun 1;64(6):648–54.
68. Biassoni R. The human leukocyte antigen (HLA)-C-specific ‘activatory’ or ‘inhibitory’ natural killer cell receptors display highly homologous extracellular domains but differ in their transmembrane and intracytoplasmic portions. *J Exp Med.* 1996 Feb 1;183(2):645–50.
69. Mingari MC, Ponte M, Cantoni C, Vitale C, Schiavetti F, Bertone S, et al. HLA-class I-specific inhibitory receptors in human cytolytic T lymphocytes: molecular characterization, distribution in lymphoid tissues and co-expression by individual T cells. *Int Immunol.* 1997 Apr 1;9(4):485–91.
70. Schönberg K, Sribar M, Enczmann J, Fischer JC, Uhrberg M. Analyses of HLA-C-specific KIR repertoires in donors with group A and B haplotypes suggest a ligand-instructed model of NK cell receptor acquisition. *Blood.* 2011 Jan 6;117(1):98–107.
71. Trowsdale J. Genetic and Functional Relationships between MHC and NK Receptor Genes. *Immunity.* 2001 Sep 1;15(3):363–74.
72. Charles A Janeway J, Travers P, Walport M, Shlomchik MJ. The major histocompatibility complex and its functions. *Immunobiol Immune Syst Health Dis 5th Ed [Internet].* 2001 [cited 2019 Jul 20]; Available from: <https://www.ncbi.nlm.nih.gov/books/NBK27156/>
73. Wagtmann N, Biassoni R, Cantoni C, Verdiani S, Malnati MS, Vitale M, et al. Molecular clones of the p58 NK cell receptor reveal immunoglobulin-related molecules with diversity in both the extra- and intracellular domains. *Immunity.* 1995 May;2(5):439–49.
74. Vilches C, Parham P. KIR: Diverse, Rapidly Evolving Receptors of Innate and Adaptive Immunity. *Annu Rev Immunol.* 2002;20(1):217–51.
75. Olcese L, Lang P, Vély F, Cambiaggi A, Marguet D, Bléry M, et al. Human and mouse killer-cell inhibitory receptors recruit PTP1C and PTP1D protein tyrosine phosphatases. *J Immunol.* 1996 Jun 15;156(12):4531–4.
76. Lanier LL, Corliss BC, Wu J, Leong C, Phillips JH. Immunoreceptor DAP12 bearing a tyrosine-based activation motif is involved in activating NK cells. *Nature.* 1998 Feb;391(6668):703.
77. Uhrberg M, Valiante NM, Shum BP, Shilling HG, Lienert-Weidenbach K, Corliss B, et al. Human Diversity in Killer Cell Inhibitory Receptor Genes. *Immunity.* 1997 Dec 1;7(6):753–63.
78. Parham P. MHC class I molecules and KIRs in human history, health and survival. *Nat Rev Immunol.* 2005 Mar;5(3):201–14.
79. Shilling HG, Guethlein LA, Cheng NW, Gardiner CM, Rodriguez R, Tyan D, et al. Allelic Polymorphism Synergizes with Variable Gene Content to Individualize Human KIR Genotype. *J Immunol.* 2002 Mar 1;168(5):2307–15.
80. Gumperz JE, Valiante NM, Parham P, Lanier LL, Tyan D. Heterogeneous phenotypes of expression of the NKB1 natural killer cell class I receptor among individuals of different human histocompatibility leukocyte antigens types appear genetically regulated, but not linked to major histocompatibility complex haplotype. *J Exp Med.* 1996 Apr 1;183(4):1817–27.
81. Khakoo SI, Thio CL, Martin MP, Brooks CR, Gao X, Astemborski J, et al. HLA and NK Cell Inhibitory Receptor Genes in Resolving Hepatitis C Virus Infection. *Science.* 2004 Aug 6;305(5685):872–4.
82. Manser AR, Weinhold S, Uhrberg M. Human KIR repertoires: shaped by genetic diversity and evolution. *Immunol Rev.* 2015;267(1):178–96.

Bibliography

83. Hsu KC, Chida S, Geraghty DE, Dupont B. The killer cell immunoglobulin-like receptor (KIR) genomic region: gene-order, haplotypes and allelic polymorphism. *Immunol Rev.* 2002;190(1):40–52.
84. Jiang W, Johnson C, Jayaraman J, Simecek N, Noble J, Moffatt MF, et al. Copy number variation leads to considerable diversity for B but not A haplotypes of the human KIR genes encoding NK cell receptors. *Genome Res.* 2012 Oct;22(10):1845–54.
85. Hsu KC, Liu X-R, Selvakumar A, Mickelson E, O'Reilly RJ, Dupont B. Killer Ig-Like Receptor Haplotype Analysis by Gene Content: Evidence for Genomic Diversity with a Minimum of Six Basic Framework Haplotypes, Each with Multiple Subsets. *J Immunol.* 2002 Nov 1;169(9):5118–29.
86. Chazara O, Xiong S, Moffett A. Maternal KIR and fetal HLA-C: a fine balance. *J Leukoc Biol.* 2011;90(4):703–16.
87. Uhrberg M, Parham P, Wernet P. Definition of gene content for nine common group B haplotypes of the Caucasoid population: KIR haplotypes contain between seven and eleven KIR genes. *Immunogenetics.* 2002 Jul 1;54(4):221–9.
88. Colonna M, Borsellino G, Falco M, Ferrara GB, Strominger JL. HLA-C is the inhibitory ligand that determines dominant resistance to lysis by NK1- and NK2-specific natural killer cells. *Proc Natl Acad Sci U S A.* 1993 Dec 15;90(24):12000–4.
89. Hilton HG, Parham P. Missing or altered self: human NK cell receptors that recognize HLA-C. *Immunogenetics.* 2017;69(8–9):567–79.
90. Colonna M, Spies T, Strominger JL, Ciccone E, Moretta A, Moretta L, et al. Alloantigen recognition by two human natural killer cell clones is associated with HLA-C or a closely linked gene. *Proc Natl Acad Sci U S A.* 1992 Sep 1;89(17):7983–5.
91. Colonna M, Brooks EG, Falco M, Ferrara GB, Strominger JL. Generation of allospecific natural killer cells by stimulation across a polymorphism of HLA-C. *Science.* 1993 May 21;260(5111):1121–4.
92. Moretta A, Vitale M, Bottino C, Orengo AM, Morelli L, Augugliaro R, et al. P58 molecules as putative receptors for major histocompatibility complex (MHC) class I molecules in human natural killer (NK) cells. Anti-p58 antibodies reconstitute lysis of MHC class I-protected cells in NK clones displaying different specificities. *J Exp Med.* 1993 Aug 1;178(2):597–604.
93. Wagtmann N, Rajagopalan S, Winter CC, Peruui M, Long EO. Killer cell inhibitory receptors specific for HLA-C and HLA-B identified by direct binding and by functional transfer. *Immunity.* 1995 Dec 1;3(6):801–9.
94. Mandelboim O, Reyburn HT, Valés-Gómez M, Pazmany L, Colonna M, Borsellino G, et al. Protection from lysis by natural killer cells of group 1 and 2 specificity is mediated by residue 80 in human histocompatibility leukocyte antigen C alleles and also occurs with empty major histocompatibility complex molecules. *J Exp Med.* 1996 Sep 1;184(3):913–22.
95. Winter CC, Gumperz JE, Parham P, Long EO, Wagtmann N. Direct Binding and Functional Transfer of NK Cell Inhibitory Receptors Reveal Novel Patterns of HLA-C Allotype Recognition. *J Immunol.* 1998 Jul 15;161(2):571–7.
96. Moesta AK, Norman PJ, Yawata M, Yawata N, Gleimer M, Parham P. Synergistic Polymorphism at Two Positions Distal to the Ligand-Binding Site Makes KIR2DL2 a Stronger Receptor for HLA-C Than KIR2DL3. *J Immunol.* 2008 Mar 15;180(6):3969–79.

Bibliography

97. Ponte M, Cantoni C, Biassoni R, Tradori-Cappai A, Bentivoglio G, Vitale C, et al. Inhibitory receptors sensing HLA-G1 molecules in pregnancy: decidua-associated natural killer cells express LIR-1 and CD94/NKG2A and acquire p49, an HLA-G1-specific receptor. *Proc Natl Acad Sci U S A*. 1999 May 11;96(10):5674–9.
98. Rajagopalan S, Bryceson YT, Kuppusamy SP, Geraghty DE, van der Meer A, Joosten I, et al. Activation of NK cells by an endocytosed receptor for soluble HLA-G. *PLoS Biol*. 2006 Jan;4(1):e9.
99. Moradi S, Berry R, Pymm P, Hitchen C, Beckham SA, Wilce MCJ, et al. The Structure of the Atypical Killer Cell Immunoglobulin-like Receptor, KIR2DL4. *J Biol Chem*. 2015 Apr 17;290(16):10460–71.
100. Biassoni R, Pessino A, Malaspina A, Cantoni C, Bottino C, Sivori S, et al. Role of amino acid position 70 in the binding affinity of p50.1 and p58.1 receptors for HLA-Cw4 molecules. *Eur J Immunol*. 1997 Dec;27(12):3095–9.
101. Stewart CA, Laugier-Anfossi F, Vély F, Saulquin X, Riedmuller J, Tisserant A, et al. Recognition of peptide–MHC class I complexes by activating killer immunoglobulin-like receptors. *Proc Natl Acad Sci*. 2005 Sep 13;102(37):13224–9.
102. Naiyer MM, Cassidy SA, Magri A, Cowton V, Chen K, Mansour S, et al. KIR2DS2 recognizes conserved peptides derived from viral helicases in the context of HLA-C. *Sci Immunol*. 2017 Sep 15;2(15):eaal5296.
103. Liu J, Xiao Z, Ko HL, Shen M, Ren EC. Activating killer cell immunoglobulin-like receptor 2DS2 binds to HLA-A*11. *Proc Natl Acad Sci*. 2014 Feb 18;111(7):2662–7.
104. Graef T, Moesta AK, Norman PJ, Abi-Rached L, Vago L, Aguilar AMO, et al. KIR2DS4 is a product of gene conversion with KIR3DL2 that introduced specificity for HLA-A*11 while diminishing avidity for HLA-C. *J Exp Med*. 2009 Oct 26;206(11):2557–72.
105. Blokhuis JH, Hilton HG, Guethlein LA, Norman PJ, Nemat-Gorgani N, Nakimuli A, et al. KIR2DS5 allotypes that recognize the C2 epitope of HLA-C are common among Africans and absent from Europeans. *Immun Inflamm Dis*. 2017 Jul 6;5(4):461–8.
106. Gumperz JE, Litwin V, Phillips JH, Lanier LL, Parham P. The Bw4 public epitope of HLA-B molecules confers reactivity with natural killer cell clones that express NKB1, a putative HLA receptor. *J Exp Med*. 1995 Mar 1;181(3):1133–44.
107. Döhning C, Scheidegger D, Samaridis J, Cella M, Colonna M. A human killer inhibitory receptor specific for HLA-A1,2. *J Immunol*. 1996 May 1;156(9):3098–101.
108. Pende D, Biassoni R, Cantoni C, Verdiani S, Falco M, Donato C di, et al. The natural killer cell receptor specific for HLA-A allotypes: a novel member of the p58/p70 family of inhibitory receptors that is characterized by three immunoglobulin-like domains and is expressed as a 140-kD disulphide-linked dimer. *J Exp Med*. 1996 Aug 1;184(2):505–18.
109. Garcia-Beltran WF, Hölzemer A, Martus G, Chung AW, Pacheco Y, Simoneau CR, et al. Open conformers of HLA-F are high-affinity ligands of the activating NK-cell receptor KIR3DS1. *Nat Immunol*. 2016 Sep;17(9):1067–74.
110. Houchins JP, Lanier LL, Niemi EC, Phillips JH, Ryan JC. Natural killer cell cytolytic activity is inhibited by NKG2-A and activated by NKG2-C. *J Immunol*. 1997 Apr 15;158(8):3603–9.
111. Fauriat C, Andersson S, Björklund AT, Carlsten M, Schaffer M, Björkström NK, et al. Estimation of the size of the alloreactive NK cell repertoire: studies in individuals homozygous for the group A KIR haplotype. *J Immunol Baltim Md 1950*. 2008 Nov 1;181(9):6010–9.

Bibliography

112. Yawata M, Yawata N, Draghi M, Partheniou F, Little A-M, Parham P. MHC class I-specific inhibitory receptors and their ligands structure diverse human NK-cell repertoires toward a balance of missing self-response. *Blood*. 2008 Sep 15;112(6):2369–80.
113. Trowsdale J, Barten R, Haude A, Stewart CA, Beck S, Wilson MJ. The genomic context of natural killer receptor extended gene families. *Immunol Rev*. 2001;181(1):20–38.
114. Borrego F, Ulbrecht M, Weiss EH, Coligan JE, Brooks AG. Recognition of human histocompatibility leukocyte antigen (HLA)-E complexed with HLA class I signal sequence-derived peptides by CD94/NKG2 confers protection from natural killer cell-mediated lysis. *J Exp Med*. 1998 Mar 2;187(5):813–8.
115. Braud VM, Allan DSJ, O’Callaghan CA, Söderström K, D’Andrea A, Ogg GS, et al. HLA-E binds to natural killer cell receptors CD94/NKG2A, B and C. *Nature*. 1998 Feb;391(6669):795.
116. Lanier LL. NKG2D receptor and its ligands in host defense. *Cancer Immunol Res*. 2015 Jun;3(6):575–82.
117. Cosman D, Müllberg J, Sutherland CL, Chin W, Armitage R, Fanslow W, et al. ULBPs, Novel MHC Class I-Related Molecules, Bind to CMV Glycoprotein UL16 and Stimulate NK Cytotoxicity through the NKG2D Receptor. *Immunity*. 2001 Feb 1;14(2):123–33.
118. Jan Chalupny N, Sutherland CL, Lawrence WA, Rein-Weston A, Cosman D. ULBP4 is a novel ligand for human NKG2D. *Biochem Biophys Res Commun*. 2003 May 23;305(1):129–35.
119. Manser AR, Scherenschlich N, Thöns C, Hengel H, Timm J, Uhrberg M. KIR Polymorphism Modulates the Size of the Adaptive NK Cell Pool in Human Cytomegalovirus-Infected Individuals. *J Immunol Baltim Md 1950*. 2019 15;203(8):2301–9.
120. Wu Z, Sinzger C, Frascaroli G, Reichel J, Bayer C, Wang L, et al. Human Cytomegalovirus-Induced NKG2Chi CD57hi Natural Killer Cells Are Effectors Dependent on Humoral Antiviral Immunity. *J Virol*. 2013 Jul;87(13):7717–25.
121. Schlums H, Cichocki F, Tesi B, Theorell J, Beziat V, Holmes TD, et al. Cytomegalovirus Infection Drives Adaptive Epigenetic Diversification of NK Cells with Altered Signaling and Effector Function. *Immunity*. 2015 Mar 17;42(3):443–56.
122. Lanier LL, Corliss B, Wu J, Phillips JH. Association of DAP12 with activating CD94/NKG2C NK cell receptors. *Immunity*. 1998 Jun;8(6):693–701.
123. Wu J, Song Y, Bakker AB, Bauer S, Spies T, Lanier LL, et al. An activating immunoreceptor complex formed by NKG2D and DAP10. *Science*. 1999 Jul 30;285(5428):730–2.
124. Lieto LD, Maasho K, West D, Borrego F, Coligan JE. The human CD94 gene encodes multiple, expressible transcripts including a new partner of NKG2A/B. *Genes Immun*. 2006 Jan;7(1):36–43.
125. Kaiser BK, Barahmand-Pour F, Paulsene W, Medley S, Geraghty DE, Strong RK. Interactions between NKG2x immunoreceptors and HLA-E ligands display overlapping affinities and thermodynamics. *J Immunol Baltim Md 1950*. 2005 Mar 1;174(5):2878–84.
126. Orbelyan GA, Tang F, Sally B, Solus J, Meresse B, Ciszewski C, et al. Human NKG2E is expressed and forms an intracytoplasmic complex with CD94 and DAP12. *J Immunol Baltim Md 1950*. 2014 Jul 15;193(2):610–6.
127. Dukovska D, Fernández-Soto D, Valés-Gómez M, Reyburn HT. NKG2H-Expressing T Cells Negatively Regulate Immune Responses. *Front Immunol*. 2018;9:390.

Bibliography

128. Kim D-K, Kabat J, Borrego F, Sanni TB, You C, Coligan JE. Human NKG2F is expressed and can associate with DAP12. *Mol Immunol*. 2004 May 1;41(1):53–62.
129. Moretta A, Biassoni R, Bottino C, Mingari MC, Moretta L. Natural cytotoxicity receptors that trigger human NK-cell-mediated cytotoxicity. *Immunol Today*. 2000 May;21(5):228–34.
130. Sivori S, Pende D, Bottino C, Marcenaro E, Pessino A, Biassoni R, et al. NKp46 is the major triggering receptor involved in the natural cytotoxicity of fresh or cultured human NK cells. Correlation between surface density of NKp46 and natural cytotoxicity against autologous, allogeneic or xenogeneic target cells. *Eur J Immunol*. 1999;29(5):1656–66.
131. Brandt CS, Baratin M, Yi EC, Kennedy J, Gao Z, Fox B, et al. The B7 family member B7-H6 is a tumor cell ligand for the activating natural killer cell receptor NKp30 in humans. *J Exp Med*. 2009 Jul 6;206(7):1495–503.
132. Shiroishi M, Tsumoto K, Amano K, Shirakihara Y, Colonna M, Braud VM, et al. Human inhibitory receptors Ig-like transcript 2 (ILT2) and ILT4 compete with CD8 for MHC class I binding and bind preferentially to HLA-G. *Proc Natl Acad Sci U S A*. 2003 Jul 22;100(15):8856–61.
133. Apps R, Gardner L, Moffett A. A critical look at HLA-G. *Trends Immunol*. 2008 Jul 1;29(7):313–21.
134. Kim S, Poursine-Laurent J, Truscott SM, Lybarger L, Song Y-J, Yang L, et al. Licensing of natural killer cells by host major histocompatibility complex class I molecules. *Nature*. 2005 Aug;436(7051):709.
135. He Y, Tian Z. NK cell education via nonclassical MHC and non-MHC ligands. *Cell Mol Immunol*. 2017 Apr;14(4):321–30.
136. Salle H de la, Hanau D, Fricker D, Urlacher A, Kelly A, Salamero J, et al. Homozygous human TAP peptide transporter mutation in HLA class I deficiency. *Science*. 1994 Jul 8;265(5169):237–41.
137. Furukawa H, Yabe T, Watanabe K, Miyamoto R, Miki A, Akaza T, et al. Tolerance of NK and LAK activity for HLA class I-deficient targets in a TAP1-deficient patient (bare lymphocyte syndrome type I). *Hum Immunol*. 1999 Jan 1;60(1):32–40.
138. Fernandez NC, Treiner E, Vance RE, Jamieson AM, Lemieux S, Raulet DH. A subset of natural killer cells achieves self-tolerance without expressing inhibitory receptors specific for self-MHC molecules. *Blood*. 2005 Jun 1;105(11):4416–23.
139. Orr MT, Murphy WJ, Lanier LL. “Unlicensed” Natural Killer cells dominate the response to cytomegalovirus infection. *Nat Immunol*. 2010 Apr;11(4):321–7.
140. Elliott JM, Wahle JA, Yokoyama WM. MHC class I-deficient natural killer cells acquire a licensed phenotype after transfer into an MHC class I-sufficient environment. *J Exp Med*. 2010 Sep 27;207(10):2073–9.
141. Brodin P, Lakshmikanth T, Johansson S, Kärre K, Höglund P. The strength of inhibitory input during education quantitatively tunes the functional responsiveness of individual natural killer cells. *Blood*. 2009 Mar 12;113(11):2434–41.
142. Sim MJW, Stowell J, Sergeant R, Altmann DM, Long EO, Boyton RJ. KIR2DL3 and KIR2DL1 show similar impact on licensing of human NK cells. *Eur J Immunol*. 2016 Jan;46(1):185–91.

Bibliography

143. Enqvist M, Ask EH, Forslund E, Carlsten M, Abrahamsen G, Béziat V, et al. Coordinated Expression of DNAM-1 and LFA-1 in Educated NK Cells. *J Immunol*. 2015 May 1;194(9):4518–27.
144. Goodridge JP, Jacobs B, Saetersmoen ML, Clement D, Hammer Q, Clancy T, et al. Remodeling of secretory lysosomes during education tunes functional potential in NK cells. *Nat Commun*. 2019 Jan 31;10(1):514.
145. Raulet DH, Vance RE. Self-tolerance of natural killer cells. *Nat Rev Immunol*. 2006 Jul;6(7):520.
146. Wu MF, Raulet DH. Class I-deficient hemopoietic cells and nonhemopoietic cells dominantly induce unresponsiveness of natural killer cells to class I-deficient bone marrow cell grafts. *J Immunol*. 1997 Feb 15;158(4):1628–33.
147. Joncker NT, Raulet DH. Regulation of NK cell responsiveness to achieve self tolerance and maximal responses to diseased target cells. *Immunol Rev*. 2008 Aug;224:85–97.
148. Brodin P, Kärre K, Höglund P. NK cell education: not an on-off switch but a tunable rheostat. *Trends Immunol*. 2009 Apr 1;30(4):143–9.
149. Joncker NT, Fernandez NC, Treiner E, Vivier E, Raulet DH. NK Cell Responsiveness is Tuned Commensurate with the Number of Inhibitory Receptors for Self MHC Class I: the Rheostat Model. *J Immunol Baltim Md 1950*. 2009 Apr 15;182(8):4572–80.
150. Guia S, Jaeger BN, Piatek S, Mailfert S, Trombik T, Fenis A, et al. Confinement of activating receptors at the plasma membrane controls natural killer cell tolerance. *Sci Signal*. 2011 Apr 5;4(167):ra21.
151. Staaf E, Hedde PN, Bagawath Singh S, Piguet J, Gratton E, Johansson S. Educated natural killer cells show dynamic movement of the activating receptor NKp46 and confinement of the inhibitory receptor Ly49A. *Sci Signal*. 2018 Feb 13;11(517).
152. Elliott JM, Yokoyama WM. Unifying concepts of MHC-dependent natural killer cell education. *Trends Immunol*. 2011 Aug;32(8):364–72.
153. Chalifour A, Scarpellino L, Back J, Brodin P, Devèvre E, Gros F, et al. A Role for cis Interaction between the Inhibitory Ly49A receptor and MHC class I for natural killer cell education. *Immunity*. 2009 Mar 20;30(3):337–47.
154. Boudreau JE, Liu X-R, Zhao Z, Zhang A, Shultz LD, Greiner DL, et al. Cell-Extrinsic MHC Class I Molecule Engagement Augments Human NK Cell Education Programmed by Cell-Intrinsic MHC Class I. *Immunity*. 2016 Aug 16;45(2):280–91.
155. Tay CH, Welsh RM, Brutkiewicz RR. NK cell response to viral infections in beta 2-microglobulin-deficient mice. *J Immunol*. 1995 Jan 15;154(2):780–9.
156. Kristensen AB, Kent SJ, Parsons MS. Contribution of NK Cell Education to both Direct and Anti-HIV-1 Antibody-Dependent NK Cell Functions. *J Virol*. 2018 Jun 1;92(11):e02146-17.
157. Tarek N, Le Luëdec J-B, Gallagher MM, Zheng J, Venstrom JM, Chamberlain E, et al. Unlicensed NK cells target neuroblastoma following anti-GD2 antibody treatment. *J Clin Invest*. 2012 Sep;122(9):3260–70.
158. Jenne DE, Tschopp J. Granzymes, a Family of Serine Proteases Released from Granules of Cytolytic T Lymphocytes upon T Cell Receptor Stimulation. *Immunol Rev*. 1988;103(1):53–71.
159. Smyth MarkJ, Trapani JA. Granzymes: exogenous proteases that induce target cell apoptosis. *Immunol Today*. 1995 Apr 1;16(4):202–6.

Bibliography

160. Trapani JA. Granzymes: a family of lymphocyte granule serine proteases. *Genome Biol.* 2001;2(12):reviews3014.1-reviews3014.7.
161. Susanto O, Trapani JA, Brasacchio D. Controversies in granzyme biology. *Tissue Antigens.* 2012;80(6):477–87.
162. Voskoboinik I, Whisstock JC, Trapani JA. Perforin and granzymes: function, dysfunction and human pathology. *Nat Rev Immunol.* 2015 Jun;15(6):388–400.
163. Henkart PA, Millard PJ, Reynolds CW, Henkart MP. Cytolytic activity of purified cytoplasmic granules from cytotoxic rat large granular lymphocyte tumors. *J Exp Med.* 1984 Jul 1;160(1):75–93.
164. Podack ER, Young JD, Cohn ZA. Isolation and biochemical and functional characterization of perforin 1 from cytolytic T-cell granules. *Proc Natl Acad Sci.* 1985 Dec 1;82(24):8629–33.
165. Shinkai Y, Takio K, Okumura K. Homology of perforin to the ninth component of complement (C9). *Nature.* 1988 Aug;334(6182):525–7.
166. Pham CTN, Ley TJ. Dipeptidyl peptidase I is required for the processing and activation of granzymes A and B in vivo. *Proc Natl Acad Sci U S A.* 1999 Jul 20;96(15):8627–32.
167. D'Angelo ME, Bird PI, Peters C, Reinheckel T, Trapani JA, Sutton VR. Cathepsin H is an additional convertase of pro-granzyme B. *J Biol Chem.* 2010 Jul 2;285(27):20514–9.
168. Voskoboinik I, Thia M-C, Fletcher J, Ciccone A, Browne K, Smyth MJ, et al. Calcium-dependent Plasma Membrane Binding and Cell Lysis by Perforin Are Mediated through Its C2 Domain A CRITICAL ROLE FOR ASPARTATE RESIDUES 429, 435, 483, AND 485 BUT NOT 491. *J Biol Chem.* 2005 Apr 3;280(9):8426–34.
169. Praper T, Beseničar MP, Istinič H, Podlesek Z, Metkar SS, Froelich CJ, et al. Human perforin permeabilizing activity, but not binding to lipid membranes, is affected by pH. *Mol Immunol.* 2010 Sep 1;47(15):2492–504.
170. House IG, House CM, Brennan AJ, Gilan O, Dawson MA, Whisstock JC, et al. Regulation of perforin activation and pre-synaptic toxicity through C-terminal glycosylation. *EMBO Rep.* 2017;18(10):1775–85.
171. Sutton VR, Davis JE, Cancilla M, Johnstone RW, Ruefli AA, Sedelies K, et al. Initiation of apoptosis by granzyme B requires direct cleavage of bid, but not direct granzyme B-mediated caspase activation. *J Exp Med.* 2000 Nov 20;192(10):1403–14.
172. Poe M, Blake JT, Boulton DA, Gammon M, Sigal NH, Wu JK, et al. Human cytotoxic lymphocyte granzyme B. Its purification from granules and the characterization of substrate and inhibitor specificity. *J Biol Chem.* 1991 May 1;266(1):98–103.
173. Masson D, Nabholz M, Estrade C, Tschopp J. Granules of cytolytic T-lymphocytes contain two serine esterases. *EMBO J.* 1986 Jul;5(7):1595–600.
174. Masson D, Zamai M, Tschopp J. Identification of granzyme A isolated from cytotoxic T-lymphocyte-granules as one of the proteases encoded by CTL-specific genes [Internet]. *FEBS Letters.* 1986 [cited 2019 Jul 19]. Available from: <https://febs.onlinelibrary.wiley.com/doi/abs/10.1016/0014-5793%2886%2981537-X>
175. Metkar SS, Mena C, Pardo J, Wang B, Wallich R, Freudenberg M, et al. Human and mouse granzyme A induce a proinflammatory cytokine response. *Immunity.* 2008 Nov 14;29(5):720–33.

Bibliography

176. Buzza MS, Zamurs L, Sun J, Bird CH, Smith AI, Trapani JA, et al. Extracellular Matrix Remodeling by Human Granzyme B via Cleavage of Vitronectin, Fibronectin, and Laminin. *J Biol Chem*. 2005 Jun 24;280(25):23549–58.
177. YOSHIKAWA Y, HIRAYASU H, TSUZUKI S, FUSHIKI T. Granzyme A Causes Detachment of Alveolar Epithelial A549 Cells Accompanied by Promotion of Interleukin-8 Release. *Biosci Biotechnol Biochem*. 2008 Sep 23;72(9):2481–4.
178. Tang H, Li C, Wang L, Zhang H, Fan Z. Granzyme H of Cytotoxic Lymphocytes Is Required for Clearance of the Hepatitis B Virus through Cleavage of the Hepatitis B Virus X Protein. *J Immunol*. 2012 Jan 15;188(2):824–31.
179. Grossman WJ, Verbsky JW, Tollefsen BL, Kemper C, Atkinson JP, Ley TJ. Differential expression of granzymes A and B in human cytotoxic lymphocyte subsets and T regulatory cells. *Blood*. 2004 Nov 1;104(9):2840–8.
180. Sayers TJ, Brooks AD, Ward JM, Hoshino T, Bere WE, Wiegand GW, et al. The Restricted Expression of Granzyme M in Human Lymphocytes. *J Immunol*. 2001 Jan 15;166(2):765–71.
181. Bratke K, Kuepper M, Bade B, Virchow JC, Luttmann W. Differential expression of human granzymes A, B, and K in natural killer cells and during CD8⁺ T cell differentiation in peripheral blood. *Eur J Immunol*. 2005 Sep;35(9):2608–16.
182. Sedelies KA, Sayers TJ, Edwards KM, Chen W, Pellicci DG, Godfrey DI, et al. Discordant Regulation of Granzyme H and Granzyme B Expression in Human Lymphocytes. *J Biol Chem*. 2004 Jun 18;279(25):26581–7.
183. Wang L, Li Q, Wu L, Liu S, Zhang Y, Yang X, et al. Identification of SERPINB1 As a Physiological Inhibitor of Human Granzyme H. *J Immunol*. 2013 Feb 1;190(3):1319–30.
184. Bade B, Boettcher HE, Lohrmann J, Hink-Schauer C, Bratke K, Jenne DE, et al. Differential expression of the granzymes A, K and M and perforin in human peripheral blood lymphocytes. *Int Immunol*. 2005 Nov;17(11):1419–28.
185. Smyth MJ, O'Connor MD, Trapani JA. Granzymes: a variety of serine protease specificities encoded by genetically distinct subfamilies. *J Leukoc Biol*. 1996 Nov;60(5):555–62.
186. Grossman WJ, Revell PA, Lu ZH, Johnson H, Bredemeyer AJ, Ley TJ. The orphan granzymes of humans and mice. *Curr Opin Immunol*. 2003 Oct;15(5):544–52.
187. Haddad P, Jenne D, Tschopp J, Clément MV, Mathieu-Mahul D, Sasportes M. Structure and evolutionary origin of the human granzyme H gene. *Int Immunol*. 1991 Jan;3(1):57–66.
188. O'Leary NA, Wright MW, Brister JR, Ciuffo S, Haddad D, McVeigh R, et al. Reference sequence (RefSeq) database at NCBI: current status, taxonomic expansion, and functional annotation. *Nucleic Acids Res*. 2016 Jan 4;44(D1):D733-745.
189. Fellows E, Gil-Parrado S, Jenne DE, Kurschus FC. Natural killer cell–derived human granzyme H induces an alternative, caspase-independent cell-death program. *Blood*. 2007 Jul 15;110(2):544–52.
190. Hou Q, Zhao T, Zhang H, Lu H, Zhang Q, Sun L, et al. Granzyme H induces apoptosis of target tumor cells characterized by DNA fragmentation and Bid-dependent mitochondrial damage. *Mol Immunol*. 2008 Feb;45(4):1044–55.
191. Ewen CL, Kane KP, Bleackley RC. Granzyme H induces cell death primarily via a Bcl-2-sensitive mitochondrial cell death pathway that does not require direct Bid activation. *Mol Immunol*. 2013 Jul;54(3–4):309–18.

Bibliography

192. Edwards KM, Kam C-M, Powers JC, Trapani JA. The Human Cytotoxic T Cell Granule Serine Protease Granzyme H Has Chymotrypsin-like (Chymase) Activity and Is Taken Up into Cytoplasmic Vesicles Reminiscent of Granzyme B-containing Endosomes. *J Biol Chem*. 1999 Oct 22;274(43):30468–73.
193. Froelich CJ, Orth K, Turbov J, Seth P, Gottlieb R, Babior B, et al. New Paradigm for Lymphocyte Granule-mediated Cytotoxicity TARGET CELLS BIND AND INTERNALIZE GRANZYME B, BUT AN ENDOSOMOLYTIC AGENT IS NECESSARY FOR CYTOSOLIC DELIVERY AND SUBSEQUENT APOPTOSIS. *J Biol Chem*. 1996 Nov 15;271(46):29073–9.
194. Jans DA, Briggs LJ, Jans P, Froelich CJ, Parasivam G, Kumar S, et al. Nuclear targeting of the serine protease granzyme A (fragmentin-1). *J Cell Sci*. 1998 Sep 1;111(17):2645–54.
195. Fujisaki H, Kakuda H, Shimasaki N, Imai C, Ma J, Lockey T, et al. EXPANSION OF HIGHLY CYTOTOXIC HUMAN NATURAL KILLER CELLS FOR CANCER CELL THERAPY. *Cancer Res*. 2009 May 1;69(9):4010–7.
196. Lozzio CB, Lozzio BB. Human chronic myelogenous leukemia cell-line with positive Philadelphia chromosome. *Blood*. 1975 Mar;45(3):321–34.
197. Lozzio BB, Lozzio CB. Properties and usefulness of the original K-562 human myelogenous leukemia cell line. *Leuk Res*. 1979 Jan 1;3(6):363–70.
198. Gong JH, Maki G, Klingemann HG. Characterization of a human cell line (NK-92) with phenotypical and functional characteristics of activated natural killer cells. *Leukemia*. 1994 Apr;8(4):652–8.
199. Graham FL, Smiley J, Russell WC, Nairn R. Characteristics of a human cell line transformed by DNA from human adenovirus type 5. *J Gen Virol*. 1977 Jul;36(1):59–74.
200. DuBridges RB, Tang P, Hsia HC, Leong PM, Miller JH, Calos MP. Analysis of mutation in human cells by using an Epstein-Barr virus shuttle system. *Mol Cell Biol*. 1987 Jan;7(1):379–87.
201. Pear WS, Nolan GP, Scott ML, Baltimore D. Production of high-titer helper-free retroviruses by transient transfection. *Proc Natl Acad Sci U S A*. 1993 Sep 15;90(18):8392–6.
202. Rasheed S, Nelson-Rees WA, Toth EM, Arnstein P, Gardner MB. Characterization of a newly derived human sarcoma cell line (HT-1080). *Cancer*. 1974;33(4):1027–33.
203. Frohn C, Schlenke P, Ebel B, Dannenberg C, Bein G, Kirchner H. DNA typing for natural killer cell inhibiting HLA-Cw groups NK1 and NK2 by PCR-SSP. *J Immunol Methods*. 1998 Sep 1;218(1):155–60.
204. Vilches C, Rajalingam R, Uhrberg M, Gardiner CM, Young NT, Parham P. KIR2DL5, a Novel Killer-Cell Receptor with a D0-D2 Configuration of Ig-Like Domains. *J Immunol*. 2000 Jun 1;164(11):5797–804.
205. Bøyum A, Fjerdingsstad HB, Martinsen I, Lea T, Løvhaug D. Separation of Human Lymphocytes from Citrated Blood by Density Gradient (Nycoprep) Centrifugation: Monocyte Depletion Depending upon Activation of Membrane Potassium Channels. *Scand J Immunol*. 2002;56(1):76–84.
206. Fang I-J, Trewyn BG. Application of Mesoporous Silica Nanoparticles in Intracellular Delivery of Molecules and Proteins. In: *Methods in Enzymology* [Internet]. Elsevier; 2012 [cited 2019 Sep 17]. p. 41–59. Available from: <https://linkinghub.elsevier.com/retrieve/pii/B9780123918604000033>

Bibliography

207. Best BP. Cryoprotectant Toxicity: Facts, Issues, and Questions. *Rejuvenation Res.* 2015 Oct;18(5):422–36.
208. McKinnon KM. Flow Cytometry: An Overview. *Curr Protoc Immunol.* 2018 Feb 21;120:5.1.1-5.1.11.
209. Demchenko AP. Beyond annexin V: fluorescence response of cellular membranes to apoptosis. *Cytotechnology.* 2013 Mar;65(2):157–72.
210. Bock GN, Chess L, Mardiney MR. The prevention of clumping of frozen-stored leukocyte populations by EDTA. *Cryobiology.* 1972 Jun;9(3):216–8.
211. Penack O, Gentilini C, Fischer L, Asemissen AM, Scheibenbogen C, Thiel E, et al. CD56 dim CD16 neg cells are responsible for natural cytotoxicity against tumor targets. *Leukemia.* 2005 May;19(5):835–40.
212. Uhrberg M. The CD107 mobilization assay: viable isolation and immunotherapeutic potential of tumor-cytolytic NK cells. *Leukemia.* 2005 May;19(5):707–9.
213. Fujiwara T, Oda K, Yokota S, Takatsuki A, Ikehara Y. Brefeldin A causes disassembly of the Golgi complex and accumulation of secretory proteins in the endoplasmic reticulum. *J Biol Chem.* 1988 Dec 5;263(34):18545–52.
214. Jung T, Schauer U, Heusser C, Neumann C, Rieger C. Detection of intracellular cytokines by flow cytometry. *J Immunol Methods.* 1993 Feb 26;159(1):197–207.
215. Foster B, Prussin C, Liu F, Whitmire JK, Whitton JL. Detection of Intracellular Cytokines by Flow Cytometry. *Curr Protoc Immunol.* 2007;78(1):6.24.1-6.24.21.
216. Weston SA, Parish CR. New fluorescent dyes for lymphocyte migration studies: Analysis by flow cytometry and fluorescence microscopy. *J Immunol Methods.* 1990 Oct 4;133(1):87–97.
217. Tag-it Violet Proliferation and Cell Tracking Dye [Internet]. [cited 2019 Aug 1]. Available from: <https://www.biolegend.com/en-us/products/tag-it-violet-proliferation-and-cell-tracking-dye-12697>
218. Yang TT, Cheng L, Kain SR. Optimized codon usage and chromophore mutations provide enhanced sensitivity with the green fluorescent protein. *Nucleic Acids Res.* 1996 Nov 15;24(22):4592–3.
219. Patterson GH, Knobel SM, Sharif WD, Kain SR, Piston DW. Use of the green fluorescent protein and its mutants in quantitative fluorescence microscopy. *Biophys J.* 1997 Nov;73(5):2782–90.
220. Vermes I, Haanen C, Reutelingsperger C. Flow cytometry of apoptotic cell death. *J Immunol Methods.* 2000 Sep 21;243(1):167–90.
221. Cheuk ATC, Mufti GJ, Guinn B. Role of 4-1BB:4-1BB ligand in cancer immunotherapy. *Cancer Gene Ther.* 2004 Mar;11(3):215–26.
222. Hrvatin S, Deng F, O'Donnell CW, Gifford DK, Melton DA. MARIS: method for analyzing RNA following intracellular sorting. *PLoS One.* 2014;9(3):e89459.
223. Mullis K, Faloona F, Scharf S, Saiki R, Horn G, Erlich H. Specific enzymatic amplification of DNA in vitro: the polymerase chain reaction. *Cold Spring Harb Symp Quant Biol.* 1986;51 Pt 1:263–73.
224. Testi M, Andreani M. Luminex-Based Methods in High-Resolution HLA Typing. In: Bugert P, editor. *Molecular Typing of Blood Cell Antigens* [Internet]. New York, NY: Springer New York;

Bibliography

- 2015 [cited 2019 Aug 23]. p. 231–45. (Methods in Molecular Biology). Available from: https://doi.org/10.1007/978-1-4939-2690-9_19
225. Zhang X-Y, La Russa VF, Bao L, Kolls J, Schwarzenberger P, Reiser J. Lentiviral Vectors for Sustained Transgene Expression in Human Bone Marrow-Derived Stromal Cells. *Mol Ther*. 2002 May 1;5(5):555–65.
226. Paddison PJ, Caudy AA, Bernstein E, Hannon GJ, Conklin DS. Short hairpin RNAs (shRNAs) induce sequence-specific silencing in mammalian cells. *Genes Dev*. 2002 Apr 15;16(8):948–58.
227. Pelletier J, Sonenberg N. Internal initiation of translation of eukaryotic mRNA directed by a sequence derived from poliovirus RNA. *Nature*. 1988 Jul;334(6180):320–5.
228. Jang SK, Kräusslich HG, Nicklin MJ, Duke GM, Palmenberg AC, Wimmer E. A segment of the 5' nontranslated region of encephalomyocarditis virus RNA directs internal entry of ribosomes during in vitro translation. *J Virol*. 1988 Aug;62(8):2636–43.
229. Adam MA, Ramesh N, Miller AD, Osborne WR. Internal initiation of translation in retroviral vectors carrying picornavirus 5' nontranslated regions. *J Virol*. 1991 Sep;65(9):4985–90.
230. Ghattas IR, Sanes JR, Majors JE. The encephalomyocarditis virus internal ribosome entry site allows efficient coexpression of two genes from a recombinant provirus in cultured cells and in embryos. *Mol Cell Biol*. 1991 Dec;11(12):5848–59.
231. Hannon GJ, Chubb A, Maroney PA, Hannon G, Altman S, Nilsen TW. Multiple cis-acting elements are required for RNA polymerase III transcription of the gene encoding H1 RNA, the RNA component of human RNase P. *J Biol Chem*. 1991 Dec 5;266(34):22796–9.
232. Kozak M. At least six nucleotides preceding the AUG initiator codon enhance translation in mammalian cells. *J Mol Biol*. 1987 Aug 20;196(4):947–50.
233. GZMH - Anti-GZMH Antibodies, shRNA, siRNA & Gene Information | Sigma-Aldrich [Internet]. [cited 2018 Jun 28]. Available from: <https://www.sigmaaldrich.com/catalog/genes/GZMH?lang=de®ion=DE>
234. Pearson JD, Zhang J, Wu Z, Thew KD, Rowe KJ, Bacani JTC, et al. Expression of granzyme B sensitizes ALK+ ALCL tumour cells to apoptosis-inducing drugs. *Mol Cancer*. 2014 Aug 29;13:199.
235. GPP Web Portal - Clone Details [Internet]. [cited 2018 Jun 28]. Available from: <https://portals.broadinstitute.org/gpp/public/clone/details?cloneId=TRCN0000006445>
236. Sanger F, Nicklen S, Coulson AR. DNA sequencing with chain-terminating inhibitors. *Proc Natl Acad Sci U S A*. 1977 Dec;74(12):5463–7.
237. McIlroy D, Cartron P-F, Tuffery P, Dudoit Y, Samri A, Autran B, et al. A triple-mutated allele of granzyme B incapable of inducing apoptosis. *Proc Natl Acad Sci U S A*. 2003 Mar 4;100(5):2562–7.
238. Sun J, Bird CH, Thia KY, Matthews AY, Trapani JA, Bird PI. Granzyme B encoded by the commonly occurring human RAH allele retains pro-apoptotic activity. *J Biol Chem*. 2004 Apr 23;279(17):16907–11.
239. Oboshi W, Watanabe T, Hayashi K, Nakamura T, Yukimasa N. QPY/RAH haplotypes of the GZMB gene are associated with natural killer cell cytotoxicity. *Immunogenetics*. 2018 Jan 1;70(1):29–36.

Bibliography

240. Sandrin V, Boson B, Salmon P, Gay W, Nègre D, Le Grand R, et al. Lentiviral vectors pseudotyped with a modified RD114 envelope glycoprotein show increased stability in sera and augmented transduction of primary lymphocytes and CD34+ cells derived from human and nonhuman primates. *Blood*. 2002 Aug 1;100(3):823–32.
241. Pietschmann T, Heinkelein M, Heldmann M, Zentgraf H, Rethwilm A, Lindemann D. Foamy Virus Capsids Require the Cognate Envelope Protein for Particle Export. *J Virol*. 1999 Apr;73(4):2613–21.
242. Stitz J, Buchholz CJ, Engelstädter M, Uckert W, Bloemer U, Schmitt I, et al. Lentiviral Vectors Pseudotyped with Envelope Glycoproteins Derived from Gibbon Ape Leukemia Virus and Murine Leukemia Virus 10A1. *Virology*. 2000 Jul 20;273(1):16–20.
243. Dull T, Zufferey R, Kelly M, Mandel RJ, Nguyen M, Trono D, et al. A third-generation lentivirus vector with a conditional packaging system. *J Virol*. 1998 Nov;72(11):8463–71.
244. Manceur AP, Kim H, Mistic V, Andreev N, Dorion-Thibaudeau J, Lanthier S, et al. Scalable Lentiviral Vector Production Using Stable HEK293SF Producer Cell Lines. *Hum Gene Ther Methods*. 2017;28(6):330–9.
245. GRCh38 - hg38 - Genome - Assembly - NCBI [Internet]. [cited 2020 May 19]. Available from: https://www.ncbi.nlm.nih.gov/assembly/GCF_000001405.26/
246. Dobin A, Davis CA, Schlesinger F, Drenkow J, Zaleski C, Jha S, et al. STAR: ultrafast universal RNA-seq aligner. *Bioinformatics*. 2013 Jan;29(1):15–21.
247. Liao Y, Smyth GK, Shi W. featureCounts: an efficient general purpose program for assigning sequence reads to genomic features. *Bioinforma Oxf Engl*. 2014 Apr 1;30(7):923–30.
248. Love MI, Huber W, Anders S. Moderated estimation of fold change and dispersion for RNA-seq data with DESeq2. *Genome Biol*. 2014 Dec 5;15(12):550.
249. Anti-Biotin antibodies - Secondary antibodies - Antibodies - MACS Flow Cytometry - Products - Miltenyi Biotec - Deutschland [Internet]. [cited 2019 Aug 24]. Available from: <https://www.miltenyibiotec.com/DE-en/products/macs-flow-cytometry/antibodies/secondary-antibodies/anti-biotin-antibodies-rea746-1-50.html>
250. Shelley CS, Silva ND, Georgakis A, Chomienne C, Arnaout MA. Mapping of the Human CD11c (ITGAX) and CD11d (ITGAD) Genes Demonstrates That They Are Arranged in Tandem Separated by No More Than 11.5 kb. *Genomics*. 1998 Apr 15;49(2):334–6.
251. Lopez-Vergès S, Milush JM, Pandey S, York VA, Arakawa-Hoyt J, Pircher H, et al. CD57 defines a functionally distinct population of mature NK cells in the human CD56dimCD16+ NK-cell subset. *Blood*. 2010 Nov 11;116(19):3865–74.
252. Henson SM, Akbar AN. KLRG1—more than a marker for T cell senescence. *Age*. 2009 Dec;31(4):285–91.
253. Elpek KG, Rubinstein MP, Bellemare-Pelletier A, Goldrath AW, Turley SJ. Mature natural killer cells with phenotypic and functional alterations accumulate upon sustained stimulation with IL-15/IL-15R α complexes. *Proc Natl Acad Sci*. 2010 Dec 14;107(50):21647–52.
254. Müller-Durovic B, Lanna A, Covre LP, Mills RS, Henson SM, Akbar AN. Killer Cell Lectin-like Receptor G1 (KLRG1) inhibits NK cell function through activation of AMP-activated Protein Kinase. *J Immunol Baltim Md 1950*. 2016 Oct 1;197(7):2891–9.
255. Freudenthal PS, Steinman RM. The distinct surface of human blood dendritic cells, as observed after an improved isolation method. *Proc Natl Acad Sci U S A*. 1990 Oct;87(19):7698–702.

Bibliography

256. Postigo AA, Corbí AL, Sánchez-Madrid F, de Landázuri MO. Regulated expression and function of CD11c/CD18 integrin on human B lymphocytes. Relation between attachment to fibrinogen and triggering of proliferation through CD11c/CD18. *J Exp Med*. 1991 Dec 1;174(6):1313–22.
257. Keizer GD, Borst J, Visser W, Schwarting R, Vries JE de, Figdor CG. Membrane glycoprotein p150,95 of human cytotoxic T cell clone is involved in conjugate formation with target cells. *J Immunol*. 1987 May 15;138(10):3130–6.
258. Rubtsov AV, Rubtsova K, Kappler JW, Jacobelli J, Friedman RS, Marrack P. CD11c-Expressing B Cells Are Located at the T Cell/B Cell Border in Spleen and Are Potent APCs. *J Immunol Baltim Md 1950*. 2015 Jul 1;195(1):71–9.
259. Masuda N, Ohnishi T, Kawamoto S, Monden M, Okubo K. Analysis of chemical modification of RNA from formalin-fixed samples and optimization of molecular biology applications for such samples. *Nucleic Acids Res*. 1999 Nov 1;27(22):4436–43.
260. Li Y, Hermanson DL, Moriarity BS, Kaufman DS. Human iPSC-Derived Natural Killer Cells Engineered with Chimeric Antigen Receptors Enhance Anti-tumor Activity. *Cell Stem Cell*. 2018 Aug 2;23(2):181-192.e5.
261. Taouk G, Hussein O, Zekak M, Abouelghar A, Al-Sarraj Y, Abdelalim EM, et al. CD56 expression in breast cancer induces sensitivity to natural killer-mediated cytotoxicity by enhancing the formation of cytotoxic immunological synapse. *Sci Rep*. 2019 Jun 19;9(1):1–17.
262. Vermes I, Haanen C, Steffens-Nakken H, Reutellingsperger C. A novel assay for apoptosis Flow cytometric detection of phosphatidylserine expression on early apoptotic cells using fluorescein labelled Annexin V. *J Immunol Methods*. 1995 Jul 17;184(1):39–51.
263. Technical Data Sheet: Fixable Viability Dye eFluor™ 780 [Internet]. [cited 2019 May 31]. Available from: <https://www.thermofisher.com/document-connect/document-connect.html?url=https%3A%2F%2Fassets.thermofisher.com%2FTFS-Assets%2FSLSG%2Fmanuals%2F65-0865.pdf&title=VGVjaG5pY2FsIERhdGEgU2hlZXQ6IEZpeGFibGUgVmlhYmlsaXR5IER5ZSBRmx1b3ImdHJhZGU7IDc4MA==>
264. Vogel C, Marcotte EM. Insights into the regulation of protein abundance from proteomic and transcriptomic analyses. *Nat Rev Genet*. 2012 Apr;13(4):227–32.
265. Hruz T, Laule O, Szabo G, Wessendorp F, Bleuler S, Oertle L, et al. Genevestigator v3: a reference expression database for the meta-analysis of transcriptomes. *Adv Bioinforma*. 2008;2008:420747.
266. Schleyen JS, Baur N, Kammerer R, Nelson PJ, Rohrmann K, Gröne EF, et al. Cytotoxic markers and frequency predict functional capacity of natural killer cells infiltrating renal cell carcinoma. *Clin Cancer Res Off J Am Assoc Cancer Res*. 2006 Feb 1;12(3 Pt 1):718–25.
267. Ascoli CA, Aggeler B. Overlooked benefits of using polyclonal antibodies. *BioTechniques*. 2018 Aug 9;65(3):127–36.
268. Rönnerberg E, Calounova G, Sutton VR, Trapani JA, Rollman O, Hagforsen E, et al. Granzyme H Is a Novel Protease Expressed by Human Mast Cells. *Int Arch Allergy Immunol*. 2014;165(1):68–74.
269. Ramsborg CG, Papoutsakis ET. Global transcriptional analysis delineates the differential inflammatory response interleukin-15 elicits from cultured human T cells. *Exp Hematol*. 2007 Mar;35(3):454-464.e4.

Bibliography

270. Tremblay-McLean A, Coenraads S, Kiani Z, Dupuy FP, Bernard NF. Expression of ligands for activating natural killer cell receptors on cell lines commonly used to assess natural killer cell function. *BMC Immunol.* 2019 Jan 29;20(1):8.
271. Schwartzkopff S, Gründemann C, Schweier O, Rosshart S, Karjalainen KE, Becker K-F, et al. Tumor-associated E-cadherin mutations affect binding to the killer cell lectin-like receptor G1 in humans. *J Immunol Baltim Md 1950.* 2007 Jul 15;179(2):1022–9.
272. Nelson-Rees WA, Daniels DW, Flandermeyer RR. Cross-contamination of cells in culture. *Science.* 1981 Apr 24;212(4493):446–52.
273. Drexler HG, Uphoff CC. Mycoplasma contamination of cell cultures: Incidence, sources, effects, detection, elimination, prevention. *Cytotechnology.* 2002 Jul;39(2):75–90.
274. Jiang S, Munker R, Andreeff M. Bcl-2 is expressed in human natural killer cells and is regulated by interleukin-2. *Nat Immun.* 1996 1997;15(6):312–7.
275. Romero V, Fellows E, Jenne DE, Andrade F. Cleavage of La protein by granzyme H induces cytoplasmic translocation and interferes with La-mediated HCV-IRES translational activity. *Cell Death Differ.* 2009 Feb;16(2):340–8.
276. Andrade F, Fellows E, Jenne DE, Rosen A, Young CSH. Granzyme H destroys the function of critical adenoviral proteins required for viral DNA replication and granzyme B inhibition. *EMBO J.* 2007 Apr 18;26(8):2148–57.
277. Waterhouse NJ, Trapani JA. H is for helper: granzyme H helps granzyme B kill adenovirus-infected cells. *Trends Immunol.* 2007 Sep;28(9):373–5.

Acknowledgments

So many people have supported me on my journey to completing this project. I would like to thank all of them.

First and foremost, however, I would like to thank my supervisor, Prof. Dr Markus Uhrberg, for giving me the opportunity to do this project and for suggesting the research topic. I also want to thank him for his great enthusiasm, his patience, his highly stimulating professional input and, of course, the trust he has placed in me. Without him, this project would neither have been possible nor have come to fruition.

My thanks also go to Dr Johannes Fischer for giving me the opportunity to do this project at his institute, and for the provision of the buffy coat blood samples used here. My thanks also go to Prof. Dr Gesine Kögler for provision of the cord blood samples used here.

I would also like to thank Dr Hans-Ingo Trompeter for his wonderful support when I worked on the overexpression (and knockdown) vectors and inserts. His advice on the optimum protocols to be used and the best way to record them, as well as his explanations regarding the underlying principles, were invaluable for the success of that part of this study.

Special thanks go to Prof. Dr Helmut Hanenberg for helping me design a protein overexpression protocol and for letting me work in his laboratory to put this protocol into effect. Many thanks also go particularly to Dr Constanze Wiek, as well as to Ms Corinna Haist and Mr Arthur Bister for teaching me how to optimise and apply the aforementioned overexpression protocol as well as for their support whenever things did not go to plan. Of course, I also thank all four of them for providing me with the necessary reagents and apparatus.

I would also like to thank Ms Nadine Scherenschlich and Dr Angela Manser for KIR-typing my blood donor samples, and for HLA-C-typing those that I did not type myself, and Ms Scherenschlich for regularly ensuring that my cell lines were not contaminated with *Mycoplasma*.

My thanks also go to Dr Maryam Hejazi and Dr Angela Manser for helping me with troubleshooting, both during my experiments and when I wrote this report.

The three of them, as well as Dr Sandra Weinhold, Dr Sarah Reusing, Ms Sabrina Bennstein and Ms Teresa Becker also have my thanks for providing me with additional blood samples from their own experimental stock, as well as for the stimulating discussions I was able to have with them, including regarding certain experimental setups. Their words of encouragement but also their great ability to spot errors and thus help me correct them have been extremely helpful to me.

I also thank Dipl. Ing. Katharina Raba for her invaluable support whenever there were problems with the flow cytometer and for her considerable genius in fixing it. I also thank her for sorting my cell samples via fluorescence-activated cell sorting, and her advice on how best to prepare cells prior to this process.

Acknowledgments

I also thank Dr Jürgen Enczmann and colleagues at the HLA laboratory at the ITZ for HLA-Bw4/Bw6 typing my samples.

I would also like to thank everyone else at the Institute of Transplantation Diagnostics and Cell Therapeutics, University Hospital Düsseldorf, Germany, who have supported me along the way.

My thanks also go to Prof. Dr Lutz Walter and his group at the Primate Genetics Laboratory at the German Primate Center in Göttingen, Germany, for RNA deep sequencing my transduced NK-92 cells.

I wholeheartedly thank those people who kindly donated their blood for this project! Without them, none of these experiments would have been possible!

I would like to end by thanking my family and James from the bottom of my heart. Without their support I would not be where I am today. Thank you for always being there for me.

Thank you!